Exploring the mechanisms of synaptotropic arbor growth in Drosophila

Constance, William Duncan

Awarding institution:
King's College London

EXPLORING THE MECHANISMS OF SYNAPTOTROPIC ARBOR GROWTH IN *DROSOPHILA*

A thesis submitted jointly to King's College London and The National University of Singapore for the degree of Doctor of Philosophy

2016

William D. Constance

Abstract

The role of synapses as junctions of information transfer is well understood, however the exact role they play in the early development of neuronal arborisations is unclear. Studies in the vertebrate central nervous system (CNS) by Vaughn led him to posit the 'synaptotropic hypothesis' whereby the stabilisation of exploratory filopodia/branches is strongly correlated with nascent synapse formation.

By pioneering a novel *in vivo* system, I have been able to show for the first time in *Drosophila* that the growth of complex arborisations occurs by synaptotropic-like mechanisms. Using live imaging during the pupal stages I see that the elaborate axonal arborisations of pleural motoneurons are built by dynamic interactions with their postsynaptic partners. Fluorescently labelled proteins show that this process involves the early assembly of synaptic components at sites of growth and branching.

Using two independent binary expression systems to live image the pre- and postsynaptic elements I see a complementary pairing of hemi-synapses during growth. Arbor growth requires the trans-synaptic signalling of the synaptic cell adhesion molecules Nlg/Nrx which selectively stabilise exploratory axonal branches. Whole null mutants and local manipulations show that signalling through these molecules directs growth in a tropic manner.

Published data on arbor growth in the *Xenopus* visual system forwards that Nlg/Nrx signalling is required for synapse formation, which in turn allows synaptic activity to stabilise branches. Using calcium imaging, in combination with pharmacological approaches, I have mapped the development of activity in my system. By silencing neurotransmission using TTX and single cell genetic mosaic approaches I find that the growth of these arborisations occurs without activity. Taken together these

data point toward an important activity-independent role for proto-synapses during the development of arbor shape.

These findings point to a mechanism of complex arbor construction from a simple iterated program of development, the principles of which may be evolutionarily conserved across taxa. Since arbor growth defects are associated with a number of neurodevelopmental disorders, such a model for this mode of growth in a genetically tractable system like the fly could have important implications for therapeutic research.

Acknowledgements

As someone who learnt more about barnacles than brain cells as an undergraduate, I was fortunate to find a position with a sympathetic supervisor who embarked as a scientist from a similar position. I was even luckier to have the pleasure to work under the mentorship of someone as relentlessly enthusiastic as Darren Williams. Darren's wide and wonderful fascinations and the philosophy with which he approaches them are inspiring and something I would be happy to inherit even a little of. I give him my unreserved gratitude for allowing me the opportunity to work in his lab and make such a fantastic project my own.

I would also like to express my gratitude to my supervisor at NUS, Yusuke Toyama. Yusuke has been an exceptionally hospitable host during my visits and, like Darren, generates an infectious excitement for learning.

My thanks also go out to the many kind people within the centre who have provided support and reagents. This includes Laura Andreae, who was always on hand to provide support and invaluable advice as a second supervisor, Eric Blanc, who put many hours into writing code for our analysis and Jon Clarke for trusting me with his brand new confocal. In addition, I'd like to thank the many people from further afield who have generously provided reagents, in particular Hermann Aberle.

I'd like to thank the past and present members of the Williams lab - Nico, Chris, Karen, Catalina, Alina, Sam, Amrita and Sinzi - for their help, friendship and, in many cases, for the countless beers we have shared in the Miller.

I owe a special thanks to Helen, who has been there with love, friendship and support whenever I have needed it.

Finally, I give my utmost thanks to my mum, dad and sister who have always been there with unending love and encouragement.

Table of Contents

List of Figures and Tables

Page

Chapter 3

Aims and Objectives

Live imaging of the optic tecta of fish and frogs has uncovered *in vivo* evidence in support of Vaughn's synaptotropic model of arbor growth. However, there are a number of fundamental questions regarding this mode of growth that these studies were unable to address. Chiefly: does this mechanism involve a genuine pairing of pre- and postsynaptic elements? Which proteins are involved in this process? And is there a requirement for synaptic transmission?

The fruit fly offers a genetically tractable venue for tackling these outstanding questions, however as of yet no model for exploring this mode of complex arbor growth exists in this system. For these reasons, the objectives of this study were thus:

1. To develop a system in *Drosophila* in which to study the growth of complex neuronal arborisations live and *in vivo*.
2. To identify using fluorescently labelled proteins if *Drosophila* use the same mode of synapse mediated arbor growth which has been reported in vertebrate systems.
3. If so, to establish if this mechanism involves the pairing of hemisynapses belonging to synaptic partners.
4. To explore a role for synaptic transmission in this mode of growth.

Chapter 1

General Introduction

The arborisations of neurons have long been held as important for understanding the nervous system. Ramón y Cajal realised that rather than being a continuous reticulum, the nervous system is a network of individual cells connected by their tree-like arborisations. He formulated that 'nervous impulses' are passed through these networks with a directionality which he called "dynamic polarisation", something which is evident from the arrows in many of his later drawings (Ramón y Cajal, 1898). As a consequence of this he saw the structure and organisation of neuron trees as being fundamental to the way in which information flows within the nervous system. In addition to these ideas, using neuron structure as a means of identifying the hundreds of neuron cell types has been pivotal to our understanding of neuron function and of the specification of cell type during neurodevelopment. As our methods for distinguishing between these types improves, their numbers are expected to increase by an order of magnitude (Sanes and Masland, 2015). Invertebrate neurons have a long history, having been used widely for studying nervous system structure and function since they were first labelled using Golgi's technique by Nansen in the late 19th century (Bullock and Horridge, 1966; Edwards and Huntford, 1998). Their popularity stems largely from the fact that their neurites are large and accessible and bear significant resemblance to those of vertebrates at the structural and molecular level. What is more, unlike most vertebrate neurons, many invertebrate neurons can be reliably identified from preparation to preparation. Although neurons from larger insects have been used for the study of their nervous systems (Bate, 1976a; Truman and Reiss, 1976; Shepherd and Laurent, 1992), modern molecular and genetic tools for precisely labelling and manipulating single neurons in *Drosophila* has made it a most powerful tool.

The importance of arbor morphology

Nervous systems host a huge diversity of branching structures, the size, shape and position of which are tightly linked to neuron function. This is evident from the wide range of developmental neuropathologies which are associated with defects in arbor growth including intellectual disability (Kaufmann and Moser, 2000), schizophrenia (Kalus *et al.*, 2000) and autism spectrum disorder (Durand *et al.*, 2012).

There are numerous features of nervous system function which arbor shape impacts. For one, arbor morphology is directly correlated with a neuron's intrinsic electrophysiological properties. In cultured explants of the mammalian cortex it was discovered that dendritic morphology is a strong predictor of neuronal firing patterns, with bursting cells tending to possess relatively more complex dendritic arborisations than single-spiking cells (Chagnac-Amatai *et al.*, 1990; Mason and Larkman, 1990; Yang *et al.*, 1996). Although the membrane properties of these cells were also found to vary, pointing to differences in ion channel compositions and densities, this indicates that arbor size and shape is an important determinant of the electrical properties of neurons. In support of this, computer modelling of cortical neurons in which membrane properties were kept constant showed that by changing arbor morphology alone the full range of spiking patterns recorded in neurons *in vivo* could be reproduced (Mainen and Sejnowski, 1996; van Ooyen *et al.*, 2002; van Elburg and van Ooyen, 2010). The firing patterns of neurons *in vivo* are known to vary, both within and between classes, and are intimately linked with neuronal function (Turner *et al.*, 1995; Dégenètais *et al.*, 2002). Therefore, one important role of arbor morphology would appear to be in the generation of this physiological diversity.

Neuronal arborisations are the platforms for information exchange within nervous systems. Consequently, for a neuron to play a meaningful role within a circuit it

must establish its arborisations the correct 'neural space' for making appropriate synaptic connections. This is particularly evident from the widespread organisation of neuronal networks into topographic 'maps' which are representations of the external world (Schwartz, 1977; Vassar *et al.*, 1994; Kaas; 1997; Landgraf *et al.*, 2003; Talavage *et al.*, 2004). These organisations facilitate the processing of sensory information and ultimately the downstream coordination of behaviours. One such example of this is the continuous 'somatotopic' mapping of the receptive fields of interneurons in the central ganglia of locusts. These interneurons receive input from the sensory afferents originating in the legs (Siegler and Burrows, 1986). By recording from single interneurons whilst stimulating the leg sensilla it was demonstrated that the arborisations of these interneurons are organised into functional maps with relation to the location of receptive fields along the legs (Burrows and Newland, 1994; Newland and Burrows, 1997). This is a clear demonstration that the spatial arrangement of arborisations relative to one another is fundamental for the accurate transmission of information.

In addition to their location in space, the size and shape of arborisations also dictate the role of neurons within their networks. This is a result of determining the number of partners with which they can make synaptic connections. An example if this is well illustrated by differences in the size of the input arborisations of the first order interneurons in different species of bees. The sweat bee *Megalopta genalis* forages by night and therefore requires exceptional optical sensitivity. Using Golgi staining it was shown that these interneurons in this species construct input arborisations in the visual lamina with much broader fields than their equivalents in the diurnal species *Apis melifera* (Ribi, 1975; Greiner *et al.*, 2004). These neurons are believed to be involved in visual processing. Therefore, by sampling from a greater number of ommatidia the

authors propose that these allow the bees a greater visual sensitivity at the cost of decreased spatial resolution.

The mechanisms that sculpt arbor shape

The mechanisms which regulate arbor morphology and position during development have also been the focus of much study. One means by which neuron growth is known to be controlled is by attractive and repulsive molecular guidance cues (Kalil *et al.*, 2011). Using *Drosophila*, it has been shown that guidance cues derived from non-synaptic partner cells can establish the patterning of dendrites during nervous system development by causing target cells to construct arborisations using a common coordinate system (Brierley *et al.*, 2009; Mauss *et al.*, 2009). This was shown to take place without activity and even in the absence of synaptic targets suggesting that it represents a simple, hard-wired means of setting up neural networks by providing common 'meeting-places' for synaptic partners. One of the signalling pathways shown to be involved in this process in *Drosophila*, the ligand-receptor pair Slit/Robo, has since been found to play a comparable role in zebrafish by regulating the laminar organisation of retinal ganglion cell axons in the tectum, perhaps pointing to an evolutionary conserved mechanism for encoding connectivity (Nikolaou and Meyer, 2015).

Another means by which the spatial organisation of arborisations is achieved in a number of systems is through tiling (Wässle *et al.*, 1981, Grueber *et al.*, 2002; Sagasti *et al.*, 2005). In this manner arborisations achieve non-overlapping arrangements with their homotypic neighbours allowing uniform, non-redundant coverage of input or output territories (Grueber and Sagasti, 2010). One case which has been particularly well studied is the tiling of the *Drosophila* body wall by the input arborisations of the multi-dendritic dendritic arborisation (da) somatosensory neurons

(Grueber *et al*, 2002). The class IV da dendrites generate large arborisations with contiguous territories which cover most of the larval body wall. Ablations of single Class IV da neurons led to the invasion of the vacant territory by neighbouring homotypic cells which generated larger arborisations, whereas duplications of class IV cells led to the generation of smaller arborisations which maintained a tiling pattern (Grueber *et al.*, 2003). Together this suggests that tiling is achieved by repulsive homotypic interactions. The molecular basis behind this repulsion is not well understood, however in mutants of the cadherin family protein Flamingo (Fmi) the arborisations of class IV da neurons were found to significantly overlap (Kimura *et al.*, 2006). Fmi has been shown to bind homophilically *in vitro* suggesting that it mediates repulsive homotypic interactions between these cells (Usui *et al.*, 1999). Interestingly, not all instances of tiling can be explained by homotypic interactions. In the retina of Brn3b mutant mice for example, in which ~80% of retinal ganglion cells are lost, the remaining retinal ganglion cells were found to construct dendritic arborisations with size and spacing no different to those in wild types (Lin *et al.*, 2004). This suggests that tiling in this case takes place in the absence of repulsive homotypic interactions. As an alternative, it has been suggested that the size of retinal ganglion cell dendrites and their density within retina may be limited by intrinsic programs of development.

Much of what we know about the intrinsic control of arbor growth comes from studies on the *Drosophila* da neurons. The type-specific morphology of the dendritic arborisations of these cells is associated with expression profiles of particular cohorts of transcription factors. The class I neurons for example, which have the least complex arborisations are characterised by expression of the BTB/zinc finger transcription factor *abrupt*, while class IV neurons, which have the most complex arborisations, express the COE transcription factor *knot*. Cell-autonomous transcriptional regulation has been shown to account for a great deal of the dendritic morphology of the da neurons. Loss

of Abrupt in single cells results in a loss of the defining branching pattern of the Class I dendrites, whilst its misexpression in other classes is sufficient to cause them to take on a simple class I morphology (Li *et al.*, 2004; Sugimura *et al.*, 2004). These observations point out that certain aspects of morphology can be set by transcription factor codes. The downstream targets of these transcription factors are still being uncovered, however common targets appear to be proteins involved in cytoskeletal remodelling which could regulate branching patterns (Jinushi-Nakao *et al.*, 2007; Ferreira *et al.*, 2014). Intrinsic programs of arbor growth such as those seen in the *Drosophila* da neurons may explain why isolated neurons grown in culture are still able to generate type-specific arbor morphologies (Montague and Friedlander, 1989; Montague and Friedlander, 1991; Neale *et al.*, 1993). This being said, the da dendritic arborisations are a special case since, unlike most arborisations, they do not receive afferent input. As a result, the biology of these neurons may be very different.

In addition to achieving patterned arrangements with one another, neurons also often display robust patterns of isoneural spacing between 'sister' branches, thus minimising the overlap and therefore the redundancy of their territories (Grueber and Sagasti, 2005). Consequently, it has been considered that neurons must also be able to recognise and avoid themselves. In *Drosophila*, loss of the immunoglobin (Ig) superfamily protein DSCAM1 has been associated with aberrant branching, collapse of processes, self-crossing and abnormal branch spacing of the arborisations of a number of peripheral and central neurons, including da sensory neuron dendrites, olfactory projection neuron dendrites and mushroom body (MB) axons (Wang *et al.*, 2002; Hummel *et al.*, 2003; Zhan *et al.*, 2004; Zhu *et al.*, 2006; Soba *et al.*, 2007). Alternative splicing of *DSCAM1* in *Drosophila* has the potential to generate as many as 19,008 proteins with distinct extracellular domains (Schmucker *et al.* 2000). What is more, these isoforms demonstrate strong homophilic interactions *in vitro*, but interact weakly

with other isoforms, raising the possibility of their role in a 'code' for connectivity (Wojtowicz *et al.*, 2004). Expression of a single isoform of *DSCAM1* chosen at random in single da or MB neurons in *DSCAM1* mutants was sufficient to rescue the arbor growth phenotypes of these cells (Zhan *et al.*, 2004, Soba *et al.*, 2007). On the other hand, however, when a single isoform was expressed in multiple neighbouring cells these adopted a pattern reminiscent of self-avoidance (Soba *et al.*, 2007). Together these data imply that rather than coding for connectivity, *DSCAM1* in *Drosophila* in fact provides a 'non-connectivity' code which enables branches of the same neurons to avoid each other yet coexist with their neighbours. Although the splice diversity of DSCAMs in vertebrates is far lower than in invertebrates, comparable arbor growth phenotypes are observed in protocadherin mutants (Lefebvre *et al.*, 2012). Furthermore, these adhesion proteins also bind homophilically and have potentially thousands of splice isoforms, leading to the speculation that they perform a similar role in vertebrates. Interestingly, in addition to acting as a cell adhesion molecule, *Drosophila* DSCAM1 has been shown to act as a receptor for the axon guidance molecule Netrin (Andrews *et al.*, 2008). In this capacity DSCAM1 was found to promote midline crossing of axons in the developing embryonic CNS via a mechanism distinct from its function as a cell adhesion molecule. What is more, binding of the midline signalling molecule Slit to DSCAM1 has more recently been shown to regulate the local outgrowth of axon branches in the developing adult *Drosophila* CNS by modulating repulsive isoform specific interactions (Dascenco *et al.*, 2015). These examples highlight the complex integration of the multiple layers of regulatory mechanisms which act to sculpt neuron arbor growth.

It would seem that a combination of these mechanisms is used to instruct arbor growth, none of which are mutually exclusive. With the technological advances in live imaging which have been made in recent years, evidence has accumulated to suggest

that arbor growth in densely populated neural tissues such as the brain is an incredibly dynamic process involving interactions between the exploratory branches of partner cells (Cooper and Smith, 1992; Dailey and Smith, 1996; Ziv and Smith, 1996; Wu and Cline, 1998; Niell *et al.*, 2004; Meyer and Smith, 2006) It has therefore been proposed that in addition to the mechanisms described above, a significant contribution to arbor construction is derived from these dynamic interactions. What the molecular mechanisms are that underlie this however are yet to be conclusively shown.

Chapter 2

Development of the abdominal pleural neuromuscular system – a new model of arbor growth in *Drosophila*

2.1 Introduction

Arbor morphology is a key determinant of a neuron's connectivity and function and is therefore central to its role within a network. On average, each of the approximately 100 billion neurons in the human brain makes around 7,000 synaptic connections with, in some cases, thousands of different synaptic partners (Palkovitis *et al.*, 1971; Pakkenberg *et al.*, 2003). From what we understand of the genome it lacks the capacity for encoding specific 'blue-prints' for constructing the enormous diversity of arbor morphologies required for this scale of connectivity. Alternatively, in an effort to understand the mechanisms of arbor growth, focus has been directed at searching for simple generative rules of development, or 'algorithms of growth', which when played out at a local level could optimise connectivity in different developmental contexts (Hassan and Hiesinger, 2015).

One idea for such an 'algorithm' was developed by Vaughn *et al.* in the late 70s and early 80s from observations of fixed samples of rat and mouse spinal cords (1974, 1988). Using electron microscopy, it was observed that synapses exist on some of the filopodia situated at the tips of motoneuron dendritic growth cones. It was imagined that these could confer selective stability to subsets of filopodia, which would then differentiate to become permanent parts of the dendritic arbor (Vaughn *et al.*, 1974). Iterations of this process could give rise to the 'strings' of synapses, which were found to stud the lengths of dendritic branches later in development. Alongside this, using Golgi staining it was recognised that dendrites only extend into territories following the

arrival of their afferent partners (Vaughn *et al.*, 1988). Together these observations provided the foundation for the synaptotropic hypothesis of arbor growth. This theory puts forward that by selectively stabilising exploratory filopodia, synapse formation directs arbor growth preferentially into regions rich in synaptic partners in a tropic manner (i.e. by orientating growth towards an external stimulus) (Vaughn, 1989) (Fig. 1). Consistent with this, other labs around the same time demonstrated that Purkinje cells generate substantially smaller and less complex dendritic arborisations when their synaptic partners are reduced in number *in vivo*, suggesting that synapse formation exerts a tropic influence on growing arborisations (Bradley and Berry 1976a, Bradley and Berry 1976b).

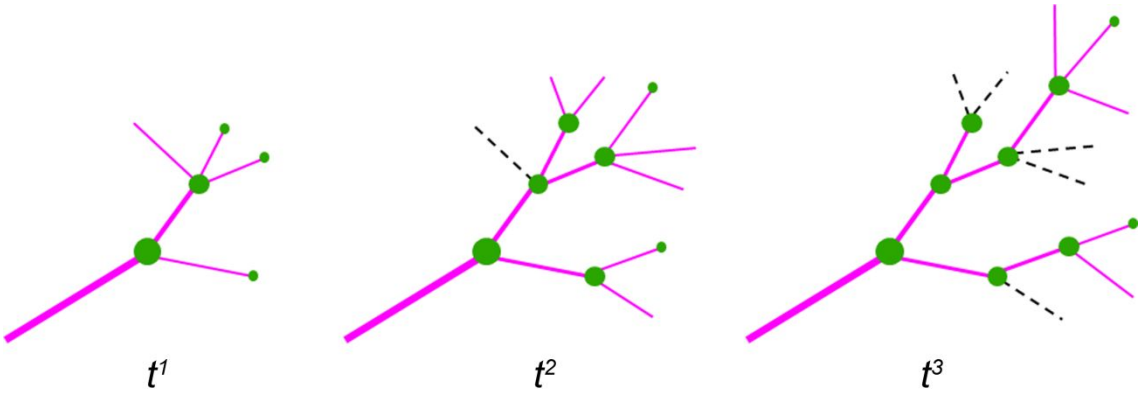

Figure 1. The synaptotropic hypothesis of arbor growth (adapted from Niell *et al.*, 2006) (t^1) exploratory filopodia (thin magenta lines) grow from established synaptic contacts (green dots) (t^2) filopodia on which synapses are formed are selectively stabilised, whereas those that fail to form synapses are lost (dotted lines) (t^1) iterative rounds of this process directs arbor growth into regions rich in synaptic partners.

This innovative thinking by Vaughn and colleagues required an insightful imagination since the fixed material from which their hypothesis was conceived was unable to convey the dynamics required for such an exploratory, interaction-dependent mode of growth. Since then, advances in live cell labelling and microscopy techniques have opened the door to live-imaging based evidence in support of these ideas. Rapid time-lapse imaging of growing axonal and dendritic arborisations in cultured explants of

vertebrate brains as well is *in vivo* has revealed that arbor construction *in situ* is indeed a highly dynamic process, involving the extension and retraction of exploratory filopodia over a matter of minutes (Kaethner and Stuermer, 1992; Dailey and Smith, 1996; Wu *et al.*, 1999). What is more, in a manner predicted by Vaughn *et al.*, arbor growth has been demonstrated to involve the stabilisation and maturation of only small numbers of these filopodia (Dailey and Smith, 1996; Wu and Cline, 1998; Niell *et al.*, 2004; Meyer and Smith, 2006). In addition to these observations, in dissociated cultures of hippocampal cells it was found that filopodia are stabilised by the formation of contacts with prospective synaptic partners (Cooper and Smith, 1992; Ziv and Smith, 1996). These contact sites have been shown to rapidly recruit pre- and postsynaptic machineries and mature into synapses capable of evoked neurotransmission, thus demonstrating a synaptotropic-like relationship between synapse formation and filopodia stability *in vitro* (Ziv and Smith, 1996; Ahmari *et al*, 2000; Friedman *et al.*, 2000).

Providing evidence for a synaptotropic mechanism of arbor growth *in vivo* however has been much more difficult. Even by today's standards visualising interactions between synaptic partners in such a complex tissue as the brain is impractical. Nevertheless, targeted expression of synaptic components in single cells in the brains of fish and frogs has provided live evidence for a role of hemi-synapse formation in the growth of axonal and dendritic arborisations via synaptotropic-like mechanisms. In growing retinal ganglion cell dendritic arborisations clusters of the synaptic vesicle associated proteins Synaptobrevin and Synaptophysin have been shown to stabilise at growth cones and on the tips of exploratory filopodia (Alsina *et al.*, 2001; Meyer and Smith, 2006; Ruthazer *et al.*, 2006). Likewise, the postsynaptic protein PSD-95 was shown to form stable puncta on the tips of filopodia of growing optic tectum cell dendritic arborisations (Niell *et al.*, 2004). In line with the synaptotropic

hypothesis, the stabilisation of these puncta was correlated with the selective stabilisation of subsets of filopodia (Niell *et al.*, 2004; Meyer and Smith *et al.*, 2006). In addition to awarding stability to filopodia, these studies found that stable synaptic puncta also act as nucleation sites for new branch growth. This suggests that synapses play a dual role in synaptotropic arbor growth by stabilising branches/filopodia and promoting growth. Iterative rounds of these processes were found to generate axonal and dendritic branches studded with synaptic puncta just as Vaughn *et al.* had suggested.

Although synaptotropic-like growth has now been identified in a number of systems, the molecular mechanisms behind it remain poorly understood. As components which play an early role in synapse assembly, synaptic cell adhesion molecules prove likely candidates for establishing stabilising contacts between exploratory filopodia. In *Xenopus*, disrupting signalling between the heterophilic partners Neurexin and Neuroligin resulted in reduced optic tectum cell filopodia stability and smaller and less complex dendritic arbors (Chen *et al.*, 2010). Conversely, overexpression of *Nlg* in optic tectum cells caused the hyper-stabilisation of dendritic filopodia. Taken together these data indicate the involvement of Nlg-Nrx interactions in a synaptotropic-like mechanism by conferring stability to filopodia. In addition to this it was found that the hyper-stabilisation effect of overexpressed *Nlg* was reversed by blockade of NMDA receptors, leading the authors to suggest that neurotransmission is required for the consolidation of these nascent contacts (Chen *et al.*, 2010). This is supported by an abundance of evidence from other work showing that blocking NMDA or AMPA receptor mediated transmission leads to smaller dendritic arbors and more unstable axonal arbors in vertebrates *in vivo* (Rajan and Cline, 1998; Rajan *et al.*, 1999; Sin *et al.*, 2002). In retinal ganglion cell axonal arborisations visual activity was found to increase the stability of branches marked by stable presynaptic puncta, but

destabilise branches without puncta, suggesting that, at least in the case of axons, activity plays a role by 'use-testing' synaptic contacts. Expanding on this idea, in *Xenopus* activity-dependent regulation has been suggested to take place via machineries required for activity-dependent plasticity, since both disruptions to *CaM-Kinase II* or protein kinase *Mζ (PKMz)*, which are involved in the long-term potentiation of synapses, have been shown to promote optic tectum cell dendritic arbor growth *in vivo* (Wu and Cline, 1998; Liu *et al.*, 2009). Although this may seem counter intuitive, the authors suggest that synaptic strengthening via these pathways acts to increase stability and therefore curtail arbor growth (Liu *et al.*, 2009). In a similar fashion, protein kinase A (PKA) has been shown to regulate the growth of an identified central dendritic arborisation in *Drosophila* in response to neurotransmission. Ostensibly therefore *PKA* may play a similar role in regulating arbor growth in *Drosophila* as *CaM-Kinase II* does in *Xenopus* (Tripodi *et al.*, 2008).

The evidence for synaptotropic growth from vertebrate models is convincing, but clearly many questions remain regarding its molecular basis. Although comparable mechanisms of synaptotropic-like growth appear to direct the growth of optic tectum cell dendritic arborisations and retinal ganglion cell axonal arborisations - known synaptic partners in the optic tectum - it would be incredibly difficult to determine if this involves the formation of synapses between these cells *in vivo*. Thus, so far, no clear evidence exists to support the involvement of hemi-synapse pairings in this mode of growth. Furthermore, which synaptic components are required at these putative contacts for conferring stability and promoting growth remains largely unknown. In addition, although synaptic activity has been implicated, the evidence to support this is fragmentary and too little to generate a compelling model for an activity-dependent mechanism.

The genetic tractability of *Drosophila* and the ability to reliably label and manipulate identical cells in different preparations make it an ideal model for tackling these outstanding questions on the mechanisms of synaptotropic growth. However, as of yet no such mode of growth has been observed outside of vertebrates. Using a previously unexplored population of axonal arborisations which develop during the pupal stage of the fly I present here a new model for exploring the mechanisms of complex arbor growth live and *in vivo* with a view to answering some of these questions.

2.2 Results

New tools for exploring complex arbor growth in Drosophila

Two models that have been used extensively to study neuronal arbor development in *Drosophila* are the output terminals of the larval motoneurons and the peripheral neurites of the multidendritic dendritic arborisation (da) sensory neurons (Fig. 1A). These systems have proved to be a rich vein for identifying the cellular and molecular mechanisms of arbor growth. The larval neuromuscular junction has revealed the fundamental aspects of synaptic maturation and plasticity and the da neurons the intrinsic and extrinsic factors that shape arborisation growth. Despite this, like all models they have limitations. On the one hand the da sensory neurons elaborate their neurites directly onto the epidermis and receive no synaptic input, whereas on the other hand the NMJ is relatively simple and its terminal target specific muscles with a rigid one-to-one connectivity. Both arborisations also show slow incremental growth, with the addition of branches or boutons over long periods. This lack of dynamism is seen in the temporally colour coded projection of a 10 -minute time-lapse of a larval NMJ in the third instar (Fig. 1B). These features present a stark contrast to the overwhelming majority of arborisations in central nervous systems which have much greater arbor complexities and achieve their patterns of connectivity via dynamic, self-organising mechanisms.

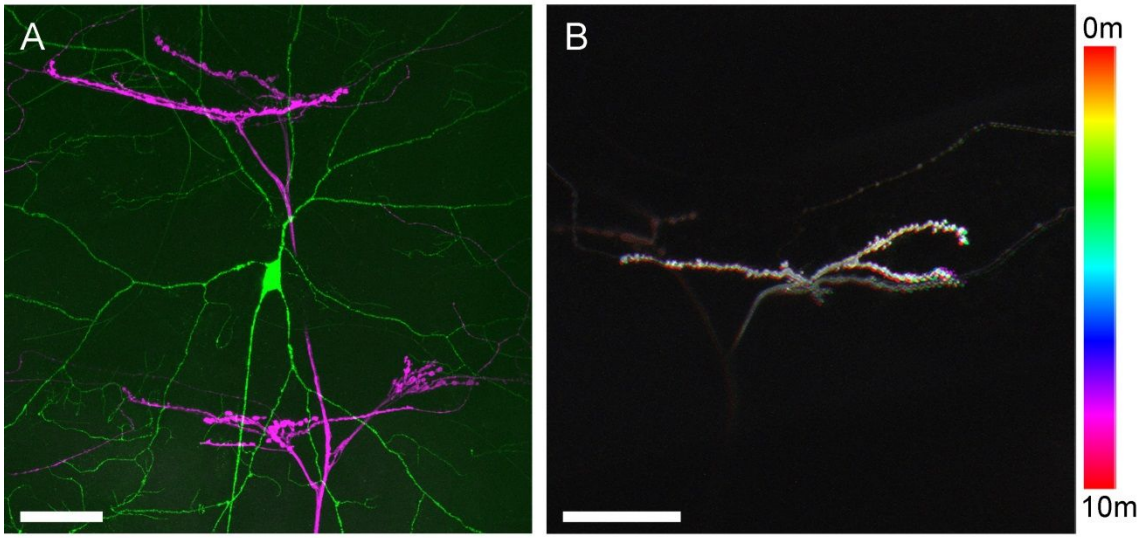

Figure 1. Existing models for studying arbor growth live in *Drosophila* (A) A class IV dendritic arborisation (da) sensory neuron ddaC (green) and the motoneuron axon terminals (magenta) innervating muscle pairs 1/9 (top) and 2/10 (bottom) in a wandering L3 larva. **(B)** A temporal colour coded projection of a time series taken at 1 minute intervals shows the dynamics of a motoneuron terminal innervating muscle 9 in an L3 wandering larva. To inhibit muscle contractions this larva was injected with 0.5mM TTX. C4da, ddaC neuron revealed with: *PPK*-GAL4>dsRed; motoneurons: *VGlut*-GAL4>myr::GFP. Scale bars: 50*μ*m.

In a search for an alternative model, the axonal arborisations of the motoneurons which innervate the abdominal pleural muscles of adult *Drosophila* were uncovered as promising candidates (Williams, *pers comm*). In each hemisegment from A1-A7 two of these motoneurons project from the lateral branch of the peripheral nerve and innervate 15-18 parallel muscle fibres, which span the extent of the pleura from the ventral limits of the tergites to the dorsal limits of the sternites (Fig. 2A). With the benefit of being close to the body wall this tissue can be easily imaged through the pupal cuticle after dissecting away the pupal case (Fig. 2B). In contrast to the neuromuscular junctions of the larva these arborisations are highly complex, with total branch numbers from 50 to over 100, as opposed to single figures, and branch orders of as many of 16, as opposed to no more than 2 or 3.

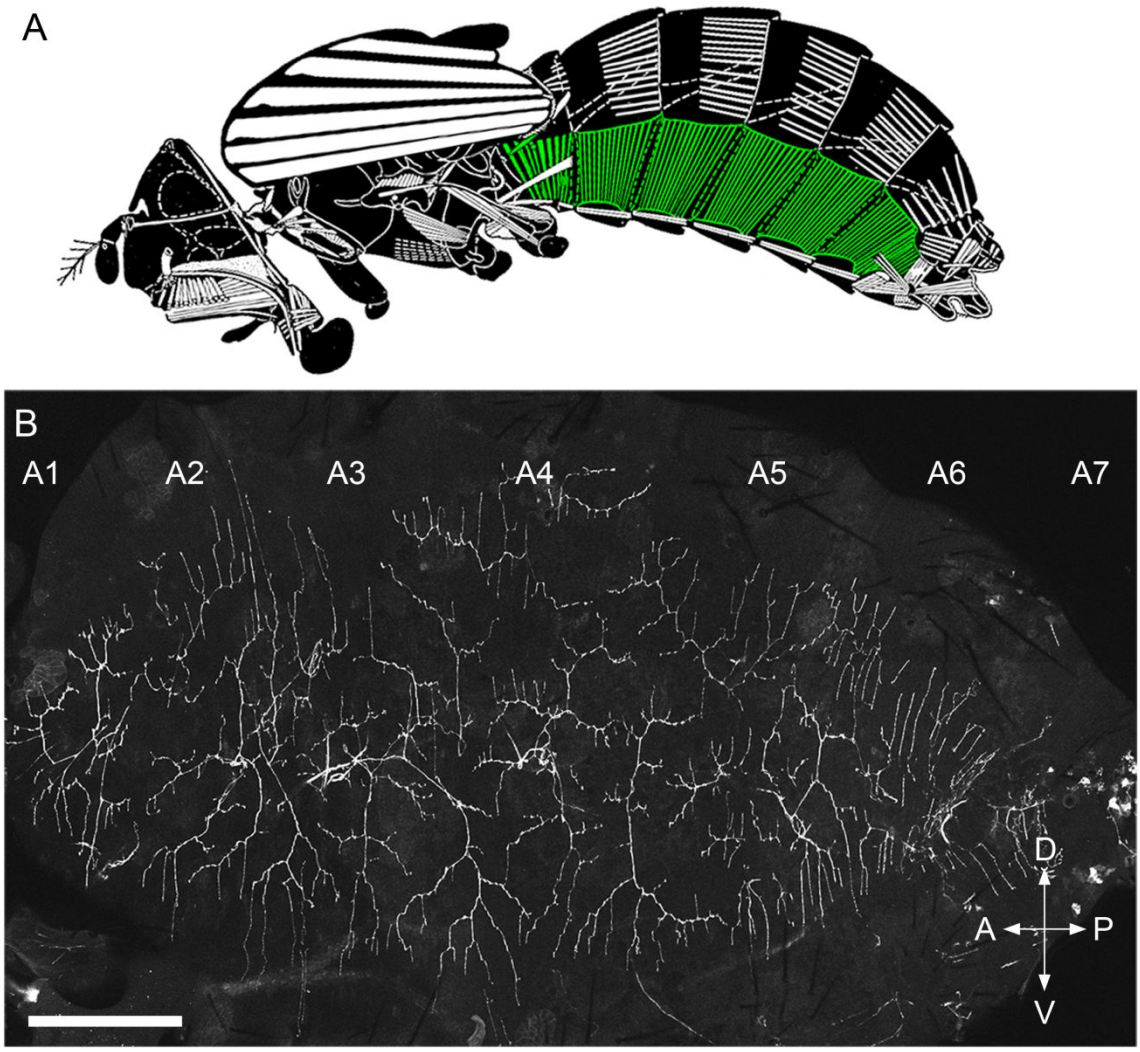

Figure 2. The pleural neuromuscular system of the *Drosophila* adult (A) A schematic of the somatic musculature of the *Drosophila* adult, adapted from Miller (1950), with pleural muscles highlighted in green **(B)** Tiled confocal z-stacks show the full complement of motoneuron axon terminals occupying the pleural region of one flank of an adult abdomen. Motoneurons express myr::GFP under the control of OK371-GAL4. The abdominal segments, demarcated by the tergites, are labelled from A1 to A7. Indicated by the axis key, all images are presented in this orientation unless stated otherwise. Scale bar: 250μm.

The variable innervation pattern of the pleural motoneuron axons points to the absence of rigid, target-specific pre-patterning (Figs. 2B&3A). Colour coding of the muscles and motoneurons by segment reveals that the growth of these arborisations is unconstrained by segment boundaries (Fig. 3A&B). This clear lack of growth constraints gives rise to variations in the size, shape, topology and area of coverage of the arborisations. Despite this apparent lack of targeting the arborisations achieve a

consistent spatial organisation with regularly sized, non-overlapping domains, which cover the entire pleural region. These dorsal domains are further impinged upon by a group of motoneurons which originate from the dorsal branches of the peripheral nerves to innervate the dorsal extremes of the pleural muscles (Fig. 3A). However, these are not the focus of this study.

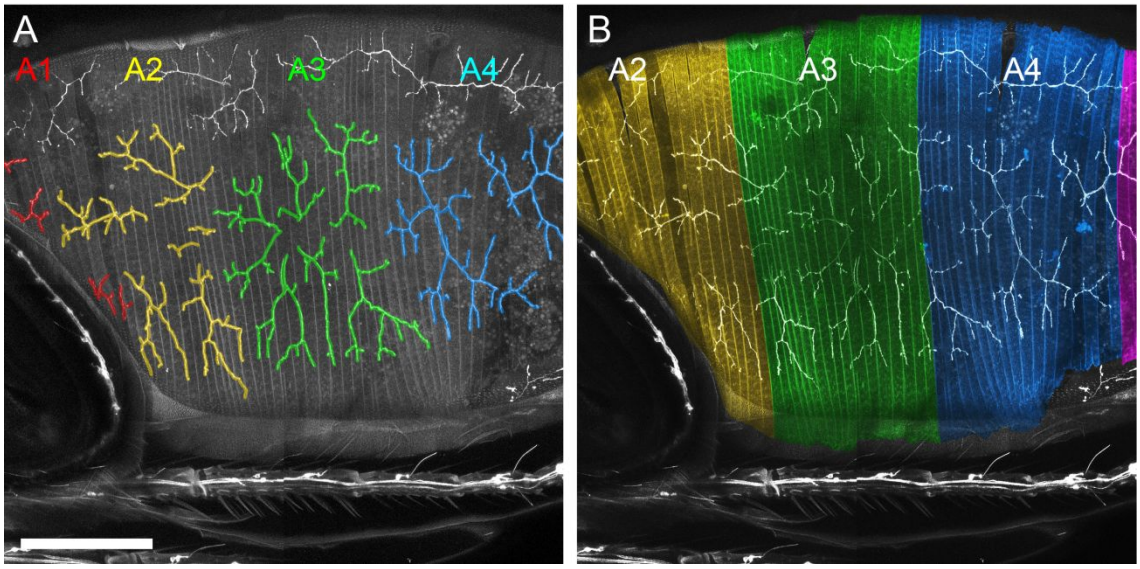

Figure 3. Innervation patterns of Motoneuron on pleural muscles (A) The axonal arborisations in hemisegments A1-A4 in a pupa at 80h APF colour coded by the segment from which they originate. The non-highlighted segments above these belong to the motoneuron axons which exit the dorsal branch of the peripheral nerve. Beneath and to the left are the sensory organs of the leg and wing **(B)** The pleural muscles of the same animal also colour coded by segment and superimposed upon the motoneurons. Motoneurons: *VGlut*-LexA>myr::GFP; muscles: *Mef2*-Gal>mtdTomato. Scale bar: 150μm.

Pleural motoneuron axonal growth is dynamic

Being an adult specific structure, the pleural neuromuscular junctions are constructed during the pupal-adult transition. Much like embryogenesis, during metamorphosis the great majority of adult specific tissues are generated *de novo* from populations of progenitor cells making it an excellent model of early aspects of development. Unlike embryogenesis however, which lasts only around 22h at 25˚C, metamorphosis takes around 96h, offering greater potential for resolving discrete

developmental events; particularly motoneuron axon arbor development which takes place within 4 hours in the embryo compared to 50+ hours in the pupa. Alongside this, the combination of the superficial position of these tissues and the immobility of the pupa enables continuous *in vivo* time-lapse imaging of these events.

To explore the development of the pleural motoneuron axons, the arborisations in a hemisegment of A3 were live imaged at approximately 12h intervals from 24h to 84h after puparium formation (APF) (Fig. 4). As described by Currie and Bate (1991), by 24h APF the larval musculature in the abdominal segments as well as the nerves that innervate it are almost entirely removed through cell death and phagocytosis. This leaves a single nerve trunk in each hemisegment which maintains four contacts with the epidermis during pupariation and allows continued innervation of the persistent larval muscles. By 24h APF the axons of the pleural motoneurons have been remodelled and are tipped with a population of filopodia. Over the course of the next 36 hours the axon terminals undergo a dynamic phase of outgrowth and branching which is correlated with the formation of many more filopodia. At approximately 60h APF this elaborative phase comes to an end and most of the filopodia are lost. Following this there is a period of refinement and a thickening of the distal branches with the formation of bouton-like varicosities along the lengths of all but the most proximal branches. By 84h APF arbor morphology is indistinguishable from that found at the pharate adult stage.

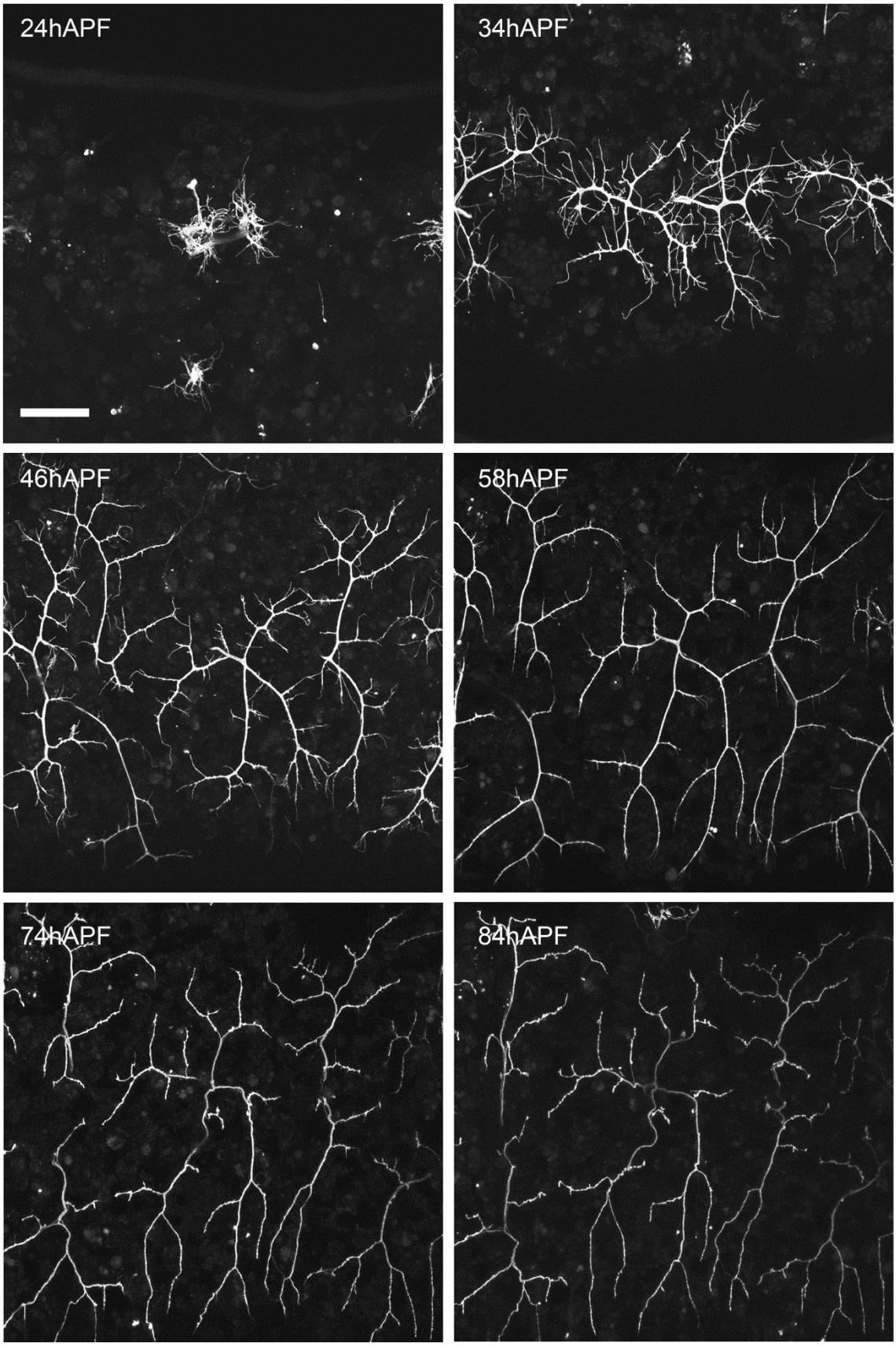

Figure 4. The developmental timeline of the pleural axonal arborisations. A time series taken at between 10h and 14h intervals follows the growth of a pair of axon terminals in segment A3 expressing myr::GFP under OK371 control. Scale bar: 50μm.

To better resolve the early phases of arbor construction shorter, higher frequency time-lapse image sequences were taken. The dynamic behaviour of a pair of motoneurons at 32h APF can be appreciated with a colour coded projection of a 10-minute time-lapse sequence with 2 minute intervals (Fig. 5A). In contrast to the relatively static larval motoneuron axon terminals displayed in Fig. 1, the developing terminals of the pleural motoneurons explore their environment by means of highly motile filopodia. This exploration takes place almost exclusively in the plane of the body wall in which the pleural muscles are closely orientated. This alone gives the first indication that these processes are exploring the local environment and undergoing multiple rounds of interaction with their postsynaptic targets.

Focusing on an early branch over longer a period of growth, a sequence of images taken at 40 minute intervals reveal the more substantial morphological changes that occur during arbor outgrowth (Fig 5B). It becomes clear that the majority of filopodia are transient and that their turnover is high, since large numbers are lost and generated between each frame. Despite this largely transient population, a small number of persistent filopodia play a crucial role in growth by pioneering branch growth: In the first frame of the sequence a number of filopodia extend beyond the branch terminal to explore its surroundings. One of these is stabilised and by 40 minutes has matured, becoming an extension of the branch (Fig. 5B). Following this, additional filopodia are generated along this newly established segment and the sequence begins again. By 140 minutes' iterative rounds of filopodia exploration and stabilisation have extended the branch further and have produced a pair of new branch points. In addition to these constructive events, a branch also retracts over this time period and collapses into a single filopodia. This highlights the inherent instability and continuous remodelling of the arborisations at this early stage. Together these progressive and

regressive phenomena make up the basic operations behind the construction of these complex arborisations.

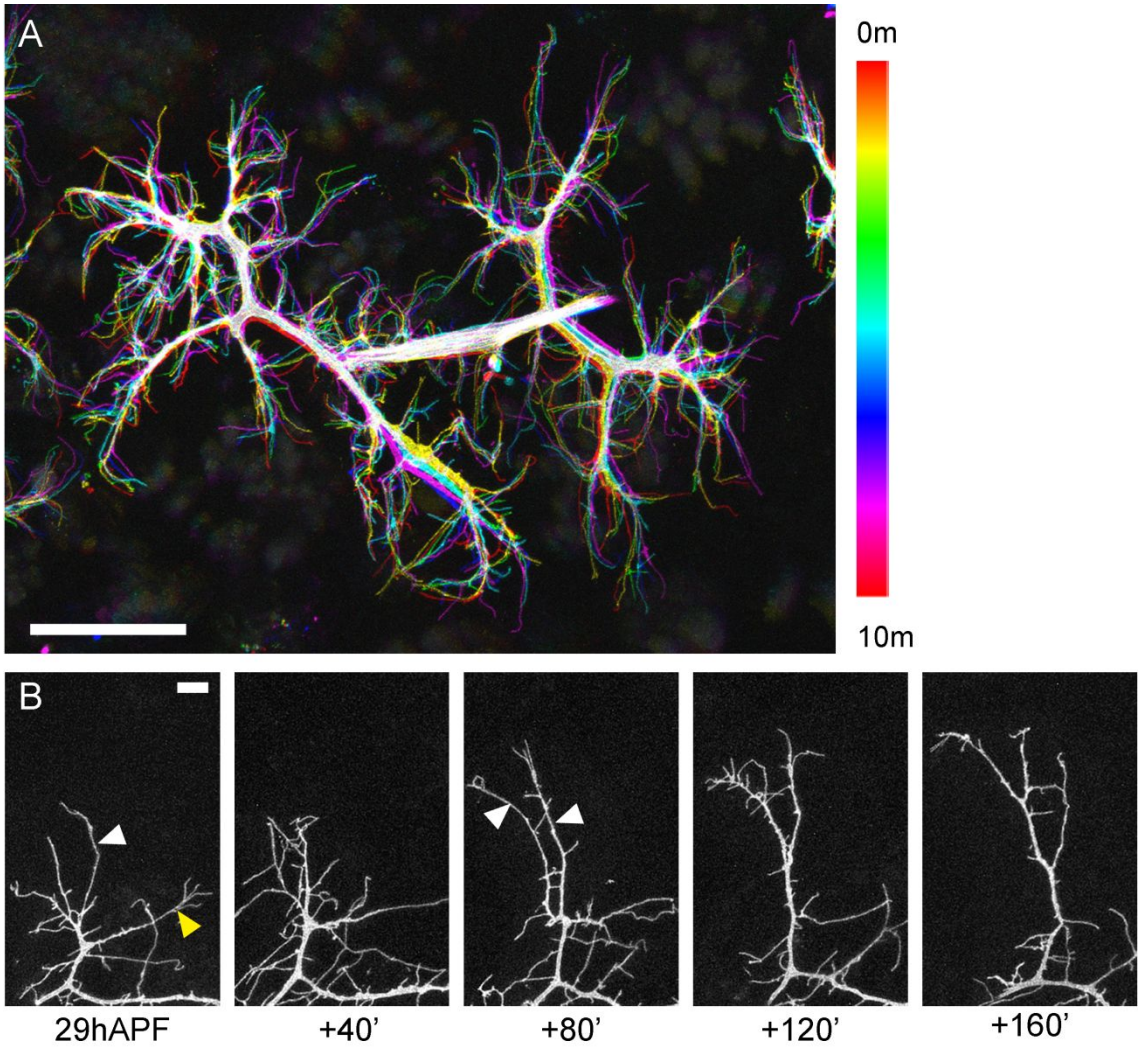

Figure 5. The early dynamics of axon arbor growth (A) A temporally colour coded projection of a time-lapse with 2 minute intervals shows the dynamics of a pair of arborisations at 32h APF **(B)** A sequence of images taken at 40 minute intervals shows the extension and branching of a segment at 29h APF. The white arrows indicate filopodia that become stabilised. The yellow arrow indicates a branch that retracts. This image sequence is rotated clockwise and flipped horizontally making dorsal left and anterior top. Motoneurons are expressing myr::GFP under the control of OK371-GAL4. Scale bars: 50μm (A) 10μm (B).

Throughout this thesis, I will often use the terms branch and filopodia. As a result, it is important at the onset to define what I mean when I use the terms i.e. to make a distinction between these structures. According to anatomical and molecular

criteria, filopodia are considered to be thin (>0.3μm), motile protrusions with cytoskeletons comprised of parallel filaments of F-actin (Matilla and Lappalainen, 2009). In terms of branches, in developing neurons these are more voluminous and less dynamic with cores consisting of parallel microtubule fibres and fewer F-actin structures. In many cases the interface between these structures is a veil-like lamellipodia structure at the leading edge, or growth cone, of the branch. These structures contain dense networks of F-actin which surround the splayed endings of the microtubules protruding from branch terminals.

In an effort to distinguish between these features within the pleural motoneurons I have used markers for both specific cytoskeletal components, expressed using OK371-GAL4. In accordance with the above descriptions, F-actin was revealed by Lifeact::Ruby. Lifeact::Ruby was found to be enriched in filopodia and at branch tips, but at lower levels in the branches themselves (Fig. 6A). Time-lapse sequences of this reporter show a clear retrograde flow of actin (data not shown). Alongside this I labelled microtubules with the plus end marker *CLIP170*::GFP (Stramer *et al.*, 2010). A strong expression of *CLIP170*::GFP decorates all microtubules. These were found to occupy branches but were entirely excluded from the filopodia. As such the branches have a blunt-ended appearance (Fig. 6B).

Using this labelling of the cytoskeleton and the accepted morphological definitions, this has provided a systematic means of feature classification. The caveat however is that 'in reality' these are very dynamic structures and constant changes, for example the invasion of maturing filopodia by microtubule filaments, produces more of a continuum of feature types. Every effort has been made to be consistent in the analysis using this classification.

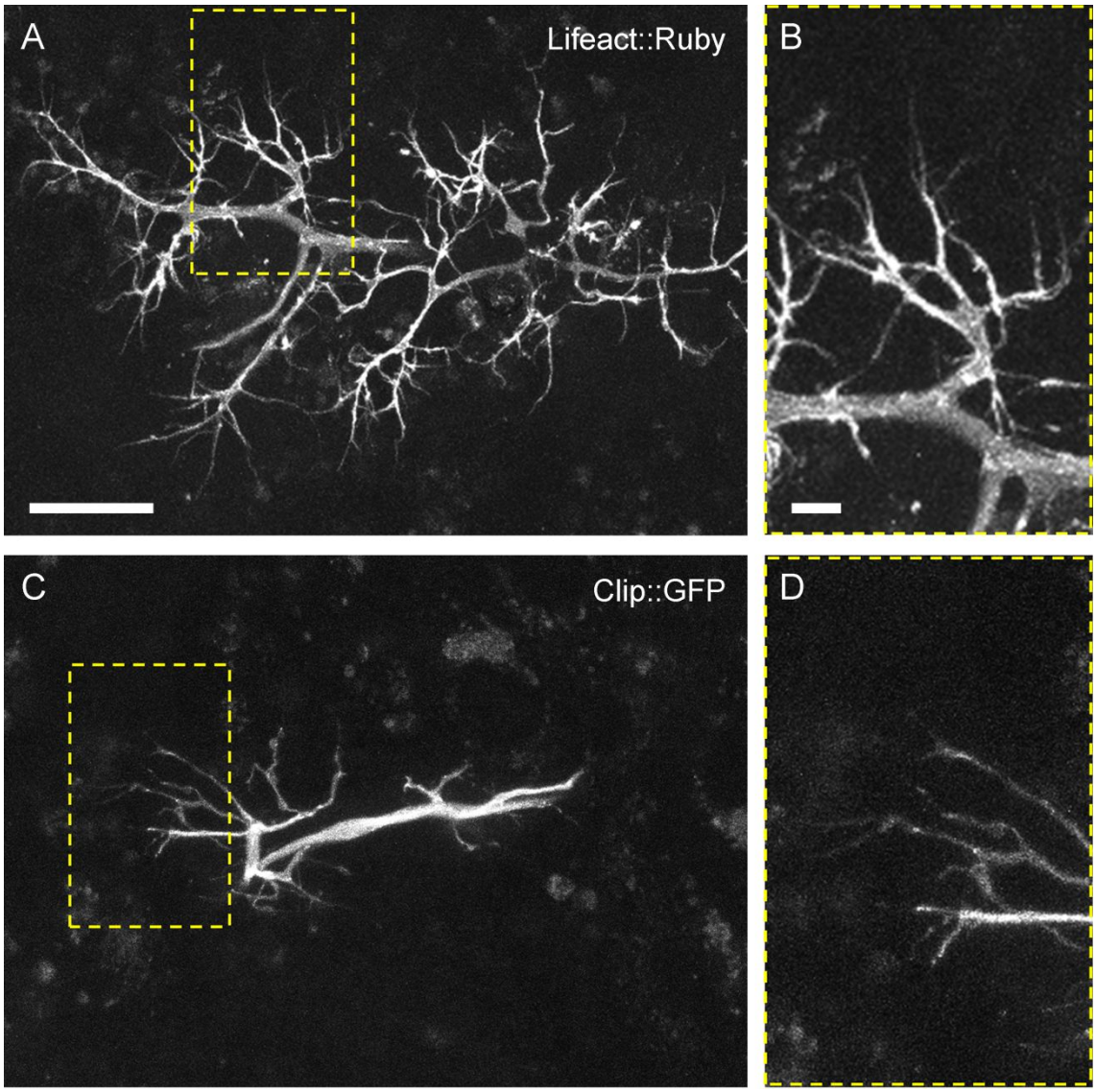

Figure 6. Cytoskeletal markers distinguish early arbor features (A) A pair of arborisations at 35h APF expressing Lifeact::Ruby under the control of OK371-GAL4 **(B)** A cutaway reveals the enrichment of actin in filopodia **(C)** A pair of arborisations at 30h APF expressing *Clip170*::GFP under the control of OK371-GAL4 **(D)** A cutaway reveals the presence of tubulin in branches but not in filopodia. Scale bar: 25μm (A&C) 10μm (B&D).

The development of the synaptic partners is concurrent

The observations of early filopodia dynamics raised intriguing questions concerning their role in arbor construction. Based on their behavior an appealing idea was that they drive growth via interactions with the postsynaptic muscle cells.

To explore the developmental of both pre- and postsynaptic partners I generated a set of reagents that allowed me to visualise and manipulate these cell types using independent binary expression systems. A comprehensive set of studies using fixed material revealed how the adult abdominal muscles of *Drosophila* are generated from a population of persistent *twist* expressing, mesodermal cells, associated with the peripheral nerves of the larva (Bate *et al.* 1991, Currie and Bate 1991). These imaginal muscle precursors originate from a single, embryonically born cell in each hemisegment which, over the course of larval life, divides to produce 6 small sets of myoblasts (8-15 cells). At the onset of pupariation these units resume proliferation and by 13h APF begin migrating outwards along the nerves to meet the motoneuron growth cones at around 20h APF. Using live imaging I set about describing the development of these tissues. By 26h APF, fusion of the myoblasts has produced sets of immature myotubes in each hemisegment which are aligned with a dorsoventral polarity (Fig. 7A). These are supplied with fusion competent cells from a mass of proliferating progenitors at the centre of each muscle cluster (Fig. 7B). Interestingly, like the axon terminals at this stage, these nascent myotubes are festooned with exploratory, filopodia-like protrusions, hereon termed myopodia (Ritzenthaler and Chiba, 2002).

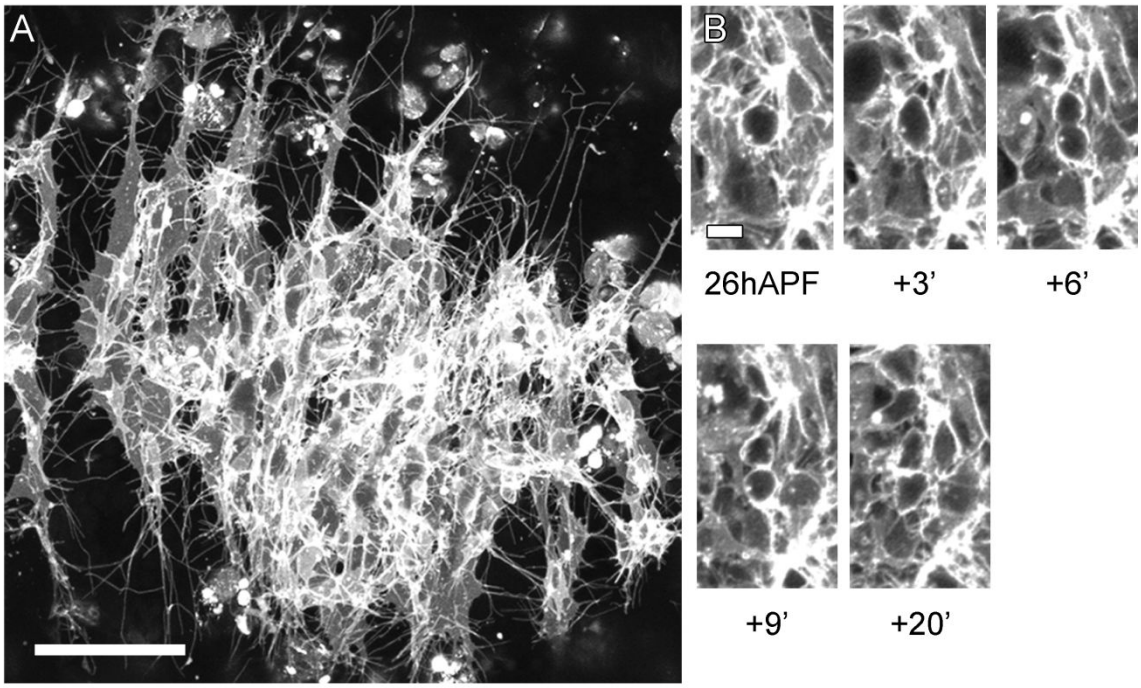

Figure 7. The development of the pleural muscles is concurrent with axon arbor growth (A) The developing pleural muscles within a hemisegment at 26h APF. Myopodia sprout from the newly established myotubes **(B)** Centered upon this mass of cells a time series captures the division of a myoblast. Muscles are expressing myr::GFP under the control of *Mef2*-GAL4. Scale bars: 50μm (A) 5μm (B).

Using independent GAL4/UAS and LexA/LexAop binary expression allowed the developing muscles and motoneurons to be visualised in spectrally distinct channels. This revealed that at 30h APF the axons are embedded within the dense cluster of myoblasts, for which they act as a scaffold. The terminal branches and filopodia however radiate outwards to make contact with the developing myotubes (Fig. 8).

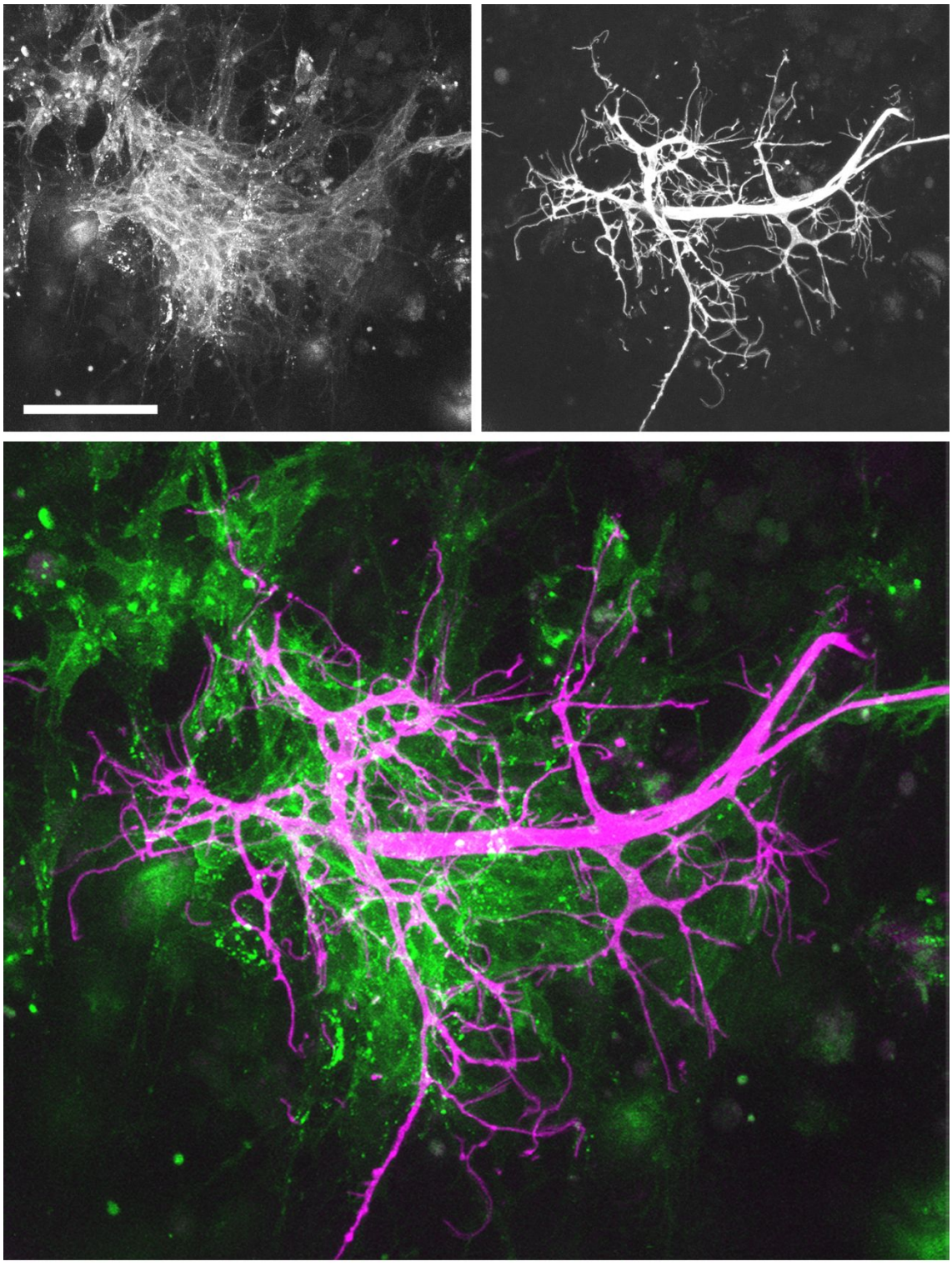

Figure 8. Independent binary expression systems reveal the intimate development of the pleural synaptic partners. Imaging of the muscles and motoneurons in separate channels demonstrates the close development of these cells at 30h APF. Motoneurons: *VGlut*-LexA>myr::GFP; muscles: *Mef2*-GAL4>mtdTomato. Scale bar: 50μm.

Although dual channel imaging allowed the best means of resolution for distinguishing between cell types, single channel imaging proved better for capturing dynamic interactions. To achieve this, cytoplasmic GFP was expressed simultaneously in the muscles, using the muscle specific driver *Mef2*-GAL4, and in the motoneurons using the glutamatergic neuron specific driver OK371-GAL4 (Fig. 9). The colour rendering of motoneuron branches at 31h APF emphasises the intimate relationship between these partners at this early stage of development (Fig. 9A). The proximal axon segments, closest to the nerve, are enveloped by a cluster of myoblasts. At the other extreme, the distal branches and filopodia extend outwards making contacts with multinucleate myotubes that clearly separated from each other.

Tracking the growth of a branch terminal over 2 hours reveals the dynamics of the interactions between these cells (Fig. 9B). Indicated by the yellow arrow, at time 0 the branch terminates with a contact onto a myotube. From this point, exploratory filopodia are generated. By 40 minutes one of these has spanned the gap to make contact with the next posterior myotube. This contact is consolidated and the filopodia matures, becoming an extension of the branch which bridges between the myotubes. From this new branch segment, more filopodia extend and the cycle of exploration and stabilisation begins again. By 120 minutes' iterations of these processes have extended the branch once more and produced a new branch point. From watching such footage, it is possible to see tension building up between two partners that are touching.

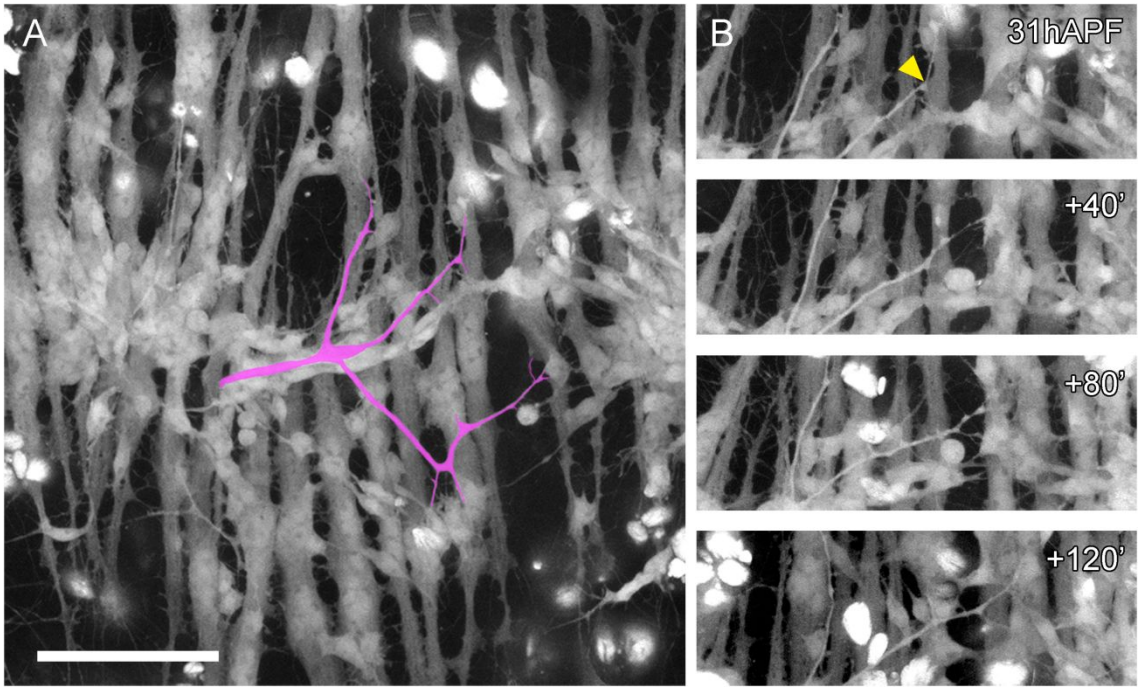

Figure 9. Single channel imaging captures dynamic interactions between the growing pleural muscles and motoneuron axons (A) The muscles and motoneurons in a hemisegment at 31h APF expressing cytoplasmic GFP under the control of OK371-GAL4 and *Mef2*-GAL4. A segment of the more posterior motoneuron axon is false coloured in magenta **(B)** A time series with 40 minute intervals focusing on a portion of this segment captures interactions between the synaptic partners. The bright, round objects are phagocytes which have engulfed GFP expressing larval tissues. Scale bar: 70μm.

Pleural motoneuron growth is plastic

As described earlier, the pleural motoneurons exhibit a degree of variation in their morphology and do not exhibit rigid one-to-one connectivity patterns seen in the larval neuromuscular system. These observations of dynamic early growth strongly suggest that morphology is an emergent product of self-organising interactions between the different components in the system. If this were correct two predictions should be true: Firstly, were a neuron bestowed an increased capacity for growth that the resultant arborisation would occupy a larger territory than normal. Secondly, that in the event of an increase in the size of the postsynaptic field available for the axonal arborisation to grow in that would respond to occupy the newly available space/resource.

To test the first prediction, I employed a 'flip out' strategy to generate mosaics with individual pleural motoneurons expressing *DP110*, the active subunit of phosphoinositide 3-kinase. The motoneurons were also labelled with GFP to mark the clones. DP110 is a signal transducer downstream of the insulin-like receptor in the mTor pathway. The overexpression of this protein has been shown to bring about increases in cell size (Leevers *et al.*, 1996, Brierley *et al.* 2009). I found that overexpressing *DP110* in single motoneurons from late larval or pre-pupal stages generated strikingly larger arborisations compared than their wild type equivalents (Fig. 10B&D). Some examples of these clones generated arborisations wide enough to cover 3 segments along the with anteroposterior axis. Such extensive coverage is never observed for wild type arborisations (Figs. 10A&C).

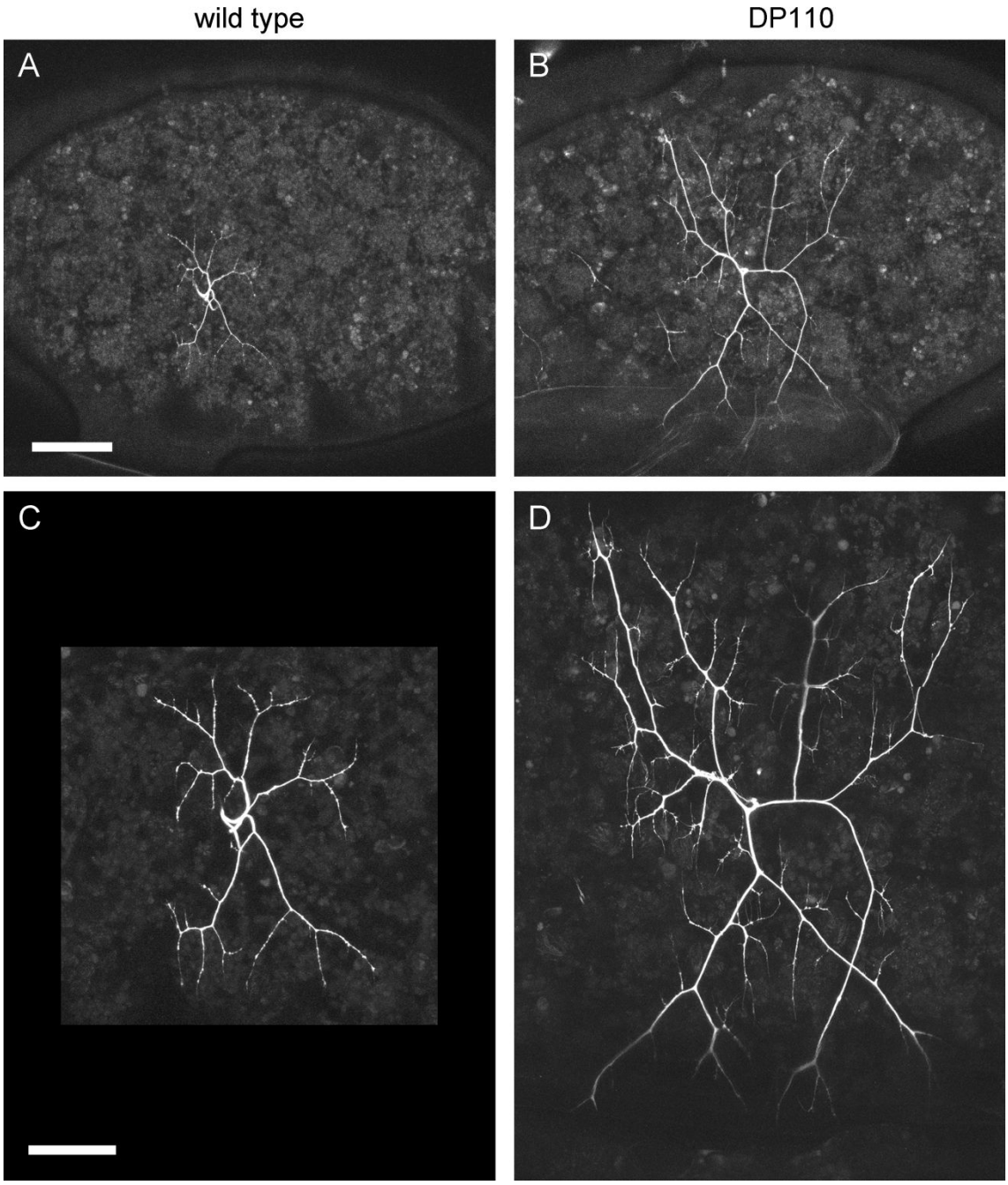

Figure 10. *DP110* expressing motoneuron clones occupy far larger territories than their wild type equivalents (A&B) Lateral views of abdominal flanks at approximately 55h APF containing single motoneuron clones expressing cytoplasmic GFP (left) or cytoplasmic GFP and *DP110*::CaaX (right) **(C&D)** Images taken at a higher magnification provide more detailed images of these cells. Scale bars: 150μm (A&B) 50μm (C&D).

To test the second prediction, the arborisations of one hemisegment were removed at an early stage in development by ablating the lateral branch of the nerve at 27h APF. This in effect generated an additional hemisegment of unoccupied

postsynaptic territory. The developing arborisations in the next anterior segment were then recorded for the following 8.5h (Fig. 11A). Soon after axotomy the ablated arborisations showed features of degeneration including membrane blebbing/swelling, branch retraction, followed by the engulfment of fragments by macrophages. As the next anterior arborisations elaborated, branches that were growing in a posterior direction continued to grow far beyond their normal range to invade the territory that the axotomy had freed up. By 8.5 hours post-axotomy the ablated cells had fully degenerated, but for 3 small branches stemming from the nerve. The 'cleared territory' was completely occupied by invasive branches from the anterior neighbors, as well as by branches originating from a ventral position, likely belonging to one of the motoneurons that normally innervate the ventral longitudinal muscles. For comparison, the growth of a pair of arborisations over the same duration in an uninjured control is presented in shown in Fig. 11B. These terminals did not grow in an asymmetric manner, instead elaborating radially within their segmental domain. This is emphasised by the registration of equivalent neurons from each experiment by their positions relative to the nerve (Fig. 11C). A possible explanation for the lack of invasive branches from the posterior segment is the slight development delay of the pleural arborisations from anterior to posterior, giving the more anterior segment an additional advantage in growth.

Imaging arbor growth following axotomy demanded a complex procedure involving the use of both a 2-photon confocal microscope for cutting, and a laser scanning confocal microscope for long term imaging. Adding to this, variation in the thermodynamics of laser energy transfer between samples meant that successful ablations with acceptable degrees of collateral damage to the surrounding tissue were relatively rare and many samples were unusable. As a result, the sample size was low (n=1). Although the effects of the ablation were striking and spoke strongly to the idea

of tropic growth, a repeat of this experiment would be desirable in order to strengthen any conclusions.

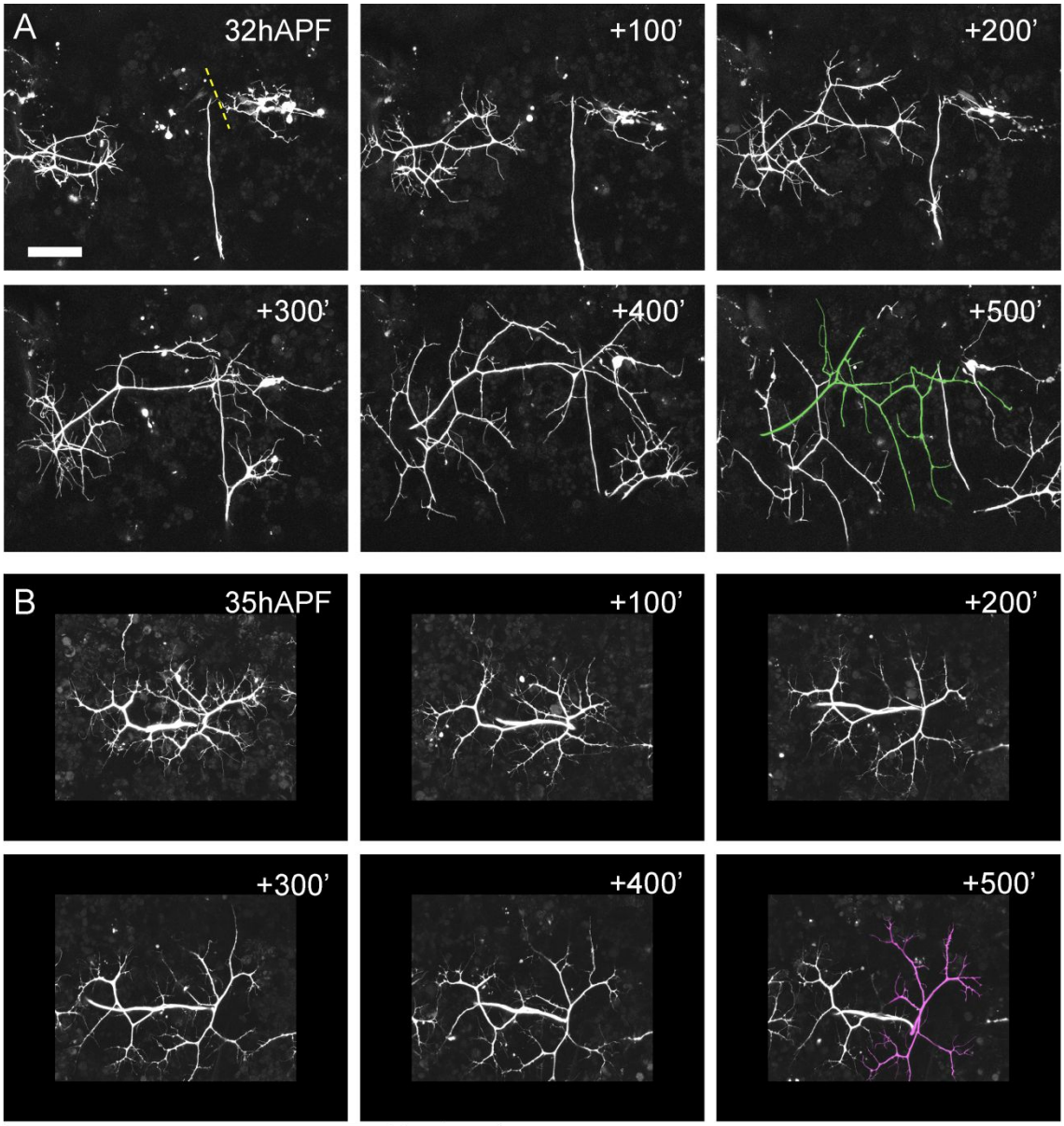

Figure 11. Axotomy demonstrates the plasticity of axon arbor growth (A) Beginning at 32h APF, a time series with 100 minute intervals shows the growth of a pair of arborisations following ablation of the arborisations in the next posterior segment. A dashed yellow line indicates the ROI of the 2-photon laser used to perform the cut **(B)** An equivalent time series shows the growth of a pair of arborisations in an undamaged pupa from 35h APF **(C)** In the final frame of each movie the most posterior of the pair of arborisations is false coloured

in magenta. Registration of these by their entry points to the nerve reveals the asymmetric growth of the arborisations in the ablation experiment. Motoneurons are expressing cytoplasmic GFP under the control of OK371-GAL4. Scale bar: 50μm.

The arrival of presynaptic machineries and their localisation within developing arborisations

Live imaging of axonal and dendritic arborisations in the brains of fish and frogs shows a robust correlation between the localisation of synaptic proteins and arbor construction from very early in development (Alsina *et al.*, 2001; Niell *et al.*, 2004; Javaherian and Cline, 2005; Meyer and Smith, 2006). As seen with these systems used in these studies, I have just shown that the axonal arborisations of the pleural motoneurons grow synchronously with their postsynaptic partners. With this in mind I wanted to know the localisation of synaptic proteins during the growth of these motoneuron arborisations.

To observe the location of presynaptic machineries I chose to express a RFP tagged version of Bruchpilot (BRP) along with membrane localised myr::GFP using OK371-GAL4. BRP is an ELKS/CAST family protein which plays an important role in the organisation and function of the active zone cytomatrix (CAZ), principally clustering voltage-gated Ca^{2+} channels and tethering synaptic vesicles close to the synaptic membrane (Kittel *et al.*, 2006; Wagh *et al.*, 2006; Fouquet *et al.*, 2009; Matkovic *et al.*, 2013). In both vertebrates and invertebrates active zone components such as BRP have been demonstrated to arrive at the presynapse as pre-packaged units contained within specialised dense-core vesicles, often termed Piccolo-Bassoon transport vesicles (PTVs) in reference to the vertebrate AZ proteins (Shapira *et al.*, 2003). I found BRP::RFP to be trafficked within the axons as discrete puncta. These puncta seem to rapidly shuttle between nodes, where they often remain stable (Fig. 12B). From the

very earliest stages of arbor growth large numbers of BRP::RFP puncta become concentrated in the axon terminals. Interestingly the majority of these puncta localise at branch points and the bases of filopodia (Fig. 12A). Quantification reveals that in axon terminals between 30h and 35h APF 85% (±6.4% S.D, n=5) of all puncta are localised to branch points/the bases of filopodia, and 82% (±4.65% S.D, n=5) of branch points/the bases of filopodia host a punctum (Fig. 12C).

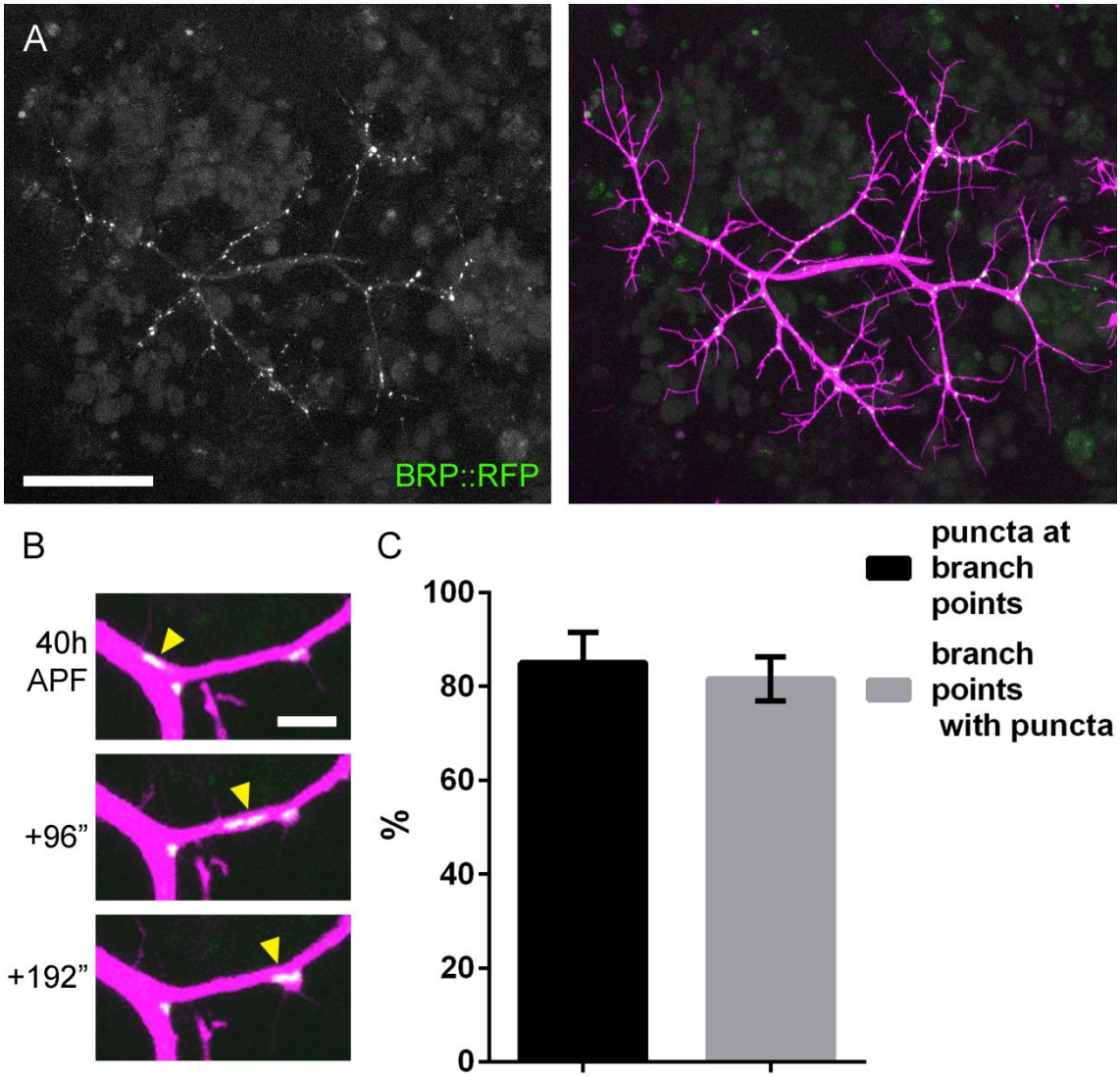

Figure 12. The arrival of Bruchpilot at the pleural axon terminals (A) UAS-*BRP*::RFP expressed under the control of OK371-GAL4 in a pair of axonal arborisation at 35h APF. Co-expression of myr::GFP (magenta) reveals BRP::RFP puncta to be localised almost exclusively to branch points and the bases of filopodia **(B)** A time series at 40h APF demonstrates the shuttling of a BRP::RFP punctum between branch points where it is stabilised. **(C)** The distribution of BRP::RFP puncta in arborisations between 30h and 35h APF. Error bars are standard deviation. Scale bars: 50μm (A) 5μm (B).

Arbor growth and BRP punctum formation is tightly coupled

To visualise the dynamics of presynaptic puncta in the pleural motoneurons, time-lapse movies of *BRP*::RFP expressing arborisations were taken at 2 minute intervals. A time series of a growing branch at 30h APF reveals the typical relationship between branch extension and BRP::RFP puncta formation (Fig. 13). At the beginning of the sequence a branch terminal has a forked end bearing two growth cone-like projections; the thicker of which contains a stable BRP::RFP punctum. While the punctum containing projection retracts within the following 19 minutes, the other matures; thickening to become part of the branch and recruiting a punctum of its own. This new node acts as a point of growth for additional exploratory filopodia. By 87 minutes one of these filopodia has stabilised and matured, producing a new growth cone-like structure from which the sequence begins again. Iterations of this process deposit a string of stable BRP containing nodes in the wake of the leading edge of the branch with the appearance of bolts anchoring the arborisation to its substrate.

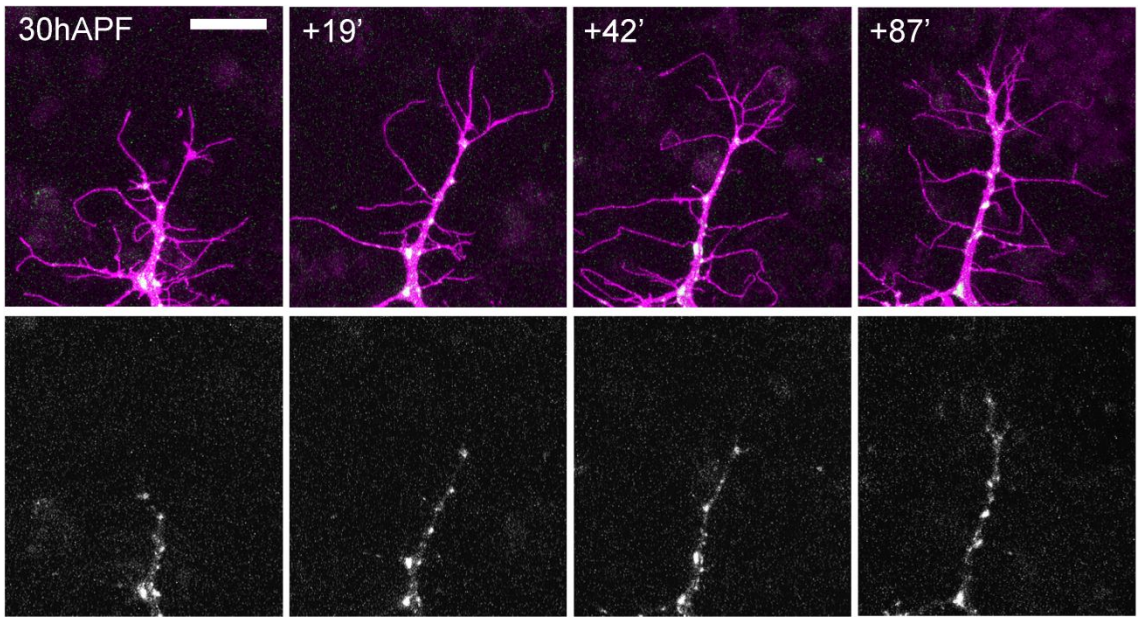

Figure 13. BRP puncta form in the wake of growing branches. A time series lasting 87 minutes shows the elongation of a branch segment expressing myr::GFP and *BRP*::RFP under OK371-GAL4 control. Stable BRP::RFP puncta are deposited in a row behind the extending growth cone. Images are rotated anti-clockwise making dorsal left. Scale bar: 20μm.

Many of the punctum-containing nodes deposited behind extending growth cones continue to act as sites of filopodia emergence. A sequence focused on a branch segment at 32h APF demonstrates how filopodia at these sites can be the precursors to new branches (Fig. 14). At time 0 a filopodium projects from a position marked by a small BRP::RFP punctum. 16 minutes later this protrusion has matured into a growth cone which bears an array of filopodia. By 49 minutes the base of this growth cone has widened, forming the foundation of a branch point, and a BRP::RFP punctum has been recruited to its tip. As in the preceding sequence, successive iterations of filopodia extension and stabilisation generate a new branch segment studded with BRP::RFP puncta.

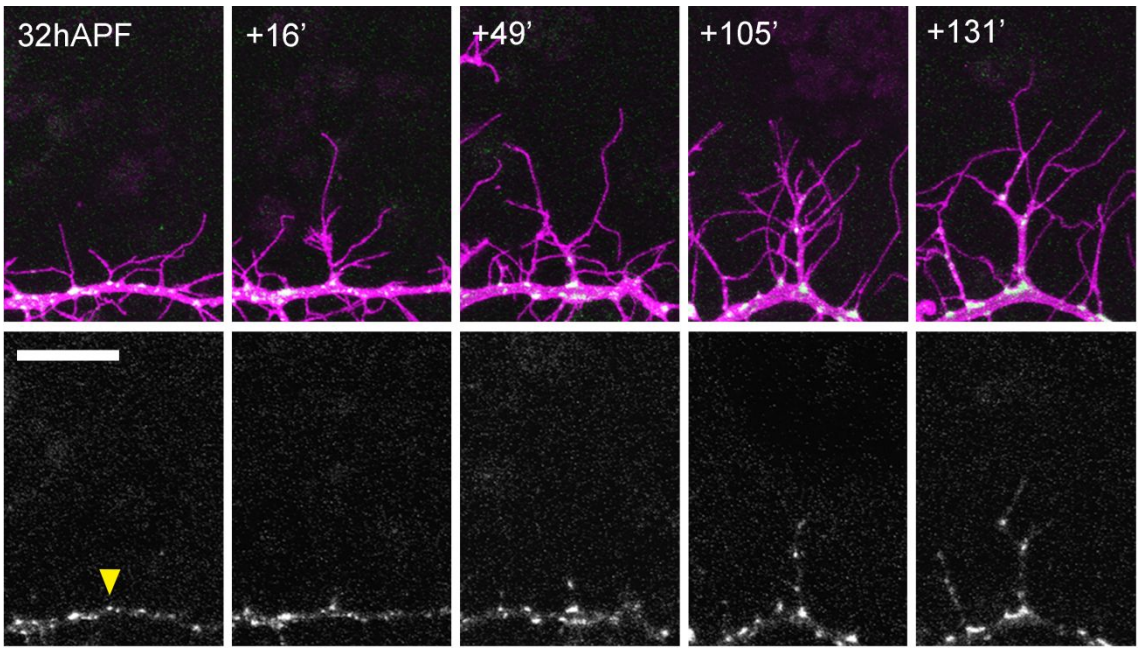

Figure 14. New branches develop from filopodia at nodes marked by BRP::RFP puncta. A time series lasting 131 minutes shows the maturation of a filopodia, indicated by the yellow arrow, into a branch. Subsequent rounds of filopodia extension and stabilisation produce a new segment studded with BRP::RFP puncta. Motoneurons expressing myr::GFP and *BRP*::RFP under the control of OK371-GAL4. Scale bar: 20μm.

BRP puncta are correlated with filopodia growth and survival

The stabilisation of filopodia on growing zebrafish retinal ganglion cell axons was correlated with the formation and stabilisation of accumulations of a GFP labelled synaptic vesicle associated protein, Synaptophysin (Syp), at their tips. In the present system however, BRP::RFP puncta were rarely observed to enter filopodia and never to stabilise at their tips. As a result, no such relationship was found. However, an interesting relationship emerged demonstrating the preferential emergence of filopodia from sites marked with stable BRP::RFP puncta. High frequency time-lapse imaging revealed that many filopodia emerge from existing BRP::RFP puncta or else recruit a punctum soon after their formation (Fig. 15A). Furthermore, the few filopodia which were not seen to recruit a BRP::RFP punctum rapidly collapsed (Fig. 15B). An analysis of 83 filopodium generation events from 3 time-lapse movies of arborisations between 30h and 33h APF found that 36.0% (± 12.6% S.D) of filopodia emerge from existing BRP puncta and a further 48.1% (± 10.7% S.D) recruit a punctum within 20 minutes of their formation (Fig. 15C). The remaining 16.0% (± 11.9% S.D) of filopodia failed to recruit a punctum altogether. As was initially observed, this suggests that filopodia grow preferentially from sites also occupied by presynaptic machineries. In addition, the observations suggested that filopodia survival is correlated with existence of puncta at their bases. To evaluate this possibility, I compared the survival times of newly generated filopodia with and without puncta at their bases. As predicted, filopodia which did not emerge from a punctum, or recruit a punctum following their formation, were always eliminated within 20 minutes of their emergence (Fig. 15D). On the other hand, although almost 60% of filopodia which did recruit puncta were also eliminated within 20 minutes, 33.3% survived between 20 and 60 minutes and a further 12.5% persisted for over an hour (measured from 24 filopodia with puncta, and 24 filopodia without puncta from 3 time-lapse movies of arborisations between 30h and 33h APF).

Statistical analysis showed that the lifetime of filopodia which are associated with BRP::RFP puncta at their bases (21.7 ± 20.3 minutes S.D., n = 24) is significantly longer than those which fail to recruit puncta (3.8 ± 2.8 minutes S.D., n = 24) (Mann-Whitney U = 73.0, $p < 0.0001$, two-tailed). This suggests that only filopodia which are associated with puncta at their bases go on to develop into permanent branches.

It should be noted that this analysis was to some degree limited by two issues. Firstly, as demonstrated, a small fraction of filopodia are stabilised and develop into branches. In the instances where this occurred, the resultant branch continued to be considered as the filopodium. Secondly, at the leading edges of branches the extreme density of filopodia made tracking individuals extremely difficult, particularly given their propensity to 'merge' with one another. For this reason, I was limited to measuring filopodia stemming from more sparsely populated regions, such as less crowded growth cones, branch nodes and along the lengths of branches. Although this obviously poses a bias, many observations of densely populated branch tips, which invariably contain stable BRP puncta, suggest that the situation in the case of these is no different.

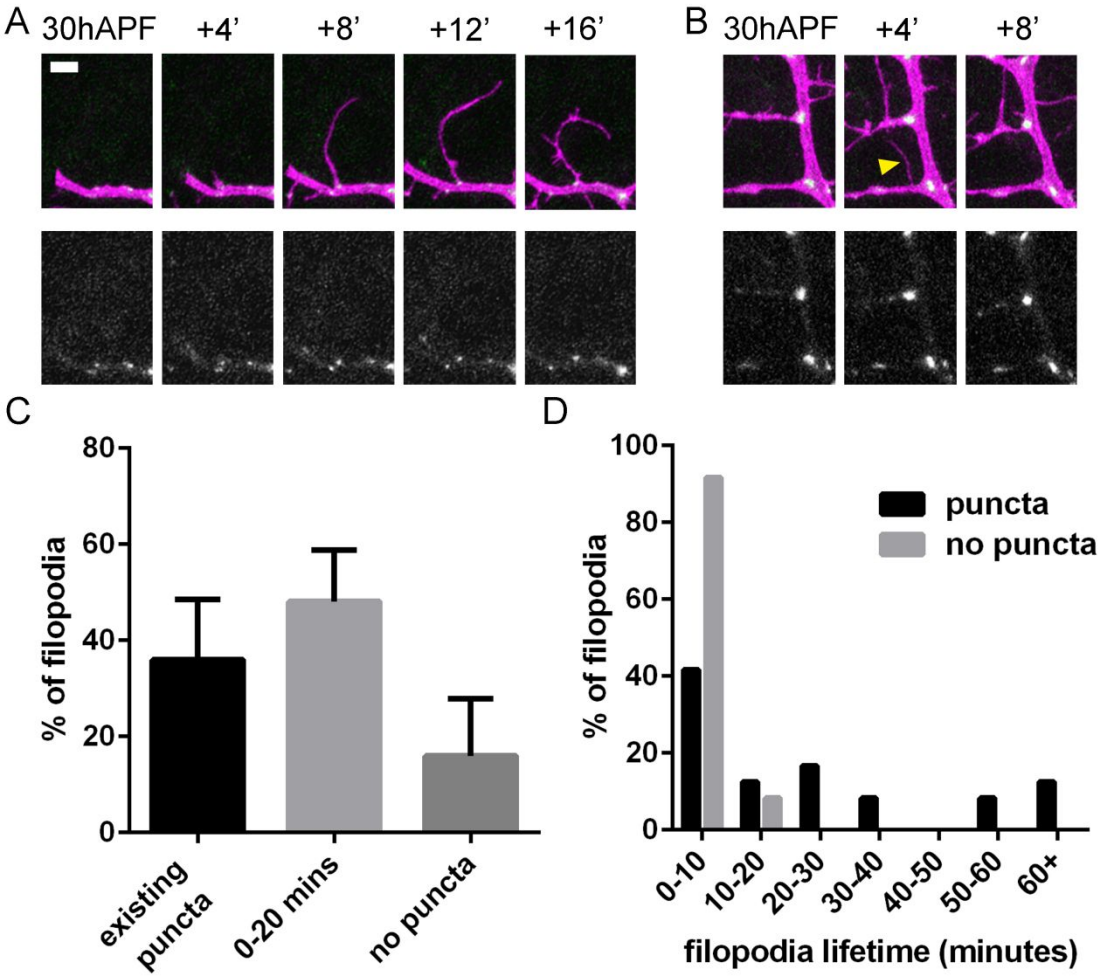

Figure 15. BRP puncta are correlated with filopodia growth and survival (A&B) Time series with 4 minute intervals showing filopodia formation on myr::GFP and *BRP*::RFP expressing arborisations at 30h APF. (A) A filopodia projects from an existing BRP::RFP punctum and continues growing for the remainder of the sequence. (B) Indicated by a yellow arrow, a filopodium emerges from a location which is not marked by a BRP punctum and is eliminated within 4 minutes **(C)** The proportions of filopodia that (i) are born from an existing punctum, (ii) recruit a punctum within 20 minutes and (iii) do not recruit a punctum *et al*. Error bars are standard deviation **(D** The lifetimes of filopodia recorded from their emergence shown in a histogram with 20 minute bins. Scale bar: 5*μ*m.

Global changes in BRP distribution through arbor development

The distribution of presynaptic puncta during early arbor development is strongly suggestive of a role for synapse assembly in growth and branching. To explore if this distribution changes over the course of development, *BRP*::RFP expressing arborisations were imaged at 12h intervals from 34h to 58h APF (Fig. 16A). As already established, at 36h APF, the apex of elaborative arbor growth, puncta are located

almost exclusively at branch points and at the bases of filopodia. By 46h APF, during the latter period of dynamic growth, BRP::RFP puncta are still found at the vast majority of branch points. At this stage however, a number of puncta are also found along the lengths of branches at inter-nodal positions. By 58h APF, strings of BRP::RFP puncta line all but the most proximal branches, including at branch points. In addition to this change in distribution, BRP::RFP puncta also appeared to become smaller and more homogenously sized over the course of development.

To complement the analysis of BRP::RFP puncta distribution at the early stages of growth, distributions were measured in 5 mature arborisations aged from 72h to 77h APF. At this stage, just 12.6% (±5.8% S.D) of the total puncta were found to reside at branch points, the rest being distributed along branch lengths. However, the clear majority, 89.4% (±6.7% S.D), of branch nodes were still found to host puncta (Fig. 16B). This demonstrates that although BRP puncta at branch points are relatively permanent, the overall pattern of BRP distribution shifts dramatically during the latter stages of arbor development.

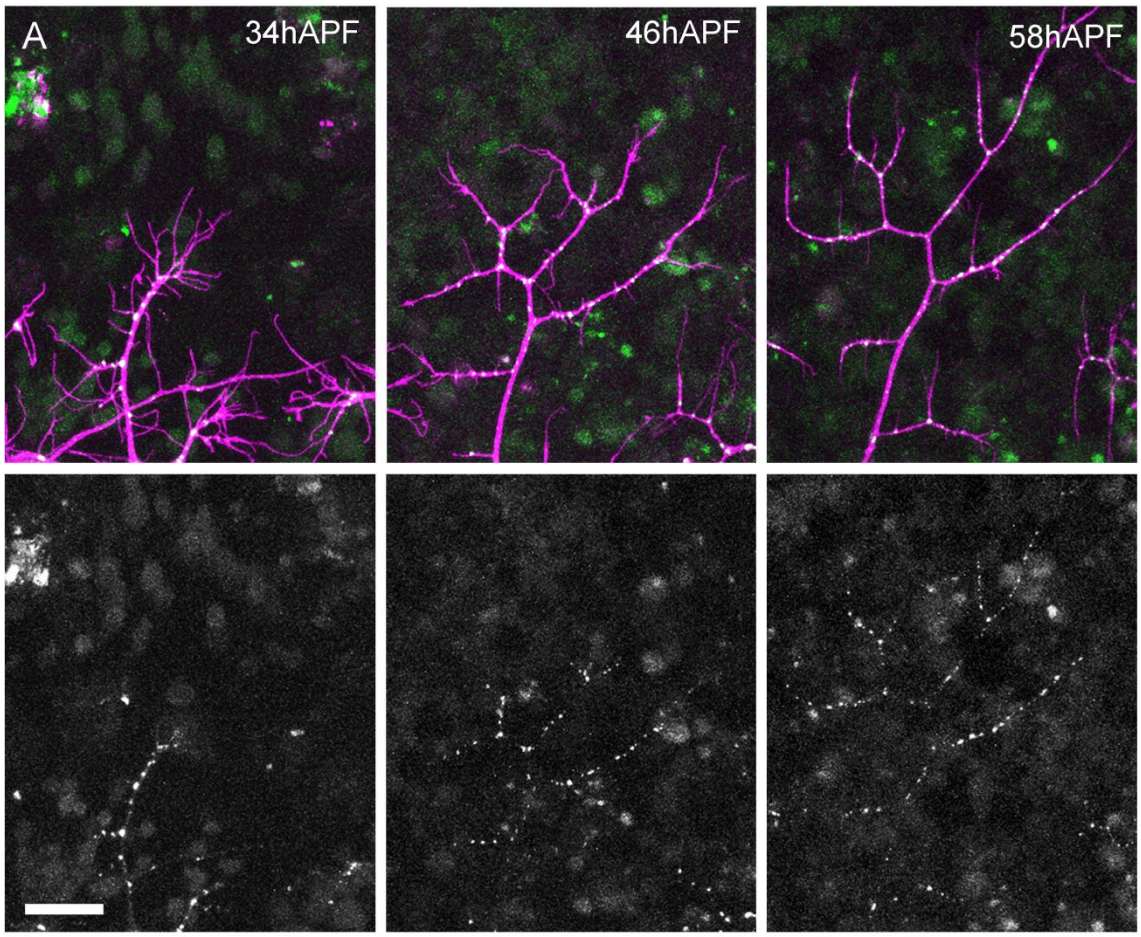

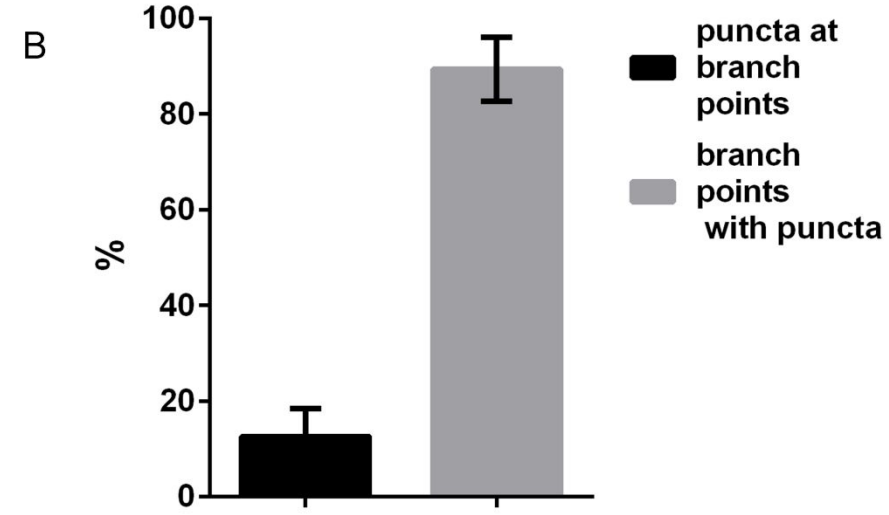

Figure 16. BRP distribution changes throughout development, but puncta at nodes persist (A) An arbor segment expressing myr::GFP and *BRP*::RFP under the control of OK371-GAL4 at 34h, 46h and 58h APF. The distribution of BRP::RFP puncta shifts between these times from being almost exclusively at branch points to lining the lengths of branches **(B)** The distribution of BRP::RFP puncta in arborisations between 72h and 77h APF. Error bars are standard deviation. Scale bar: 25μm.

Colocalisation of active zone components and synaptic vesicle proteins reveals different subcellular domains

Like CAZ components, synaptic vesicle (SV) associated proteins have been shown to arrive at presynaptic terminals in dedicated packages known as synaptic vesicle protein transport vesicles (STVs) (Zhai *et al.*, 2001). To observe how these apparently independently trafficked classes of proteins are organised at the pleural axon terminals, *BRP*::RFP was co-expressed with a GFP labelled variant of the SV associated protein *Synaptotagmin1* (*Syt1*) under the control of OK371-GAL4. Syt1 is a Ca^{2+} sensitive protein which embeds within SV membranes and is believed to coordinate synchronised SV fusion in response to Ca^{2+} influx via interactions with the SNARE machinery (Südhof, 2013).

Like BRP::RFP, Syt1::GFP is found concentrated in the terminals of the pleural motoneurons axons at 30h APF (Fig. 17A). Compared to BRP::RFP however, Syt1::GFP forms aggregations that cover a larger area and are more diffuse. Despite this it is clear that SV components are localised to nodes where they coincide with and overlap the smaller BRP::RFP puncta. As with BRP::RFP, at this early stage Syt1::GFP is almost completely absent from inter-nodal positions. At 70h APF the strings of BRP::RFP puncta which line the branches of the arborisations are again all coincident with Syt1::GFP aggregations (Fig. 17B). However, at this stage these aggregations are far more punctate, overlapping only marginally with those of BRP::RFP.

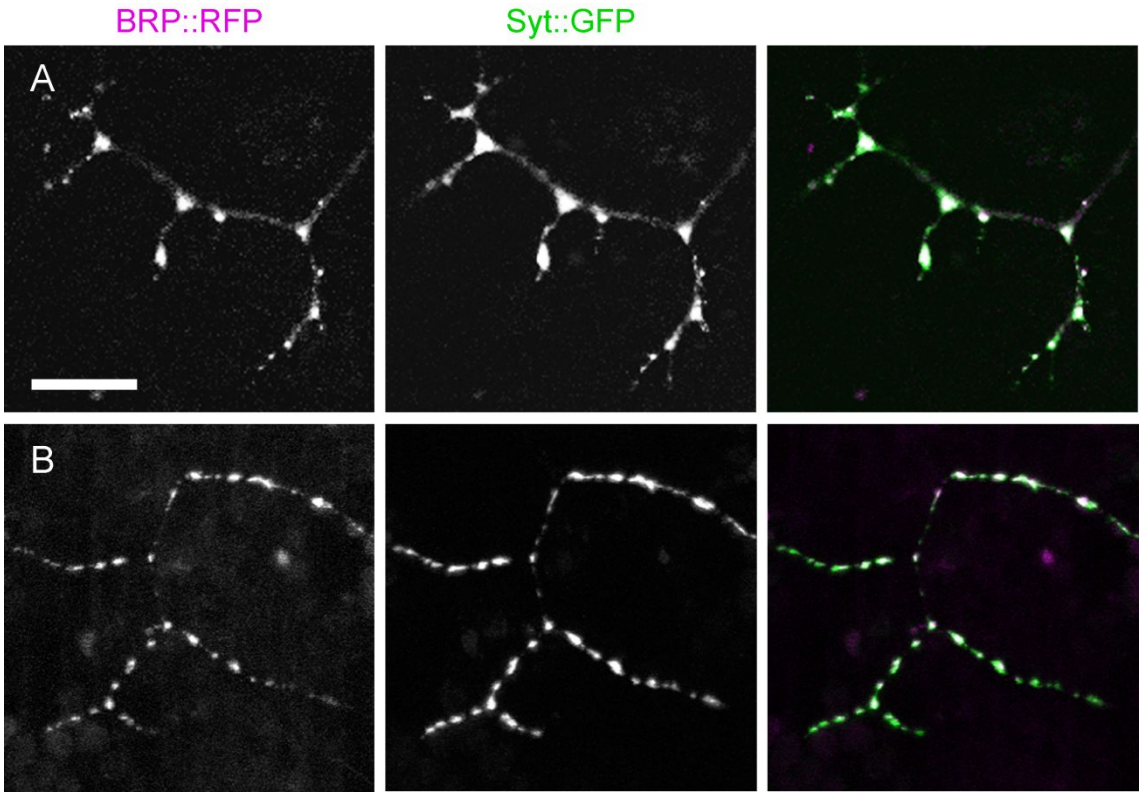

Figure 17. Presynaptic machineries colocalise from early in development (A+B) Segments of arborisations at 30h APF (A) and 70h APF (B) expressing *BRP*::RFP and *Syt1*::GFP under the control of OK371-GAL4. At 30h APF Syt1 aggregations overlay BRP puncta at branch nodes. At 70h APF Syt1 and BRP puncta are coincident along the lengths of branches and at branch nodes.

Fluorescently labelled protein traps of native proteins confirm the distributions of presynaptic components

An important consideration which had to be taken into account is whether exogenously supplied synaptic components truly reflect the localisation of native proteins. As the fluorescently labelled markers I used in the previous experiments relied on artificially expressing presynaptic markers under the control of an exogenous GAL4/UAS binary system I needed to validate this. Often these concerns can be evaluated by immunohistochemical staining of fixed preparations. Unfortunately, the fragility of the developing pupal body wall made this option unviable until the later stages of arbor development, obviously long after the time we need to know about. As an alternative for visualising early native protein distributions I decided to use protein

trap lines in which endogenous proteins are fluorescently labelled. These tools are generated by the insertion of a synthetic GFP exon flanked by splice acceptor and splice donor sites into an intron between the coding exons of an endogenous gene. Since the GFP sequence in these elements are in the native protein under the control of the native cis-regulatory machine it provides a powerful tool to look at the timing and location of the expression of these proteins.

For this task, I used a *vesicular glutamate transported* (*VGlut*), a *Syt1*, and a *BRP* protein trap. These were imaged concurrently with membrane targeted mCD8::Cherry expressed under OK371-GAL4 control. To assess early distribution imaging was performed between 30h and 33h APF (Fig. 18). The distribution of the synaptic vesicle associated proteins, VGlut and Syt1, were indistinguishable from the distribution of overexpressed UAS-*Syt1*::GFP; both had diffuse rather than punctate aggregations which were concentrated at branch points and the bases of filopodia and typically absent from along the lengths of branches. Likewise, as with its UAS counterpart, BRP had a punctate distribution at branch points and the bases of filopodia, although these accumulations did appear marginally smaller in diameter.

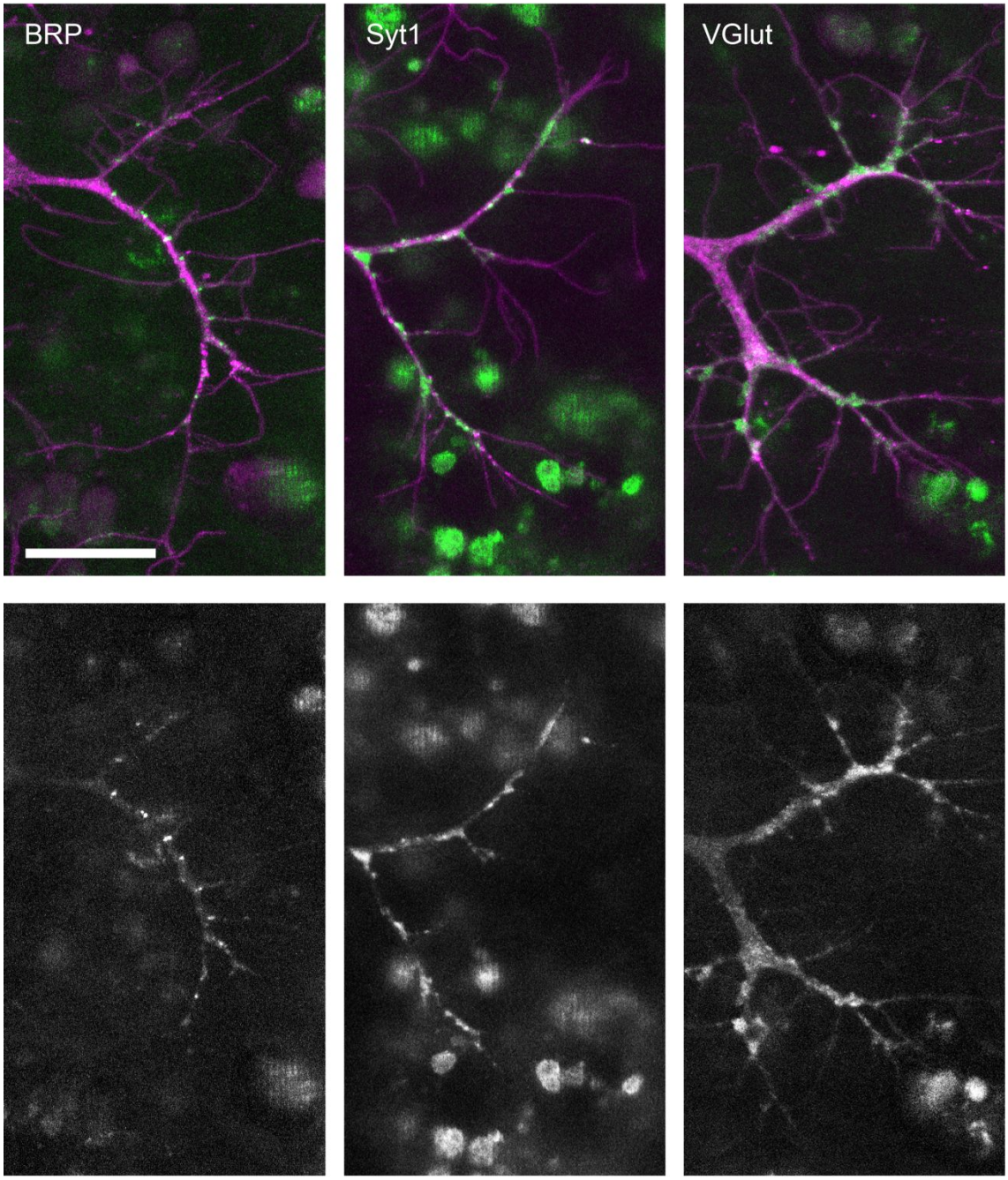

Figure 18. Protein trap lines verify the early subcellular distribution of presynaptic components. Native GFP tagged presynaptic proteins in axon terminals expressing mCD8::Cherry (magenta) under the control of OK371-GAL4. Like the UAS variant, endogenous BRP forms puncta which are localised to branch points and the bases of filopodia. This image is rotated clockwise making dorsal right. The endogenous versions of synaptic vesicle associated proteins VGlut and Syt1 also localise to these sites but in larger and more diffuse aggregations than BRP, as was seen with UAS-Syt1::GFP. Scale bar: 20μm.

2.3 Discussion

A new model for complex arbor growth in Drosophila

Drosophila has lacked for a system in which to explore the construction of complex, synapse-forming arborisations live and *in vivo*. To address this shortcoming, I have pioneered a novel system in which the growth of a population of elaborate axonal arborisations and their synaptic partners can be time-lapse imaged *in vivo* for the duration of their development. With the advantage of the unparalleled genetic tools available to *Drosophila* this innovation has allowed me to dissect the cellular and molecular mechanisms underlying the construction of such structures in more depth than has ever before been possible.

Drosophila nervous system development, like other invertebrate systems studied, has been considered relatively hard-wired; from the stereotyped proliferation of identifiable neuronal stem cells and the lineages they generate, to the predictable connectivity patterns of synaptic partners in both the central and peripheral nervous systems (Belote and Baker, 1987; Bate, 1976b; Jefferis *et al.*, 2001; Hiesinger *et al.*, 2006; Karuppudurai *et al.*, 2014). Nowhere is this more apparent than at the larval neuromuscular junction, where motoneuron axons plug in to segmentally repeated arrays of target muscles in a highly specific molecularly determined manner (Sink and Whittington, 1991; Chiba *et al.*, 1993).

Using time-lapse imaging with high temporal resolutions I have shown that, unlike the larval motoneurons, the pleural motoneurons of the pupa construct complex axonal arborisations with variable patterns of innervation and branching in a process with close parallels to the development of neurons in vertebrates. Like the growth of axonal and dendritic arborisations in vertebrate brains these axon terminals undergo an initial phase of exuberant, dynamic outgrowth involving a high turnover of exploratory

filopodia with lifetimes in the region of minutes (Dailey and Smith, 1996; Wu *et al.*, 1999). Growth and branching is achieved by the selective stabilisation of subsets of these predominantly transient filopodia; a process which was first described from observations of hippocampal cultures and has since been confirmed in vertebrate nervous systems *in vivo* (Cooper and Smith, 1992; Niell *et al.*, 2004; Meyer and Smith, 2006). What is more, like vertebrate arborisations, this elaborative phase was found to comprise a significant degree of remodelling involving the pruning of more substantial branches (Kaethner and Stuermer, 1992). Following arbor construction a period of refinement brings about the loss of filopodia, the cessation of branch dynamics and the formation of synaptic boutons along the lengths of axon branches; a process which is ostensibly analogous to the formation of presynaptic varicosities and postsynaptic spines on vertebrate axonal and dendritic arborisations which occurs during the latter stages of growth (Harris *et al.*, 1992). These resemblances are strongly suggestive that the pleural motoneuron axons follow a vertebrate-like mode of arbor construction driven by a local trial and error mechanism of exploration.

Growing axon branches are stabilised locally by interactions with the muscles

In vertebrate central nervous systems, the selective stabilisation of exploratory axonal and dendritic filopodia which is fundamental to arbor growth has been proven to depend on interactions between prospective synaptic partners (Cooper and Smith, 1992; Ziv and Smith, 1996; Jontes *et al.*, 2000). Concurrent imaging of the pleural muscles and motoneurons indicated that the same is true within this system. In contrast with the development of the larval neuromuscular junction, in which motoneuron axons contact sets of fully developed muscle fibres, the pleural motoneurons develop concurrently and in close association with their synaptic partners (Bate *et al.*, 1991). From the earliest stages of arbor growth the proximal axon

branches are intertwined with a mass of proliferating myoblasts while more distal branches and filopodia radiate outwards to make contacts with the extending myotubes. Time-lapse imaging of these partners during the period of arbor elaboration pointed to a close linkage between these interactions and constructive events whereby exploratory filopodia are generated from points of established contact and are stabilised by the consolidation of new contacts. Like growing vertebrate dendrites, the developing muscles were discovered to host dense populations of dynamic filopodia-like processes (myopodia). It is possible that these protrusions provide the stabilising substrate for axonal filopodia in much the same way as dendritic filopodia are thought to in vertebrate brains. This speculation is supported by previous findings showing that myopodia act as recognition sites for exploratory axonal growth cones during the innervation of the larval musculature (Ritzenthaler and Chiba, 2002; Kohsaka and Nose, 2009). Myopodia on which contacts are established were found to selectively mature into nascent postsynaptic sites, not unlike the way dendritic filopodia in vertebrates are believed to develop into stable synapse bearing dendritic spines (Fiala *et al.*, 1998; Kohsaka *et al.*, 2007).

Pleural MNs adjust to changes in their size and the available postsynaptic field

These observations of dynamic, interaction-driven growth suggest that rather than following rigid blueprints, arbor construction is an emergent property born from iterative rules of interaction played out during development at a local level. This would imply that a large component of arbor growth is determined by extrinsic interactions. To test this idea, motoneuron clones were conferred an increased capacity for growth by overexpression of *DP110*. Given this 'metabolic advantage' in size over their neighbouring homologous pleural motoneurons, and therefore a head start in growth, these cells built arborisations which occupied far larger postsynaptic territories than

usual. In addition to going further to demonstrate an absence of target-specific connectivity this suggests that arbor size is not defined by intrinsic limitations for growth. As an alternative test of to look at the plasticity of the system the size of the available postsynaptic field was manipulated by the denervation of a single abdominal hemisegment. In much the same way as was reported following the removal of dendrites from small regions of fish and rat retinas, neighbouring neurons generated larger and more asymmetric arborisations to exploit the vacant postsynaptic field (Perry and Linden, 1982; Hitchcock, 1989). In contrast with the experiment in which *DP110* was expressed, this axotomy demonstrates the morphological plasticity of wild type neurons and their capacity to respond to changes in the availability of substrate/synaptic partners. In addition, these data suggest that the extremes of arbor growth are limited by interactions between neighbouring arborisations. Conceivably this is achieved through repulsive cell-cell contacts mediated by cell-surface molecules, the kind of which are known to give rise to the tiling of arborisations in the visual and somatosensory systems of vertebrates and invertebrates (Wässle *et al*, 1981; Grueber *et al.*, 2002; Sagasti *et al.*, 2005; Millard *et al.*, 2007). Alternatively, such spatial organisations of arborisations have been shown to arise from activity based competition, as is the case for retinal ganglion cell axons in zebrafish (Hua *et al.*, 2005; Fredj *et al.* 2010), activity-independent competition, as appears to be sufficient to regulate the innervation of vertebrate muscles by single motoneuron axons (Costanzo *et al.*, 2000), or even via secreted cues such as those involved in axon guidance (McLaughlin and O'Leary, 2005; Kalil and Dent, 2014).

Arbor construction follows a synaptotropic-like mechanism of growth

One interpretation of these results is that arbor growth is directed preferentially into synaptogenic regions via a tropic mechanism. This would follow the prediction of

Vaughn and colleagues who forwarded the idea that synapse formation directs arbor growth by selectively stabilising branches in a process they dubbed synaptotropic growth (1974, 1988 and 1989). Since the conception of this hypothesis from observations of fixed tissue, live imaging of fluorescently tagged synaptic proteins has unearthed correlations between synapse formation and branch stability and growth in the brains of fish and frogs via synaptotropic-like mechanisms (Alsina *et al.*, 2001; Niell *et al.*, 2004; Javaherian and Cline, 2005; Meyer and Smith, 2006; Ruthazer *et al*, 2006). To explore the possibility that a similar mechanism drives the construction of the pleural neuromuscular system, nascent presynapse formation in the developing arborisations was visualised by time-lapse imaging of motoneurons expressing a fluorescently tagged presynaptic CAZ component (*BRP*::RFP). From the earliest stages of arbor growth BRP puncta localised within the axon terminals almost exclusively at sites of branch growth and filopodia emergence, providing a direct correlation between the assembly of presynaptic machineries and arbor construction. These puncta were found to translocate rapidly between these sites in a manner characteristic of synaptic protein transport vesicles (Zhai *et al.*, 2001; Sabo *et al.*, 2006). Moreover, a significant proportion of these puncta are well above the diffraction-limited diameters expected of active zones, suggesting that at least some of these BRP::RFP aggregations represent vesicular packets of synaptic proteins. In work performed in other labs, the pause sites of such packets have been demonstrated to be sites of nascent contacts between exploratory branches of synaptic partners (Ahmari, *et al.*, 2000; Washbourne *et al*, 2005; Sabo *et al.*, 2006). This corresponds with the observations of growth and branching from sites in close apposition with the muscle fibres, suggesting that stable assemblies of BRP::RFP represent established points of contact between the synaptic partners. In growing hippocampal cultures the arrival of presynaptic components at nascent axodendritic contacts is soon followed by the recruitment of postsynaptic

machineries, and within one hour these hemi-synapse pairings are capable of activity evoked neurotransmission (Ziv and Smith, 1996; Ahmari *et al*, 2000; Friedman *et al.*, 2000). In the pleural motoneuron axons BRP::RFP puncta were also found to colocalise with clusters of the synaptic vesicle associated protein Syt1::GFP. Since these machineries are believed to be trafficked independently it is reasonable to suggest that these common points of assembly also represent genuine presynaptic specialisations.

Time-lapse imaging of BRP::RFP in motoneuron axons revealed a close association between nascent presynapse assembly and branch growth. BRP::RFP puncta are stabilised in growth cones concurrently with their formation, or very soon after, and destabilised and lost during growth cone retraction. By virtue of this, strings of nodes marked with BRP::RFP puncta are deposited in the wake of advancing growth cones which chart the progression of successful branch stabilisation events. Identical sequences of events were recorded in the axons of both zebrafish retinal ganglion cells and Mauthner cells indicating an analogous mechanism of growth (Jontes *et al.*, 2000; Meyer and Smith, 2006). My observations point to a structural role of synapses during arbor construction as anchor points between synaptic partners in addition to suggesting that exploratory growth occurs preferentially from nascent synaptic contacts. In support of this it was found that the overwhelming majority (84%) of filopodia emerge from puncta or recruit a punctum to their bases within minutes of their formation. My study is not the first to identify such a relationship (Alsina *et al.*, 2001; Niell *et al.*, 2004; Javaherian and Cline, 2005; Meyer and Smith, 2006; Ruthazer *et al*, 2006), however it is the first to demonstrate a correlation between the lifetimes of filopodia and the existence of puncta at their bases. Every filopodium which failed to establish a punctum at its base was eliminated within 20 minutes, suggesting that none of this population mature to become permanent arbor features. This evidence points to two potential

scenarios: (1) filopodia which do not stem from puncta are incapable of forming stabilising contacts, or (2) the formation of stabilising contacts by filopodia results in the recruitment of puncta to their bases. It is clear however that puncta formation does not always precede filopodia growth since the largest proportion (48%) recruit puncta only after their emergence. This indicates that BRP at least is not required for the promotion of growth but is rather recruited secondarily. Since active zone proteins such as BRP are believed to arrive at nascent synapses as pre-packaged units, this suggests that this mechanism does not require synapses capable of evoked neurotransmission. This is consistent with the failure of this study to implicate the assembly of active zone machineries on the tips of filopodia with their selective stabilisation as has been observed in vertebrates (Niell *et al.*, 2004; Meyer *et al.*, 2006). A possibility therefore is that the synaptotropic-like mechanism described here is accomplished by specialised membrane domains, or proto-synapses, consisting of more basic trans-synaptic adhesion complexes.

To explore the long-term fate of presynaptic assemblies established during early growth, *BRP*::RFP expressing motoneurons were repeatedly imaged at 12 hour intervals. This showed that puncta stabilised at branch points are predominantly permanent, adding weight to the notion of their structural importance. However, towards the latter stages of growth the distribution of synaptic puncta shifted from being predominantly located at branch points to being arranged along the lengths of axon branches. A remarkably similar change in the distribution of synapses on dendritic arborisations in the spinal cords of rodents was resolved with electron microscopy by Vaughn *et al.*, who found that during early arbor development 80% of synapses are located at growth cones and very few along dendrite branches, whereas at later stages of development the majority of synapses were located primarily along branch lengths (1974). Likewise, live imaging of axonal arborisations in the *Xenopus* tectum showed

that during early growth the vast majority of presynaptic clusters were located at branch points whereas in mature arborisations synapses are distributed predominantly along terminal axon branches (Alsina *et al.*, 2001). This suggests that in each of these systems nascent synapse/protosynapse formation plays specific developmental roles in determining arbor shape. In addition to this organisational change it was also noted that presynaptic puncta decrease in diameter towards the later stages of arbor growth, becoming closer in size to individual active zones. This might indicate that during early growth presynaptic puncta do not represent synapses, but are in fact storage points for synaptic machineries recruited by nascent trans-synaptic complex for redistribution to synapses during later development.

Conclusions

This work describes a population of complex arborisations in the fly which grow in a dynamic, trial and error manner with remarkable similarities to the growth of complex arborisations in vertebrate brains. Moreover, it demonstrates a synaptotropic-like mechanism underlying this mode of growth for the first time outside of vertebrates. In contrast with vertebrates though, the stabilising and growth promoting effects imparted by this mechanism do not appear to depend on the maturation of nascent presynapses into units possessing the full complementation of molecular machineries necessary for evoked neurotransmission. From these observations, and with evidence drawn from other studies, I propose a series of events underlying this process whereby (1) contacts between axonal filopodia and myopodia or myotubes result in the formation of adhesive trans-synaptic complexes (2) these complexes facilitate the cytoskeletal remodelling required for the maturation of subsets of these filopodia into branches (3) vesicular transport packets containing presynaptic proteins rapidly arrive and are stabilised at these trans-synaptic domains (4) further cytoskeletal remodelling

promotes the generation of new exploratory filopodia. The sequence of steps 3 and 4 appears to be interchangeable. Despite the particular differences between this mechanism of synaptotropic growth and mechanism described in vertebrates, the core principles remain the same.

These morphological data suggest the existence of a universal ‘algorithm of growth’ for building complex arborisations in different developmental settings. Via local, trial and error sculpting of arbor shape this mechanism offers a versatile means by which to build functionally effectual structures in an environment which is relatively scarce in suitable synaptic contacts.

Chapter 3

Exploring the role of the synaptic cell adhesion molecules Neurexin-Neuroligin in synaptotropic growth mechanisms

3.1 Introduction

The synaptotropic hypothesis posits that arbor morphology is determined by the stabilising action of synapse formation between growing synaptic partners. Synaptic cell adhesion molecules are perfectly suited to coordinate this process by providing structural stability to nascent contacts and bringing additional pre- and postsynaptic machineries into close apposition. These molecules which bind heterophilically or homophilically across the synaptic cleft belong to a wide range of protein classes including neurexins, neuroligins, cadherins, leucine rich repeat trans-membrane (LRRTM) proteins, ephs and ephrins. Despite the term 'adhesion molecule' these proteins perform diverse functions including cell-cell recognition, coordinating synapse assembly and linking the synapse to intracellular signalling pathways (Dalva *et al.*, 2007; Missler *et al.*, 2012). What is more, these functions can be modulated acutely, for example by phosphorylation, proteolytic cleavage and synaptic activity, positioning these proteins as key regulators of synaptic structure and function (Chubykin *et al.*, 2007; Bozdagi *et al.*, 2010; Ko *et al.*, 2011; Peixoto *et al.*, 2012). However, despite their importance, the exact contribution these molecules make to building complex tree-like architectures through synapse formation is poorly understood.

Perhaps the best studied of all synaptic cell adhesion molecules, and the only ones for which synapse specific functions have been shown, are the neurexins (Nrxs) and neuroligins (Nlgs) (Südhof, 2008). Canonically, postsynaptic Nlgs bind to the extracellular laminin/neurexin/sex-hormone (LNS) domains of presynaptic Nrxs via

catalytically inactive extracellular acetylcholinesterase domains and have been shown to form trans-synaptic complexes *in vivo* (Ushkaryov *et al.*, 1992; Ichtchenko, *et al.*, 1995; Nguyen and Südhof, 1997; Tsetsenis *et al.*, 2014). This being said, electron microscopy has revealed Nrxs to be in the postsynaptic membranes of some synapses in vertebrates, and at least one of the *Nlg* homologues in *Drosophila* (*Nlg2*) is required presynaptically for normal synapse function (Taniguchi *et al.*, 2007; Chen *et al.*, 2012). On top of this, evidence is mounting to show that both Nrxs and Nlgs interact with a diverse range of additional proteins via their extracellular domains, pointing to their involvement in numerous molecular pathways which may or may not be functionally redundant (Sugita *et al.*, 2001; Siddiqui *et al.*, 2010; Xu *et al.*, 2010). The importance of both *Nrxs* and *Nlgs* for nervous system function is highlighted by the extremely elevated risk of autism and other cognitive diseases associated with mutations in both of these gene families (Jamain *et al.*, 2003; Chih *et al.*, 2004; Feng *et al.*, 2006; Kim *et al.*, 2008; Tabuchi *et al.*, 2011). Adding to this, defects in synaptic transmission resulting from mutations in *Nlgs* and *Nrxs* in both vertebrates and invertebrates indicate that this importance is evolutionarily conserved across taxa (Li *et al.*, 2007; Banovic *et al.*, 2010).

Nrxs and *Nlgs* play diverse roles at the synapse from early assembly to mature function. Each of these proteins possesses intracellular PDZ-binding motifs enabling them to recruit synaptic components during synaptic maturation. Nrxs for example have been shown to be essential for coupling presynaptic Ca2+ channels to the synaptic release machinery at vertebrate synapses via interactions with PDZ domain proteins (Missler *et al.*, 2003). Nlgs on the other hand have been shown to bind and recruit PDZ domain protein PSD-95, a central organiser of the postsynaptic density which is essential for the proper apposition of glutamate receptors to presynaptic release zones at excitatory synapses (Irie *et al.*, 1997; Mondin *et al.*, 2011). In addition to this,

interactions between Nrxs and the different homologues and/or splice variants of Nlgs have been shown to a specify vertebrate synapses as excitatory or inhibitory (Graf *et al.*, 2004; Chih *et al.*, 2005; Chih *et al.*, 2006; Chubykin *et al.*, 2007). In fact, the differential binding affinities of Nlg and Nrx splice isoforms presents a potential trans-synaptic signalling 'code' for determining connectivity or synapse specificity, although quite what role this 'code' plays is yet to be shown.

The role of *Nrxs* and *Nlgs* as synaptic organisers is widely accepted. However, their requirement during the initial stages of synapse formation is more controversial. *In vitro* both *Nrx* and *Nlg* have been shown to be strongly synaptogenic. *Nlgs* expressed in non-neuronal cells are sufficient to induce the formation of presynaptic elements in cultured neurons, whilst *Nrxs* are sufficient to induce the formation of postsynaptic elements (Scheiffele *et al.*, 2000; Dean *et al.*, 2003; Chih *et al.*, 2003; Graf *et al.*, 2004). Likewise, overexpression of *Nlgs in vivo* leads to elevated numbers of synapses in vertebrate brains, whilst overexpression of *Nrx* in *Drosophila* motoneurons leads to an increased number of presynaptic boutons (Li *et al.*, 2007; Dahlhaus *et al.*, 2010; Schnell *et al.*, 2012). Adding to this, RNAi mediated knockdown of *Nlgs in vitro* and *in vivo* causes significant reductions in the number of synapses as well as in the number of presynaptic spines (Chih *et al.*, 2005; Kwon *et al.*, 2012). This would suggest that *Nlg* and *Nrx* are central to the initiation of synapse formation. However, to counter this, mice lacking all 3 *Nlg* homologues, known to be expressed at high levels in the brain, showed no differences in synapse density when compared to wild type controls (Varoqueaux *et al.*, 2006). Similarly, loss of all 3 *α-Nrxs* also failed to effect brain synapse densities (Missler *et al.*, 2003). This being said, these experiments failed to take into account the increasing number of other adhesion proteins, particularly LRRTMs, which are being shown to function redundantly with Nlgs at vertebrate synapses (Ko *et al.*, 2009; Siddiqui *et al.*, 2010; Ko *et al.*, 2011; Soler-Llavina *et al.*,

2011). Furthermore, the failure to remove *β-Nrxs*, which are known to induce postsynapse assembly in cultured neurons by binding to Nlgs or LRRTMs, makes it impossible to discount a role for Nrx signalling in synapse formation in vertebrates (Scheiffele *et al.*, 2000; Ko *et al.*, 2009). In *Drosophila* loss of *Nlg1* or *Nrx* leads to reductions in synapse numbers at the neuromuscular junction suggesting that, in the fly at least, Nlg/Nrx signalling is important for establishing synapses.

Evidence is emerging to suggest that the action of Nlg/Nrx signalling is regulated by synaptic activity. The increase in synapse number and synaptic strength mediated by *Nlg1* overexpression in cultured hippocampal cells was found to be completely reversed by chronic blockade of NMDA mediated glutamate transmission (Chubykin *et al.*, 2007). Adding to this, Nlg1 in vertebrates has been shown to be phosphorylated by CaM-Kinase II, suggesting that its modulation in response to synaptic transmission takes place via this activity-dependent plasticity pathway (Bemben *et al.*, 2014). Adding to this, acute RNAi mediated silencing of *Nlg1* in the amygdalae of rats suppressed long term potentiation and inhibited the formation of new memories (Kim *et al.*, 2008). Together these data suggest that Nlg/Nrx signalling is directly linked to the activity-dependent regulation of synapse function, and could potentially play a role in the 'use-testing' of synaptic connections speculated to take place during synaptotropic growth (Ruthazer *et al.*, 2006; Chen *et al.*, 2010).

The action of Nlg and Nrx would appear to make them strong candidates to play a role in synaptotropic growth. However very little evidence has been uncovered linking their function to changes in arbor morphology. As with synapse density, the deletion of *Nlgs* and *Nrxs* in mice had no overt impacts on brain structure (Varoqueaux *et al.*, 2006; Dudanova *et al.*, 2007). However, these results are subject to the same limitations listed before. What is more, the studies did not perform detailed

investigations into the effects of *Nlg* or *Nrx* deletion on arbor morphology. In contrast, cell-autonomous knockdown of *Nlg* in *Xenopus* tectal cells using morpholinos or dominant negative Nlg1 resulted in substantially smaller and less complex dendritic arborisations *in vivo* (Chen *et al.*, 2010). This appeared to be a result of the impaired ability of dendritic filopodia to become stabilised. Using soluble Nrx to block endogenous Nrx signalling, this was determined to be a result of reduced Nlg-Nrx interactions. These dendritic arborisations have been shown previously to grow via a synaptotropic-like mechanism, indication a that Nlg/Nrx interactions play a role in this mode of growth by stabilising nascent contacts between synaptic partners. This is supported by i*n vitro* evidence showing that *Nlg1* overexpression in dissociated hippocampal cells increases the likelihood of dendritic filopodia making stable contacts with presynaptic elements (Arstikaitis *et al.*, 2011). That being said, these studies could not show that Nlg/Nrx signalling influences filopodia stability at a local level, as would be predicted by the synaptotropic hypothesis. Nor could it be shown conclusively that this signalling is played out trans-synaptically between synaptic partners. On top of this, results generated by the use of morpholinos should be treated with caution since 15-20% of morpholino based knock downs have been found to produce off-target effects (Ekker and Larson, 2001). Therefore ideally, an alternative approach should be taken for these findings to be verified.

Intuitively synaptic cell adhesions molecules should be expected to play a central role in establishing connectivity and arbor morphology. However, the evidence to support this is scant and somewhat unclear. Studies in vertebrates have been limited by the high functional redundancy of these proteins as well as the difficulties in labelling and manipulating small numbers of cells and visualising interactions between synaptic partners. With my new model of synaptotropic-like arbor growth in the fly I have used live imaging to explore the importance of these proteins in stabilising nascent contacts

between dynamically growing synaptic partners, which has so far been impossible in other systems.

3.2 Results

Trans-synaptic Neurexin-Neuroligin signalling is required for normal arbor growth

As described above the trans-synaptic signalling activity of the cell adhesion molecules Neurexin and Neuroligin is believed to play significant roles in synapse biology and has been implicated in synaptotropic growth. To determine if presynaptic Neurexin (Nrx) or postsynaptic Neuroligin1 (Nlg1) play roles in the construction of the pleural neuromuscular junctions, homozygous mutants were generated using classical loss of function alleles described by Li *et al.* (2007) and Banovich *et al.* (2010). These mutants are null, yet the flies survive through to pharate adult stages. Motoneuron arborisations were live imaged in pupal abdomens by expression of myr::GFP under the control of the glutamatergic neuron specific driver *VGlut*-LexA.

Broad overviews of arbor morphology in hemisegments A3 to A5 in mature *Nrx* null, *Nlg1* null and wild type control specimens demonstrate the gross arbor growth defects observed in these mutants (Fig. 1). In both cases the axonal arborisations appear stunted and underdeveloped which leads to a general disruption in their coverage of the pleural region. This is most obvious from the large areas of the muscle field that are not innervated compared to wild type.

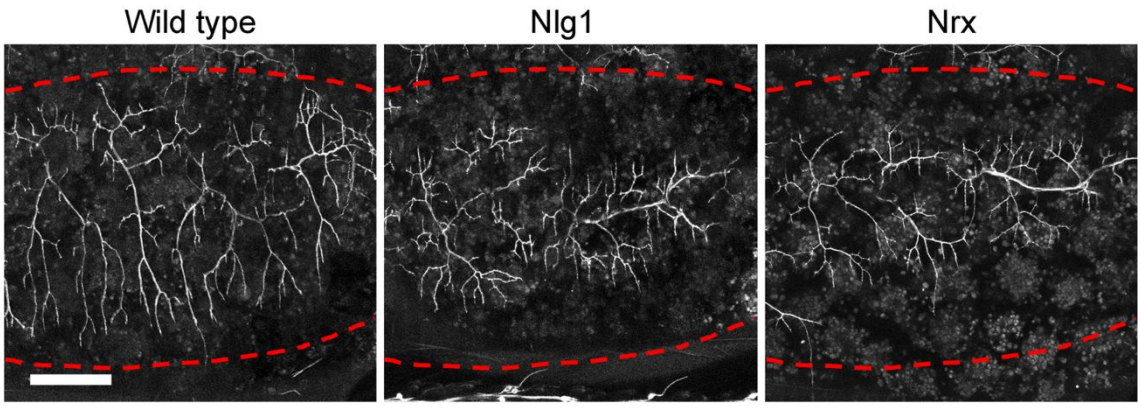

Figure 1. Deficiencies in arbor coverage of the pleural regions in *Nlg1* and *Nrx* nulls. Lateral abdominal views show the motoneuron axon arborisations in hemisegments A3-A5 in a wild type, an *Nlg1* null and an *Nrx* null aged between 76h and 78h APF. The red dashes indicate the contours of the pupal abdomen and the approximate limits of the pleural region. Motoneurons are expressing myr::GFP under the control of *VGlut*-LexA. Scale bar: 100μm.

To better describe these phenotypes and explore their significance I used morphometric methods to analyse the data. Although the pleural neuromuscular junctions display variations in arbor morphology, as described in chapter 1, trends in size and shape clearly distinguish arborisations of different segmental identities. Adding to this, differences in body size between the adult sexes introduces a further confounding variable. For these reasons, only, arborisations from the same sex and with equivalent anatomical identities were compared in the analyses in the interests of objectivity. In this case these were the anterior most arborisations of segment A3 (abbreviated as A3A) of females.

Higher magnification examples of *Nrx* and *Nlg1* null A3A arborisations alongside a wild type control at 75h APF reveal in more detail the arbor growth defects seen in the mutants (Fig 2A). At a glance, the images in Fig. 2A point towards reductions in arbor coverage and cumulative branch length in both mutants, but seem similar in arbor complexity. To quantify these differences reconstructions of late stage arborisations from 70h to 80h APF were generated using a semi-automated method and analysed in a bespoke software package (see methods). As predicted, the area of coverage of *Nrx* and *Nlg1* mutant arborisations was significantly lower than those of the wild type controls (Figs. 2B) (*Nlg1* [29616 ± 3259μm^2, n = 11] versus controls [47455 ± 2298μm^2, n = 13], $t(22) = 15.67$, $p < 0.0001$; *Nrx* [32692 ± 4565μm^2, n = 8] versus controls, $t(19) = 9.89$, $p < 0.0001$, Student's t-tests, two-tailed). This was also found to be true for the cumulative branch lengths (Fig. 2C) (*Nlg1* [1785 ± 265μm, n = 11] versus controls [2251 ± 140μm, n = 13], $t(22) = 5.51$, $p < 0.0001$; *Nrx* [1758 ± 306μm, n

= 8] versus controls, t(19) = 5.07, p < 0.0001, Student's t-tests, two-tailed). Conversely, a comparison of the same groups revealed no significant differences in the total numbers of branches (Fig. 2D) (*Nlg1* [86.0 ± 14.7, n = 11] versus controls [84.4 ± 11.0, n = 13], t(22) = 0.31 p = 0.76; *Nrx* [91.9 ± 23.3, n = 8] versus controls, t(19)= 1.00 p = 0.33, Student's t-tests, two-tailed). Compared with each other, *Nlg1* and *Nrx* mutants displayed no statistically significant differences in any of these measurements (for arbor area t(17) = 1.72, p = 0.10, for arbor length t(17) = 0.20, t(17) = 0.68, p = 0.84, for branch number p = 0.51, Student's t-tests, two-tailed). To evaluate arbor complexity and topology the Strahler method of branch ordering was applied to the arborisations (Fig. 2E). As with total branch number, the topological organisations of the arborisations of each of the condition showed no statistical difference. Firstly, the highest order of branching of the groups was not significantly different (Nlg1 [n = 11] versus controls [n = 13], t(22) = 0.41, p = 0.67; *Nrx* [n = 8] versus controls, t(19) = 0.27, p = 0.79, Student's t-tests, two-tailed). This also held true for the total number of terminal (1^{st} order) branches (*Nlg1* [n = 11] versus controls [n = 13], t(22) = 0.36, p = 0.72; *Nrx* [n = 8] versus controls, t(19) = 0.99, p = 0.33, Student's t-tests, two-tailed); a trend which continued for subsequent orders, with each group showing remarkably similar numbers of branches at every level.

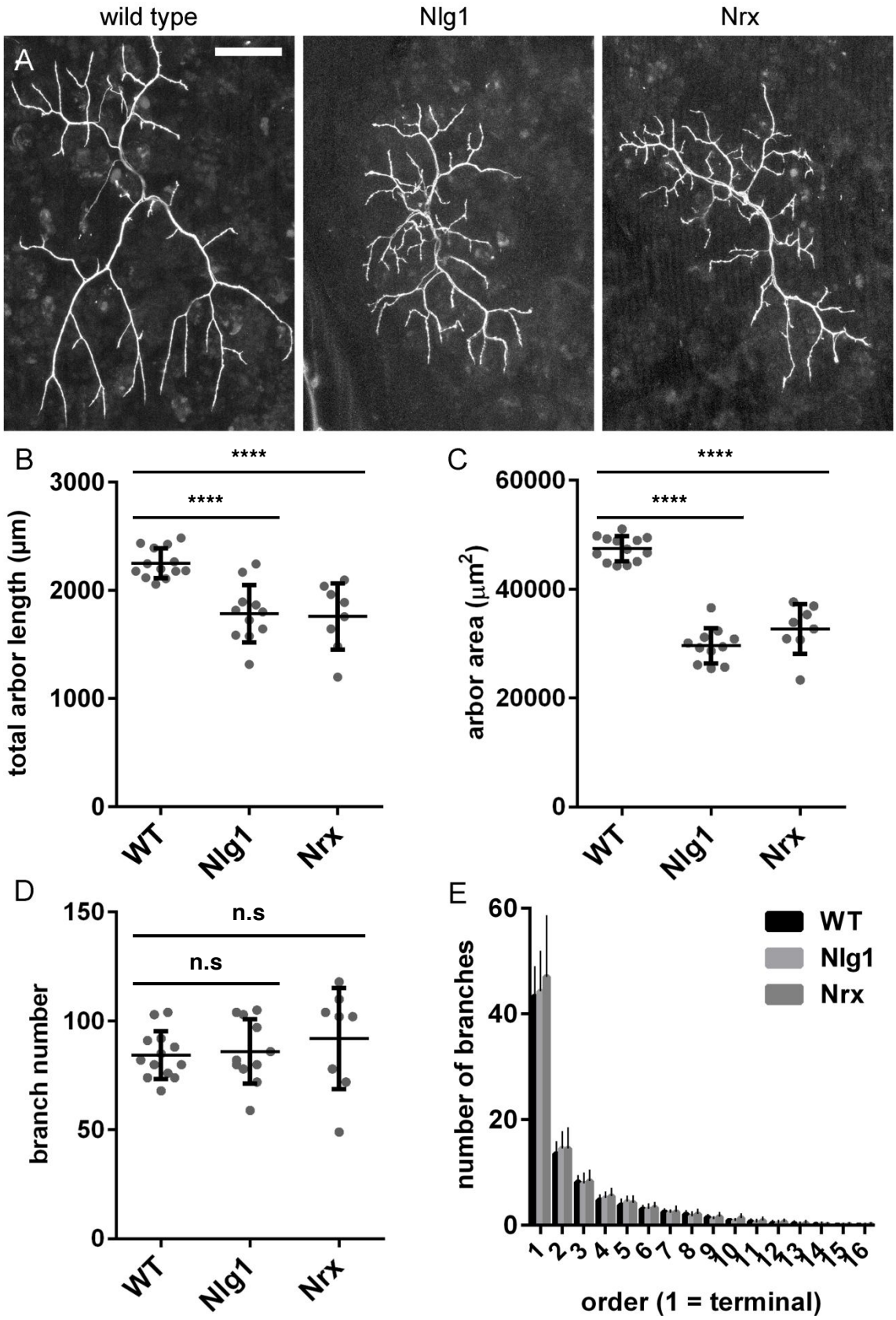

Figure 2. Morphometric analyses of Nlg1 and Nrx mutant arborisations (A) A3A axonal arborisations of females in a wild type, an Nrx null and an Nlg1 null expressing myr::GFP under *VGlut*-LexA control. For clarity, the arborisations of neighbouring neurons have been edited out using the image processing software FIJI **(B-C)**

Quantifications of total arbor length, arbor area and branch number **(E)** Arbor complexity measured by Strahler ordering. Branches were ordered from the distal tips (lowest) to the primary axon (highest). Error bars are standard deviation. Scale bar: 50μm.

In addition to these measurable defects, a variety of subtler morphological abnormalities were identified in the mutants that are better described qualitatively. Both Nlg1 and Nrx null arborisations occasionally produce exceptionally long, narrow and predominantly unbranched processes that arise at distal parts of the arborisation (Fig. 3A). Unlike typical axon terminals, which invariably innervate the internal surfaces of the pleural muscles, these projections were found to regularly grow along the sides of muscle fibres (within the inter-muscle space) or along the superficial muscle surfaces. Furthermore, in contrast with the rest of the terminals in the mutants and the wild type, these filaments fail to form synaptic boutons. For these reasons, in addition to the difficulties posed in imaging them, these structures were not in the analyses. Another defect which was also found in the arborisations of Nlg1 and Nrx mutants is best described as deficit in their adhesive integrity at the interface with the muscle. This manifests as the delamination of the more proximal axon branches from the muscle surfaces. Although not obvious in collapsed z-stacks, it is made clear in transverse projections by the unevenness of the arborisations of the mutants in this orientation compared with those of the wild types (Fig. 3B). A final phenotype observed in both mutants is a conspicuous splitting, or defasciculation, of individual axons (Fig. 3C). This splitting occurs basally, generally at the primary axon, and is usually followed by reconvergence of the fibres nearer the tips of the distal branches. Although this phenomenon is sometimes observed in wild types it is far less overt, perhaps due to a lesser degree of occurrence or a greater tightness of the fascicles. In addition to these, an aberration observed only in Nrx mutants is the continued generation of filopodia into much later stages of development than would be expected normally. Using time-lapse

imaging these filopodia were determined to transient and therefore were not considered as part of the established arborisations for the reconstructions (Fig. 3D).

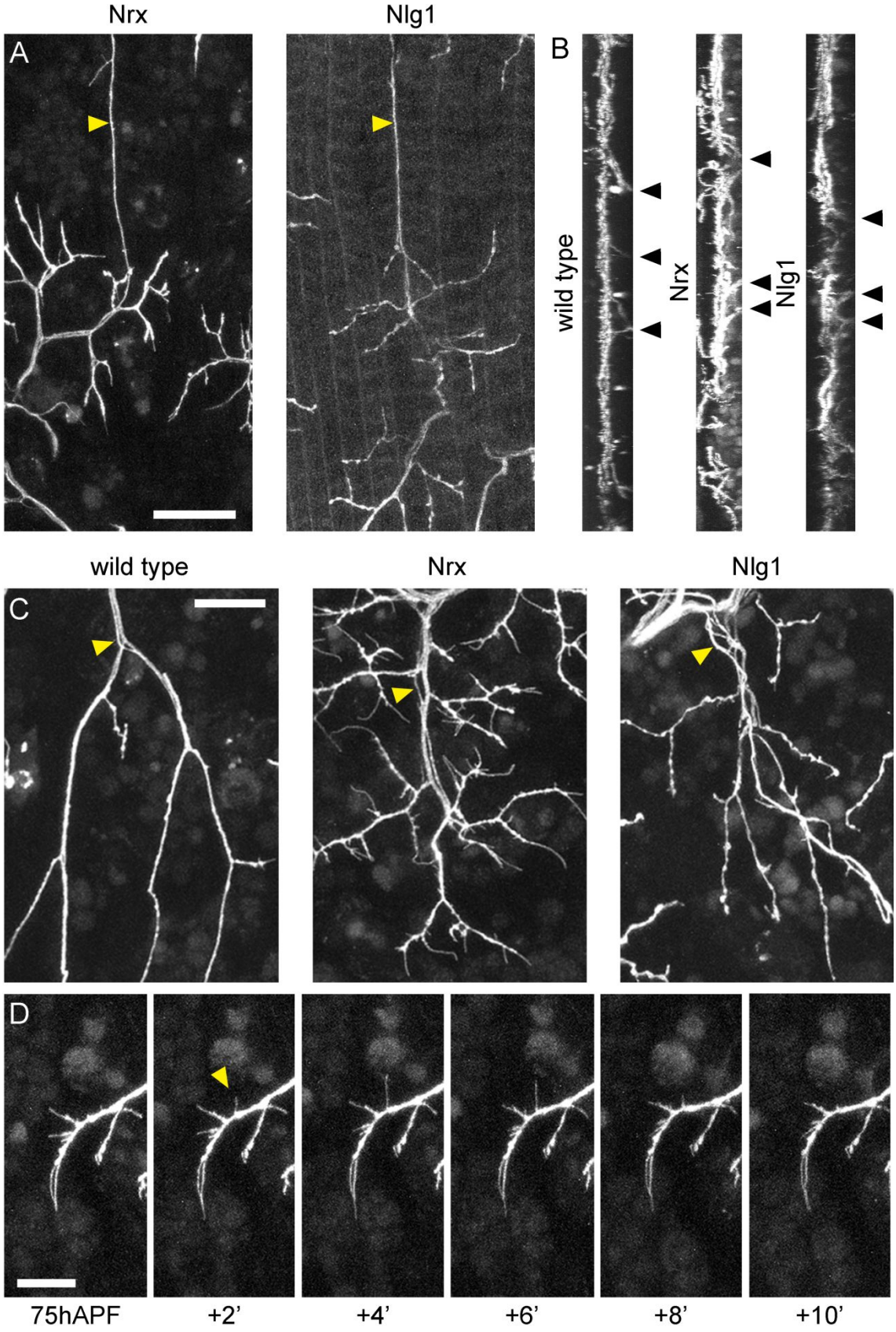

Figure 3. Additional qualitatively assessed arbor defects in Nlg1 and Nrx nulls (A) Yellow arrows indicate the abnormally long filaments found on the arborisations of *Nrx* and *Nlg1* nulls at 75h APF. In the case of Nlg1, MHC promotor driven CD8-

Shaker::GFP reveals the muscle membranes indicating that the escaping process runs within the space where 2 muscle fibres meet **(B)** In samples between 74h and 78h APF transverse projections show the irregularity of the arborisations of both nulls in this orientation relative to the wild type, a result of their delamination from the muscle. Black arrows indicate the points of entry of the axons to the nerve **(C)** Defasciculation of axons of nulls and a wild type aged between 70h and 80h APF indicated by the yellow arrows **(D)** An image sequence with 2 minute intervals demonstrates the extension and retraction of exploratory filopodia from a branch of an Nrx null arborisation at 75h APF. Motoneurons are expressing myr::GFP under *VGlut*-LexA control. Scale bars: 30*μ*m (A) 20*μ*m (C-D).

Nrx and Nlg1 puncta localise to growing motoneuron axonal terminals

Morphometric analysis of mature arborisations shows a requirement of Nrx-Nlg signalling in the construction of the pleural axonal arborisation. However, when, where and how this signalling impacts growth was not clear. To gain insight into these matters, Nlg1 distribution was visualised live in the pleural muscles by expression of a GFP labelled variant of full-length *Nlg1* (*Nlg1*::GFP) under the control of the muscle specific driver *Mef2*-GAL4. To observe the relationship of this component with the growing presynaptic terminals myr::tdTomato was expressed concurrently using glutamatergic neuron specific driver *VGlut*-LexA.

Live imaging at 35h APF reveals that the developing muscles form Nlg1::GFP puncta which appose exclusively to branches of the axonal arborisations (Fig. 4A). In addition to these strong localisations/punctate distributions we see a diffuse covering of Nlg1::GFP which exposes the entire muscle membrane. At higher magnifications, it is clear that these puncta are concentrated at branch points and beneath filopodia laden growth cones (Fig. 4B). This is similar in many ways to the localisation of presynaptic proteins, but unlike presynaptic BRP::RFP, numerous Nlg1::GFP puncta are also found at the very tips and along the lengths of filopodia themselves. Many of these puncta appear to ‘exist’ in the gaps between adjacent myotubes. This is likely to be due to myopodia which extend from muscle cells and can be revealed by labelling muscle

cells with a membrane bound reporter. These motile protrusions populate the inter-muscle spaces and are therefore likely to the hosts of these Nlg1::GFP puncta (Fig. 4D).

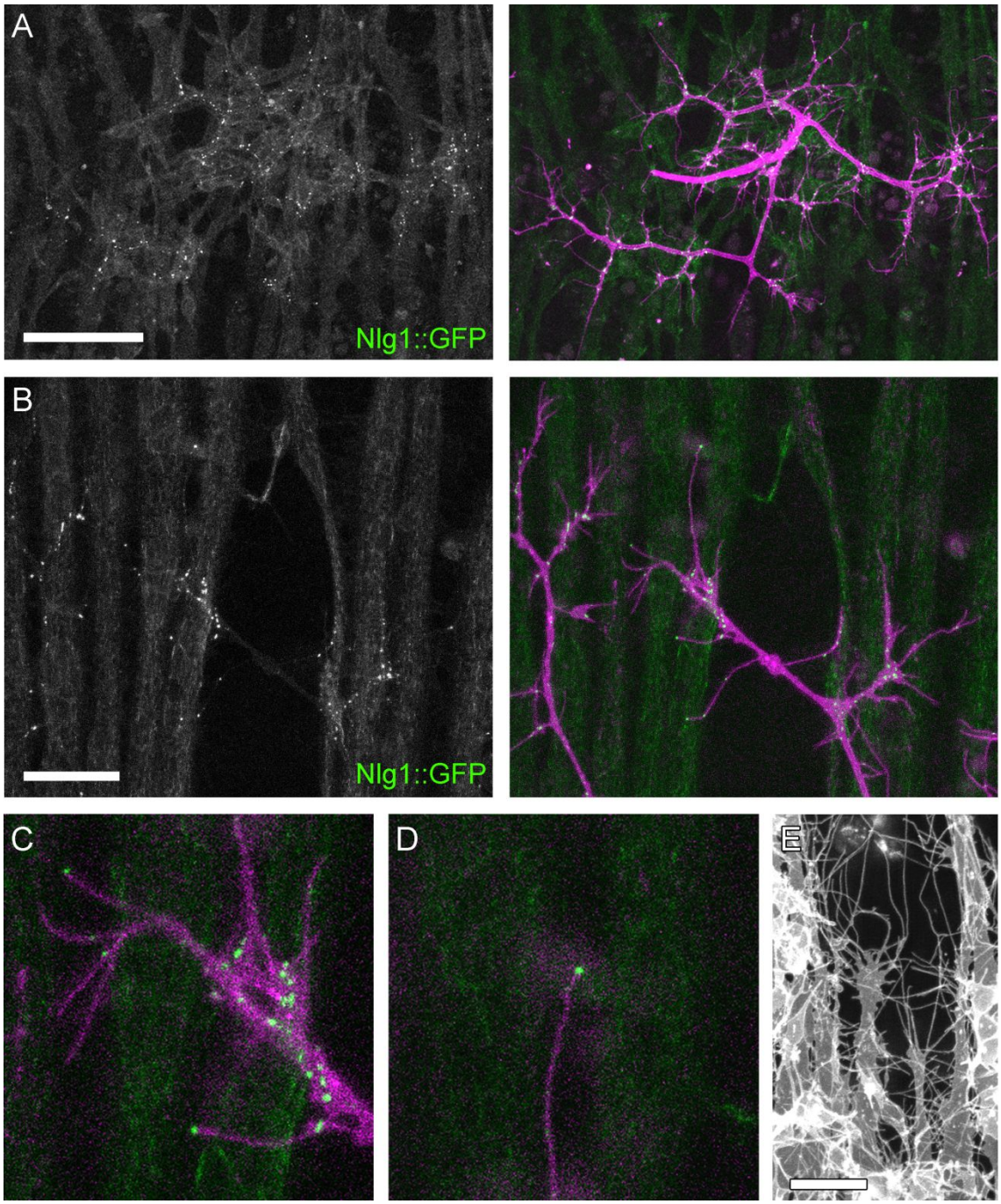

Figure 4. Live imaging reveals the subcellular distribution of Nlg1::GFP in axon terminals during early arbor growth (A) The pleural muscles in a hemisegment at 35h APF expressing *Nlg1*::GFP (green) under *Mef2*-GAL4 control. Motoneurons (magenta) are expressing myr::tdTomato under *VGlut*-LexA control. Nlg1::GFP puncta are distributed exclusively along the axon terminals **(B)** A higher magnification image shows the concentration of Nlg1::GFP puncta at a branch terminal at 38h APF **(C&D)**

Cutaways show the apposition of Nlg1::GFP puncta to filopodia and the points of filopodia growth **(E)** Myopodia growing from myotubes at 35h APF are revealed by myr::GFP expressed under the control of *Mef2*-GAL4. Scale bars: 50μm (A) 20μm (B).

To observe the subcellular localisation of Nrx in the developing arborisations a GFP tagged *Nrx* construct was overexpressed in motoneurons along with membrane targeted mCD8::Cherry under the control of OK371-GAL4. Unfortunately, the particularly low level of fluorescence of Nrx::GFP and its susceptibility to photobleaching made detailed imaging of this presynaptic component difficult. Nevertheless, it is still clear that Nrx::GFP has a punctate distribution within growing axon terminals, particularly where filopodia are generated on branches and also on the tips as well as on tips and along the lengths of distal filopodia (Fig. 5). As with Nlg1::GFP in the muscles, Nrx has a more diffuse coverage along the entire axonal membrane.

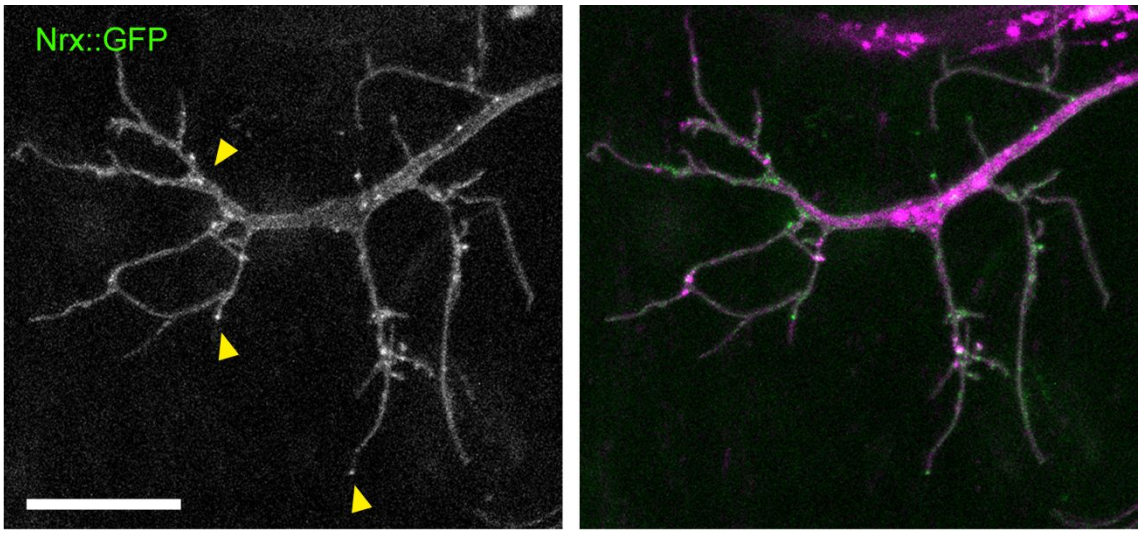

Figure 5. Live imaging reveals the subcellular distribution of Nrx::GFP during early arbor growth. A segment of an arborisation at 35h APF expressing *Nrx*::GFP and mCD8::Cherry under the control of OK371-GAL4. Indicated by the yellow arrows, Nrx::GFP puncta localise to growth cones and within filopodia. Scale bar: 15μm.

Nlg1 functions locally by stabilising filopodia during early arbor growth

To explore if a relationship exists between Nlg1::GFP puncta distribution and branch growth. Growing arborisations in animals aged from 35h to 40h APF were imaged at 1 minute intervals. An 18-minute sequence of a branch segment demonstrates that both the Nlg1::GFP puncta located at branch points and those apposed to filopodia are stable at these sites (Fig. 6A). In addition, this footage points to a relationship between the apposition of Nlg1 puncta to filopodia tips and the selective stabilisation of these protrusions: In the first frame of the series a total of 9 filopodia exist, 5 of which host puncta at their tips. Over the duration of the sequence all 5 of the filopodia associated with puncta remain anchored in position and persist for the full duration of the sequence. Conversely, the filopodia which are not marked by puncta are far more motile and ultimately 3 of the 4 are fully retracted and lost. In addition to these pre-existing filopodia, a number of filopodia are generated over the course of the series, every one of these also fails to recruit a punctum and is eventually eliminated. Interesting, two cases also occur in which Nlg1 puncta at the tips of filopodia clearly act as the limits of retraction following extension of the filopodia.

To assess the implication of these observations a comparison was performed between the lifetimes of filopodia with Nlg1::GFP puncta and filopodia without puncta from 2 time-lapse movies (for both groups n = 16). Due to the susceptibility of Nlg1::GFP and myr::tdTomato to photobleaching, high frequency imaging sessions were limited to approximately 20 minutes. Thus, very few incidents were observed in which newly generated filopodia recruit an Nlg1::GFP punctum. To circumvent this, only filopodia in existence at the beginning of recording were considered for the analysis. I found that 100% of the filopodia that did not appose a punctum were eliminated within 10 minutes of recording. In contrast with this, just 6.3% of filopodia with an Nlg1 punctum were eliminated within the same time. A further 25% of these

were lost within 20 minutes, although the clear majority, 68.8%, survived for longer than the duration of the analysis (Fig. 6B). Statistical analysis found that filopodia which are apposed to puncta have significantly longer lifetimes that those which are not (with puncta = 19.4 minutes (± 2.8 S.D), n = 44, without puncta = 10.7 (± 6.8 S.D), n = 49, Mann-Whitney U = 305.5, $p < 0.0001$, two-tailed).

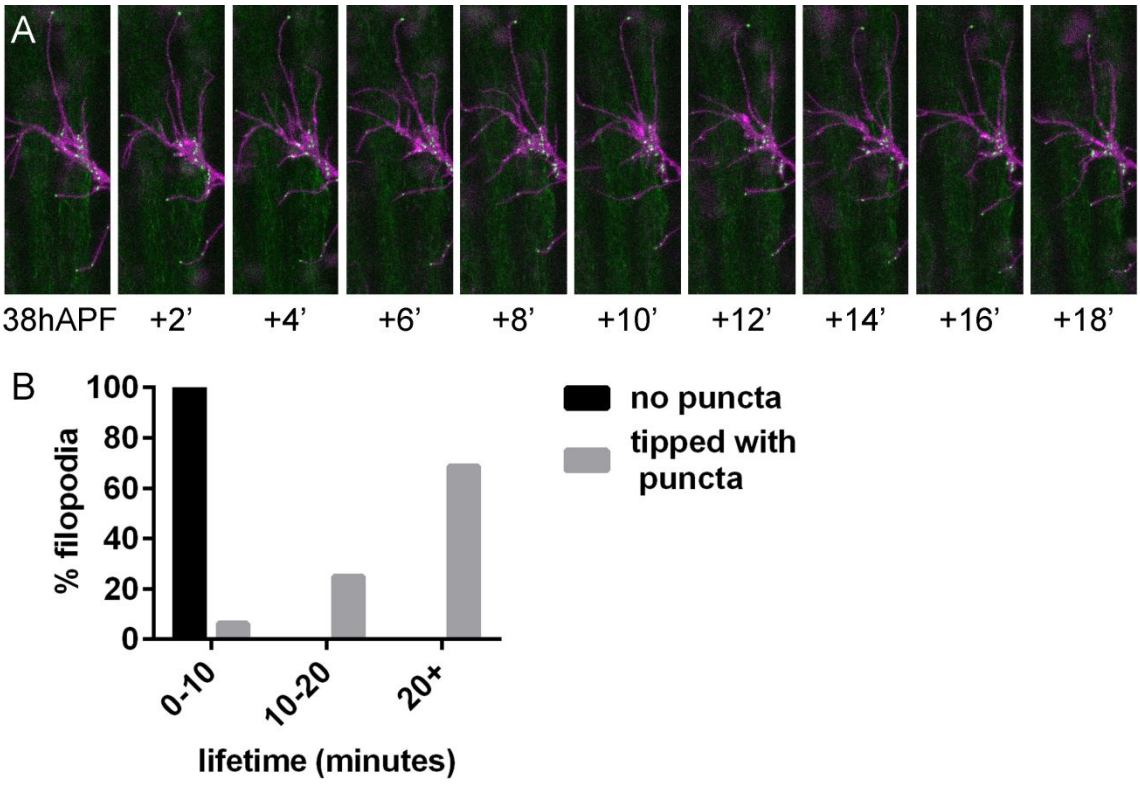

Figure 6. Nlg1::GFP puncta distribution is correlated with the selective stabilisation of filopodia (A) A sequence of images at 2 minute intervals showing the relationship between Nlg1::GFP puncta distribution and branch dynamics at 38h APF **(B)** The lifetimes of 16 filopodia with and 16 filopodia without puncta at their tips displayed in a histogram with 20 minute bins. These measurements were from 2 time-lapse movies of arborisations at 40h APF taken at 1 minute intervals.

Branch growth is preceded by the formation of Nlg1 puncta upon exploratory filopodia and their selective stabilisation

The relationship between Nlg1::GFP puncta and branch dynamics strongly suggests that Nlg1 has a stabilising influence on dynamic filopodia. This raises questions regarding both the mechanism of Nlg1 recruitment to filopodia and the

longer-term consequences of these trans-synaptic interactions. High frequency time-lapse imaging provided a rare few examples which shed light on these matters. Shown in the time series in Fig. 7, exploratory filopodia extend from a branch terminal at 35h APF. One of these makes contact with the left most muscle fibre and by 9 minutes has recruited a small accretion of Nlg1::GFP close to its tip. By 13 minutes this accretion has expanded into a conspicuous punctum. Concurrent with this, the filopodium thickens and splits; producing what appear to be the foundations of a nascent growth cone. Principally, these data demonstrate that Nlg1 puncta precipitate directly upon exploratory filopodia, i.e. they coalesce. In addition, it suggests that as well as eliciting a stabilising effect, Nlg1 might also act to promote the cytoskeletal reorganisation required for branch maturation and growth.

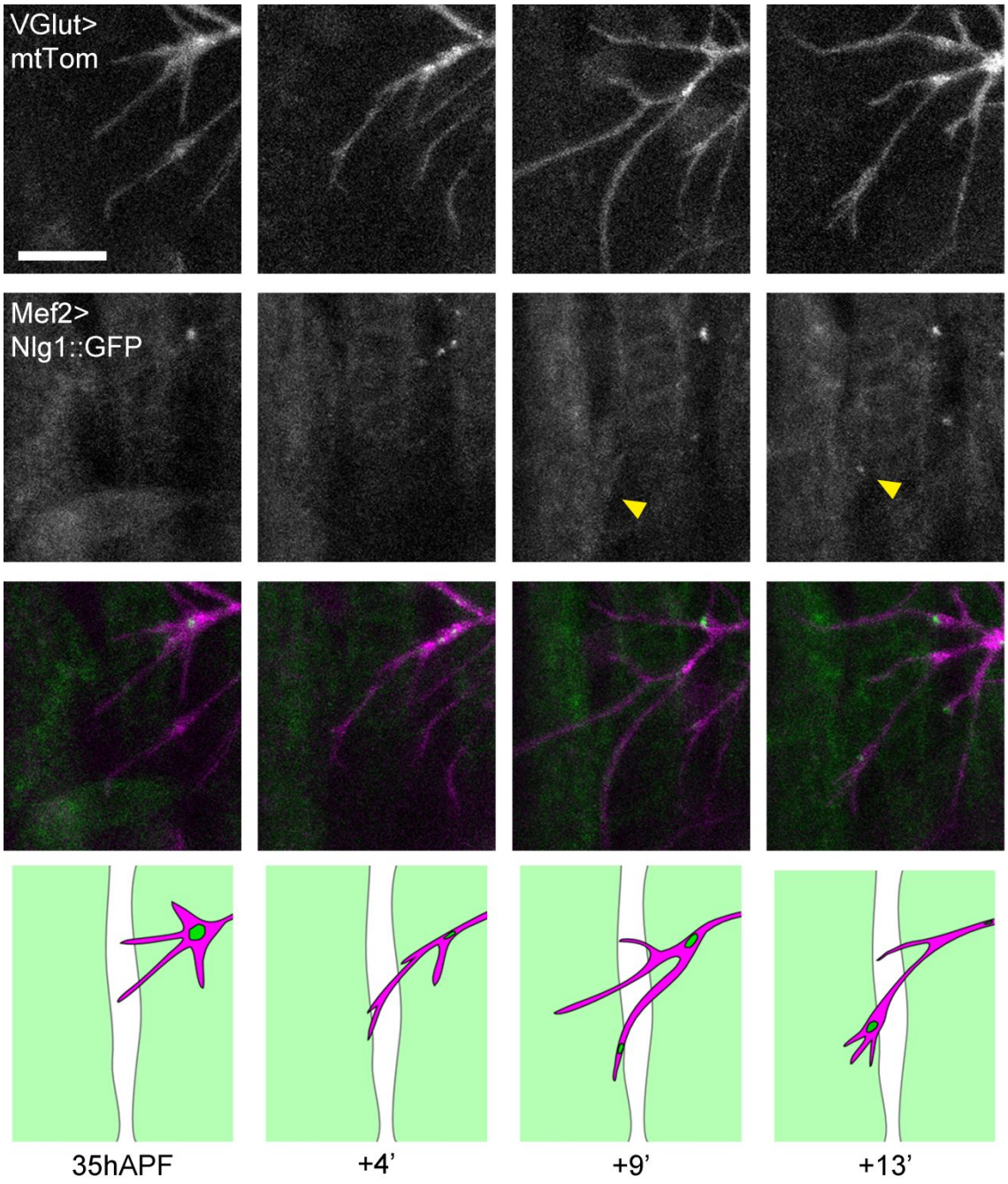

Figure 7. Nlg1::GFP condenses on the tips of exploratory filopodia. A time series shows the accretion of Nlg1::GFP in apposition with an exploratory filopodium at 35h APF. Maturation of this accretion into a conspicuous punctum is coincident with a thickening and branching of the filopodial tip. These events are modelled in the schematic. Motoneuron: *VGlut*-LexA>myr::tdTomato; muscle: *Mef2*-GAL4>*Nlg1*::GFP. Scale bar: 20μm.

To understand the significance of these observations in the greater context of arbor growth, longer time-lapses were taken at lower rates of acquisition. In Fig. 8 a time series following a branch segment as it traverses a field of muscles demonstrates

the typical relationship between Nlg1::GFP puncta dynamics and branch growth. For orientation, the muscle fibres are numbered anterior to posterior (1 to 4). In the initial frame the leading edge of the branch sits above a cluster of Nlg1::GFP puncta which mark a well-established contact with the first fibre. From this centre of exploratory growth, a filopodium bridges the gap to the second muscle where a pair of nascent contacts are marked by Nlg1::GFP puncta close to the filopodium tip (the small misalignment is a result of the latency of imaging between each channel). By 20 minutes this stabilised filopodium has matured, becoming an extension of the branch, and the contacts marked by Nlg1 puncta now mark the positions of new filopodia emergence. At 75 minutes the contact with muscle 2 is well consolidated and has recruited many more Nlg1::GFP puncta; now appearing much like the growth cone that was initially in positioned over muscle 1. By 110 minutes additional filopodia generated at this new node have recruited puncta themselves and the sequence begins again. By 185 minutes' iterations of extension and stabilisation which occur concomitantly with Nlg1::GFP puncta formation have extended the leading edge of the branch onto the 3rd muscle fibre.

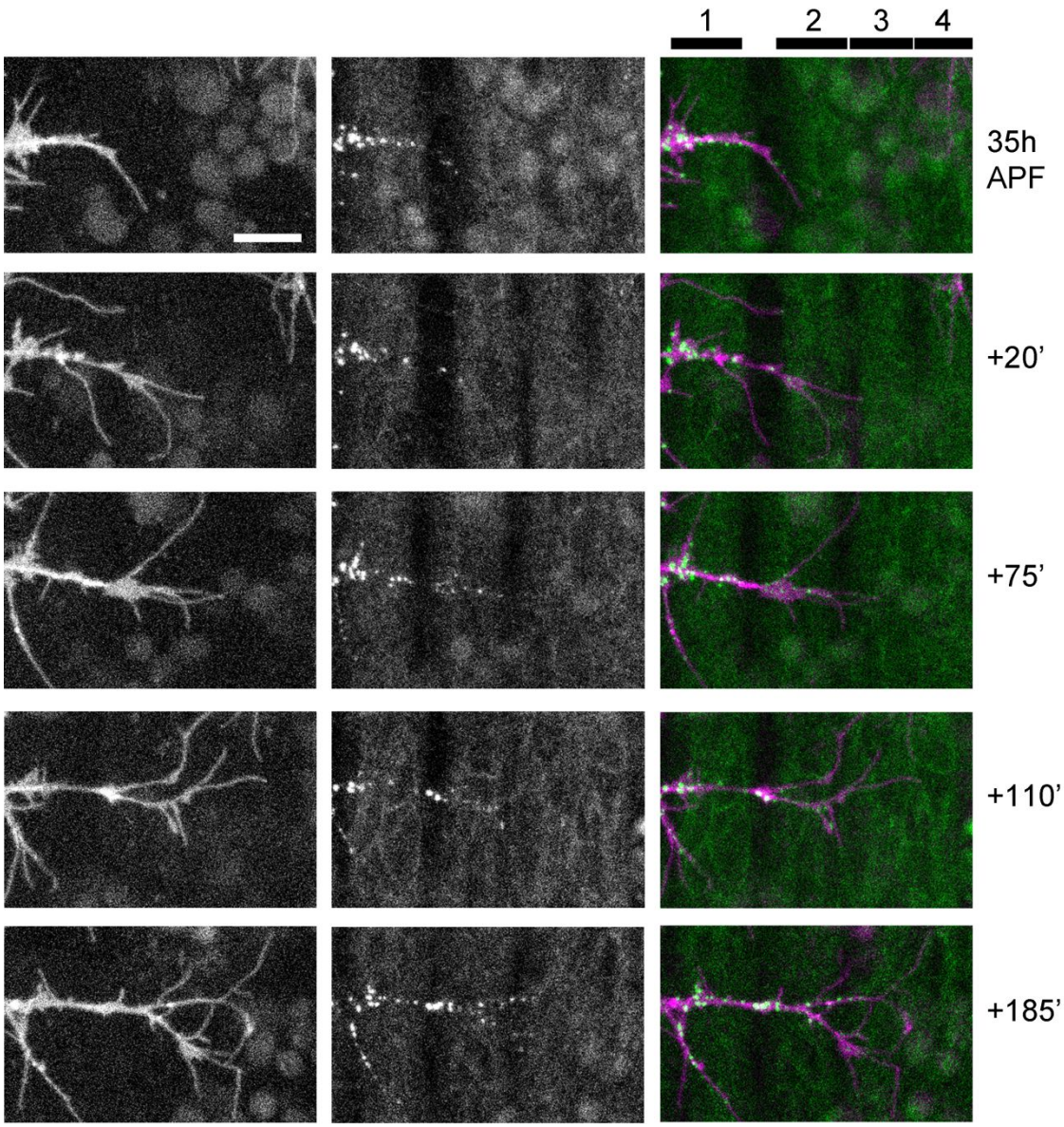

Figure 8. Long term time-lapse imaging demonstrates the relationship between Nlg1::GFP puncta formation and branch growth. A series of images taken from a time-lapse sequence with 5 minute intervals shows the extension of a branch at 35h APF in relation to Nlg::GFP puncta formation. The muscles are labelled by their positions from left to right. Rounds of filopodia extension stabilisation are concomitant with the formation of Nlg1::GFP puncta on these processes. Motoneurons: *VGlut*-LexA>myr::tdTomato; muscles: *Mef2*-GAL4>UAS-*Nlg1*::GFP. Scale bar: 20*μ*m.

An important point to address here is whether the expression of this GFP tagged construct itself causes a phenotype. Banovich *et al.*, (2010) describe that overexpression of *Nlg1*::GFP specifically in muscles does not significantly impact the growth of larval neuromuscular junctions. This was contrasted with the overexpression of an untagged version of *Nlg1* which caused reductions in synaptic terminal size and

bouton numbers. The untagged construct was found to be expressed at a much higher level. To test if postsynaptic *Nlg1*::GFP expression causes a growth phenotype in this system, mature arborisations in animals expressing *Nlg1*::GFP under *Mef2*-GAL4 control were compared with wild type equivalents (Fig. 9). As was found with the larval neuromuscular junctions, no obvious growth phenotype was observed in a background of *Mef2*-GAL4 driven *Nlg1*::GFP expression.

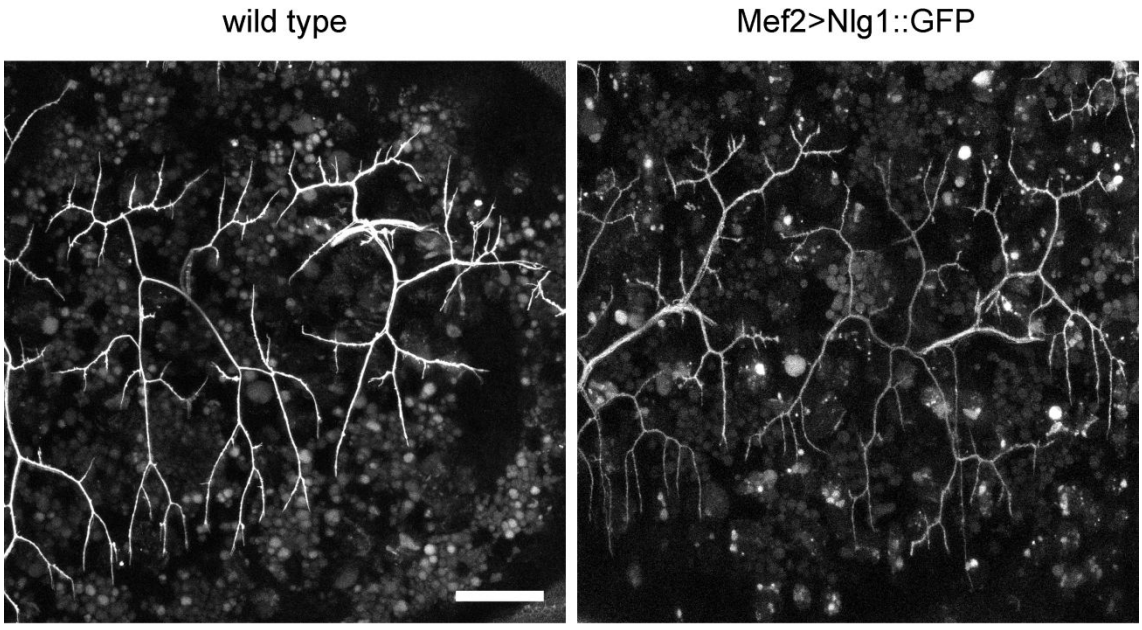

Figure 9. Postsynaptic *Nlg1*::GFP expression causes no overt arbor growth phenotypes. Arborisations in hemisegments A4 and A5 in pupae between 70h and 80h APF. In the right-hand panel motoneurons are expressing myr::tdTomato driven by *VGlut*-LexA in a background of *Mef2*-GAL4 driven *Nlg1*::GFP expression. In the left controls are expressing myr::GFP driven by *VGlut*-LexA. Scale bar: 50*μ*m.

Nlg1 null arborisations display a deficit in tension generation during early growth

If, as the data suggests, Nlg1 signalling plays a stabilising role during the elaborate phase of arbor growth, one would expect to see abnormalities in the arborisations at this early stage in development. Fig. 10A displays a section of an Nlg1 null arborisation at 36h APF together with a wild type equivalent. A distinction that immediately draws attention is that the branches of the mutant are more tortuous. To

assess the significance of this, primary, secondary and tertiary branches (ordered from the branch tips and excluding filopodia) from wild type and Nlg1 null arborisations aged between 30 and 36h APF were scored using an index of straightness (Monier *et al.*, 2010). This measurement calculates the proportional difference between the actual length of a branch and the hypothetical straight line distance between its ends (nodes). The outputs are plotted as percentages of the actual length (Fig. 10B). As estimated by eye, Nlg1 null branches (4.58 ± 3.05% S.D, n = 23) were significantly less straight than those of wild types (2.85 ± 1.76% S.D, n = 22) (p = 0.02, Student's t-test, two-tailed).

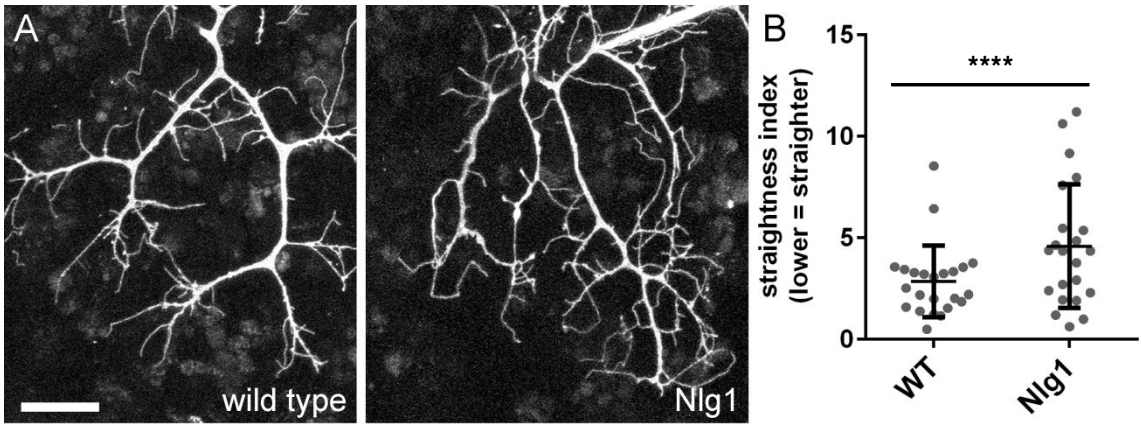

F**igure 10. Branches of Nlg1 nulls are less straight during the period of dynamic arbor growth (A)** A segment of a wild type arborisation at 33h APF and an Nlg1 null arborisation at 36h APF expressing myr::GFP under *VGlut*-LexA control **(B)** Straightness of 23 control branches from 5 arborisations and 22 Nlg1 null branches from 3 arborisations as percentages of straight line distance between the branch nodes. Error bars are standard deviation. Scale bar: 25.

A potential reason for this discrepancy in branch straightness is an impaired ability of the Nlg1 mutants to generate traction forces and therefore branch tension. One means by which the tensile state of a tissue can be inferred is by measuring its recoil kinetics following a lesion. To achieve this, branches of *Nlg1* nulls and wild type controls were severed using a 2-photon laser and imaged at 2 frames per second for the subsequent 30 seconds (Fig. 11A). In the case of the controls, ablation was often followed by a conspicuous separation of the severed ends of the branch as well as changes in the branching angles at the nodes. In contrast, upon ablation many

of the Nlg1 null branches appeared to show very little change in either of these qualities. To quantify these observations, recoil was calculated at 5 second intervals following ablation by measuring the change in distance between the rear most positions of the nodes of each branch. These values were normalised by division with the initial distance between the nodes, of which they are plotted as percentages (Fig. 11B). For both groups the greatest rate of recoil was observed during the first 5 seconds after ablation. However for the controls this was marginally more. This inequality increased and by 20 seconds, when the recoil of both groups had plateaued, the extent of the recoil of the control branches (9.72 ± 2.41% S.D, n = 7) was significantly greater than that of the mutants (4.75 ± 2.94% S.D, n = 6) ($p = 0.006$, Student's t-test, two-tailed).

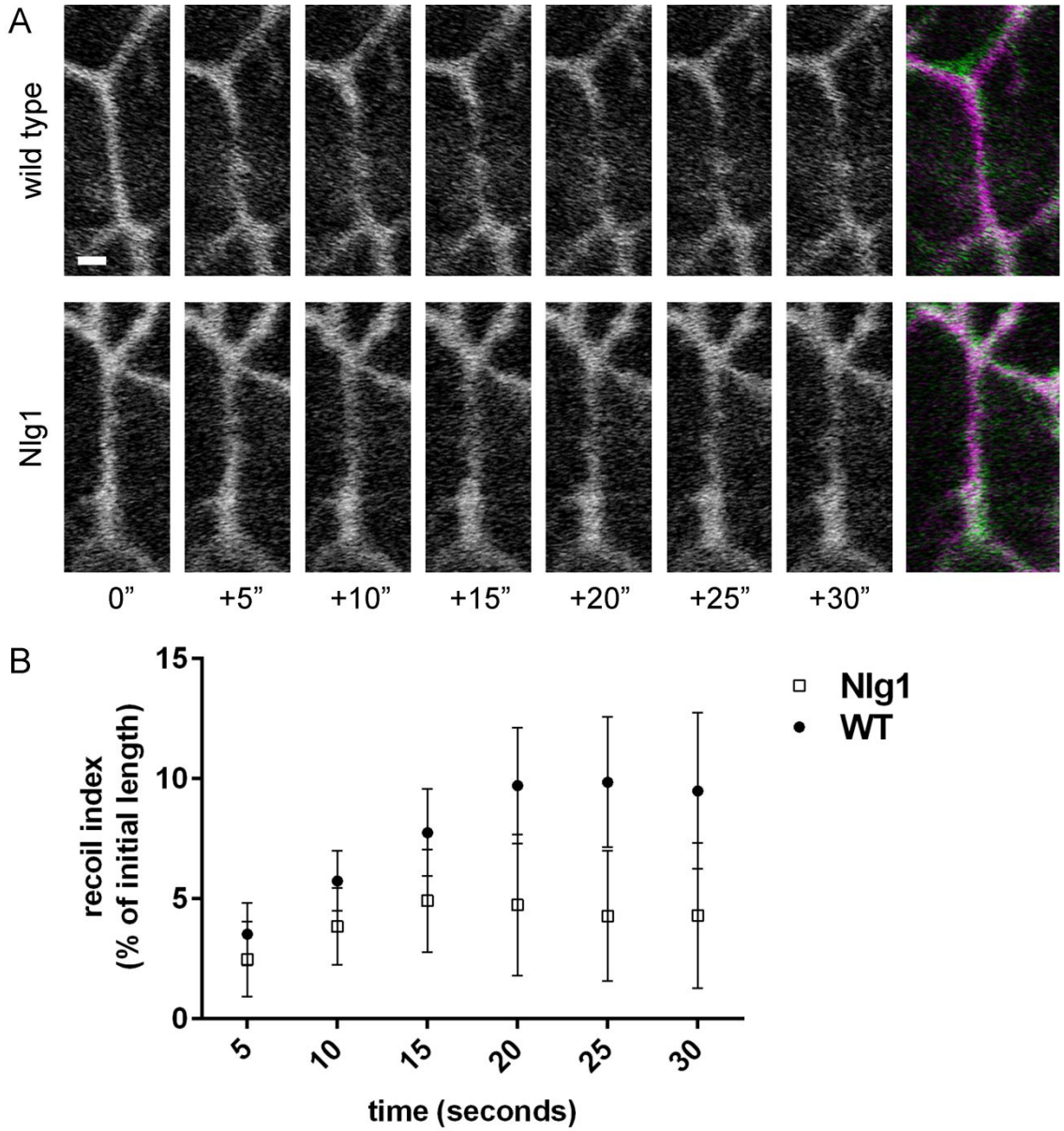

Figure 11. (A) Nlg1 null arborisations have a tension generation deficit during early arbor growth. Sequences of images 5 seconds apart show the recoil kinetics of a branch of a control arborisation at 36h APF and a branch of an Nlg1 null at 37h APF over 30 seconds following ablation with a 2-photon laser. The final frame of each sequence shows a composite of the frames at 0 seconds and 30 seconds. Motoneurons are expressing myr::GFP driven by *VGlut*-LexA **(B)** The recoil of 7 wild type branches and 6 Nlg1 null branches between 33h and 37h APF as a percentage of the branch lengths prior to ablation. Scale bars are standard deviation. Scale bar: 5μm.

The growth of the pleural arborisations is sensitive to Nlg1 levels from early in development

To determine if the pleural arborisations are responsive to Nlg1 signalling during the earliest stages of arbor growth, full length, untagged *Nlg1* (*Nlg1*-Untagged) was driven specifically in muscles using *Mef2*-GAL4. As mentioned, before the untagged version is known to be expressed at higher levels than the GFP tagged variant. To visualise the motoneurons myr::GFP was expressed under the control of *VGlut*-LexA.

From the very earliest stages of arbor development the growth of the axon terminals was disrupted by these elevated levels of postsynaptic Nlg1 (Figs. 12A&B). In comparison with those of wild types, these arborisations had compact, flattened branches, resembling large, filopodia-laden lamellipodia/growth cones. The effects of this gain of function were sustained and irrevocable; resulting in mature arborisations with broad, flattened arbor terminals that were greatly reduced in length and complexity in comparison with the controls (Figs. 12C&D). Interestingly, these branches also maintain a large number of filopodia into much later stages of development than would be expected normally. In contrast to evidence from the null experiments in which Nlg1 was removed globally, this targeted manipulation of Nlg1 signalling shows that it is sufficient to disrupt growth in a wild type neuron.

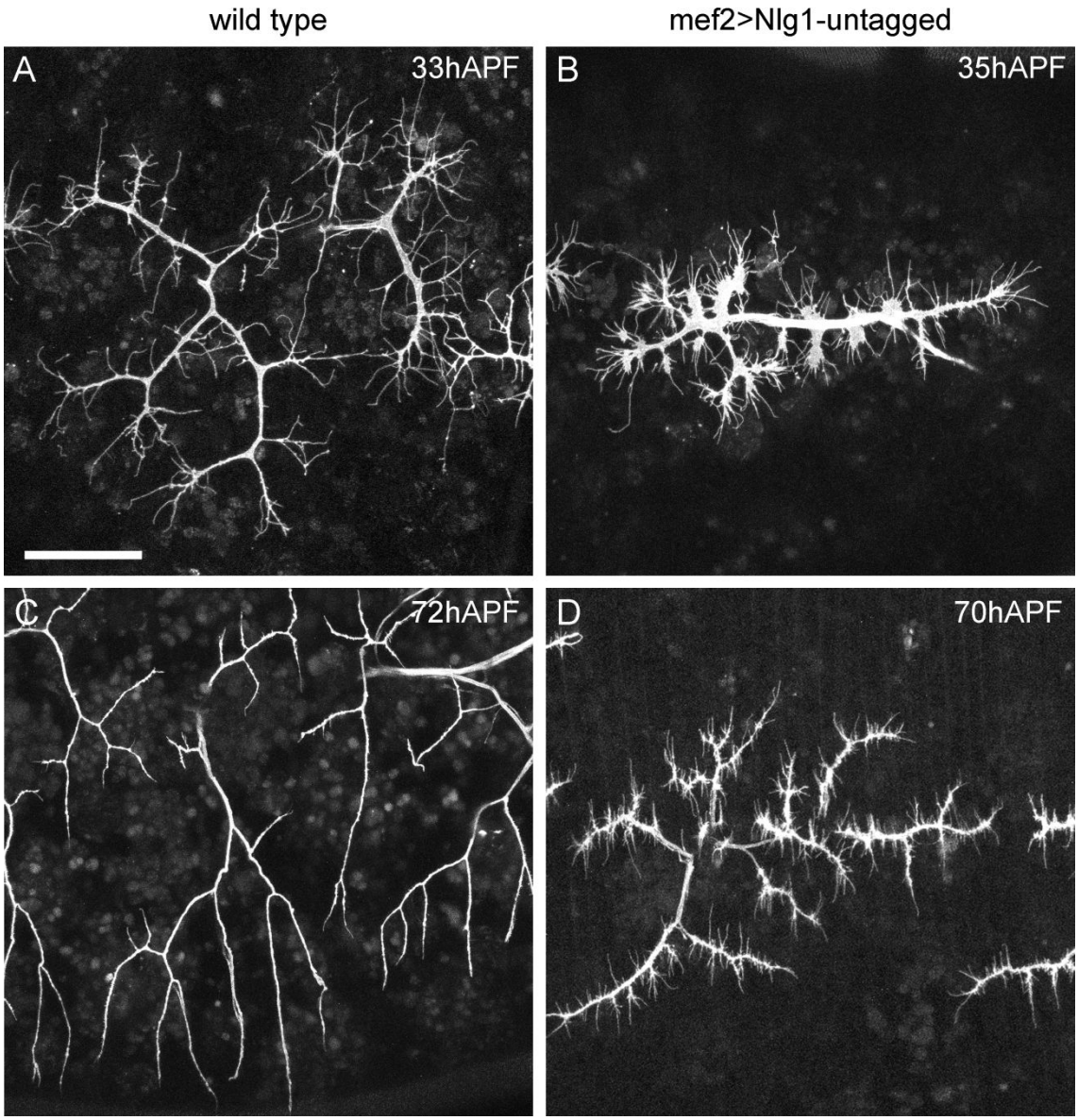

Figure 12. Increased postsynaptic Nlg1 levels have an impact on early presynaptic arbor growth (A-D) Arborisations expressing myr::GFP under *VGlut*-LexA control in wild type controls (left) and in backgrounds of *Mef2*-GAL4 *Nlg1*-Untagged expression (right) at early and late stages of arbor development. Scale bar: 50μm.

Local manipulations of Nlg1 expression result in local changes in arbor growth

Although full overexpression of *Nlg1*-Untagged in muscles shows that the pleural motoneurons are receptive to Nlg1 from the very earliest stages of elaboration it gives no indication as to whether this signalling influences arbor growth at a local or global level. To investigate the capacity that Nlg1 signalling functions during arbor

construction I devised set of tools and a protocol to enable the manipulation of Nlg1 levels in a local fashion. To achieve this I used *Mef2*-GAL4 driven expression and restricted it to muscle clones using the 'flip-out' Gal80 system described in chapter 1. These clones were visualised by the expression of membrane targeted mtdTomato whereas the motoneurons were revealed by myr::GFP expressed under the control of *VGlut*-LexA. Demonstrated in Fig. 13, the induction of clones at late larval or pre-pupal stages generates clusters of clonal myoblasts. These fuse to produce defined bands of muscle fibres with varying levels of expression depending on their fraction of +ve myoblasts that fuse in a single myotube. This assay acts much like an *in vivo* Bonhoeffer stripe assay, providing opportunity to present growing axon terminals with different choices of substrate types and allowing the local role of signalling to be explored (Walter *et al.*, 1987).

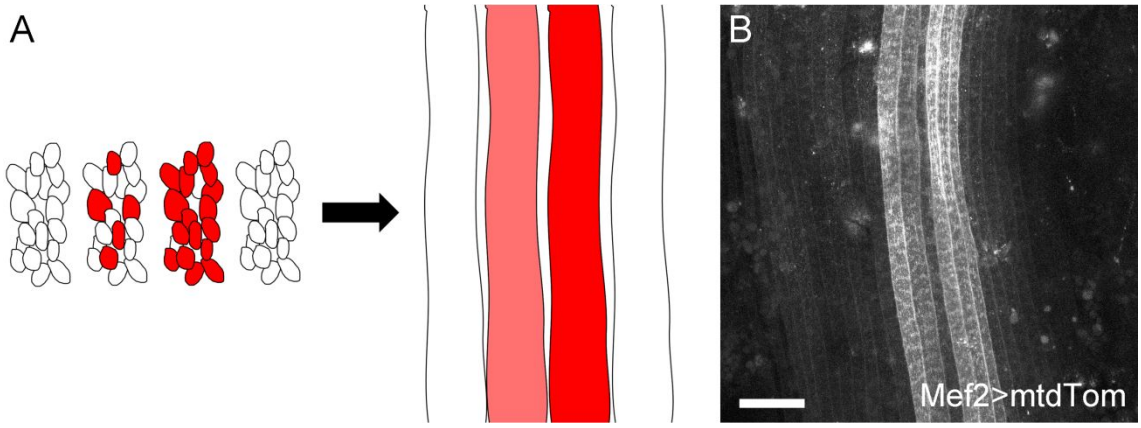

Figure 13. Gal80 'flip-out' muscle clones provide an *in vivo* stripe assay (A) A model demonstrating how stripes of muscle fibres with varying GAL4 expression levels are generated from pools of clonal myoblasts. The red cells indicate 'flipped-out' Gal80 clones **(B)** Clonal muscle fibres at 70h APF expressing mtdTomato under the control of *Mef2*-GAL4 generated using this strategy. Scale bar: 50*μ*m.

To explore the local influence of Nlg1 levels on arbor growth early, *Nlg1*-Untagged was overexpressed in muscle clones. At the later stages of arbor growth *Nlg1*-Untagged expressing clones were organised into bands of myotubes (Fig. 14A). In contrast with full postsynaptic *Nlg1*-Untagged overexpression, only arbor segments

in contact with the clonal muscles displayed the growth phenotype defined by stunted, engorged branches and a neotenous retention of filopodia. On the other hand, the segments of the same arborisations contacting wild type muscles or weakly expressing clonal fibres were morphologically typical. Interestingly, despite these symptoms of hyper-stabilisation, the branches in contact with the clones were still capable of branching and ramified with apparent preference into the territory of the high *Nlg1* expressing clones.

At the early stages of neuromuscular development clones consisted of clusters of immature myoblasts and myotubes (Fig. 14B). In these situations, arbor growth was directed disproportionally into the territories of these clonal cells in a manner highly suggestive of tropism. This is particularly evident in the magnified cutaway which demonstrates the preferential elaboration of an arbor segment onto a cluster of clonal myoblasts, leaving a segment in the non-clonal region relatively devoid of branches.

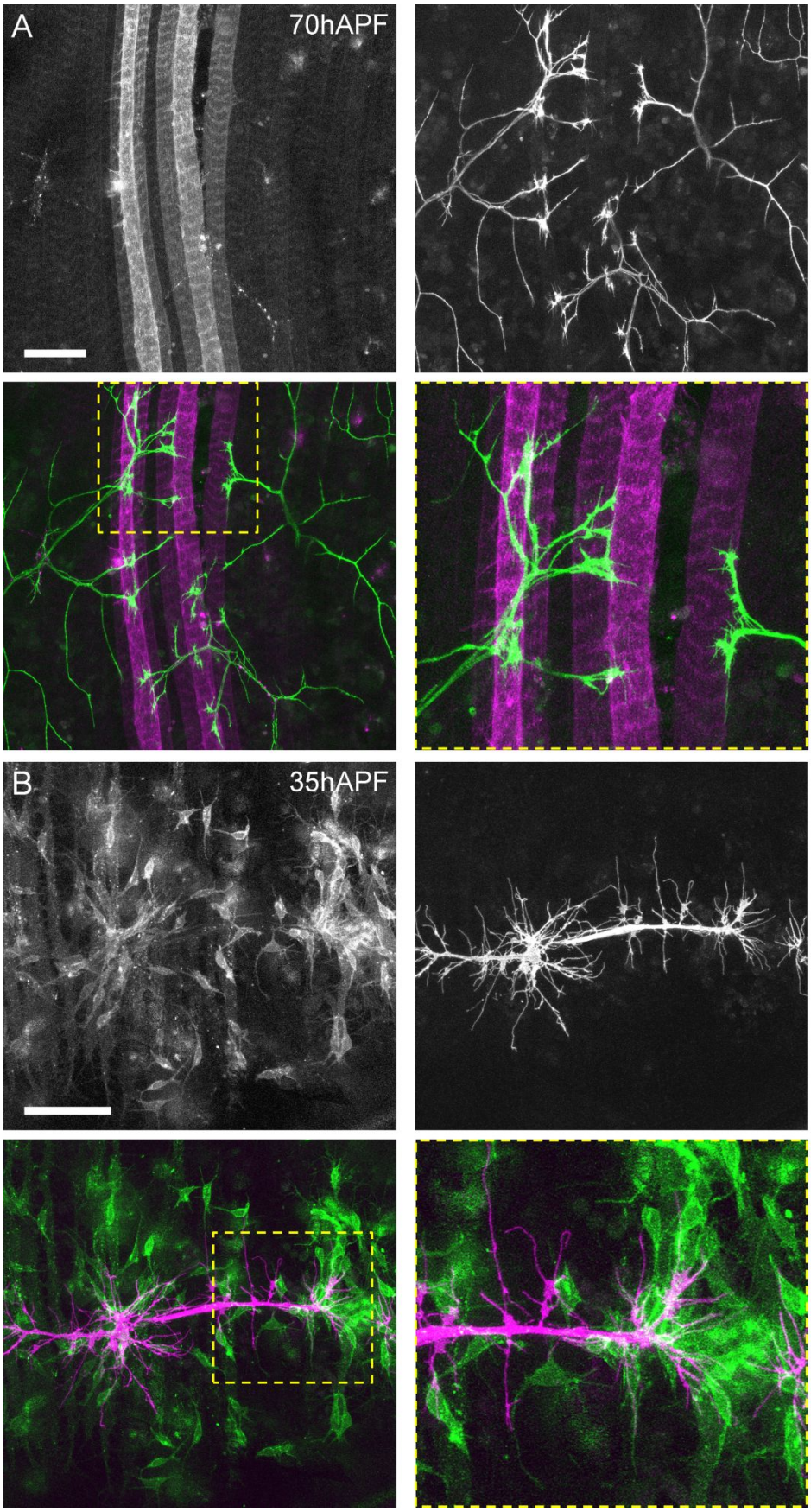

Figure 14. Local changes in Nlg1 levels elicit local changes in arbor growth (A) At 70h APF axon branches in contact with *Nlg1*-Untagged expressing muscle stripes

generated using 'flip-out' Gal80 show signs of hyper-stabilisation and preferential growth onto the clonal cells **(B)** At 35h APF motoneuron axon terminals elaborate preferentially into the territory of *Nlg1*-Untagged expressing myoblast clones. Motoneurons: *VGlut*-LexA>myr::GFP; muscle: *Mef2*-GAL4>mtdTomato. Scale bars: 50μm.

Ectopic Nlg1 overexpression reveals a tropic mechanism of arbor construction

The data presented so far implicates a role of trans-synaptic adhesion complexes in the structural development of the pleural neuromuscular junctions in a process with marked resemblances to the synaptotropic model of arbor growth first proposed by Vaughn. The synaptotropic hypothesis posits that growing arborisations will be directed preferentially into regions rich with more putative synaptic partners in a tropic manner. This was suggested already by outcome from the clonal overexpression of *Nlg1*-Untagged in muscles both early and late. However, as a more conclusive test of this mode of growth I took advantage of the anatomical organisation of the pleural system. Leaving the nerve at the same point as the pleural motoneurons are the v'ada neurons, a subtype of class IV da sensory neuron. During metamorphosis, these cells remodel to generate an adult specific morphology and generate complex 2-dimensional dendritic arborisations in the region between the pleural muscles and the epidermis of the adult abdomen (Fig. 15A). Thus, these arborisations lie directly atop those of the pleural motoneuron axons but are separated from them by the pleural muscles. Despite the clear separation in the mature system, during the outgrowth phase the neurites of each of these cells are able to interact. As a result, overexpression of *Nlg1* in the da neuron, which ordinarily has an asynaptic peripheral neuritic field, can be used to test whether a synthetic synaptotropic growth can occur between these two parties that never normally connect.

Thus *Nlg1*Δcyto::GFP or *Nlg1*-Untagged was expressed in v'ada neurons using *PPK*-GAL4 and the impact on motoneuron axon arbor growth was explored. *Nlg1*Δcyto::GFP lacks the cytoplasmic domain of the protein, but when driven in muscles was found to elicit effects on arbor growth comparable to *Nlg1*-Untagged. v'ada neurons were labelled with RFP and motoneurons were visualised by myr::GFP expression under *VGlut*-LexA control. At 50h APF exploratory motoneuron processes were found to make contact with *Nlg1*Δcyto::GFP expressing dendrites (Fig. 15B). In addition, these contacts were marked by the production of motoneuron filopodia. By 75h to 85h APF the expression of *Nlg1*-Untagged in the v'ada neurons resulted in motoneuron arborisations with stable branches which protruded between muscle fibres to make contact with the dendritic arborisations (Fig. 15E). In a number of cases additional growth from these ectopic contact sites had led to the generation of more connections and resulted in an increase in motoneuron arbor complexity. Demonstrated by branches projecting perpendicularly to the main arborisation in the transverse projection, these ectopic contacts conferred substantial changes to arbor morphology. In contrast, the branches of control neurons were found almost never to occupy the same territory as the v'ada dendritic fields and, as demonstrated by the transverse projection, produced arborisations with far more 2-dimensional configurations (Fig. 15D).

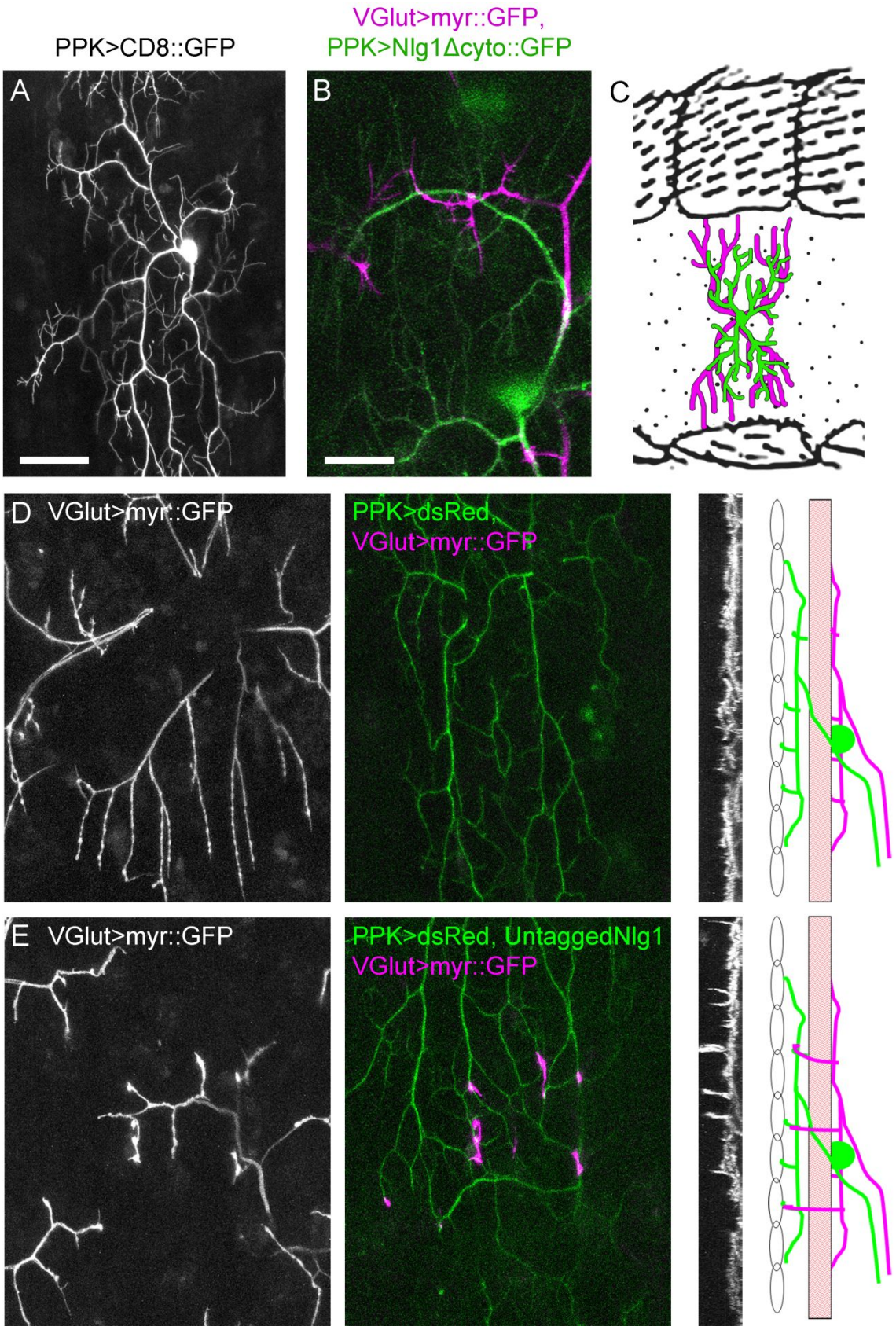

Figure 15. Ectopic expression of *Nlg1*-Untagged causes tropic changes in motoneuron arbor morphology (A) The dendritic arborisation of a v'ada sensory neuron at 80h APF expressing CD8::GFP under *PPK*-GAL4 control **(B)** Exploratory

motoneuron filopodia expressing myr::GFP under *VGlut*-LexA control (magenta) interact with dendrites of a v'ada sensory neuron expressing *Nlg1*Δcyto::GFP and dsRed under *PPK*-GAL4 control (green) at 50h APF **(C)** A schematic of the pleural region of an abdominal hemisegment shows the relative positions of the v'ada dendritic arborisation (green) and the axonal arborisations of the pleural motoneurons (magenta) (adapted from Ferris (1950) **(D&E)** Misexpression of *Nlg1*-Untagged in class IV da sensory causes motoneurons to extend branches between the muscle fibres to make contact with the dendrites of these cells. From a number of these contacts further branch growth can be seen. Transverse projections demonstrate the resultant changes in motoneuron arbor morphology. This is also illustrated in the schematic, again in a transverse orientation: The green cell represents v'ada and the magenta cell represents the motoneuron. The rectangular bar represents the muscle fibre and the ovals the epidermis. Scale bars: 25*μ*m (A, C&D) 10*μ*m (B).

Presynaptic machineries cluster at contacts induced by ectopic Nlg1 expression

An outcome predicted by the synaptotropic model is the 'stabilisation of synaptic junctions into functional connectivity patterns' (Vaughn, 1989). For this to be satisfied it should be expected that arbor segments generated via a synaptotropic mechanism would harbour synaptic terminals at maturity. To test this, abdominal filets were prepared from pharate adults expressing *Nlg1*Δcyto::GFP and CD8::GFP under the control of *PPK*-GAL4 (Fig. 16). To visualise presynaptic specialisations these were stained with an antibody against VGlut. To label nervous tissue, including the motoneurons they were stained with the neuronal membrane marker anti-Horseradish peroxidase (HRP). Indicated by the arrow in the first panel, a motoneuron branch delivers projections between a pair of muscle fibres which make contacts with the thinner dendritic processes. These contacts are marked by pronounced presynaptic varicosities. Shown in the second panel, complementary to these engorgements are intensities on the dendritic arbor, most likely marking concentrations of Nlg1Δcyto::GFP. Shown in the third panel, each presynaptic varicosity in contact with the da arborisation is marked by a conspicuous VGlut accumulation, revealing the accumulation of presynaptic machineries to these sites. The smaller aggregations of

VGlut along the length of motoneuron terminal not in contact with the sensory arborisation represent synapses onto the muscles.

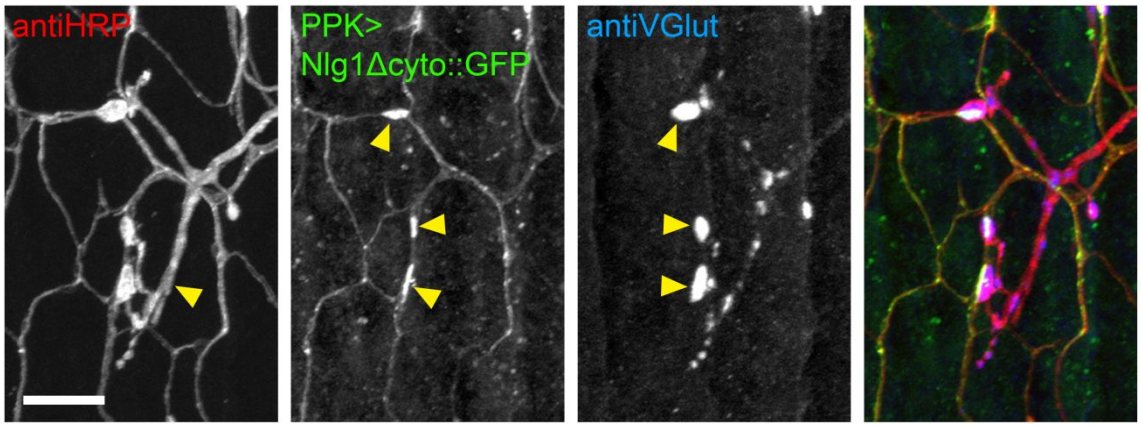

Figure 16. Presynaptic specialisations form on arbor segments generated by synaptotropic growth. From left to right: HRP reveals neuronal membranes; the arrow indicates a motoneuron branch. *Nlg1*Δcyto::GFP and CD8::GFP driven by *PPK*-GAL4 reveal the dendrites of a class IV da sensory neuron; the arrows indicate Nlg1Δcyto::GFP accumulations at contacts with the motoneuron. Anti-VGlut reveals presynaptic specialisations; the arrows indicate those at contacts with the dendrites. Scale bar: 10*μ*m.

Nlg1 and Nrx are dispensable for producing normal active zone densities

Conflicting evidence exists pertaining to the exact involvement of Nlg/Nrx signalling in synapse formation and maturation (Varoqueaux *et al.*, 2006; Chubykin *et al.* 2007). With this in mind I was interested to explore if the function of these components in the construction of the pleural neuromuscular junctions was directly coupled to a role in synapse formation. In order to test this, filets of pharate adult abdomens were prepared from *Nlg1* nulls and *Nrx* nulls as well as animals expressing *Nlg1*-untagged under *Mef2*-GAL4 control and wild type controls expressing myr::GFP under the control of *VGlut*-LexA. To visualise individual synapses these were stained with an antibody against BRP, anti-NC82, which has been used extensively to label synapses at larval NMJs (Fig. 17A).

In each condition, homogenously sized rows of BRP puncta line the terminals of the arborisations, as was observed in mature UAS-*BRP* expressing arborisations

shown in chapter 1. To the first approximation, the density of BRP puncta in the terminals of each of the nulls appeared no different from that of the controls. In addition, although the broader terminals of the gain of function arborisations resulted in greater local concentrations of puncta, the density within each terminal also appeared roughly consistent with the other conditions. To quantify these observations the density of puncta for each condition was calculated from 5 synaptic terminals (Fig. 17B). Synaptic terminals were defined as branch regions with synaptic boutons. As estimated, for each condition the density of puncta was remarkably similar, ranging between 1.0 and 1.2 puncta per μm^2. This is supported by a Kruskal Wallis analysis of variance which found no significant difference between the means of the groups (wild type = 1.22 per μm^2 (± 0.14 S.D), n = 4, *Nlg1* gain of function = 1.00 per μm^2 (± 0.21 S.D), n = 4, *Nlg1* null = 1.09 per μm^2 (± 0.12 S.D), n = 4, *Nrx* null = 1.01 per μm^2 (± 0.22 S.D), n = 4, H = 4.30, p = 0.24). This suggests that in each condition active zone assembly was able to occur as normal and that only the morphology of the arborisations was compromised by manipulating Nlg/Nrx signalling.

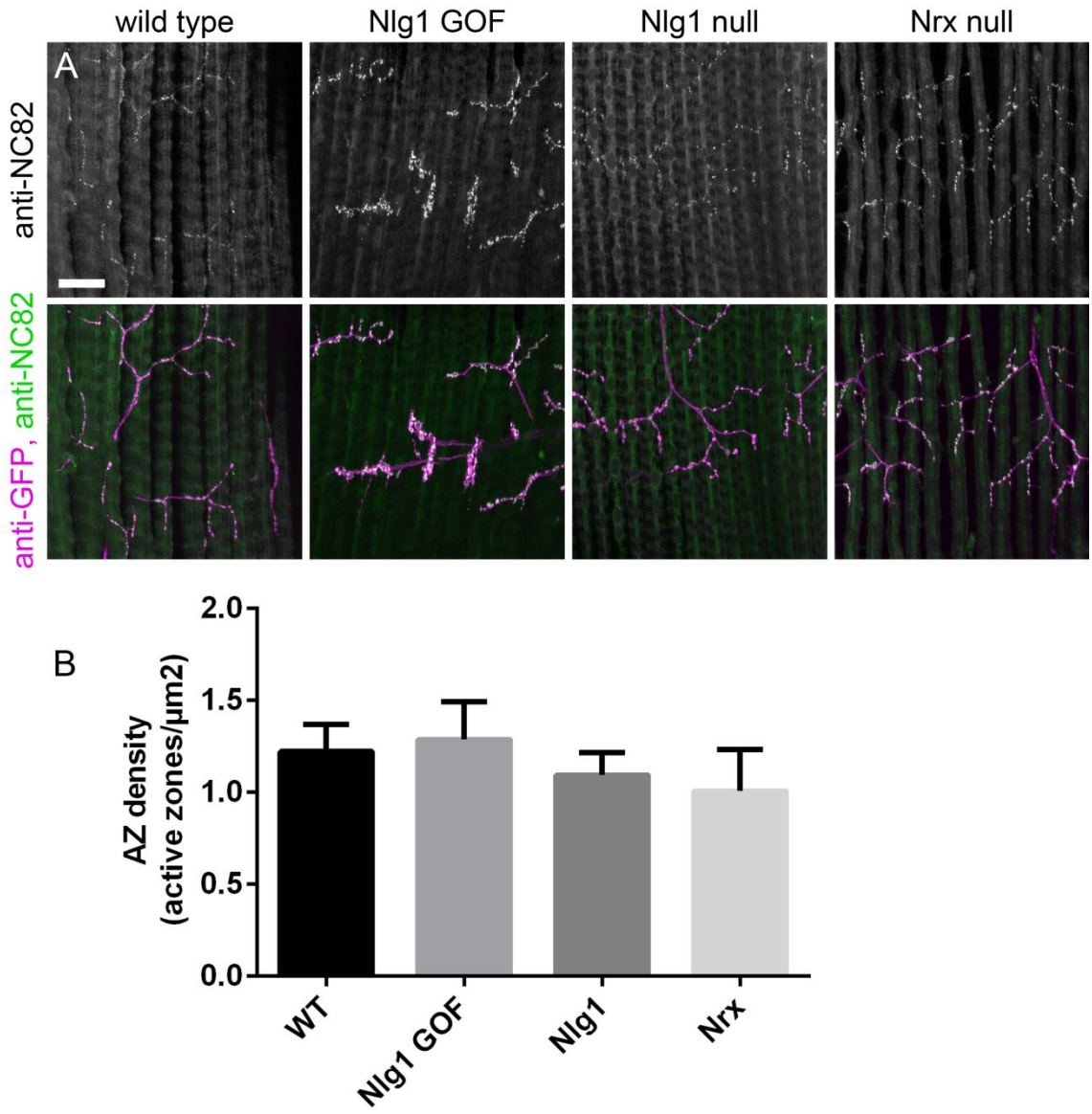

Figure 17. Active zone distribution is unaffected by manipulating Nlg/Nrx signalling (A) Antibody staining against BRP (anti-NC82) reveals active zone distributions in the synaptic terminals of *Nlg1* null, *Nrx* null, *Nlg1* gain of function and wild type controls. Myr::GFP expressed under *VGlut*-LexA control is amplified by staining against GFP **(B)** Active zone densities calculated from BRP puncta in the synaptic terminals of each of the above conditions (each measured from 5 terminals in the same sample). Error bars show standard deviation. Scale bar: 20*µ*m.

3.3 Discussion

The importance of trans-synaptic signalling complexes formed by Neurexins and Neuroligins during the assembly of neuronal circuits is evident from functional abnormalities recorded in knock-out studies on rodents and flies (Missler, *et al.*, 2003; Varoqueaux *et al.*, 2006; Chubykin, *et al.*, 2007; Li *et al.*, 2007; Banovich *et al.*, 2010). However, the degree to which these abnormalities can be ascribed to defects in arbor morphology is unclear. This has been difficult to tease apart in vertebrates due to the multiple copies of these genes and their functional overlap with other proteins. The synaptogenic properties of Neurexins and Neuroligins in culture make these proteins attractive candidates to be central players in synaptotropic growth, although there still remain questions as to their role in synapse formation *in vivo* (Scheiffele *et al.*, 2000; Dean *et al.*, 2003; Graf *et al.*, 2004; Chih *et al.*, 2005; Lee *et al.*, 2010). Using a combination of morpholinos and dominant-negative forms of Nlg and Nrx, an *in vivo* study on *Xenopus* brains has previously shown a key role for these proteins in stabilising filopodia during dendritogenesis as part of a synaptotropic-like mechanism (Chen *et al.*, 2010). With this new system of synaptotropic-like growth in the fly I explore this further and show how Nlg/Nrx mediated hemi-synapse pairings between synaptic partners contribute to this mode of growth.

Trans-synaptic Neurexin-Neuroligin signalling is essential for the generation of arbor shape

In previous work, *Drosophila Nlg1* and *Nrx* were determined to be required for the expansion of larval neuromuscular junctions following embryogenesis via the addition of synaptic boutons during larval life (Li *et al*, 2007; Banovic *et al.*, 2010). Using null alleles from these studies to observe full mutants at adult stages, this work has demonstrated that these adhesion proteins are also required during the

construction of the axonal arborisations of the pleural motoneurons. Mature arborisations of mutants exhibited severe deficiencies in total branch length and arbor coverage pointing to defects originating in early arbor growth. In previous studies, in situ hybridisation and transgenic rescues have demonstrated *Nrx* to be exclusively presynaptic and *Nlg1* to be exclusively postsynaptic at the *Drosophila* neuromuscular junction (Li *et al.*, 2007; Banovic *et al.*, 2010). This implies that the arbor growth phenotypes seen in *Nrx* nulls in the present study stem from defective trans-synaptic signalling. Since both mutants have very similar phenotypes, which could not be differentiated statistically, it is highly likely that both derive from defects in the same molecular pathway. Purified Nrx and Nlg family proteins have been shown to bind to one another via their extracellular domains in affinity purification assays (Ichtchenko *et al.*, 1995). More recently using a modified GFP Reconstitution Across Synaptic Partners (GRASP) tool in which GFP reconstitution only occurs upon Nrx-Nlg binding these proteins have also been demonstrated to form complexes across synaptic junctions *in vitro* (Tsetsenis *et al.*, 2014). Together this evidence indicates that the phenotypes exhibited here result directly from trans-synaptic interactions between Nlg1 and Nrx. It should be noted however that preliminary immunoprecipitation experiments were unable detect interactions between *Drosophila* Nrx and Nlg1 (Banovic *et al.*, 2010). In addition, these proteins have been shown to elicit different and even contradictory effects on synaptic organisation and transmission at the larval neuromuscular junction (Li *et al.*, 2007; Banovic *et al.*, 2010). What is more, *Drosophila* Nlg1 lacking an Nrx binding domain was able to partially rescue Nlg1 mutant phenotypes (Li *et al.*, 2007; Banovic *et al.*, 2010). This suggests that, at least in part, these proteins function through different molecular pathways or interact only indirectly.

The *Drosophila* larval neuromuscular junction has been a valuable tool for characterising Nlg-Nrx interactions. However, I propose that the role that these proteins

play in the present system is fundamentally different to the role that has been described for them in the larva. The growth defects of *Nlg1* and *Nrx* nulls at the larval neuromuscular junction were described as an inability to add synaptic boutons to mature, fully functioning axon terminals. As has been made clear already, this is a slow process involving the incremental addition of boutons. In contrast, the growth of the pleural neuromuscular junction is a dynamic process in which structural changes take place over a matter of minutes. What is more, at the larval neuromuscular junction Nlg1 and Nrx are thought to function by coordinating the formation of new synaptic scaffolds and aligning pre- and postsynaptic machineries. This has been shown to be dependent on interactions with active zone components including Syd1, a RhoGAP protein which plays a key role in coordinating synapse assembly, and Spinophilin, which in the context of mature synapses is believed to act as a scaffolding protein for other active zone machineries (Owald *et al.*, 2010; Owald *et al.*, 2012; Muhammad *et al.*, 2015). This contrasts with the mode of growth described for the present system which relies on the local stabilisation of filopodia by a mechanism apparently independent of active zone components (See chapter 1). As a result, I suggest that in this system Nlg/Nrx signalling plays a role during arbor growth by stabilising growing processes which is independent of a role facilitating the assembly of new synaptic apparatus.

Surprisingly branch number and complexity were unaffected by the loss of *Nlg1* or *Nrx*. This perhaps indicates that branching is regulated by an intrinsic, inflexible program of development and that only branch extension is subject to an interaction-dependent synaptotropic growth mechanism. However, this seems unlikely since branches where shown to mature from filopodia which in turn were shown to emerge from stable presynaptic puncta in a synaptotropic-like manner (see chapter 1). Alternatively, it is more likely that branching, but not branch extension, occurs under the control of fully redundant molecular mechanisms, or perhaps is determined by a

mechanism distinct from Nlg1/Nrx signalling. A potential candidate to play a role in this hypothetical pathway is the *Nlg1* homologue, *Neuroligin 2* (*Nlg2*). Unlike *Nrx* or *Nlg2* alone, double *Nlg2*/*Nrx* mutants are 2nd instar larval lethal and also exhibit more extreme larval neuromuscular junction growth phenotypes suggesting that to a significant degree these proteins operate through parallel pathways (Sun *et al.*, 2011).

In addition to the readily quantifiable phenotypes discussed above, a number of qualitative phenotypes were described in *Nlg1* and *Nrx* nulls which allude to the functions of these proteins during arbor growth. In each mutant, the arborisations generated exceptionally long, ectopic processes which failed to form synaptic varicosities. One possibility is that these represent an intrinsic element to arbor growth which is perhaps driven by bulk membrane insertion at growth cones or by the trafficking of cytoskeletal components to axon terminals. In the absence of a guidance mechanism these processes could conceivably lead to the formation of these abnormal processes. Alternatively, since these branches do not appear to host synapses, it could be imagined that these processes have adopted a redundant growth mechanism secondary to synaptotropic growth which directs them into abnormal territories. In addition to this, both mutants displayed a phenotype characterised by the splitting, or defasciculation of proximal axons. It is difficult to speculate on the cause of this, although reduced adhesion with the muscle would seem likely. Alternatively, the branch regions exhibiting by this phenotype correspond closely to the lengths of axon which are ensheathed by glia (data not shown). In other work these glia have been shown to stabilise adult *Drosophila* motoneuron axons via the neuronal cell adhesion molecule Fasciclin 2 and could conceivably also interact with axons by means of Nlg/Nrx signalling (Hebbar and Fernandes, 2010). In both mutants, the arborisations also showed distinct signs of detachment from the muscle membranes. This would appear to be clear evidence of a structural role of Nlg/Nrx interactions at synaptic junctions by

bringing the synaptic membranes into close apposition. Such a role for Nlg/Nrx signalling has been demonstrated before by ultrastructural analysis of *Nrx* null larval neuromuscular junctions (Li *et al.*, 2007). Finally, a phenotype observed only in *Nrx* nulls was the retention of exploratory filopodia until well beyond the elaborative phase of arbor development. This potentially points to a feedback mechanism by which filopodia numbers are negatively regulated by Nlg/Nrx signalling. Conceivably this could be a means of limiting arbor growth. This is perhaps similar to the influence of Nlg/Nrx signalling in the *Xenopus* tectum, where blocking Nrx signalling was found to inhibit the stabilisation of dendritic filopodia (Chen *et al.*, 2010). However, in this case the long-term impacts of these disruptions on filopodia growth were not recorded.

Neuroligin1 stabilises exploratory filopodia during early arbor growth

The morphometric analysis of mature arborisations revealed an important role for Nlg/Nrx signalling during arbor growth. Despite this, it does not indicate if this signalling contributes to the synaptotropic-like mechanism described in chapter 1. To explore when and where Nlg1 acts, GFP labelled Nlg1 was imaged live in muscles concurrently with the motoneurons using independent binary expression systems. From the earliest stages of arbor growth Nlg1::GFP was found to form puncta which align in perfect apposition to the axon branches. Since Neuroligins are believed to have a synapse-specific function, it could be assumed that these aggregations represent the postsynaptic halves of nascent hemi-synapse pairings (Südhof, 2008). Although pre- and postsynaptic elements of the same synapses are routinely observed live and *in vivo* at the *Drosophila* neuromuscular junction as well as in vertebrate cells *in vitro*, visualising these pairings in the context of complex arborisations live and *in vivo* has so far been impossible (Zito *et al.*, 1999; Craig *et al.*, 2010). By virtue of the nature of this system, my work demonstrates the formation of putative synapses between synaptic

partners in the context of a complex arborisation live and *in vivo* for the first time. To be able visualise the pairing of synaptic elements in this system we are currently constructing LexAop variants of *BRP*::RFP and *Nrx*::RFP.

High spatial resolution imaging revealed that stable Nlg1::GFP puncta concentrate at growth cones and at points of filopodia growth as well as along the lengths and at the tips of filopodia during the phase of arbor elaboration. Though more difficult to resolve, Nrx::GFP displays an equivalent punctate distribution within the motoneuron axons suggesting that these adhesion proteins are located at apposing nascent hemi-synapses. When compared to the active zone protein BRP::RFP however, these components were found to have subtly different distributions. Although the Nlg1::GFP and Nrx::GFP puncta are concentrated at points of branching and filopodia growth, these components are also arranged along the lengths of terminal branches during the early stages of growth. This perhaps suggests that during early growth only synaptic contacts at branch points mature via the recruitment of active zone proteins. In addition to this, unlike BRP::RFP, both Nrx::GFP and Nlg1::GFP also stabilise at filopodia tips. In zebrafish retinal ganglion cell axons the stabilisation of synaptic components at filopodia tips was correlated with filopodia stability, suggesting that the formation of synaptic contacts stabilises filopodia (Meyer *et al.*, 2006). To explore the existence of a similar mechanism in this system involving Nlg1, high frequency lapse imaging was performed on growing arborisations in a background of postsynaptic *Nlg1*::GFP expression. This revealed a robust relationship between filopodia stability and the existence of Nlg::GFP at their tips or along their lengths. Additionally, in a few cases stable Nlg1::GFP puncta positioned along the lengths of filopodia were seen to act as the limits of retraction during exploratory movements. Unlike the work in *Xenopus*, which demonstrated a role for Nlg/Nrx signalling in filopodia stability by disrupting interactions globally, or by causing significant

overexpression within the cell that was being imaged (Chen *et al*., 2010), this provides evidence that these proteins play a role at very local levels by stabilising individual filopodia. What is more this is the first time that synaptotropic interactions between a pair of synaptic partners have been demonstrated *in vivo*.

The observations of Nlg1::GFP puncta outside of the body of the myotubes combined with the observations of myopodia suggest that at least some synaptic contacts are formed between myopodia and filopodia. This complements the observations of Kohsaka *et al.* (2009) who showed that motoneuron axon growth cone filopodia in *Drosophila* are stabilised by myopodia tipped with the leucine rich repeat trans-membrane (LRRTM) protein Capricious during the innervation of the larval muscles, and is further evidence in support of a stabilising role of myopodia/filopodia interactions during arbor growth. From what has been shown of dynamics in vertebrate central nervous systems, one could imagine such interactions between the filopodia of two neurons.

In zebrafish, muscle innervation is pre-patterned by the clustering of acetylcholine receptors together with other postsynaptic components on muscle membranes prior to contact by motoneuron axons (Panzer *et al*., 2006). Such a mechanism does not appear to exist for the neuromuscular junctions described here. As opposed to being arranged as preformed puncta, postsynaptic Nlg1::GFP was found to coalesce at the tips of exploratory filopodia following their contact with the muscles. The diffuse covering of Nlg1::GFP on muscle membranes and Nrx::GFP on axon membranes suggests that puncta are accreted from a local supply of Nlg1 following contact formation. In a few instances the thickening and branching of filopodia was observed following the formation of an apposing punctum. This suggests that in addition to playing stabilising role, Nlg signalling contributes to synaptotropic growth by

orchestrating the cytoskeletal remodelling required for growth and branching. To explore how these processes contribute to arbor growth, longer time-lapse movies were recorded with lower rates of capture. This exposed a close relationship between Nlg1::GFP dynamics and arbor growth whereby branch extension is preceded by the formation of puncta on exploratory filopodia. Although the temporal resolution was too low to capture the selective stabilisation of subsets of filopodia, the order of events in combination with existing evidence implicating Nlg1 in filopodia stabilisation is highly indicative of a synaptotropic mechanism of branch extension involving Nlg1.

Nlg1 nulls display a tension generation phenotype during early arbor growth

If Nlg1 plays a role during early arbor growth the arborisations of *Nlg1* nulls should be expected to display differences to those of wild type neurons at this time. The most striking difference I saw was the greater 'bendiness' of the null branches. Following their stabilisation, wild type filopodia quickly straighten, indicating a rapid built up of tension. This leads to the construction of arborisations with relatively straight branches. Adding to this, observations of Nlg1::GFP revealed that filopodia apposed to Nlg1::GFP puncta are noticeably straighter than those without puncta, suggesting that tension generation is part of an *Nlg1* mediated synaptotropic mechanism. To test this idea, the relative tensile states of *Nlg1* null and wild type branches were gauged from the recoil of branch nodes following branch ablation. From this I found that branches in *Nlg1* nulls are under significantly less tension those in wild types. Could tension generation therefore be a significant factor in the construction of the pleural neuromuscular junctions? As has been demonstrated in *C. elegans*, transmembrane adhesions can contribute to neuron structure in a purely mechanical sense by acting as anchor points and preventing branch deformation (Heiman and Shaham, 2009). Furthermore, as is increasingly being found to be important in developing systems,

tensile forces can also be transduced into biochemical signals which could play a role in the stabilisation and maturation of synaptic contacts. As examples of this, a number of studies have shown neurons in culture to undergo growth in response to applied mechanical force (Bray, 1984; Lamoureux *et al.*, 2002; Smith *et al.*, 2001). It is also possible that tensile forces could induce branch stability. In fibroblasts cultures, mechanical forces exerted on the leading edges of cells results in local calcium transients via TRP channels homologous to those expressed in neurons (Wei *et al.*, 2009). Calcium influx has been demonstrated to be an important regulator of filopodia stability and dynamics and thus such a mechanism could offer a means of filopodia stabilisation in response to force generated via adhesions made with synaptic partners as part of a synaptotropic mechanism (Kater and Rehder, 1992; Lohmann *et al.*, 2002, Heiman and Shaham, 2010). Perhaps most relevantly however, mechanical forces exerted on *Drosophila* motoneuron axons were shown to restore synaptic vesicle clustering at larval neuromuscular junctions following axon ablation, thus pointing to a direct role for mechanical forces in synaptic maturation (Siechen *et al*, 2009). Regardless of its significance in terms of arbor growth, this phenotype reveals a role of Nlg1 signalling during the early growth of the axonal arborisations. That being said, this finding raises the possibility that mechanical forces might play a role in an Nlg/Nrx mediated synaptotropic mechanism. One means of testing this could be achieved by the mechanical perturbation of neuronal filopodia via the 'trapping' of membrane-bound magnetic beads, thus mimicking tension generated by the formation of a synaptic contact (Desprat *et al.*, 2008; Tyler, 2012).

If Nlg/Nrx signalling plays a role in arbor growth by stabilising filopodia it should also be expected to see a filopodia stability phenotype in *Nlg1* nulls. Although preliminary investigations of filopodia lifetimes did not yield statistically significant results between wild types and *Nlg1* nulls, the sample sizes used thus far though have

been low, and meaningful differences are likely obscured by the high rates of filopodia turnover in both conditions.

Nlg1 signalling impacts arbor growth in a cell non-autonomous manner

Global knock-outs of *Nlg1* and *Nrx* say nothing of the cell autonomy of Nlg/Nrx signalling during early arbor growth. As a result, from these experiments alone it cannot be claimed that the role of Nlg/Nrx signalling during this period is mediated by trans-synaptic complexes. To gain some insight into this, *Nlg1*-Untagged, which is known to be expressed at higher levels than *Nlg1*::GFP, was overexpressed only in muscles. From the earliest stages of neuromuscular development postsynaptic Nlg1-Untagged provoked strong gain of function effects on the growth of the arborisations of wild type neurons. For one this demonstrates that the arborisations are receptive to Nlg/Nrx signalling from the early stages of growth. Furthermore, it is highly suggestive that Nlg1 influences arbor growth in a non cell-autonomous manner, pointing to a role for the formation of trans-synaptic complexes involving postsynaptic Nlg1. This is not something that has been possible to demonstrate in vertebrate brains due to the vast unlikelihood of labelling synaptic partners. The phenotype elicited by *Nlg1*-Untagged overexpression is indicative of a hyper-stabilising effect on branch growth which results in broad, condensed arborisations at maturity. By comparison with the arborisations of *Nlg1* and *Nrx* nulls it seems that arbor growth is determined by a balance between stability and growth; too much stability and branches are bound too tightly to grow, too little stability and branches are unable to gain the traction required for growth. It could therefore be imagined from this that one means of regulating arbor growth is by 'dialling' up or down the levels of adhesion proteins

Interestingly *Nlg1* untagged overexpression also resulted in the retention of axonal filopodia until much later stages than would be expected usually. This seems at

odds with the observations of *Nrx* nulls which exhibited a similar phenotype. However, since *Nlg1* nulls showed no such phenotype, this suggests that the effect in *Nrx* nulls is mediated via an Nlg1-independent pathway. In this case, it could be interpreted that Nlg1 actually upregulates filopodia numbers, perhaps further evidence of growth role in promoting growth; however, as with any gain of function, this potentially neomorphic effect must be treated cautiously.

Nlg1 has a local influence on arbor growth

The relationship between filopodia dynamics and Nlg1::GFP puncta indicated a local action of Nlg1 signalling as part of a synaptotropic stabilisation mechanism. To test this idea, a protocol was designed to enable the local manipulation of Nlg1 levels. By generating muscle clones expressing *Nlg1*-Untagged, motoneurons were presented with a mosaic of wild type muscle and muscle enriched with Nlg1. Only the segments of axon branches in contact with the *Nlg1*-Untagged expressing clones showed the hyper-stabilisation phenotype, thus confirming that Nlg1 signalling influences arbor growth on a local scale. Furthermore, given a choice, branch growth appeared to be directed preferentially into the territory of the clonal muscles, providing the first evidence of Nlg1 mediated tropism.

Nlg1 drives growth in a synaptotropic manner

The evidence presented here suggests that Nlg/Nrx signalling directs arbor growth in a tropic manner via iterative rounds of filopodia stabilisation and growth. With inspiration from the work of Scheiffele *et al.* (2000) who demonstrated the sufficiency of *Nlg* to induce presynapse assembly when expressed in cultured HEK cells, this was tested by ectopic expression of *Nlg1*-Untagged in the multidendritic v'ada sensory neurons which do not usually make synapses in the periphery. This resulted in the formation of stable contacts between the dendrites and growing axon branches from

which further axon branch growth occurred in a synaptotropic manner, producing mature arborisations with abnormal 3 dimensional arbor shapes. I believe this is the first demonstration of synaptotropic arbor growth in an *in vivo* system. As predicted by Vaughn (1989), presynaptic machineries were recruited to these sites indicating their maturation into functional presynaptic terminals. These data raise an interesting point regarding the mechanism of synaptotropic growth in this system; since the da sensory neurons are unlikely to express glutamate receptors in their dendrites (although this is yet to be shown) and it would therefore appear that Nlg mediated synaptotropic growth is independent of neurotransmission. This corresponds with the apparent independence of synaptotropic stabilisation from active zone components suggesting perhaps that in this system synaptotropic growth takes place independently of neurotransmission. To truly test if Nlg/Nrx signalling drives synaptotropic growth and to test the cell-autonomy of this mechanism *Nlg1* null genetic mosaics would need to be generated. The lines to achieve this using MARCM are currently being built, along with Flip-Excision (FLEX)-based tools. FLEX is a tool which allows conditional control of endogenous gene expression (Fisher *et al.*, 2017). Within the FLEX construct an invertible, FRT flanked cassette encodes a splice acceptor and stop sequences in all 3 reading frames. Depending in its insertion orientation into a coding intron of a native gene, inversion of the cassette gives either a truncated protein product or can rescue the truncated protein to full-length. By taking advantage of the library of Mimic insertions made available by the Gene Disruption Project, we are generating lines capable of rescue and disruption of Nlg-1 by targeting FLEX to the 3rd coding intron of Nlg-1 via recombination mediated cassette exchange.

The role of Nlg/Nrx signalling in arbor growth is decoupled from a role in synapse formation

The roles that Nlg/Nrx signalling plays in the formation and maturation of synapses are hotly disputed. Mice lacking all 3 *Neuroligin* homologues which are expressed in the brain showed no abnormality in the density of synaptic contacts (Varoqueaux *et al.*, 2006). Likewise, mice lacking all 3 *α-Neurexins* (although not *β-Neurexins*) showed no changes in synapse density, leading the authors to conclude that Nlg/Nrx signalling is dispensable for the establishment of synapses (Missler *et al.*, 2003). This however overlooks the functional redundancy which has been demonstrated for Neurexins and Neuroligins with other cell adhesion proteins in vertebrates (Ko *et al.*, 2009; Siddiqui *et al.*, 2010; Soler-Llavina *et al.*, 2011). In contradiction with these findings, numerous studies have demonstrated the synaptogenic properties of Neurexins and Neuroligins *in vitro* (Scheiffele *et al.*, 2000; Dean *et al.*, 2003; Graf *et al.*, 2004; Chih *et al.*, 2005; Lee *et al.*, 2010). To explore the role of Nlg1 and Nrx in synapse formation in this system, presynaptic densities at the neuromuscular junctions of pharate adults were measured by staining the active zone component BRP. This revealed that in *Nlg1* nulls, *Nrx* nulls and *Nlg1*-Untagged gain of function animals the density of synapses per unit area of synaptic terminal is not considerably different. Although arbor morphology is affected in each condition, it appears that the capacity to form synapses is unaffected. This suggests that the role Nlg1/Nrx signalling plays in arbor construction is decoupled from synapse formation. This supports the observation that Nlg1::GFP and Nrx::GFP do not share the exact same distribution as BRP::RFP during early development. From these data, I put forward that the mechanism of synaptotropic growth in this system is based not on the formation of synapses but on the formation of proto-synapses built on adhesive Nlg/Nrx interactions. If this were true it would be expected that functional deficits resulting from

manipulations of these components would result from abnormalities in arbor growth, and therefore connectivity or the distribution of synapse, rather than synapse formation itself.

Conclusion

This work builds on previous work showing the importance of adhesion molecules in synaptotropic arbor growth by providing the first evidence for a role of Nlg1-Nrx mediated hemi-synapse pairing in the stabilisation of exploratory filopodia. What is more, it shows synapse-mediated tropism for the first time *in vivo*. This goes further to support the existence of a conserved mechanism of complex arbor construction between vertebrates and invertebrates. With the genetic mosaic tools, available to *Drosophila* the molecular pathways behind this mechanism and their cell-autonomy can now be explored in more depth than has before been possible.

Chapter 4

The role of synaptic activity in synaptotropic-like growth mechanisms

4.1 Introduction

The ability of neurons to modify their connections in response to activity is central to the formation of memories and to the maintenance of stable firing patterns (Citri and Malenka, 2008). These plasticity responses can involve functional changes to synapses or small scale structural changes to arbor morphology, for example the addition and removal of dendritic spines, via processes which are well described, if not yet fully understood (Yuste and Bonhoeffer, 2001). In contrast, the roles of activity and synaptic transmission in regulating the large scale structural changes which take place during early arbor growth are less clear. The synaptotropic hypothesis puts forward that synapse formation sculpts arbor shape by stabilising contacts made between synaptic partners. To build arborisations which are functionally appropriate it is an attractive idea that transmission contributes to this mechanism by 'use-testing' these nascent contacts.

In a number of species, from *Drosophila* to rodents, spontaneous, patterned activity is generated prior to the onset of experience-dependent sensory input (Gu *et al.*, 1994; Feller *et al.*, 1996; Ashworth *et al.*, 2002; Crisp *et al.*, 2008). Even after the onset of sensory input, considerable structural rearrangements to arbor morphology continue to take place during 'critical' early periods of development (Wiesel and Hubel, 1963; Sin *et al.*, 2002; Hua *et al.*, 2005; Tripodi *et al.*, 2008). As a consequence, investigating the importance of these modes of activity during nervous system development has been an active area of study.

One of the first places in which the role of activity in arbor growth was explored in depth is the mammalian visual system. When activity is blocked in the developing retinas the eye specific segregation of retinal ganglion cell axon territories in the lateral geniculate nucleus (LGN) is disrupted or lost (Shatz and Stryker, 1986; Rossi *et al.*, 2001). Furthermore, when the activity of a single eye is blocked, the axon territories of the remaining active eye are greatly expanded (Penn *et al.*, 1998). These data point to a role of activity in shaping arbor morphology by determining the outcome of competition for a synaptic resource. In conflict with this however, a number of studies have shown that activity does not play a major role in regulating arbor growth. Mice lacking the proteins Munc13 or Munc18, which are essential for spontaneous and evoked neurotransmitter release, build brains with grossly normal cytoarchitecture and synapse densities (Verhage *et al.*, 2000; Varoquoaeux *et al.*, 2002). Similarly, *Xenopus* larvae when immobilised for their full pre-motile development using a combination of chemicals or drugs display normal swimming behaviours upon their recovery and construct dendritic arborisations of normal complexity and size (Harrison 1904, Haverkamp and Oppenheim, 1986; Haverkamp, 1986). This suggests that activity is not required for arbor construction or for establishing the connectivity required for normal behaviour. It is very much possible that these contradictory findings reflect fundamental differences in the requirements of activity for normal arbor growth in different systems/species. This being said, these studies were somewhat limited. We now know that the drugs used in many of these studies, such as Chlorobutanol, TTX and lidocaine, fail to block all forms of early activity or neurotransmission which could play a role in growth (Gu *et al.*, 1994; Wong *et al.*, 2000; Lohmann *et al.*, 2002; Andreae *et al.*, 2012). Furthermore, without detailed time-lapse imaging of changes to arbor morphology *in vivo* it is impossible to get a complete picture of the importance of

activity to growth i.e. they may develop differently but look similar with endpoint morphometric analysis.

Much of what we know about the influence of activity on the dynamics of arbor construction comes from live imaging of zebrafish and *Xenopus* optic tecta. Although the findings from this work have not been entirely consistent, it is becoming clear that activity impacts axonal and dendritic arbor growth in subtly different ways. When NMDA receptor (NMDAR) mediated glutamate transmission is blocked globally, growing optic tectum cell (OTC) dendrites respond with a decrease in branch turnover, ultimately resulting in smaller dendritic arborisations (Rajan and Cline, 1998; Rajan *et al.*, 1999). On the other hand, the same treatment results in increased rates of branch addition and retraction of retinal ganglion cell (RGC) axonal arborisations, but does not lead to significant changes in arbor size and shape (Rajan *et al.*, 1999; Hua *et al.*, 2005, Fredj *et al.*, 2010). One study however observed that RGC axonal arborisations in globally silenced zebrafish brains had elongated peripheral branches which extended into wider territories than expected, suggesting that activity is required for refining, or sharpening, axon territories, perhaps in a competition-dependent manner as appears to be the case in the vertebrate LGN (Schmidt *et al.*, 2000). Together these data indicate that activity stimulates dendritic branch growth whilst simultaneously stabilising and slowing the growth of dynamic axon branches. This is supported by the fact that visual stimulation increases OTC dendrite outgrowth, but slows the growth of RGC axon arborisations (Sin *et al.*, 2002; Ruthazer *et al.*, 2006).

In contrast, when single RGCs or OTCs are silenced in otherwise active brains, their responses are quite different. Whereas globally silenced OTC dendrites show no response to light (Sin *et al.*, 2002), the dendrites of single cells silenced by overexpression of a dominant-negative glutamate receptor are destabilised by visual

stimulation, resulting in the retraction of branches (Haas *et al.*, 2006). This suggests that visually stimulated activity at least shapes dendritic arbor growth via a competition-based mechanism, perhaps by stabilising co-active synapses in a Hebbian-like manner. In contrast to globally silenced RGCs, the axon arbor morphology of singularly silenced cells is dramatically affected. The polarity of this effect however has been found to be diametrically opposite by different studies. One study found that silencing single RGCs using TeTxLC resulted in greatly enlarged axonal arborisations (Fredj *et al.*, 2010). On the other hand, silencing by expression of a mutant form of *Synaptobrevin 2* resulted in arborisations which were much smaller (Hua *et al.*, 2005). Although the reasons behind these conflicting results are not clear, it does suggest that, like the growth of OTC dendrites, activity impacts axon arbor growth in a manner dependent on competitive interactions.

Evidence suggests that OTC dendritic arborisations and RGC axonal arborisations grow via synaptotropic-like mechanisms, whereby synaptic elements promote branch growth and confer selective stability to filopodia (Niell *et al.*, 2004; Meyer and Smith, 2006). As a consequence, attempts have been made to explore the role that activity might play in this mechanism. Chen *et al.* (2010) showed that Nlg-Nrx interactions contribute to arbor growth by stabilising filopodia in a putatively synaptotropic manner. Furthermore, it was found that the hyper-stabilising effect of *Nlg* overexpression on OTC dendritic filopodia could be reversed by blocking NMDAR mediated transmission. This was taken to suggest that glutamate signalling is required to consolidate transient contacts mediated by Nlg/Nrx interactions as part of a synaptotropic-like mechanism. This assumption fits with other work which has shown that Nlg recruits NMDARs to nascent synapses via interaction with PSD-95 domain proteins, and that NMDAR mediated transmission confers stability to growing OTC dendritic branches (Barrow *et al.*, 2002; Sin *et al.*, 2002). Despite this it has yet to be

demonstrated that such an activity-dependent mechanism selectively stabilises small numbers of filopodia in a manner predicted by the synaptotropic hypothesis. On the other hand, the most compelling evidence of a role for activity in synaptotropic axon arbor growth comes from the work of Ruthazer *et al.* (2006). In this work, it was shown that visually evoked activity simultaneously increased the stability of branches marked by intense presynaptic puncta, whilst destabilising branches marked by weak or no puncta. This appears to reconcile activity-dependent axon arbor growth with synaptotropism by demonstrating a mechanism of transmission based 'use-testing' of synapses. Whether this mechanism contributes to major structural changes however is yet to be shown.

A problem many investigations into activity-dependence of arbor growth have faced is the inability of pharmaceuticals or genetic tools to reliably and precisely supress all forms of activity or neurotransmission. Many early attempts to silence transmission used TTX (Kaethner and Stuermer, 1994). It has since been shown however that much of the early activity in nervous systems is generated independently of voltage-gated sodium channel-dependent action potentials (Gu *et al.*, 1994; Wong *et al.*, 2000; Lohmann *et al.*, 2002). Likewise, blockade of receptors may be incomplete, or fail to consider the full complement of receptor types at the synapse. Furthermore, the possibility that spontaneously released neurotransmitter may play a role in arbor growth has recently gained traction. In culture, it has been found that spontaneous neurotransmission is at much higher levels during early arbor growth than in mature neurons (Andreae *et al.*, 2012). Moreover, it was shown that this form of neurotransmission has a specific role in shaping dendritic arbors by stimulating growth and branching (Andreae and Burrone, 2015). Similarly, in *Drosophila* spontaneous neurotransmission has been shown to have a specific role in regulating motoneuron axon arbor expansion during larval life (Choi *et al.*, 2014). Perhaps the most complete

knock down of synaptic transmission in vertebrates *in vivo* has been achieved by the generation of choline acetyl-transferase (ChAT) mutant mice, in which neurotransmitter acetylcholine (Ach) is unable to be biosynthesised (Misgeld *et al.*, 2002; Brandon *et al.*, 2003). In these animal's muscles became hyper-innervated by motoneuron axons which generated far greater numbers of terminal branches than usual. In contrast, no such phenotype was observed in animals paralysed *in utero* using TTX (Houenou *et al.*, 1987). Although this does not demonstrate a role for spontaneous neurotransmission, it does highlight the importance of considering the efficacy of different methods of silencing activity.

Our understanding of the molecular mechanisms underlying the activity-dependent regulation of arbor growth is still in its infancy. In the growing retina of the chick, localised neurotransmitter evoked calcium activity has been correlated with the stabilisation of RGC dendritic filopodia *in vivo* (Lohmann *et al.*, 2002). What is more, it was found that filopodia could be selectively stabilised by the local uncaging of calcium, demonstrating a calcium-dependent mechanism of filopodia stabilisation. In both *Xenopus* RGC axonal arborisations and OTC dendritic arborisations CaM-Kinase II activity has been shown to stabilise growing branches (Wu and Cline, 1998; Zou and Cline, 1999). It therefore seems likely that this plasticity associated pathway acts downstream of calcium activity to stabilise filopodia, how this is achieved though is yet to be shown. Very little is known about the retrograde signals which could regulate activity-dependent axon arbor growth and the pathways by which they might act, although two candidates, BDNF and arachidonic acid, have been shown to regulate the growth of RGC axonal arborisations in *Xenopus* or zebrafish, and as such are potential candidates to play a signalling role in synaptotropic growth (Alsina *et al.*, 2001; Schmidt *et al.*, 2004).

Evidence from a number of systems supports a role for activity in shaping arbor morphology. However, the degree to which this stems from a role in influencing the outcome of early contacts between synaptic partners, as opposed to later, competition-based refinements is unclear. Tackling these questions has been challenging due to the limited number of systems in which growing arborisations can be live imaged *in vivo* whilst concurrently manipulating activity. *Drosophila* presents the best model for reliably and precisely manipulating neurotransmission. By taking advantage of this I have explored the role of activity in this new model of synaptotropic-like growth in the fly.

4.2 Results

Using GCaMP to map the development of the pleural motoneurons

The role of activity and synaptic transmission during nervous system development has received enormous interest, and in some areas, it is well known which developmental processes these phenomena control. In the specific context of synaptotropic growth however, the involvement of their role is still poorly understood and existing studies have produced conflicting results. To explore the role of activity in the synaptotropic-like growth of the pleural neuromuscular junction I began by mapping the electrical development of the pleural motoneurons using the genetically encoded calcium indicator GCaMP6m as a proxy for activity.

To resolve calcium activity in the motoneurons, recordings of GCaMP6m expressing arborisations lasting 30 minutes were taken at 1 second intervals (1Hz). These data are displayed as heat-map registered kymographs (Fig. 1). In these spatiotemporal reconfigurations, each frame is collapsed in the y-axis. The resultant projections are then reassembled so that the vertical axis corresponds to the original x-axis of the images and the horizontal axis corresponds to the passage of time (or frame number) from left to right. Presented alongside these are cropped frames taken 10 seconds apart which feature representative examples of calcium events from the data set. The sudden change in pattern but not intensity represents refocusing of the microscope. Changes in GCaMP signal are represented by a change in the colour pallet i.e. towards orange/gold/white hues.

At 32h and 40h APF an absence of substantial deviations from baseline fluorescence suggest that at these early stages of dynamic arbor growth the motoneurons are largely inactive (Figs. 1A&B). Not until later during the phase of arbor elaboration, from 42h APF, were the first calcium transients recorded that were

indicative of membrane depolarisations, as indicated by the strong bar of yellow and gold (Fig. 1C). As demonstrated in the kymograph these initial events were isolated and infrequent. The single transient displayed in this example was synchronous between the 5 motoneuron arborisations within the field in focus, explaining the height of the band on the kymograph which spans the entire vertical axis. The width of the band shows that these early events were slow and sustained; reaching peaks within 1 second that lasted from 5 to 10 seconds before attenuating to base-line fluorescence over a similar duration. Soon after its initiation the frequency of calcium events rose quickly and by 48h APF activity was characterised by episodes of frequent calcium events lasting around 8 minutes interspersed by longer periods of quiescence (Fig. 1D). These episodes were found to consist of both synchronised and asynchronous transients, indicated by the bands of varying height on the kymograph. Unlike earlier transients, the events during these episodes had more rapid kinetics, peaking only for a second or 2 before attenuating over a comparable duration. Approaching maturity, at 74h APF activity continued to be defined by bouts of calcium events lasting in the region of 8 minutes (Fig. 1E). However, at this later stage these occurred more regularly, with intervals also lasting approximately 8 minutes, and included far greater number of events. As at previous stages, activity during this period occurred as both synchronised and independent events, however the kinetics at the later stage were extremely rapid, lasting no more than the duration of a frame (sampled at 1 Hz) and with no detectible periods of attenuation.

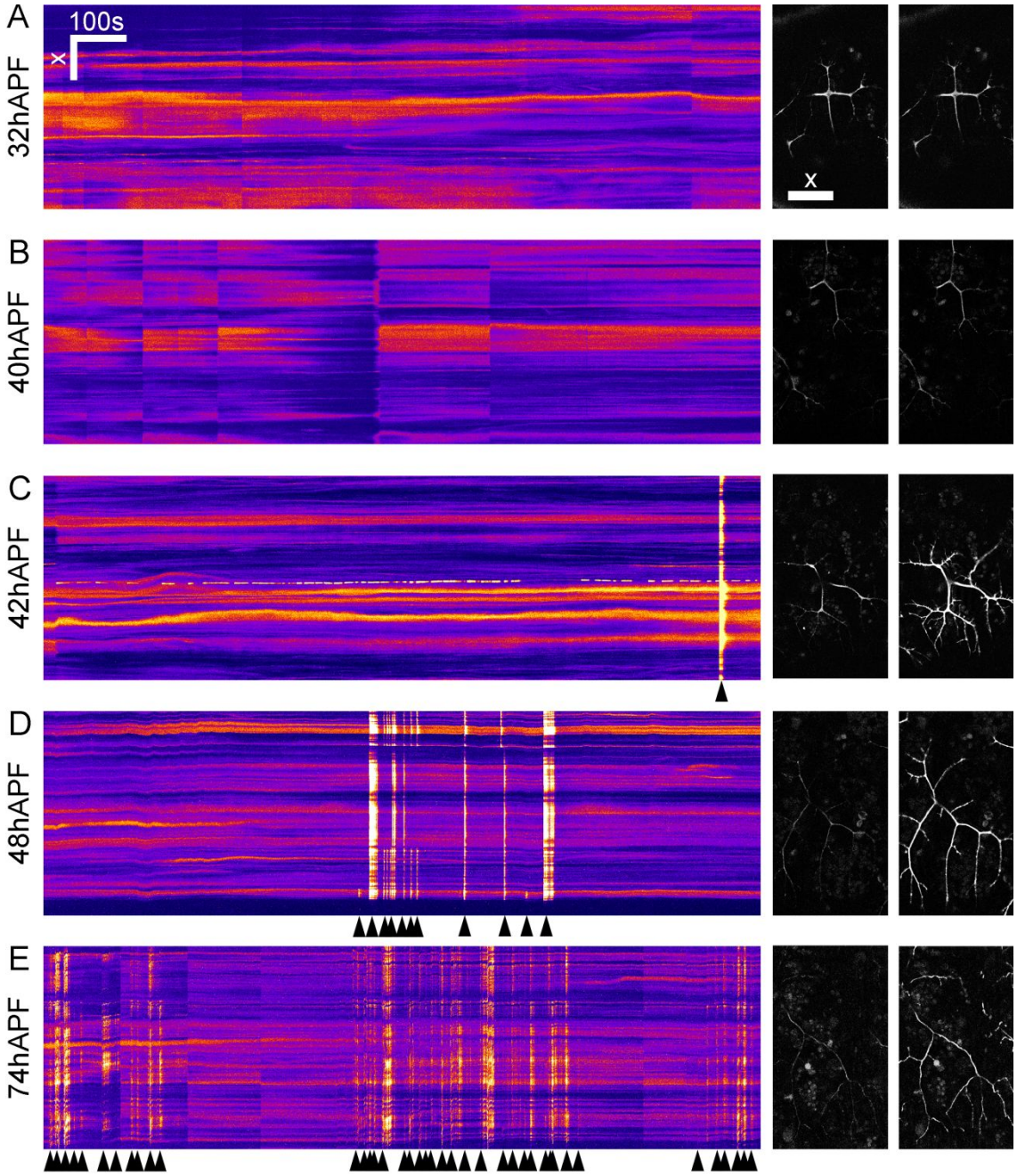

Figure 1. The development of presynaptic electrical activity (A-E) Kymographs showing calcium activity in the motoneurons from 32h to 74h APF measured by changes in GCaMP6m fluorescence. To the right of these images taken 10 seconds apart show representative examples of calcium recordings at each time point. The black arrows indicate calcium events or trains of indivisible events. Motoneurons expressing GCaMP6m under OK371-GAL4 control. Scale bar: 50μm.

Using GCaMP to map the development of the pleural muscles

To explore the parallel development of activity in the pleural muscles, GCaMP6m was expressed under the control of the muscle driver, *Mef2*-GAL4. As with the motoneurons, postsynaptic activity was recorded in 30 minute time-lapse movies (with the exception of the example at 70h APF which is marginally shorter) taken at 1 second intervals. These are represented in the kymographs in Fig. 2.

At the earliest stages of muscle development localised and sporadic calcium activity was recorded in individual myoblasts and in the immature myotubes (Fig. 2A). These events displayed variable kinetics, lasting from 3 to more than 20 seconds, but were consistently characterised by a slow and continuous rise and decay in intensity. At 40h APF this localised activity was found to persist in the few remaining unfused myoblasts, however no activity was recorded in the myotubes at this time (Fig. 2B). Only at 50h APF was the first calcium activity observed in the defined muscle fibres (Fig. 2C). These initial calcium transients propagated as waves across the pleural muscle field at rates of between 2 and 6 fibres a second and originated from both directions in the anteroposterior axis (Fig. 2E). In every case these travelled the full extent of the field in view and therefore their points of origin and termination are unknown at this stage in development. In contrast with the activity of the motoneurons at this period of development, these transients showed no obvious periodicity, instead occurring as relatively isolated events in an apparently stochastic manner. In contrast with this, by 70h APF the incidence of calcium events in muscles was far more like that of the motoneurons, with periods of frequent bursts of activity lasting approximately 8 minutes interspersed by comparable periods of quiescence (Fig. 2D). Muscle calcium events at this stage are dominated by the synchronised depolarisation of ‘blocks’ of fibres (Fig. 2F). Though the precise composition of these units of fibres varied between

these events, as demonstrated by the irregular heights of the bands on the kymograph, trends of coordinated activity among spatially related groups were clear. Unlike the earlier ‘wave-type’ events, these ‘blocks’ typically do not propagate, but instead occur simultaneously in all of the fibres involved. As indicated in Fig. 2D, a few sporadic ‘wave-type' events continued to be observed at these later stages, however at this time these were more restricted, often originating in frame and terminating abruptly.

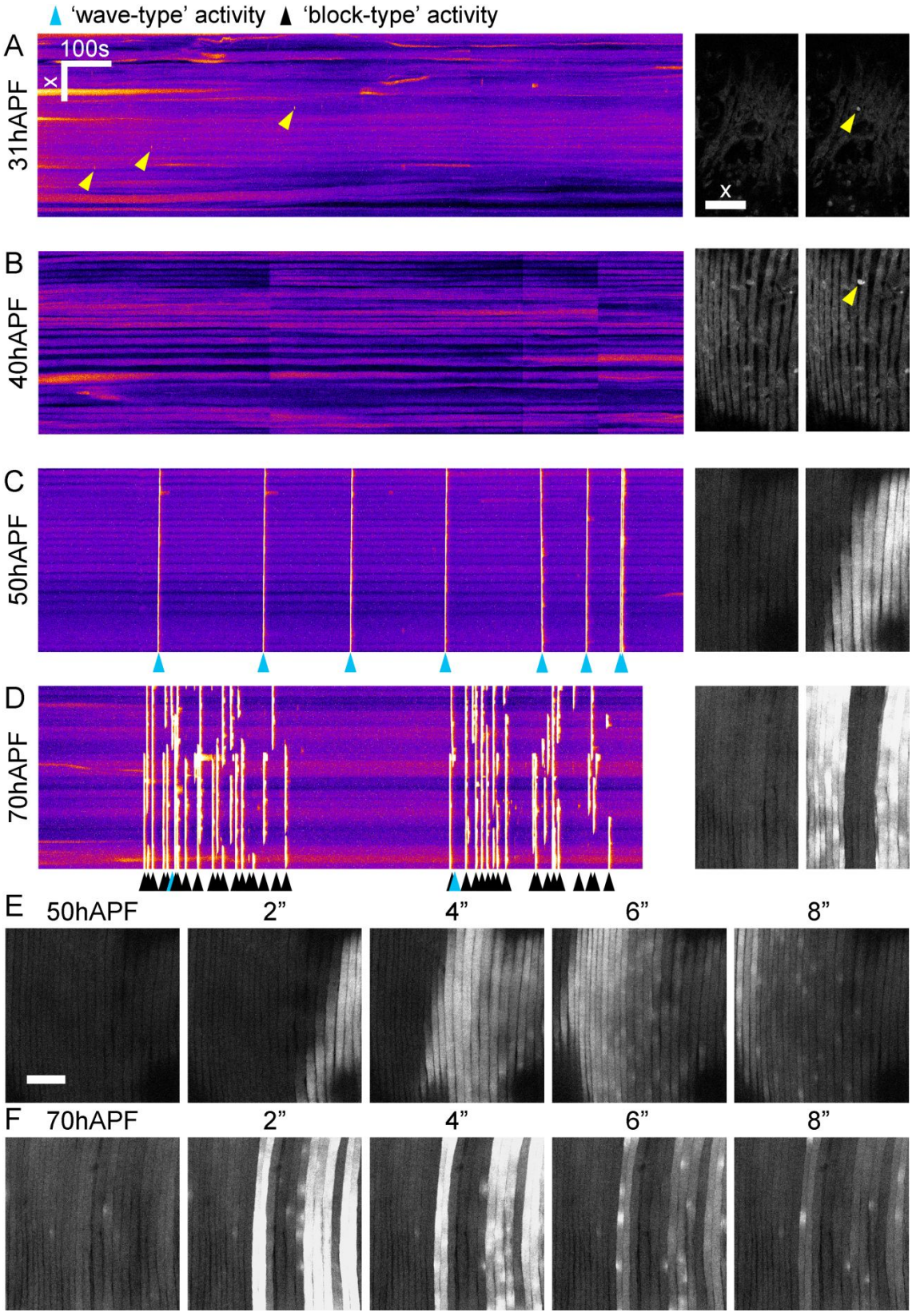

Figure 2. The development of postsynaptic electrical activity (A-D) Kymographs showing calcium activity in the muscles from 32h to 74h APF measured by changes in GCaMP6m fluorescence. To the right of these images taken 10 seconds apart show representative examples of calcium recordings at each time point. The yellow arrows indicate early, localised calcium event. The blue arrows indicate 'wave-type' activity.

The black arrows indicate 'block-type' activity **(E)** An image sequence with 2 second intervals showing the propagation of a calcium 'wave' at 50h APF **(F)** An image sequence with 2 second intervals showing an incidence of a 'block' of calcium activity at 70h APF. Muscles expressing GCaMP6m under *Mef2*-GAL4 control. Scale bars: 50μm (A-F).

Synaptic blockade suppresses 'block-type' muscle activity but not 'waves'

The timings of the calcium event development in the pleural synaptic partners display broad similarities, however at closer inspection the precise patterns of these activities appear not to become congruent until later stages of development. Leading on from this it was intriguing to investigate the dependence of postsynaptic activity on synaptic transmission over the course of development. To achieve this, I used a temperature sensitive allele of *Drosophila Dynamin*, *Shibire^{TS}*, in combination with calcium imaging in the muscles using GCaMP6m. Dynamin is a GTPase required for the scission of clathrin coated vesicles during endocytosis and thus is necessary for the recycling of neurotransmitter vesicles (Kosaka and Ikeda, 1983). At temperatures below 22^{o}C Shibire^{TS} functions normally, however beyond 30^{o}C its activity is inhibited, leading to a depletion of synaptic vesicles and a reversible synaptic blockade. I designed an improvised Peltier stage (a thermoelectric heat pump) that allowed me precise and rapid control of the temperature whilst imaging calcium events in whole intact pupae. By calibrating The Peltier device to 33^{o}C, neurotransmission could therefore be temporally restricted during live imaging. During each experiment imaging commenced at the permissive temperature (~20^{o}C), followed shortly by elevation to the restrictive temperature, before finally returning to the permissive temperature. The timings of these periods are represented by the coloured bars atop the kymographs in Fig. 3, with green corresponding to the permissive temperature and red corresponding to the restrictive temperature.

Inhibiting neurotransmission via *Shibire^{TS}* had no impact on early, localised calcium activity. Though not discernible in a kymograph, an example of such an event taking place at the restrictive temperature is demonstrated in Fig. 3A. This deduction was supported by quantification which revealed that at permissive temperatures these events occur at a rate of 3.83 (± 1.84 S.D) per minute (within the myoblast cluster of one hemisegment), compared to a rate of 3.93 (± 1.41 S.D) per minute at 33^{o}C (n = 2).

Inactivation of Shibire^{TS} also failed to suppress activity during the epoch of 'wave-type' events, and in fact correlated with an increase in its frequency. With the caveat of a small sample size, all 4 'waves' recorded in samples at 50h APF were found to occur at the restrictive temperature, as exhibited by the kymograph in Fig. 3B (n = 2). This was supported by the data from 60h to 70h APF, the period of transition from 'wave-type' to 'block-type' activity, in which elevation to the restrictive temperature also saw an increase in muscle 'waves' from 0.17 (± 0.13 S.D) per minute to 0.68 (± 0.51 S.D) per minute (n = 3) (Fig. 3C). In contrast with this however, 'block-type' activity at this stage was reduced considerably from 0.24 (± 0.35) S.D per minute to just 0.03 (± 0.04 S.D) per minute upon inactivation of Shibire^{TS} (n = 3). Interestingly, lifting the synaptic blockade was often met with brief but intense episodes of 'block-type' events, as is shown in the kymograph.

At ages between 75h and 80h APF, i.e. during the phase dominated by 'block-type' activity, the impact of Shibire^{TS} inhibition was most pronounced (Fig. 3D). At this stage 'blocks' were found to occur at a rate of 1.94 (± 0.29 S.D) per minute at the permissive temperature, however at the restrictive temperature these were reduced to 0.53 (± 0.13 S.D) per minute (n = 3). As indicated by the kymograph, many of the events that did occur during the periods of inhibition took place during the first few seconds following the raise in temperature, when a pool of neurotransmitter filled

vesicles would still have been available. Though scarcer at this stage, 'wave-type' activity once again failed to be inhibited by the inactivation of Shibire^{TS}, with 3 'wave' events recorded at the restrictive temperature and 1 recorded at the permissive temperature.

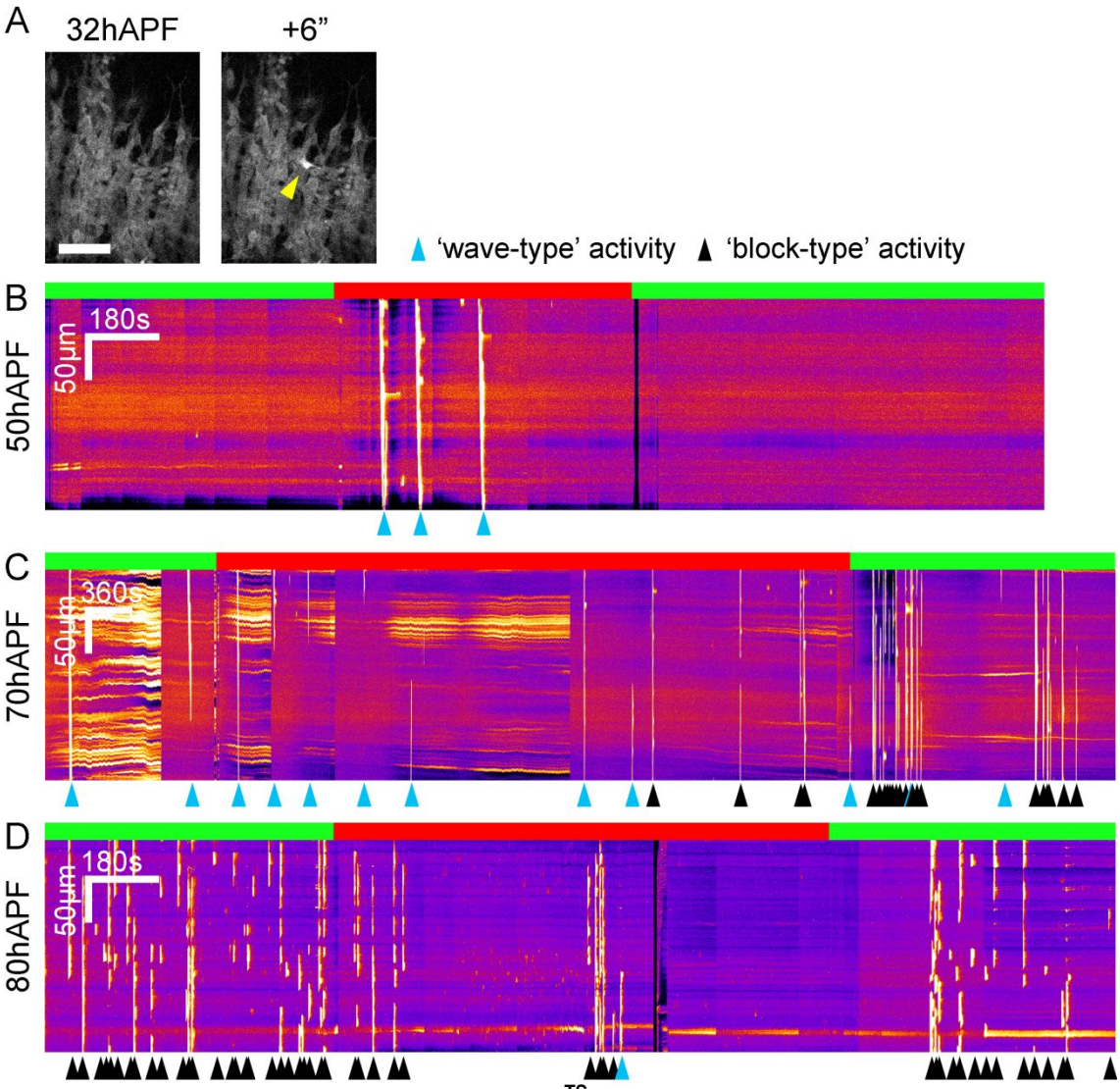

Figure 3. Synaptic blockade with Shibire^{TS} supresses 'block-type' but not 'wave-type' calcium events in the muscles (A) Sequential images 6 seconds apart showing a cluster of myoblasts at 32h APF in a Shibire^{TS} mutant demonstrate a calcium event in a single myoblast at the restrictive temperature **(B)** Kymographs at 50h, 70h and 80h APF show the rates of 'wave-type' and 'block-type' events in muscles of Shibire^{TS} mutants. Green bars represent the permissive temperature, red bars represent the restrictive temperature. Muscles expressing GCaMP6M under the control of *Mef2*-GAL4. Scale bar: 30μm.

Muscle 'blocks', but not 'waves', are dependent on motoneuron activity

As a further test of the hypothesis that early 'wave-type' is muscle autonomous, calcium activity in the muscles and motoneurons was recorded simultaneously by concurrent expression of GCaMP6m under the control of OK371-GAL4 and *Mef2*-GAL4.

In pupae aged between 60h and 65h APF, before the onset of 'block-type' events, 'wave-type' events were predominantly incongruent with motoneuron activity, with only 16.1% (± 13.7 S.D) found to be associated with motoneuron transients (n = 4) (Fig. 4A). A caveat however is that many of these 'waves' originated from beyond the limits of the field of view and therefore may possibly have been evoked elsewhere. However, of the 5 'waves' that were observed to originate within the imaging field none coincided with motoneuron activity (n = 1). In contrast to this, in pupae staged between 70h and 78h APF, 95.7% (± 3.9 S.D) of 'block events' coincided unambiguously with motoneuron activity (n = 3) (Fig. 4B). Interestingly however, at this later stage 68.9% ± (32.2 S.D) of the recorded 'waves' were also associated with motoneuron firing (n = 2).

To further dissect the relationship between motoneuron activity and the different modes of muscle activity, Tetrodotoxin (TTX) was used to pharmacologically silence motoneuron firing in pupae expressing GCaMP6m in muscles and motoneurons. TTX is a selective blocker of voltage-gated sodium channels and as a consequence suppresses action potential generation in neurons (Narahashi *et al.*, 1960). *Drosophila* muscles on the other hand, which do not use voltage-gated sodium channels for their depolarisation are unaffected by TTX. As described within the methods, 0.5mM TTX was administered to 4 animals at 73h APF by injection an hour before imaging. Demonstrated in the kymograph, in every case TTX administration resulted in complete abolition of detectable motoneuron calcium transients (n = 4) (Fig. 4C). Furthermore, at

a time predominated by ‘block-type’ muscle events under normal conditions, this mode of activity was also totally eliminated. Conversely however, the few ‘wave-type’ events at this stage failed to be suppressed by silencing motoneuron activity. Quantification of these events revealed that ‘waves’ occurred in TTX affected samples at a rate of 0.11 per minute (± 0.14 S.D) (n = 4). For contrast, in un-injected animals staged between 70h and 78h APF the rate of ‘wave-type’ activity was calculated at 0.20 per minute (± 0.24 S.D) and the rate of ‘blocks’ occurred at 0.81 per minute (± 0.77 S.D) (n = 4).

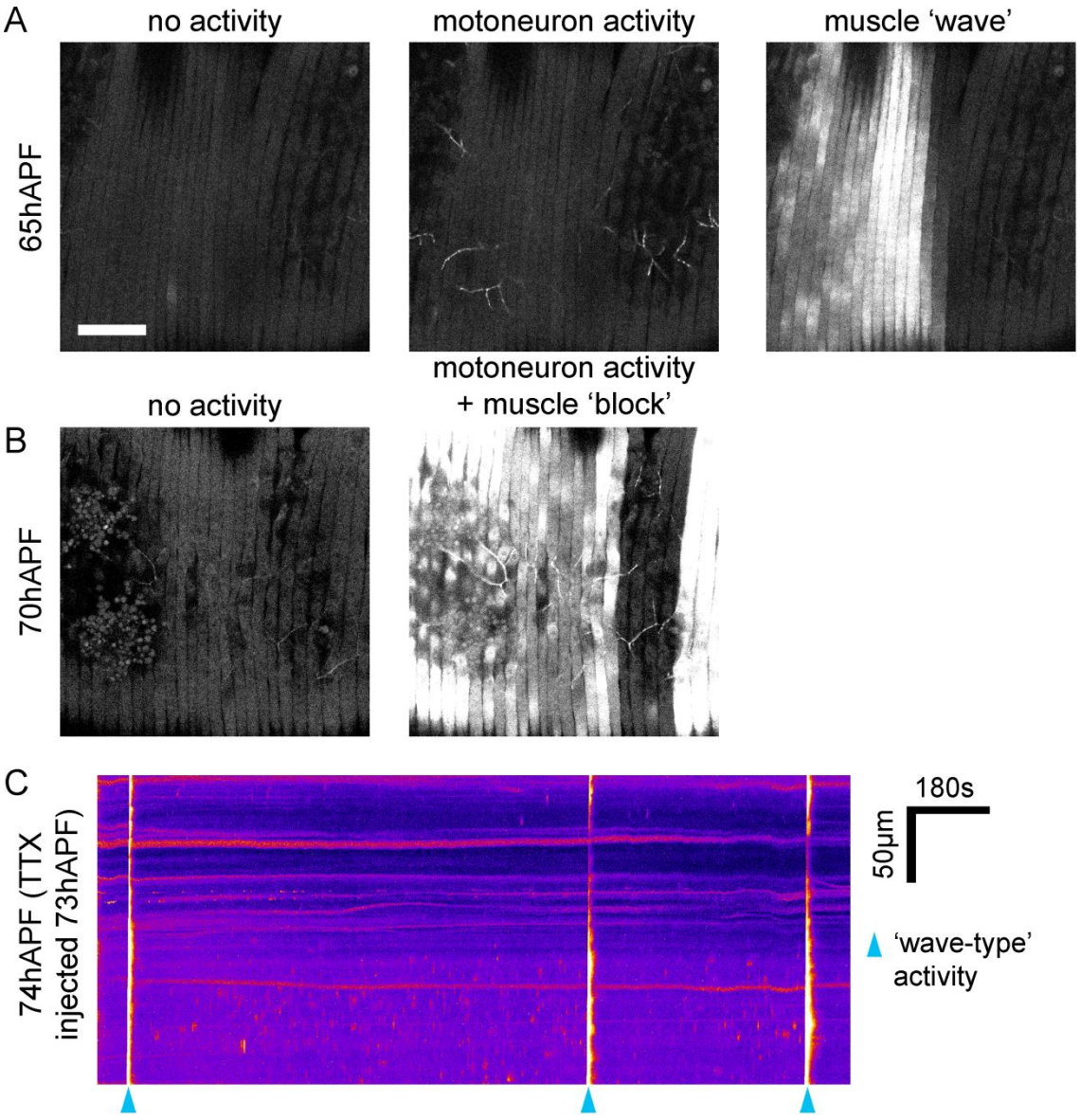

Figure 4. ‘Wave-type’ but not ‘block-type’ calcium events are independent of

activity in the motoneurons (A&B) Sequential frames from time-lapse movies showing calcium activity in the pleural muscles and motoneurons expressing GCaMP6M under the control of OK371-GAL4 and *Mef2*-GAL4. (A) At 65h APF muscle 'waves' are incongruent with motoneuron activity. (B) At 70h APF muscle 'block-type' events occur concurrently with activity in the motoneurons **(C)** A kymograph showing GCaMP6M activity at 74h APF in the pleural muscles and motoneurons of a pupa injected with 0.5mM TTX an hour prior to imaging. Scale bar: 50μm.

'Block like' activity in the muscles cannot be evoked by motoneuron activity until around 70h APF

Evidence from correlative relationships as well as pharmacological and genetic disruptions strongly suggests that postsynaptic calcium activity is independent of activity in the motoneurons until the later stages development of the pleural neuromuscular junctions. A potential reason for this is that neurotransmission is not possible at these junctions until towards the end of the pupal stages. To test this hypothesis artificial stimulation of neurotransmission was attempted by the induction of presynaptic membrane potentials using the warm sensitive ion channel TRPA1. At temperatures above 25^{o}C TRPA1 acts as a non-selective cation channel and as a result can initiate action-potentials (Hamada *et al*., 2008). Thus, mounting samples on a Peltier device bestowed the ability to induce motoneuron activity during live imaging sessions. As with the data from the *Shibire^{TS}* experiments, shifts in temperature are indicated by the coloured bars atop the kymographs (Fig. 4). However, in the case of these green corresponds to the higher permissive temperature (30^{o}C), whereas red corresponds to the lower restrictive temperature (~20^{o}C).

As a proof of principle calcium activity was recorded in motoneurons expressing *TRPA1* and GCaMP6m under the control of OK371-GAL4 at 27h APF. Although normally electrically inactive at this stage, these neurons displayed robust calcium responses in response to TRPA1 gating (Fig. 5A). To drive neurotransmission whilst

recording postsynaptic calcium activity, *TRP1A* was expressed under the control of *VGlut*-LexA and GCaMP6m expressed under the control of *Mef2*-GAL4. In samples staged between 40h and 49h APF no postsynaptic activity was observed at either the permissive or restrictive temperatures (n = 2) (Fig. 5B). Although a small number of 'wave-type' events were recorded in samples between 50 and 59h APF, in each case these occurred either during the last 10 seconds of the 2 minute periods at the permissive temperature, or else during the periods at the restrictive temperature (n = 2) (Fig. 5C). In contrast, samples staged between 68h and 72h APF displayed rapid and sustained increases in calcium activity in response to motoneuron activation with TRPA1 (5D-F). This is supported by quantification which showed that at the permissive temperature calcium events occurred at a rate of 6.15 per minute (± 5.60 S.D, n = 7) which was significantly greater than the rate of 0.93 per minute (± 0.81 S.D, n = 7) recorded at the restrictive temperature (p = 0.02, Mann-Whitney U-test, two-tailed). Interestingly, both 'wave-type' and 'block-type' activity was upregulated by TRPA1 activation at these times, with 'waves' occurring at 0.64 (± 0.69 S.D) per minute and 'blocks' at 0.29 (± 0.41 S.D) per minute at the restrictive temperature, but at 2.75 (± 1.93 S.D) and 3.40 (± 3.98 S.D) per minute respectively at the permissive temperature.

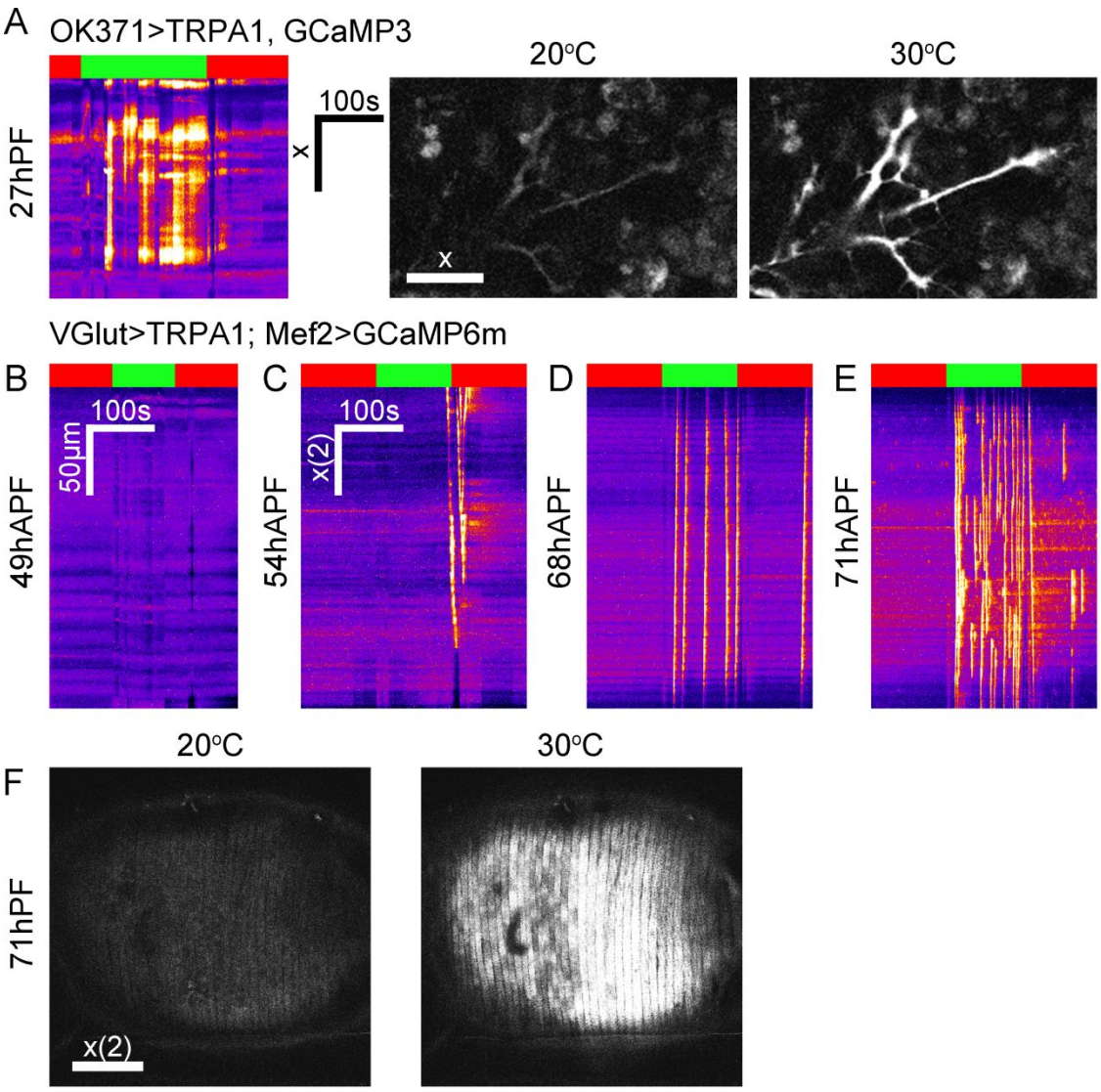

Figure 5. The activation of motoneuron using *TRPA1* does not evoke activity in the muscles until around 70h APF (A) Calcium activity in motoneurons expressing TRP1A and GCaMP3 under the control of OK371-GAL4. TRP1A gating evokes a robust calcium response at 27h APF **(B)** Calcium activity in muscles expressing GCaMP6m under the control of *Mef2*-GAL4 in a background of *VGlut*-LexA driven *TRPA1* expression. From 68h APF onwards TRPA1 gating induces trains of postsynaptic calcium events **(C)** Sequential images demonstrate calcium activity in the pleural muscles in response to presynaptic TRPA1 gating at 71h APF. Scale bars: 20μm (A), 100μm (C-F).

Genetic manipulations intended to persistently suppress presynaptic activity and neurotransmission cause motoneuron degeneration and death

These observations suggest that neurotransmission at the pleural neuromuscular junction does not start until after the main phase of elaborative arbor growth. To address directly whether the bulk of arbor construction takes place independently of activity-dependent neurotransmission I employed a number of genetic tools. These tools disrupted either presynaptic membrane depolarisations or the evoked fusion of neurotransmitter vesicles.

To inhibit evoked neurotransmitter release motoneuron clones expressing the light chain of tetanus toxin (*TeTxLc*) in addition to cytoplasmic GFP under OK371-GAL4 control were generated using the Gal-80 'flip out' technique described in chapter 1. TeTxLc cleaves the v-SNARE component neuronal-Synaptobrevin (nSyb) which is necessary for the evoked docking and fusion of neurotransmitter vesicles (Link *et al*, 1992). Chronic expression of this constitutively active toxin therefore persistently inhibits neurotransmission; a function for which it is routinely used in studies (Sweeney *et al*., 1995; Kaneko *et al*., 2000; Suster *et al*., 2002). At 45h APF the arborisations of these motoneurons appeared ostensibly normal, displaying comparable degrees of arbor complexity and coverage as those of the controls (Fig. 6A&D). By 65h APF however, *TeTxLC* expressing arborisations began to show signs of degeneration including the formation of membrane swellings and the contraction of branches. By 79h APF the arborisations displayed more advanced signs of degradation including the neuritic beading symptomatic of apoptotic cell death and were much reduced in complexity.

As an alternative approach to test the role of neurotransmission in arbor growth, I overexpressed *Shibire*^{TS} in motoneurons together with cytoplasmic GFP under the

control of OK371-GAL4. To achieve a chronic blockade during the period of motoneuron growth animals were raised at room temperature (~20^{o}C) until pupariation and then shifted to 31^{o}C until imaging. In contrast with *TeTxLc* expressing motoneurons, by 45h APF these arborisations displayed signs of degeneration and defective arbor growth including reduced arbor complexity and the formation of membrane swellings (Fig. 6B). By 66h APF the axon terminals had regressed into rudimentary arborisations surrounding varicose engorgements.

To chronically supress presynaptic electrical activity the Gal-80 'flip out' method was used to generate motoneuron clones expressing the mammalian inward-rectifying potassium channel K_{ir} *2.1* in addition to cytoplasmic GFP under the control of OK371-GAL4. This class of ion channels are involved in the repolarisation of axons following action potential generation and are open at resting membrane potential. As a result, increasing the quantity of this channel in the presynaptic membrane amplifies the efflux of K^+ ions, hyperpolarising the cell and making it less likely that the threshold for action potential generation will be reached (Johns *et al.*, 1999). By 53h APF K_{ir} *2.1* expressing motoneuron clones had failed to establish axonal arborisations *et all*, instead terminating in a frayed ending with no established branches (Fig. 6C). By 80h APF all that remained of these of these terminals were fragmented objects at the entry points to the nerves.

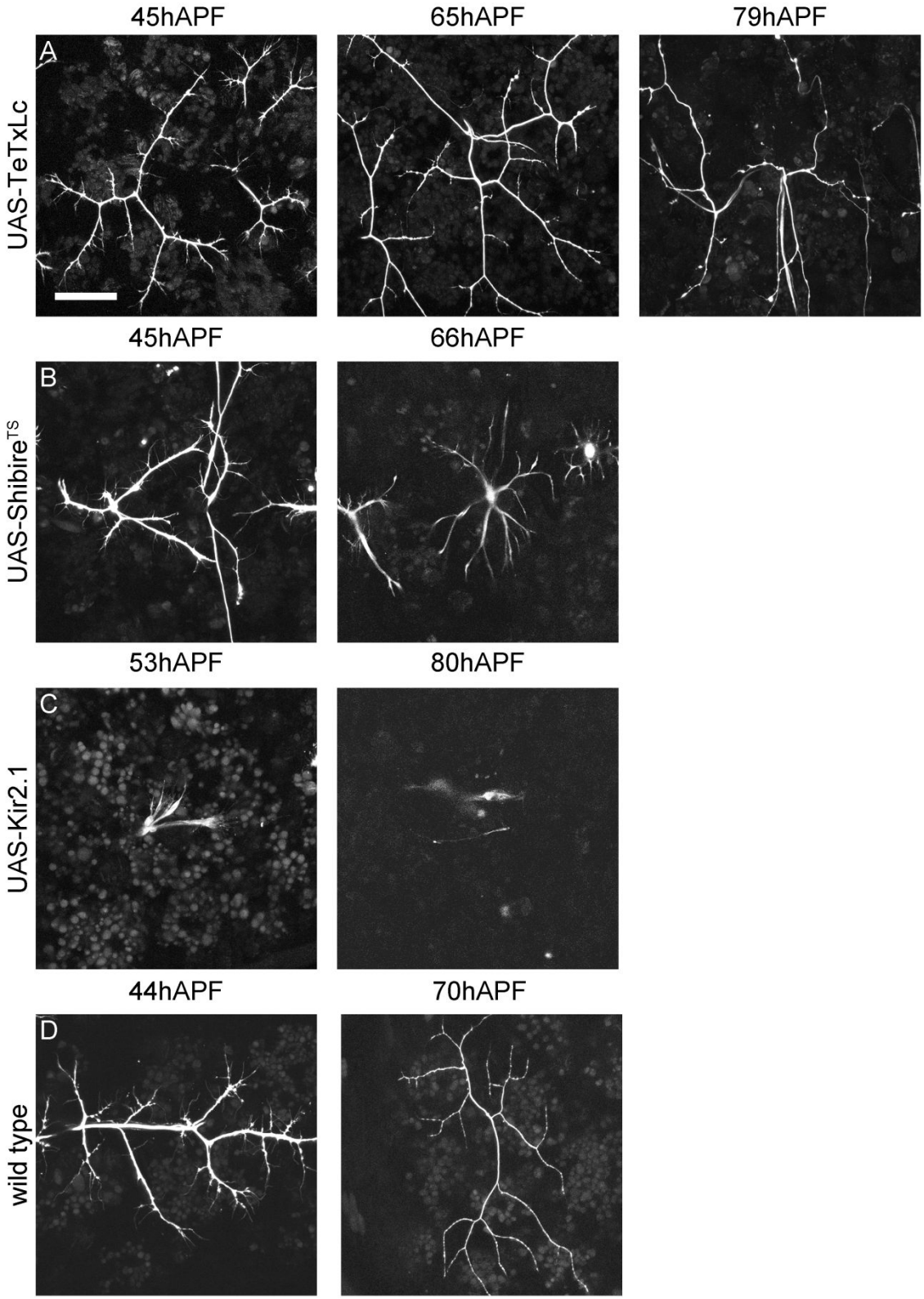

Figure 6. Cell-autonomous approaches for disrupting neurotransmission or presynaptic activity result in axonal degeneration (A) 'Flip-out' Gal80 motoneuron clones expressing *TeTxLC* and cytoplasmic GFP **(B)** Motoneurons expressing *Shibire^{TS}* and cytoplasmic GFP. Samples were raised at 20°C until pupariation followed by 31°C until imaging **(C)** 'Flip-out' Gal80 motoneuron clones expressing K_{ir} *2.1* and cytoplasmic GFP **(D)** Control 'flip-out' Gal80 motoneuron clones expressing cytoplasmic GFP. For all conditions the examples at each time point are derived from

different preparations. Motoneuron expression was driven by OK371-GAL4. Scale bar: 50μm.

TTX suppresses motoneuron activity for the full duration of dynamic arbor growth

An alternative to the genetic strategies for manipulating presynaptic activity, and therefore evoked neurotransmission, is the application of TTX. Used acutely, TTX was shown to inhibit motoneuron calcium activity as well as the generation of postsynaptic 'block-type' activity. To determine if the intravital injection of TTX suppressed or removed presynaptic activity, pupae expressing GCaMP6m under the control of OK371-GAL4 were injected with 0.5mM or 0.3mM TTX between 24h and 32h APF. These pupae were left at 25^{o}C to develop until between 72h and 78h APF when calcium activity in the pleural motoneurons was recorded by time-lapse imaging at 1Hz. To verify that injections were successful the solution included a ruby-labelled dextran. As demonstrated in Fig. 7A, in all cases the control preparations - injected with buffer and fluorescent dextran - displayed expected levels of presynaptic calcium activity for the stage of development (n=5). In the 8 TTX injected pupae however, 6 displayed no detectable calcium activity and the remaining 2 displayed only small and infrequent transients restricted locally to small branch segments.

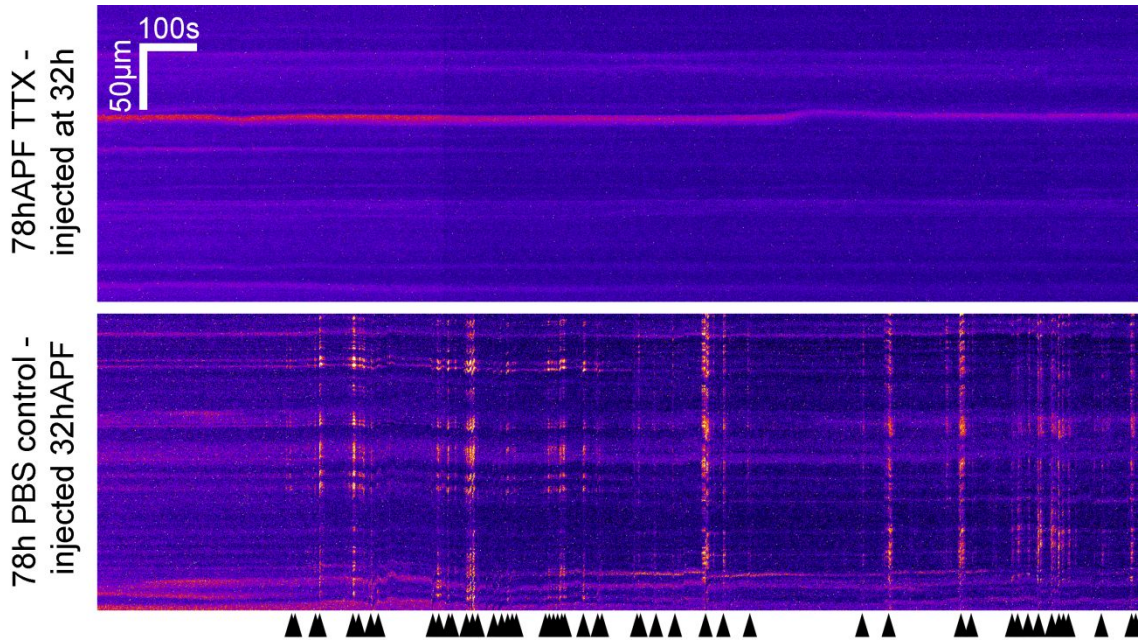

Figure 7. Injected TTX is efficacious for up to 46h. Kymographs show motoneuron calcium activity at 78h APF in pupae injected at 32h APF with TTX (top) or a control solution of PBS (bottom). GCaMP6m expression driven by OK371-GAL4. The black arrows indicate calcium events or trains of events.

Arbor construction and synapse formation is unaffected by chronic suppression of evoked activity using TTX

To investigate the impact of suppressing presynaptic activity animals expressing myr::GFP under the control of OK371-GAL4 were injected with 0.3mM TTX in PBS or a control solution of PBS at 32h APF and imaged at 79h APF. Lateral abdominal views suggest that arbor coverage in the pleural regions is no different between these conditions (Fig. 8A&D). Focusing on the arborisations of hemisegment A3 reveals that the motoneurons in each condition achieve comparable levels of arbor size and complexity and display no overt growth defects (Fig. 8B&E). Although too few samples were collected to make meaningful statistical comparisons, morphometric analysis revealed that the TTX injected pupae generated arborisations with cumulative branch lengths of 1741.3μm, (± 175.7 S.D, n=3) compared to 1991.9 μm (± 358.7 S.D, n=3) of controls, arbor areas of 38688μm^2 (± 5377 S.D) compared to 43039μm^2 (±

7733 S.D) and total branch numbers of 56 (± 4 S.D) compared to 68 (± 16). Although in each measure the arborisations of TTX injected animals trailed by a small margin, the magnitude of these discrepancies in combination with a qualitative assessment of arbor morphology suggests that they are not statistically meaningful.

To see if active zone formation was affected by silencing motoneuron activity, UAS-BRP::RFP was also expressed in these samples. In both the controls and TTX injected animals BRP::RFP formed puncta which by 79h APF were distributed in strings along the axon terminals exactly as was found in the wild-type examples in chapter 1. This suggests that the initial assembly of presynaptic specialisations is largely independent of motoneuron evoked activity.

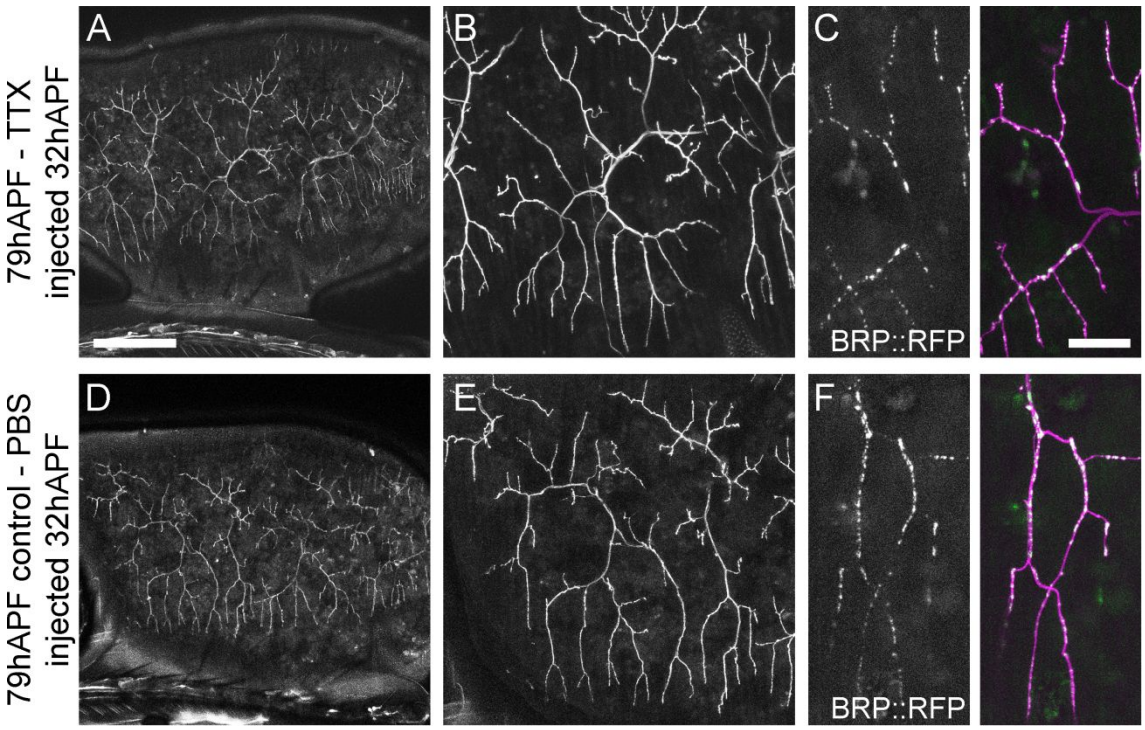

Figure 8. Chronic suppression of presynaptic activity using TTX has no effect on axon arbor growth or active zone formation (A&D) Lateral abdominal views show motoneuron arbor coverage at 79h APF in the pleural regions of pupae injected at 32h APF with (A) 0.5mM TTX or (D) a control solution of PBS **(B&E)** Higher magnification images show the arborisations in hemisegment A3 **(C&F)** UAS-BRP::RFP puncta in the synaptic terminals of these arborisations reveal the distribution of active zones. Motoneurons expressing myr::GFP and BRP::RFP under the control of OK371-GAL4. Scale bars: 150μm (A&D), 50μm (B&E), 20 (C&F).

Removing the vesicular glutamate transporter VGlut reveals arbor construction takes place without neurotransmission

In addition to evoked neurotransmission, spontaneous neurotransmitter release, responsible for miniature postsynaptic potentials (mEPSCs) or 'minis', has been shown to play a role in arbor growth and development (Choi *et al.*, 2014; Andreae and Burrone, 2015). At the pleural neuromuscular junction calcium recordings limited to the subsynaptic reticulum (SSR) using myr::GCaMP5 revealed postsynaptic activity diagnostic of spontaneous quantal release events in pharate adults (Fig. 9A). However, due to the late-stage development of the SSR - which seems to concentrate membrane tethered reporters - these events could not be seen earlier in development. To assess unequivocally a role for either spontaneous or evoked glutamate signalling in the construction of the pleural motoneuron arborisations the MARCM technique was used to generate and label single cell clones homozygous for a null allele in the *vesicular glutamate transporter* (*VGlut*). In *Drosophila*, *VGlut* encodes the single transporter responsible for filling neurotransmitter vesicles with glutamate, and is therefore essential for both evoked and spontaneous vesicular glutamate release (Daniels *et al.*, 2006).

The developmental origins of the pleural motoneurons have not been previously reported. To use the MARCM technique which relies on recombination only during mitosis I set out to determine when these neurons were born. I did this by inducing clones during the defined periods of embryonic and larval neurogenesis using the pan-neuronal driver Elav-GAL4 and looking for wild type, GFP expressing clones. Screening revealed the pleural motoneurons to be embryonically born (data not shown). To generate *VGlut* null clones the allele $dfVGlut^{2}$ was used in which the entire coding region of *VGlut* has been removed by P-element excision (Daniels *et al.*, 2006).

Clones were labelled with CD8::GFP and cytoplasmic GFP in addition to BRP::RFP under the control of the *VGlut*^{NMJX}-GAL4. This driver, which was generated by cloning of a fragment of the *VGlut* promoter, was necessary since OK371-GAL4 itself is in the locus of the *VGlut* gene (Daniels *et al.*, 2008).

DF*VGlut*^{2} homozygous motoneuron terminals in pharate adult abdominal filets stained negatively for the VGlut protein, whereas the terminals of controls were lined with rows of VGlut puncta (Fig. 9B&C). To assess the morphology of *VGlut* mutant clones, pupae were staged for live imaging at ages between 70h and 80h APF. Because MARCM clones are generated mosaically, obtaining replicates of anatomically identical cells was a matter of chance and thus numbers were low. To compensate for this, pleural motoneuron arborisations of 2 anatomical identities, A3A and A4A, were analysed. In addition, to increase sample sizes for the analyses clonal arborisations from males and females were pooled. To account for this, the same sex ratio of control arborisations was used. Control data was selected at random using a random number generator from a data set of motoneurons expressing myr::GFP under the control of *VGlut*-LexA.

The morphology of the arborisations of *VGlut* mutant clones of the anterior motoneurons of segment A4 (A4A) appeared well within the bounds of the normal variation of their wild type counterparts and displayed no obvious growth defects (Figs. 9D&E). With the caveat of being a sample size of only 3, these null clones had arbor areas of 38228μm^2 (± 6689 S.D), total arbor lengths of 1668μm (± 225 S.D) and branch numbers of 61.7 (± 7.5 S.D). This is remarkably similar to the controls, which were measured at 34978μm^2 (± 2134 S.D), 1751 μm (± 198 S.D) and 79.0 (± 1.7 S.D) respectively (n = 3). Fileting and staining these preparations with the marker of

invertebrate neurons anti-HRP revealed that *VGlut* null clones occupy typical spatial domains in relation to neighbouring arborisations (Fig. 9F).

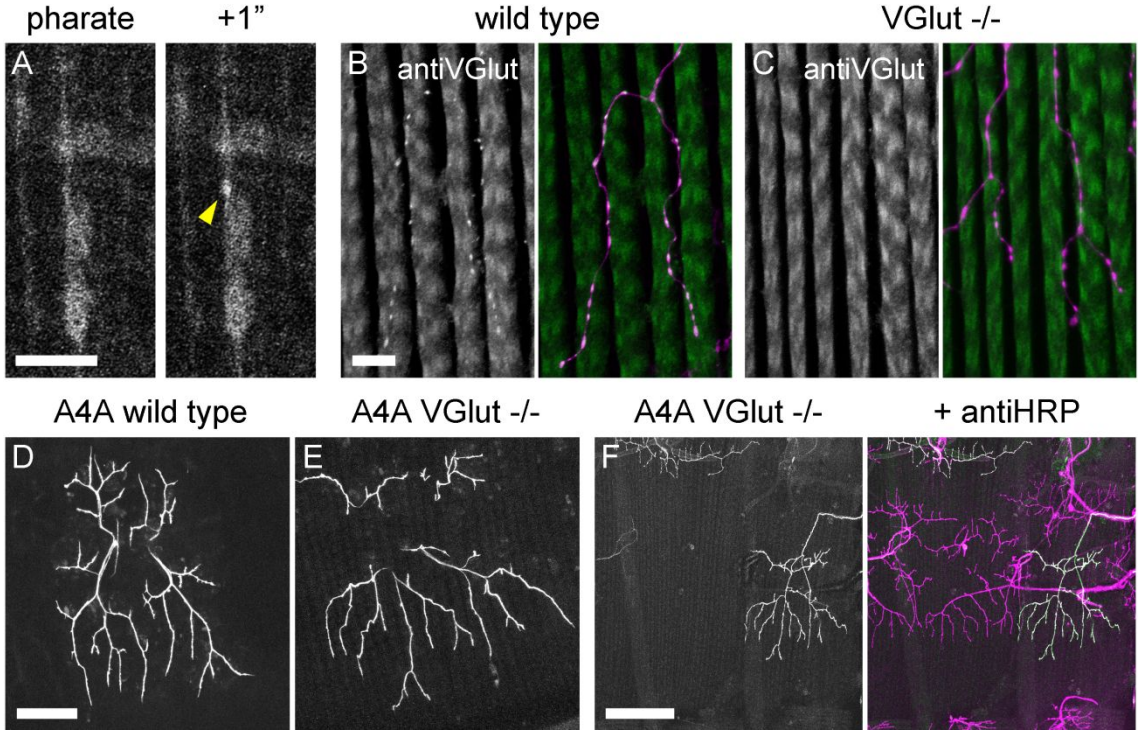

Figure 9. Silencing spontaneous and evoked glutamate transmission has no effect on axon arbor construction in motoneuron clones (A) Imaging at 0.5 frames per second reveals a ‘mini’ calcium event induced by the fusion of a single neurotransmitter vesicle at a pleural neuromuscular junction of a pharate adult expressing myrGCaMP5 under the control of *Mef2*-GAL4 **(B&C)** anti-VGlut staining of the axon terminals of a control motoneuron MARCM clone (A) and a *VGlut* null motoneuron MARCM clone (B) in pharate adult filets **(D)** An axonal arborisation of a male control A4A motoneuron expressing myr::GFP under the control of *VGlut*-LexA at 78h APF. Neighbouring arborisations have been removed using FIJI **(E)** The axonal arborisation of a male *VGlut* null A4A motoneuron MARCM clone expressing CD8::GFP, cytoplasmic GFP and *BRP*::RFP under the control of $VGlut^{NMJX}$-GAL4 at 85h APF **(F)** A fileted preparation showing the same motoneuron as in Fig. 9E with the neuronal membranes stained with anti-HRP (magenta). Scale bars: 10μm (A-C), 50μm (D&E), 150 (F).

To complement this analysis a supplementary data set was derived from the arborisations of motoneuron A3A (Fig. 10). As with the clones of A4A these were qualitatively indistinguishable from their wild type equivalents and displayed no appreciable morphological abnormalities (Fig. 10A&B). This is supported by morphometric analyses which revealed that neither the total arbor areas (46467μm^2 ±

4342 S.D in wild types [n = 4] versus 44384μm^2 ± 4069 [n = 4] in *VGlut* mutants; p = 0.66), total branch lengths (2151μm ± 268 S.D in wild types [n = 4] versus 2017μm ± 285 [n = 4] in VGlut mutants; p = 0.49) or overall branch numbers (76.5 ± 12.5 S.D of wild types [n = 4] versus 65.8 ± 9.0 [n = 4] of *VGlut* mutants; p = 0.34) differed significantly between the groups (Mann-Whitney U-tests, two-tailed) (Fig. 10C, D&E).

To assess if the formation or distribution of synapses is affected by the elimination of glutamate filled vesicles in motoneuron clones UAS-*BRP*::RFP was used to visualise presynaptic active zones. Just as was seen with motoneurons affected by TTX, mature *VGlut* mutant motoneurons achieved punctate distributions of BRP along the lengths of their terminal branches that appeared to show no obvious difference from wild type equivalents (Fig. 10F).

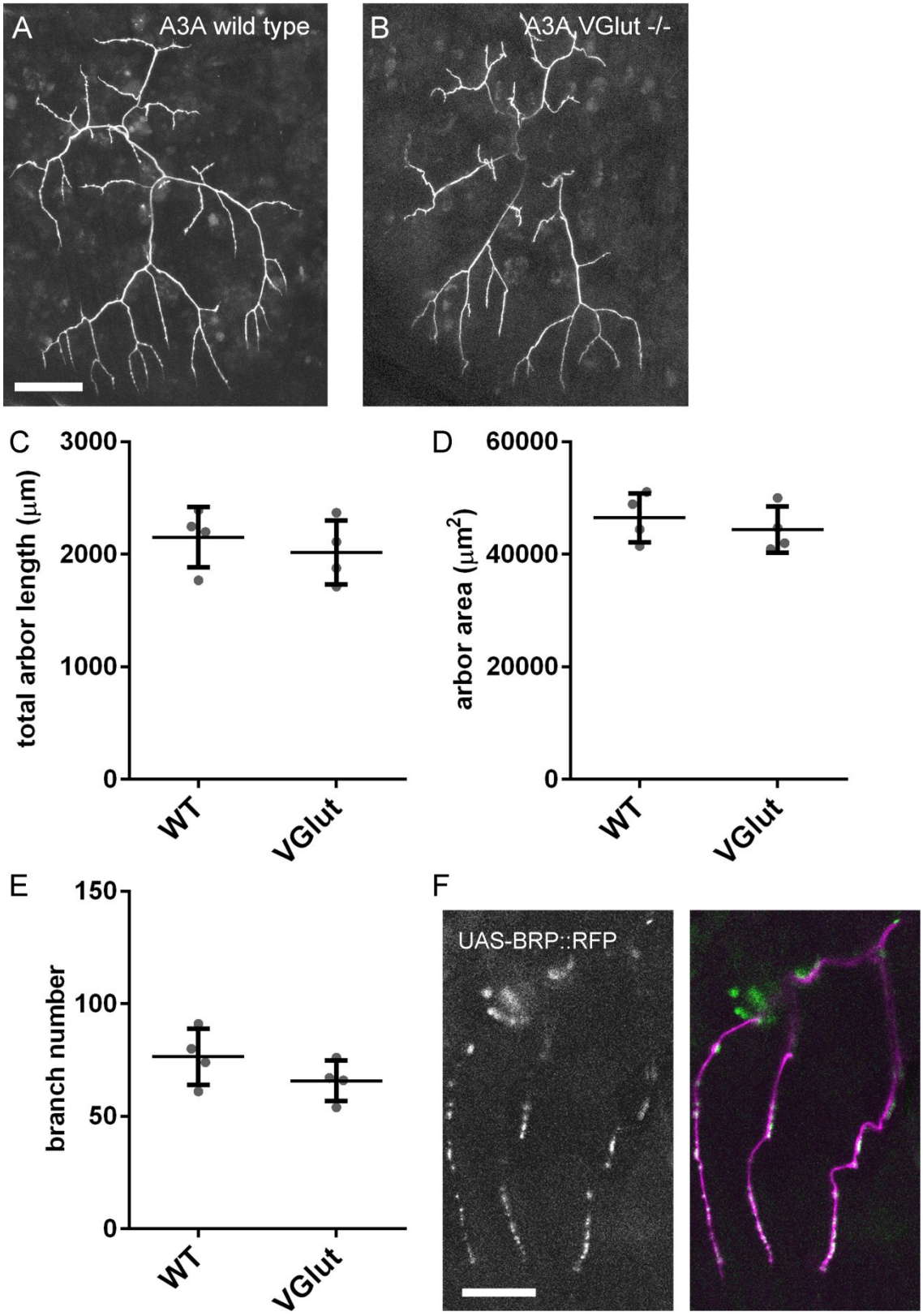

Figure 10. Arbor construction and synapse formation is independent of glutamatergic neurotransmission (A) An axonal arborisation of a female control A3A motoneuron expressing myr::GFP under the control of *VGlut*-LexA at 72h APF. Neighbouring arborisations have been removed using FIJI **(B)** An axonal arborisation of a female *VGlut* null A3A motoneuron MARCM clone expressing CD8::GFP, cytoplasmic GFP and BRP::RFP under the control of $VGlut^{NMJX}$-GAL4 at 80h APF **(C-E)**

Quantifications of total arbor length, arbor area and branch number of A3A arborisations **(F)** BRP::RFP puncta distribution in the synaptic terminals of a *VGlut* null motoneuron MARCM clone at 85h APF. Scale bars: 50μm (A&B), 20μm (F).

4.3 Discussion

The contribution of synaptic activity to the development of neural networks is a question which has been asked for over 100 years (Harrison, 1904; Weiss, 1941). From classic sensory deprivation experiments we know that activity can play an important role in in the structural development of neurons (Wiesel and Hubel, 1963; Coleman and Riesen, 1968). However, the significance of this role in terms of early arbor as networks are emerging and the mechanisms by which it operates are still unclear. Neurotransmission has been shown to have a stabilising effect on the exploratory filopodia of growing vertebrate arborisations *in vivo*, prompting the suggestion of a role for activity as part of a synaptotropic mechanism of arbor construction (Rajan and Cline, 1998; Sin *et al.*, 2002; Ruthazer *et al.*, 2006; Chen *et al.*, 2010). However, this inference is countered by evidence from a number of studies which have indicated that synaptic activity only regulates competition-dependent refinements of connectivity and has little impact on the establishment of arbor complexity and shape (Kaethner and Stuermer, 1994; Hua *et al.*, 2005; Fredj *et al.*, 2010). To add to our limited, and somewhat contradictory, understanding of the role of activity in synaptotropic growth, I took advantage of the genetic tractability of the fly to explore its importance in the development of this new model system.

Functional imaging and manipulations of synaptic activity point to an activity-independent-epoch of arbor growth

Previous work on growing dendritic arborisations in the brains of *Xenopus* led the authors to propose that neurotransmission is required for the consolidation of nascent axodendritic contacts mediated by Nlg/Nrx interactions by the recruitment of additional stabilising synaptic components (Fig. 1) (Chen *et al.*, 2010). The discovery of a comparable role for Nlg/Nrx in the present system raised the possibility of a similar

mechanism. To explore a role for evoked neurotransmission in arbor growth, the development of activity in the motoneurons was mapped using calcium imaging. This revealed that activity indicative of membrane depolarisations does not commence until after a large proportion of arbor outgrowth has already taken place. What is more, it is not until even later that activity becomes frequent enough to conceivably conduct stabilisation events. This argues against a requirement for evoked neurotransmitter release during the early period of arbor growth as part of a synaptotropic mechanism. A caveat to this however is that GCaMP serves only as a proxy for electrical activity and subthreshold transients may not have been detected. This being said, calcium imaging is a well-established and accepted means of measuring neuronal activity, and the latest generation of GCaMP tools, as used in my study, can resolve activity to the level of single action potentials (Chen *et al.*, 2013).

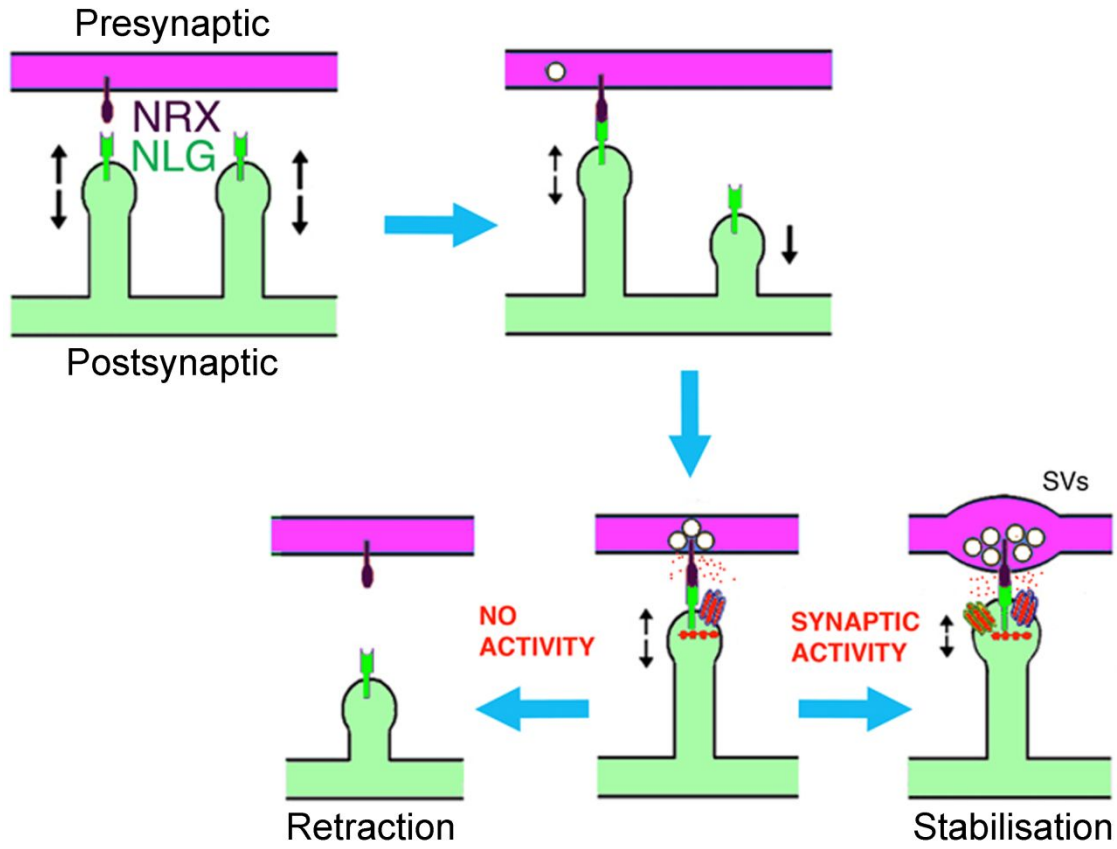

Figure 1. A model of Nlg/Nrx mediated synaptotropic arbor growth (adapted from Chen *et al.* (2010). The synapse mediated stability of filopodia in this model is a 3 part process (1) Nlg-Nrx adhesions provide transient stability to nascent axodendritic

contacts (or in the case of the neuromuscular junction, myo-axonal contacts) (2) Via intracellular PDZ domains Nlg and Nrx recruit synaptic machineries and synaptic vesicles allowing neurotransmission to occur (3) Neurotransmission leads to synaptic maturation and contact stabilisation, whereas no neurotransmission leads to synaptic disassembly and filopodia retraction.

To explore the development of postsynaptic excitation, postsynaptic activity was mapped by calcium imaging in the muscles. During the period of muscle growth, myoblasts and immature syncytial myotubes displayed localised asynchronous calcium transients. Previous work using cultured vertebrate and *Drosophila* muscles has shown that calcium influx facilitates myoblast fusion by promoting calcium-dependent membrane binding (David *et al.*, 1981; Doherty *et al.*, 2005). This occurs in the absence of neuronal cells and therefore it can be assumed that the signals seen at this stage are not a result of neurotransmission. With similarity to the development of activity in the motoneuron axons, strong activity in developed myotubes was not recorded until the later stages of arbor outgrowth, adding support to the deduction that arbor growth takes place independently of neurotransmission. In addition to this, initial 'wave-type' transients were not coincident with motoneuron activity and, unlike later congruent 'block-type' activity, were not supressed by the silencing of neurotransmission with TTX or *Shibire*^{TS}. Taken together this evidence implies that evoked neurotransmission at the pleural neuromuscular junction does not commence until after the arborisations have achieved their mature morphology.

The early 'wave-type' muscle activity described here is reminiscent of spontaneous retinal calcium waves recorded in vertebrate embryos (Ackman *et al.*, 2010). These transients have been shown to propagate via the optic nerve to the visual cortex and are proposed to carry information for patterning retinotopic maps prior to visual input (Ackman *et al.*, 2010, Kirkby *et al.*, 2013). Indeed, in ferrets, monocular blockade of the propagation of these waves using pharmaceuticals resulted in eye-

specific organisational abnormalities in cortical structure (Penn *et al.*, 1998). Electrical synapses formed by Connexins are known to be important for the long-range propagation of activity in developing vertebrate nervous systems, including for the formation and propagation of retinal waves (Fulton, 1995; Blankenship *et al.*, 2011). Likewise, it is possible that gap junctions (in invertebrates formed by Innexins) play a similar role in this system by aiding the generation of spontaneous, patterned activity in the developing muscles (Crompton *et al.*, 1995). This could perhaps form the basis for strengthening synaptic connections based on coincidence detection via a retrograde signal. Since activity in the synaptic partners appears to become gradually more congruent over time, such a 'tuning up' mechanism seems plausible. It would be interesting to explore this prospect by disrupting gap junction function or the release of calcium from internal stores during muscle development.

To investigate the hypothesis that synaptic function develops late at the pleural neuromuscular junction, motoneurons were depolarised using TRPA1 channels in an attempt to stimulate neurotransmission. From the timeline of muscle activity, it suggests that neurotransmission does not take place until the later stages of arbor growth. Likewise, it was not until after 70h APF that postsynaptic calcium activity could be elicited in this manner. These evoked responses were robust and sustained making them easily distinguishable from background activity. Combined with the pharmacological and genetic disruptions of synaptic activity this is highly suggestive that evoked neurotransmission does not play a role in early arbor growth.

To test the idea that arbor growth occurs independently of transmission, 3 different genetic tools were employed with the aim of disrupting fundamental aspects of evoked neurotransmitter release. Surprisingly, in light of the evidence against a role for synaptic activity in arbor growth, each of these appeared to produce severe, albeit

different defects in arbor growth. However, drawing from other work I argue that these effects are unrelated to a disruption of neurotransmission. Firstly, TeTxLC specifically cleaves n-Syb and has been widely shown to silence evoked neurotransmission in *Drosophila* neurons (Sweeney *et al.*, 1995; Kaneko *et al.*, 2000; Suster *et al.*, 2002). However, as well as localising to synaptic vesicles n-Syb has been found to localise to endosomal vesicles in *Drosophila* photoreceptors (Haberman *et al.*, 2012). What is more, the expression of *TeTxLC* in these cells caused a build of endosomal vesicles and neuronal degeneration which could be rescued by upregulation of a partially redundant endosomal sorting pathway, therefore demonstrating a non-synaptic function of n-Syb in endosomal sorting. Secondly, although *Shibire*^{TS} is also widely used to silence neurotransmission, its role in clathrin coated vesicle budding is ubiquitous and when inactivated in cells for long periods has been shown to cause degenerative effects related to defective endocytosis and microtubule bundling in both neuronal and non-neuronal cells (Kosaka and Ikeda, 1983; Damke *et al.*, 1994; Gonzalez-Bellido *et al.*, 2009). Lastly, the mammalian K_{ir} channels are potent inhibitors of action potential generation and are also commonly used to silence neurons in a range of systems (Nitabach *et al.*, 2002; Paradis *et al.*, 2001). However, the effects of a chronically maintained artificially low neuronal membrane potential are not well understood, and a study on hippocampal cells in culture found long term expression of K_{ir} channels to result in apoptotic cell death (Nadeau *et al.*, 2000). It is often taken as given that these tools do not cause phenotypes during development, although this may not be the case. In the present study, these manipulations elicited diverse phenotypic effects. Together with evidence from previous studies this suggests that these are a result of different defective pathways unrelated to neurotransmission.

Pharmacological and genetic mosaic approaches demonstrate a synaptotropic mode of growth independent of synaptic activity

As an alternative to using genetic tools, presynaptic activity was silenced pharmacologically using TTX. In *Drosophila*, as is the case in vertebrates, TTX selectively blocks voltage-gated calcium channels, therefore inhibiting the generation of action potentials (Wu and Ganetzky, 1980). But for a few small, localised transients, TTX remained efficacious 40h after intravital injection, indicating a strong suppression of activity for the full period of elaborative arbor growth. In affected samples the pleural motoneurons constructed arborisations no different in size, shape or complexity to the PBS injected controls. Together with the functional evidence this suggests that evoked neurotransmission is not required for the formation of arbor morphology. Similar spontaneous, localised transients to the ones shown here under TTX suppression have been observed in the growing branches of cortical neuron axonal arborisations and were found to play a role in regulating outgrowth (Kalil and Hutchins, 2011). Perhaps in the present system these transients represent a similar mode of activity which is revealed by local differences in the degree of TTX suppression.

It was speculated in chapter 2 that the synaptotropic mechanism of arbor growth described in this system relies not on the formation of mature synapses, but on the formation of Nlg/Nrx based proto-synapses. In support of this, arbor morphology was found to be severely disrupted in *Nlg1* and *Nrx* mutants whereas synapse formation appeared to be unaffected. If synapse formation were found to be activity-dependent, but not synaptotropic growth, this would provide evidence in support of a decoupling of the role of Nlg/Nrx signalling in arbor growth from synapse formation. To explore this possibility, active zones were visualised in arborisations silenced with TTX by the expression of *BRP*::RFP. This however revealed that, like arbor growth, the

initial stages of synapse formation occur independently of evoked transmission. This is perhaps not surprising considering existing evidence from *Drosophila* as well as other systems. At the larval neuromuscular junction Broadie and Bate (1993) found no abnormalities in the number of synapses or the size of synaptic terminals formed during embryogenesis when presynaptic activity was suppressed using TTX or with a temperature sensitive mutant of the voltage-gated sodium channel *para*. Similarly, in mice lacking proteins required for all forms of neurotransmitter release brain structure and synapse formation was largely unaffected (Verhage *et al.*, 2000; Varoqueaux, 2002).

An important piece of data that is missing from this experiment is the effect of TTX on calcium activity during the early stages of arbor growth. Over the course of motoneuron development the kinetics of calcium activity change from slow, graded transients to rapid spike-like transients. Comparable changes are observed during the development of vertebrate neurons which reflect different modes of calcium activity (Spitzer *et al.*, 2000; Moody and Bosma, 2005). During early development calcium elevations in vertebrate central neurons which are distinct from later electrical activity play diverse signalling roles including coordinating cell migration and establishing connectivity patterns (Penn *et al.*, 1998; Komuro and Rakic, 1996; Wong and Ghosh, 2002). By virtue of their kinetics these early transients are often categorised as spikes or waves (Spitzer *et al.*, 2000). Spikes, which are dependent on voltage gated sodium channels for their generation, are blocked with TTX (Gu *et al.*, 1994; Tang *et al.*, 2003). However, the slower waves occur independently of voltage-gated channels, instead relying on calcium induced calcium release as well as other channel types, and are therefore insensitive to TTX (Yuste *et al.*, 1992; Gu *et al.*, 1994). The resemblance of early motoneuron activity in this study to these vertebrate waves raises the prospect of

a similar mode of calcium activity which is insensitive to TTX. To draw conclusions from this data it is important that this possibility is explored.

The manipulations of synaptic activity presented so far are clearly not without limitations. What is more, there are two important considerations to which they do not attend. Firstly, it has recently been shown that spontaneous neurotransmitter release plays distinct roles in the development of some arborisations which are parallel to those of evoked transmission (Choi *et al.*, 2014; Andreae *et al.*, 2015). The recording of miniature calcium events at the pleural neuromuscular junctions raised the possibility that this mode of transmission also plays a role during the development of this system. Secondly, some studies have provided evidence that arborisations constructed via a synaptotropic mechanism only display growth effects when silenced singularly, as opposed to globally, suggesting that the role of activity is competition-dependent. The 'gold-standard' for determining gene function in *Drosophila* is using genetic mosaics to generate homozygous null clones. Therefore, to attend to both of these issues, and to provide the most direct evidence for a role of synaptic activity, I eliminated all forms of glutamate transmission in a cell-autonomous manner by the generation of *VGlut* null MARCM clones. Morphometric and qualitative analysis found no difference between the arborisations of *VGlut* Null motoneurons and those of GFP labelled wild types. This is conclusive evidence that glutamate transmission does not play a role in the constructions of the arborisations. Although all *Drosophila* motoneurons use glutamate as a primary neurotransmitter, neuromodulatory peptides including Proctolin and Octopamine are also released at some larval neuromuscular junctions (Anderson *et al.*, 1988; Monastirioti *et al.*, 2015). Therefore, although it is unlikely, it cannot be excluded that such forms of transmission are involved in the synaptotropic-like mechanism by which these arborisations are built. As was seen with silencing motoneuron activity with TTX, in *VGlut* null motoneurons active zone densities appeared no different to wild

types, lending support to the deduction that synapse formation occurs independently of neurotransmission.

Conclusions

Though its precise involvement is unclear, activity is widely regarded to play a role in regulating the growth of neuronal arborisations in vertebrate brains. In one study this was shown to take place via a synaptotropic-like mechanism by stabilising nascent contacts mediated by Nlg/Nrx (Chen *et al.*, 2010). The present study found a role for Nlg/Nrx signalling but was unable to demonstrate a subsequent requirement for neurotransmission. Together with the evidence against a role for active zone components in this mechanism, as presented in chapters 1 and 2, I forward an alternative model whereby Nlg/Nrx based proto-synapses provide the basis for a synaptotropic-mode of arbor growth which is independent of synaptic transmission (Fig. 2).

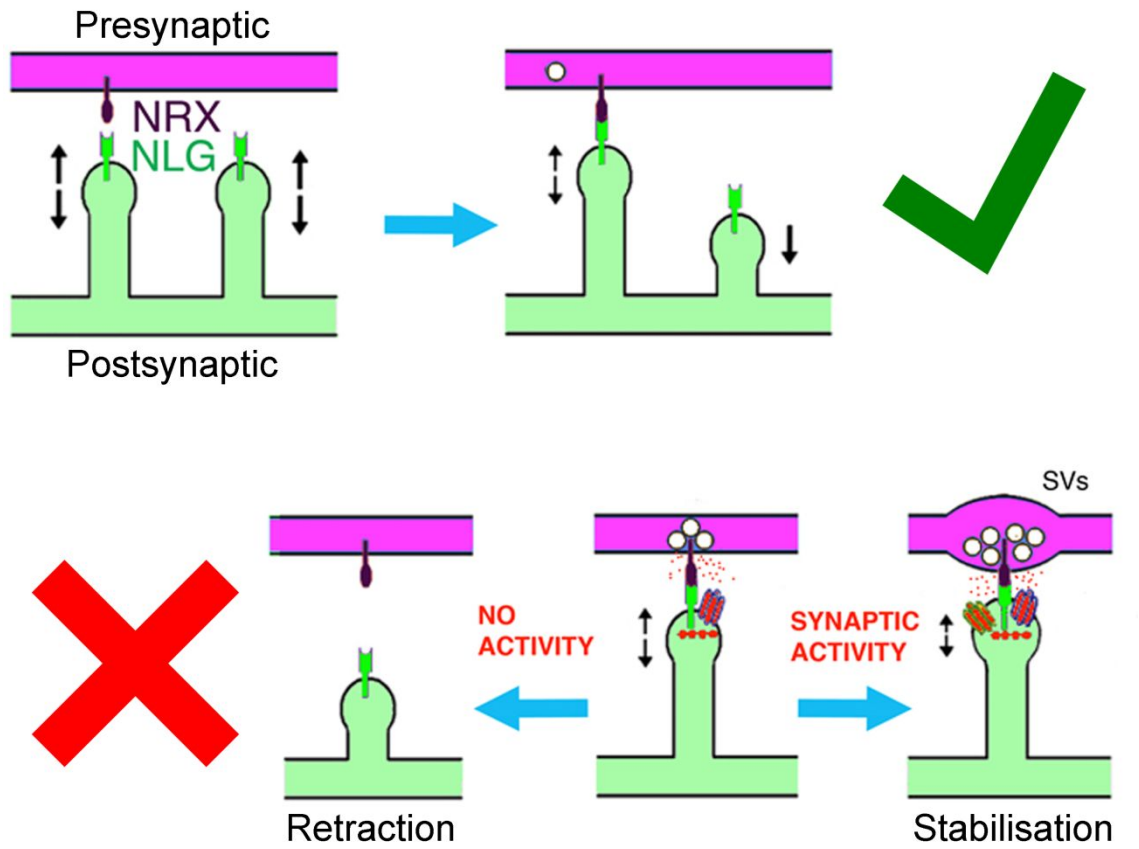

Figure 2. An activity-independent, proto-synapse mediated model of arbor growth. This model proposes that proto-synapses built around Nlg/Nrx adhesions are sufficient to provide the stabilisation and promote the cytoskeletal remodelling required for synaptotropic arbor growth.

Chapter 5

General Discussion

Previous studies of complex, synapse forming arborisations in the fly have either been limited to fixed material, and therefore could not observe dynamics, or have lacked the temporal and spatial resolution to necessary to determine the contribution of dynamic processes to arbor construction (Tripodi *et al.*, 2008; Mauss *et al.*, 2009; Zschätzsch *et al.*, 2014). What is more, in all existing systems it is impossible to observe the interactions between growing synaptic partners and the importance of this to growth and ultimate form. In this thesis, I present a new system in which a population of easily accessible, complex axonal arborisations and their synaptic partners can be live imaged for their full period of outgrowth. Unlike larval motoneuron axon terminals these exhibit major structural plasticity in their patterns of innervations and branching and grow in an exploratory, vertebrate-like, trial and error manner. With this system, I show for the first time outside of vertebrate central nervous systems that this involves the local stabilisation of exploratory branches and filopodia via a synaptotropic-like mechanism. However, in contrast with the mechanism described in vertebrates, I provide 3 lines of evidence which advocate that the molecular basis of the synaptotropic mechanism shown here is distinct and that we should reflect on the interpretation of the previous:

(1) In zebrafish retinal ganglion cell axons, the stabilisation of filopodia was shown to be preceded by the arrival and stabilisation of presynaptic components at their tips. In my system, however, synaptic machineries were never found to stabilise at the tips of filopodia and were often recruited subsequently following the emergence of filopodia.

(2) Manipulations of Nlg/Nrx signalling resulted in defective synaptotropic growth, but had little effect on the eventual number of synapses, pointing to mechanistic decoupling of synaptotropic growth and synapse formation.

(3) In a number of vertebrate systems, synaptic activity has shown to play a role in synaptotropic growth. In *Xenopus* neurotransmission was demonstrated to be required for the stabilisation of transient axodendritic contacts mediated by Nlg/Nrx adhesions. In contrast, in this system synaptotropic growth was shown to occur as normal when neurotransmission was eliminated.

From this evidence, I propose that synaptotropic growth in in the present system is mediated not by synapses but by proto-synapses that are rich in synaptic cell adhesion molecules. This mechanism allows neurons to construct functionally relevant arborisations during an activity-independent epoch of development.

This new *in vivo* model paves the way for tackling unresolved questions regarding the molecular basis of synaptotropic arbor growth which so far have been unfeasible in more complex systems. One aspect of this mode of growth which is still yet to be conclusively demonstrated is 'tropism'. As predicted by Vaughn, arborisations using synaptotropic mechanisms will preferentially grow into regions rich in synaptic partners. One means of truly testing this phenomenon would be by using mosaic techniques, such as MARCM, to generate *Nlg1* null muscle mosaics. According to Vaughn's prediction, axon branches presented with a 'choice' between two substrates would grow preferentially onto patches of wild type muscle in a manner of tropism. What is more, this experiment would provide a means of definitively demonstrating the local role of Nlg/Nrx in stabilising nascent contacts.

In addition, this system provides an opportunity explore the components required for mediating stability and growth as part of a synaptotropic mechanism. In *C. elegans* the synaptic cell adhesion molecule Syg-1 was found to regulate cytoskeletal remodelling by recruiting the F-actin interacting protein Nab1 and the WAVE regulatory complex (Chia *et al.*, 2012; Chia *et al.*, 2014). The cytoskeletal remodelling function of this cell adhesion molecule was unaffected by the loss of active zone components, suggesting that its roles in synapse formation and cytoskeletal remodelling are independent. With evident similarity, it is possible that *Drosophila* Nrx plays an equivalent role by coordinating the cytoskeletal remodelling required for growth and branching. In support of this the *Drosophila* homologue of Nab-1, Spinophilin has been shown to form a complex with Nrx *in vivo*, making it a promising candidate as a regulator of cytoskeletal remodelling in the synaptotropic-like mechanism described here (Muhammad *et al.*, 2015).

My work proposes that active zone components are not required for the synaptotropic-like growth of the pleural neuromuscular junctions. One way of testing this would be to block the assembly of active zones. As described earlier, active zones proteins are recruited to nascent synapses in vesicular packets that contain many, if not all, active zone components required for evoked neurotransmission (Zhai *et al.*, 2001; Shapira *et al.*, 2003). In *Drosophila,* a single motor protein, *Kinesin-3/Unc-104*, is responsible for trafficking these packets to axon terminals (Pack-Chung *et al.*, 2007). As such, in *Kinesin-3* nulls very few active zones formed in the synaptic boutons of embryonic motoneuron axons. Although these nulls did not hatch, the generation of *Kinesin-3* null MARCM motoneuron clones would provide a means of testing the requirement of active zone components during arbor growth. Alternatively, *Drosophila Syd-1* and *Syd2/Liprin-α* act as master organisers of active zones through partially

overlapping pathways and could be used to similar effect (Kaufmann *et al.*, 2002; Owald *et al.*, 2010; Li *et al.*, 2014).

In addition to *Nlg1*, *Nlg2* and *Nlg3* have been shown to play roles in the expansion of the larval neuromuscular junction (Sun *et al.*, 2011; Chen *et al.*, 2012; Xing *et al.*, 2014). It is possible therefore that these proteins could also play roles in the synaptotropic-like growth of the pleural muscular junction. Although *Nlg1* and *Nrx* caused distinct growth phenotypes, the axons were still able to construct relatively large arborisations with showed no difference in complexity from wild types. Therefore, it is tempting to speculate that these homologues play partially redundant roles during arbor construction, or are involved in different aspects of a synaptotropic mechanism. Since both *Nlg2* and *Nlg3* show little sign of interaction with *Nrx*, unlike *Nlg1*, this seems a likely possibility (Sun *et al.*, 2011; Chen *et al.*, 2012; Xing *et al.*, 2014). Exploring the role of these proteins and their potential interactions is therefore a priority in future experiments.

That synaptotropic-like growth is found in vertebrates and now the Ecdysozoa it will be exciting to establish if the lophotrocohozoa (annelids and molluscs) use the same mechanism, and that therefore it could be a universal toolkit for tree building in nervous systems. Indeed, if extra-terrestrials have evolved nervous system analogues in other star systems it will be interesting to determine if they use trees-like structures to help compute information and whether the growth of these structures occurs by synaptotropic-like mechanism (If so I look forward to the citations).

Chapter 6

Materials and Methods

Fly stocks

Flies were reared on a standard yeast-cornmeal-molasses diet. For time-sensitive experiments flies were raised at 25^{o}C, unless stated otherwise, or at room temperature if precise staging was not required.

Table 1. Fly stocks used in this study

Full Genotype (where known)	Shorthand	Source (where known)
W^{1118}	*W1118*	
w[1118]; P{w[+mW.hs]=GawB}VGlut[OK371]	OK371-GAL4	Gift from Hermann Aberle, (Mahr & Aberle, 2006)
y[1] w[*]; +; P{w[+mC]=GAL4-*Mef2*.R}3	*Mef2*-GAL4	Bloomington *Drosophila* Stock Centre (BDSC) 27390, (Ranganayakulu *et al*., 1996)
w[*]; P{w[+mC]=ppk-GAL4.G}2	*PPK*-GAL4	Gif from Wesley Grueber (Grueber *et al*., 2003)
P{VGlut-GAL4.D}NMJX; $_{+;+}$	$VGlut^{NMJX}$-GAL4	Gift from Aaron DiAntonio, (Daniels *et al*, 2008)
w[*]; Mi{Trojan-lexA:QFAD.2}VGlut[MI04979-TlexA:QFAD.2]/CyO, P{Dfd-GMR-nvYFP}2	*VGlut*-LexA	Gift from Matthias Landgraf (BDSC 60314)
w[*]; P{y[+t7.7] w[+mC]=10XUAS-IVS-myr::GFP}attP40	UAS-myr::GFP	Gift from Barret Pfeiffer, (Pfeiffer *et al*., 2012)
w[*]; P{10XUAS-IVS-Syn21-GFP}attP40	UAS-cytoplasmic GFP	Gift from Barret Pfeiffer, (Pfeiffer *et al*., 2012)

y[1] w[*] P{y[+t7.7] w[+mC]=10XUAS-IVS-mCD8::GFP}su(Hw)attP8	UAS-CD8::GFP	BDSC 32189
w[*]; P{y[+t7.7] w[+mC]=10XUAS-IVS-mCD8::GFP}attP40	UAS-CD8::GFP	BDSC 32186
+; +; UAS-Bruchpilot::mRFP	UAS-*BRP*::RFP	Gift from Stephan Sigrist
w[*]; P{w[+mC]=UAS-syt.eGFP}2	UAS-*Syt1*::eGFP	BDSC 6925
w[*]; P{w[+mC]=UAS-mCD8.ChRFP}2	UAS-mCD8::Cherry	BDSC 27391
w[*]; P{w[+mC]=UAS-AUG-DsRed}A	UAS-dsRed	BDSC 6282
y[1] w[1118]; Pin[1]/CyO; M{w[+mC]=UAS-mtdTomato-3xHA}ZH-86Fa/TM6B, Tb[1]	UAS-mtdTomato	BDSC 30124
y[1] w[*]; P{y[+t*] w[+mC]=UAS-Lifeact-Ruby}VIE-19A	UAS-Lifeact::Ruby	BDSC 35545
+; +; UAS-CLIP170::GFP	UAS-*CLIP170*::GFP	Gift from Brian Stramer, (Stramer *et al*., 2009)
P{w[+mC]=Dp110-CAAX}1, y[1] w[*]	UAS-*DP110*::CaaX	BDSC 25908
+; +; P{UAS-Nlg1::GFP}	UAS-*Nlg1*::GFP	Gift from Hermann Aberle, (Banovic *et al*., 2010)
+; +; P{UAS-Nlg1Untagged}	UAS-*Nlg1*-Untagged	Gift from Hermann Aberle, (Banovic *et al*., 2010)
+; +; P{UAS-Nlg1Δcyto::GFP}	UAS-*Nlg1*Δcyto::GFP	Gift from Hermann Aberle, (Banovic *et al*., 2010)
P{UAS-nrx.GFP}; +; +	UAS-*Nrx*::GFP	Gift from Hermann Aberle, (Banovic *et al*., 2010)
w*; +; P{UAS-shits1.K}3	UAS-*Shibire*^{TS}	Gift from Barret Pfeiffer, BDSC 44222
w[*]; P{y[+t7.7] w[+mC]=UAS-TrpA1(B).K}attP16	UAS-*TRPA1*	BDSC 26263
	UAS-K_{ir} *2.1*	Gift from Sean Sweeney

w[*]; P{w[+mC]=UAS-TeTxLC.tnt}G2	UAS-*TeTxLC*-G	Gift from Sean Sweeney, BDSC 28838
w[1118]; P{y[+t7.7] w[+mC]=20XUAS-IVS-GCaMP6m}attP40	UAS-GCaMP6m	BDSC 42748
w[1118]; PBac{y[+mDint2] w[+mC]=20XUAS-IVS-GCaMP6m}VK00005	UAS-GCaMP6m	BDSC 42750
w[1118]; P{y[+t7.7] w[+mC]=UAS-GCaMP3.T}attP40	UAS-GCaMP3	BDSC 32116
y[1] w[67c23]; Mi{PT-GFSTF.0}brp[MI02987-GFSTF.0]/SM6a	*BRP*::GFP	BDSC 59292
y[1] w[67c23]; Mi{PT-GFSTF.0}Syt1[MI02197-GFSTF.0]/CyO	*Syt1*::GFP	BDSC 59411
y[1] w[67c23]; Mi{PT-GFSTF.2}VGlut[MI04979-GFSTF.2]	*VGlut*::GFP	BDSC 59788
w[*]; P{y[+t7.7] w[+mC]=13XLexAop2-IVS-myr::GFP}attP40	LexAop-myr::GFP	BDSC32210
w^{*}; P{LexAop-tdTomato.Myr}su(Hw)attP5/CyO	LexAop-myr::tdTomato	Gift from Matthias Landgraf
+; +; LexAop-TRPA1	LexAop-*TRPA1*	
w[*]; P{w[+mC]=alphaTub84B(FRT.GAL80)}2/CyO ; TM2/TM6B, Tb[1]	tub<GAL80<	BDSC 38880
P{hsFLP}12, y1 w*	hsFlp	BDSC
w[1118], shi[1]	$Shibire^{TS}$	Gift from Sean Sweeney (Grigliatti *et al*., 1973)
$dNlg1^{ex2.3}$/TM6c, Sb, Tb	*Nlg1* ex1.9	Gift from Hermann Aberle, (Banovic *et al*., 2010)
Nlg1 I960, CD8-Shaker::GFP/ TM6c, Sb, Tb	*Nlg1* I960, CD8-Shaker::GFP	Gift from Hermann Aberle, (Banovic *et al*., 2010)
Df(3R)BSC747/TM6c, Sb, Tb	DFBSC747	Gift from Hermann Aberle, (Cook *et al*., 2012)

dNrx^{241}	*Nrx*^{241}	Gift from Hermann Aberle, (Li *et al*., 2007)
Df(3R)Exel6191/TM6b	DFEXEL6191	Gift from Hermann Aberle, (Parks *et al*., 2004)
DF(2L)dVGlut^{2}/CyO	DF*VGlut*^{2}	Gift from Aaron DiAntonio, (Daniels *et al*., 2006)
y[1] w[*]; P{w[+mC]=tubP-GAL80}LL10 P{ry[+t7.2]=neoFRT}40A/CyO	FRT 40A, tub-Gal80	BDSC 5192

Table 2. Genetic crosses

Figure(s)	Cross (shorthand)	Use
2.1	*PPK*-GAL4, UAS-CD8::GFP/*VGlut*-LexA, LexAop-myr::GFP	Independent labelling of class IV da sensory neurons and glutamatergic neurons
2.11	OK371-GAL4/+; UAS-cytoplasmicGFP/+	Labelling glutamatergic neurons
2.2, 2.4, 2.5, 3.1, 3.2, 3.3, 3.9, 3.10…3.1, 3.17	*VGlut*-LexA, LexAop-myr::GFP/+	Labelling glutamatergic neurons
2.3, 2.8	*VGlut*-LexA, LexAop-myr::GFP/+; *Mef2*-GAL4, UAS-mtdTomato/+	Independent labelling of muscles and glutamatergic neurons
2.6	OK371-GAL4/+; UAS-*CLIP170*::GFP/+	Labelling microtubules in glutamatergic neurons
2.6	OK371-GAL4/UAS-Lifeact::Ruby	Labelling actin in glutamatergic neurons

2.7	*Mef2*-GAL4/ UAS-myr::GFP	Labelling muscles
2.9	OK371-GAL4/+; *Mef2*-GAL4/UAS-CytoplasmicGFP	Co-labelling muscles and glutamatergic neurons
2.10, 4.6	hsFlp/+; OK371-GAL4, Tub<GAL80</+; UAS-CytoplasmicGFP/+	Mosaic labelling of glutamatergic neurons
2.10	hsFlp/UAS-*DP110*::CaaX; OK371-GAL4, tub<GAL80</+; UAS-CytoplasmicGFP/+	Mosaic expression of *DP110* in motoneurons
2.12…2.1, 4.8	OK371-GAL4/+; UAS-myrGFP, UAS-*BRP*::RFP/+	BRP:RFP localisation in glutamatergic neurons
2.12	OK371-GAL4/+; UAS-cytoplasmicGFP, UAS-*BRP*::RFP/+	BRP:RFP localisation in glutamatergic neurons
2.17	OK371-GAL4/UAS-*Syt1*::GFP;UAS-*BRP*::RFP/+	Syt1 and BRP localisation in glutamatergic neurons
2.18	OK371-GAL4, UAS-mCD8::Cherry/*BRP*::GFP	Native BRP localisation in glutamatergic neurons
2.18	OK371-GAL4, UAS-mCD8::Cherry/*VGlut*::GFP	Native VGlut localisation in glutamatergic neurons
2.18	OK371-GAL4, UAS-mCD8::Cherry/*Syt1*::GFP	Native Syt1 localisation in glutamatergic neurons
3.1…3.3, 3.10, 3.11, 3.17	*VGlut*-LexA, LexAop-myr::GFP/+; $Nlg1^{ex2.3}$/DFBSC747	Labelling glutamatergic neurons in Nlg1 nulls
3.1…3.3, 3.10, 3.11	*VGlut*-LexA, LexAop-myr::GFP/+; *Nlg*1 I960, CD8-Shaker::GFP /DFBSC747	Labelling glutamatergic neurons in Nlg1 nulls
3.1…3.3, 3.17	*VGlut*-LexA, LexAop-myr::GFP/+; Nrx^{241}/DFEXEL6191	Labelling glutamatergic neurons in Nrx nulls

3.4, 3.6, 3.7, 3.8, 3.9	*VGlut*-LexA, LexAop-myr::tdTom/LexAop-myr::tdTom/*Mef2*-GAL4, UAS-*Nlg1*::GFP/ *Mef2*-GAL4, UAS-*Nlg1*::GFP	localisation of postsynaptic Nlg1::GFP in relation to glutamatergic neurons
3.5	UAS-*Nrx*::GFP/y; OK371-GAL4, UAS-mCD8::Cherry/+	Localisation of Nrx::GFP in glutamatergic neurons
3.12, 3.17	*VGlut*-LexA, LexAop-myr::GFP/+; *Mef2*-GAL4/ UAS-*Nlg1*-Untagged	Labelling glutamatergic neurons in a background of *Nlg1*-Untagged expression in muscles
3.13, 3.14	hsFlp/+; *VGlut*-LexA, LexAop-myr::GFP, tub<GAL80</+; *Mef2*-GAL4, UAS-mtdTomato/ UAS-*Nlg1*-Untagged	Labelling glutamatergic neurons in a background of mosaic *Nlg1*-Untagged and tdTomato expression in muscles
3.15	*PPK*-GAL4, UAS-CD8::GFP/+	Labelling class IV da sensory neurons
3.15	*PPK*-GAL4 UAS-dsRed/*VGlut*-LexA, LexAop-myr::GFP; UAS-*Nlg1*::CytoGFP/+	Labelling glutamatergic neurons in a background of *Nlg1*::CytoGFP and dsRed in class IV da sensory neurons
3.15	*PPK*-GAL4 UAS-dsRed/*VGlut*-LexA, LexAop-myr::GFP; UAS-*Nlg1*-Untagged/+	Labelling glutamatergic neurons in a background of *Nlg1*-Untagged and dsRed in class IV da sensory neurons
3.16	*PPK*-GAL4, UAS-CD8::GFP/+; UAS-Nlg1::CytoGFP/+	Expression of *Nlg1*::CytoGFP and CD8::GFP in class IV da sensory neurons
4.1, 4.7	OK371-GAL4, UAS-GCaMP6m/+	Expression of GCaMP6m in glutamatergic neurons
4.2	*Mef2*-GAL4, UAS-GCaMP6m/+	Expression of GCaMP6m in muscles
4.3	*Shibire*^{TS}/y; +; *Mef2*-GAL4, UAS-GCaMP6m/+	Expression of GCaMP6m in muscles in Shibire^{TS} hemizygous males
4.4	OK371-GAL4/+; *Mef2*-GAL4, UAS-GCaMP6m/+	Expression of GCaMP6m in muscles and glutamatergic muscles
4.5	OK371-GAL4, UAS-GCaMP3/UAS-*TRPA1*	*TRPA1* and GCaMP3 expression in glutamatergic neurons
4.5	*VGlut*-LexA/+; *Mef2*-GAL4, UAS-GCaMP6m/LexAop-*TRPA1*	GCaMP6m expression in muscles in a background of *TRPA1* expression in glutamatergic neurons

4.6	hsFlp/+; OK371-GAL4, tub<GAL80</UAS-*TeTxLC*; UAS-cytoplasmicGFP/+	Mosaic expression of *TeTxLC* in motoneurons
4.6	hsFlp/+; OK371-GAL4, tub<GAL80<; UAS-cytoplasmicGFP and UAS-*Kir2.1*	Mosaic expression of *Kir2.1* in motoneurons
4.6	OK371-GAL4/+; UAS-*Shibire*^{TS}/UAS-cytoplasmicGFP	Expression of *Shibire*^{TS} and cytoplasmicGFP in glutamatergic neurons
4.9, 4.10	hsFlp, *VGlut*^{NMJx}-GAL4, CD8::GFP; FRT 40A, DF*VGlut*^{2}/FRT 40A; tub-GAL80; UAS-myr::GFP, UAS-*BRP*::RFP	Mosaic analysis of *VGlut* null motoneuron MARCM clones

Sample preparation and live imaging

For live imaging at precise developmental timings, I refined a procedure for staging and mounting whole pupae.

Pupae extraction

To guarantee accuracy in staging, samples were collected at 0h APF when the pupal cuticle is yet to develop pigment; a state which lasts only around 15 minutes. Samples were incubated at 25^{o}C on damp tissue paper in 35mm Petri dishes sealed with parafilm tape, until the desired stage. In preparation for mounting, pupae were first dried on tissue paper for 10-15 minutes before immobilisation on strips of double sided sticky tape stuck to glass slides. Pupae were extracted from their puparial cases using a combination of forceps and iridectomy scissors, by removing first the operculum and then carefully peeling away the case piece by piece.

Mounting

For short term imaging (2 hours or less) pupae were mounted on glass slides. Each pupa was positioned with the dorso-lateral aspect of one abdominal flank facing upwards. A thin layer of halocarbon oil was applied to the abdomen using a paintbrush with a single bristle. A cover slip supported by wax mounts at the corner of the pupa was then gently pressed down upon the pupa, until a complete contact was formed with the pleural region of the abdomen.

For longer term imaging, pupae were mounted in humidity maintained imaging chambers (Fig. 1). In this arrangement, a sheet of semipermeable membrane was fastened across a circular opening in a specialised steel slide by means of a rubber O-ring, forming a breathable platform for the pupa. The pupa was mounted on the membrane and encircled with a ring of petroleum jelly. The addition of a cover slip supported by wax mounts formed a completely sealed environment permeable to gasses but not liquids. For optimal humidity, pupae were situated in the chambers with small pieces of damp tissue.

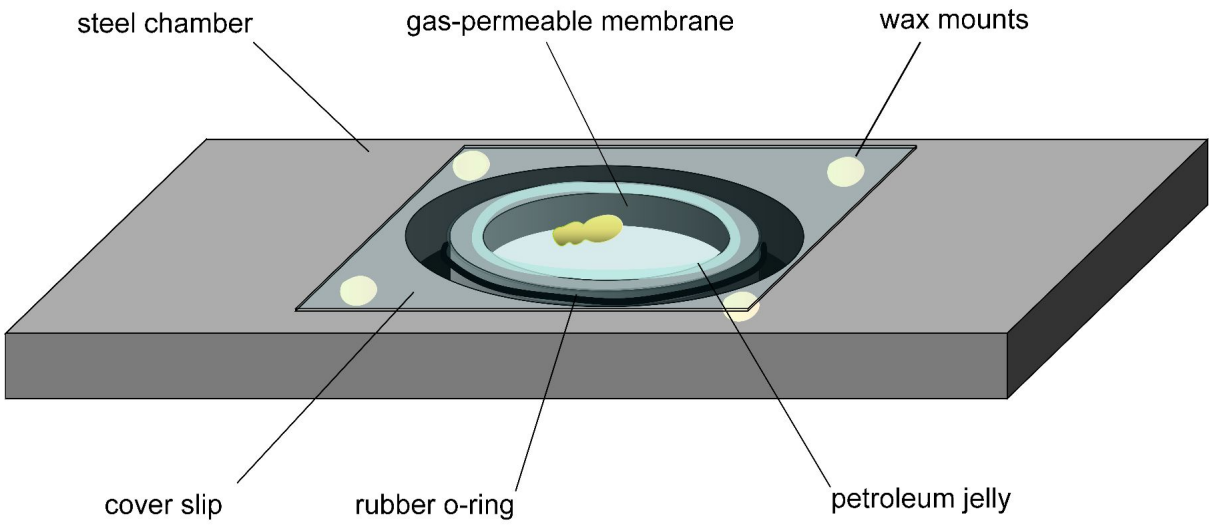

Figure. 1. Humidity maintained imaging chamber. Pupae are sealed in a compartment which prevents water loss but allows gas exchange.

For experiments requiring temperature manipulation, I devised a specialised, temperature adjustable stage. This consisted of a glass slide mounted on a 5x5cm Peltier device (Maplin Electronics Ltd., UK) which could be mounted on a regular microscope stage slide-holder. Pupae were mounted on the slide in the same way as described previously. Temperature was controlled from a 0-30v power supply unit (Rapid Electronics Ltd., UK) and calibrated using a thermocouple probe attached to a multi-meter device.

Confocal imaging

All imaging was performed using a Zeiss LSM 510 with a 20x or a 40x oil objective. This is with the exception of the imaging of Nlg::GFP and Nrx::GFP which was performed using a Zeiss LSM 880 (with the kind permission of Jon Clarke), and the imaging of branch recoil following ablation which was performed using a custom Nikon A1R in the Toyama lab, NUS.

Laser cutting

For laser cutting, samples were mounted as for live imaging, in the way appropriate for the experiment duration. Laser axotomies were performed using a femtosecond pulsed Ti-sapphire 2-photon laser (Coherent Inc., USA) mounted on a Nikon A1R confocal microscope. Before commencing each experiment a ‘practice’ sample was used to optimise the laser set-up for axon ablation. Although success varied to some degree between samples, stimulation settings of 750nm, 75% power output, 0.063 second scan speed and 1 loop were generally found to offer the best results whilst minimising the formation of destructive cavity bubbles.

Dissections and immunocytochemistry

For the preparation of abdominal wall fillets, pupae were dissected from their puparial cases as described for live imaging and transferred to Sylgard (Dow Corning, USA) lined Petri dishes. Dissections were performed in 1x phosphate buffered saline (PBS) (pH 7.3, Thermo Fisher Scientific, USA). Before dissecting, each pupa was immobilised by pinning through the head to the Sylgard using an electrolytically sharpened 0.1mm tungsten pin. The posterior of each abdomen was cut away (from approximately segment A6) using an iridectomy scissors. Incisions were made along the dorsal midline until reaching the thorax, at which point abdomens were freed from the rest of the body by cutting along the joint with the thorax. Using forceps, the resulting rectangular fillets were rolled out flat and pinned using additional tungsten pins.

Dissected samples were fixed in buffered 3.7% formaldehyde for 45 minutes at room temperature and washed three times in PBS containing 1% Triton-X100 (Sigma, USA) (PBST). Following fixation, samples were blocked in PBST containing 4% goat serum (Sigma, USA) for 45 minutes and incubated in solutions of primary antibodies made up with PBST overnight at 4^{o}C. After rinsing 3 times with PBST over the course of a day samples were incubated in solutions of secondary antibodies made up with PBST overnight at 4^{o}C. After 3 rinses with PBST and a final rinse with PBS samples were mounted on poly-L-lysine coated coverslips, dehydrated through a series of alcohol, cleared with xylene and mounted in DePeX (BDH Chemicals, UK).

Primary antibodies were used at the following concentrations: mouse anti-NC82 (DSHB, USA) 1:5, rabbit anti-VGlut-C term (kindly provided by Hermann Aberle (Mahr & Aberle, 2006)) 1:10,000, chicken anti-GFP (Invitrogen, USA) 1:1000. Secondary antibodies were used at the following concentrations: Cy3 goat anti-HRP (Jackson

Immunoresearch, USA) 1:5000, AlexaFluor 488 goat anti-Chicken (Invitrogen, USA) 1:500, Cy5 donkey anti-mouse 1:500, Cy5 donkey anti-rabbit 1:500.

Injections

To prepare for injection, pupae and larvae were first dried on tissue paper and then immobilised on strips of double sided sticky tape stuck to glass slides. To enable injection into the pupal abdomens, whilst minimising desiccation, small access holes were made at the posterior limits of the puparial cases using forceps. Glass injection needles were pulled from glass capillaries using a model p-87 micropipette puller (Sutter Instruments Co., USA) and loaded with TTX made up with PBS or a control solution, which included a ruby-labelled dextran (Thermo Fisher Scientific, USA). Injections were made using a Transjector-5246 micro-injector (Eppendorf, Germany) into the abdominal cavities. Following injection, samples were removed from the sticky tape with a damp paintbrush and allowed to develop until the required stage at 25^{o}C on damp tissue in 35mm Petri dishes sealed with parafilm tape.

Mosaic analysis

For mosaic expression of GAL4 in a manner independent of mitosis I used a GAL80 'flip-out' method of clone induction. This technique employs a ubiquitously expressed GAL80, the repressor of GAL4, which is flanked by FRT sides and can be excised using Flipase. hsFlp (*Flipase* driven under the control of a *Heat-Shock Protein-70* promoter) was used to induce clones stochastically throughout the animals. To generate small numbers of OK371-GAL4 positive motoneuron clones, or *Mef2*-GAL4 positive muscle clones in the adult abdomen, L3 wandering larvae were heat shocked for 20 minutes by incubation of vials in water a bath warmed to 37^{o}C.

The MARCM system (Lee and Luo, 1999) was used to create and label *VGlut* null motoneuron clones in otherwise heterozygous animals by mitotic recombination. In a preliminary screen of OK371-GAL4 motoneuron MARCM clones induced during the embryonic or larval waves of neurogenesis, the pleural motoneurons were found to be born embryonically. The embryonic wave of neurogenesis is short, and the survival of embryos through heat-shock low, therefore crosses were established in laying cages on a large scale (200-300 females per cage). To make clones, flies were first allowed to lay on grape jelly plates with yeast for 2 hours. Plates were then sealed with parafilm and incubated at 25^{o}C. Following this, plates were heat-shocked by incubation in a water bath at 37^{0}C for 45 minutes, rested at room temperature for 30 minutes and heat-shocked again for 30 minutes. Plates were then incubated at 25^{o}C for a further 24h when L1 larvae were transferred to vials of standard food, on which they were raised at 25^{o}C until the required stage for imaging.

Image Processing

Raw image stacks were imported into the image processing software Fiji (http://imagej.net/Fiji). For clarity, the freehand select tool was used to remove obscuring objects created by degenerating larval tissues and macrophages on a slice by slice basis. Collapsed z-projections were imported into Photoshop (Adobe, USA) for the assembly of figures. Schematic cartoons were made in Photoshop, Canvas X (ACD systems, USA) or Illustrator (Adobe, USA). To generate kymographs the reslice tool in FIJI was used to reconfigure the axis of image sequences

Statistical Analysis

Statistical analyses were performed using the software package GraphPad Prism (GraphPad Software Inc., USA). Significances correspond to the following p values: ≤0.05 = *, ≤0.01 = **, ≤0.001 = ***, ≤0.0001 = ****. For selecting between

parametric and non-parametric tests, the residuals of each data set were tested for normality.

Filopodia and puncta dynamics

Relationships between BRP::RFP and Nlg1::GFP puncta dynamics and branch growth were calculated by manually measuring and tracking puncta in FIJI. Puncta were identified by accumulations of fluorescent protein measuring 3 or more pixels in diameter at the native resolution.

Morphometric analysis

Arbor reconstructions were generated using the semi-automated plugin for FIJI, Simple Neurite Tracer. Reconstructed skeletons were imported into bespoke analysis software written by Dr Eric Blanc which computed total arbor length, total branch number, Strahler order and total arbor area (Fig. 2). Arbor area was calculated by giving branch coordinates a hypothetical 'contact distance' which represented its area of coverage. This value was set to 20μm, approximately the length of a terminal branch. In addition, this software could be used to add and delete vertices and nodes, allowing corrections to me made to tracing errors.

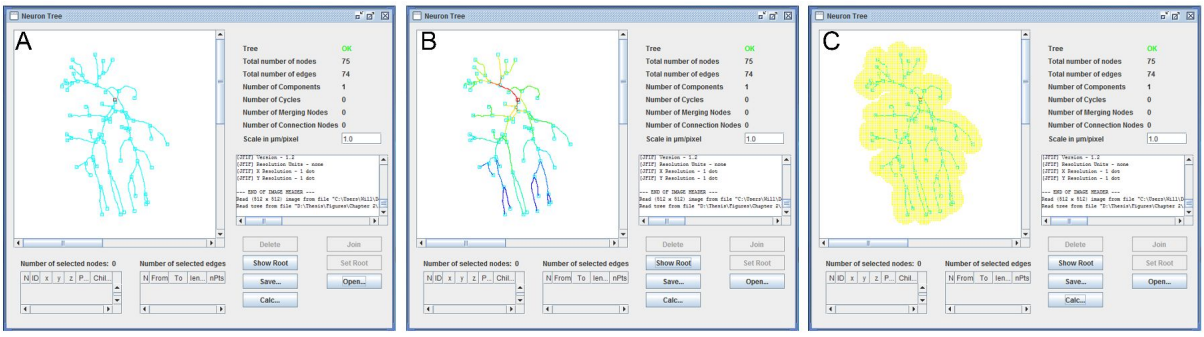

Figure. 2 Morphometric analysis software workflow. Screenshots show the software interface at different stages of morphometric analysis. (**A**) A 2D skeletonised trace upon being imported into the software, individual nodes and vertices can be modified. (**B**) Branches colour

coded according to their Strahler order. (**C**) The shaded yellow area shows the branch area, calculated with a 20μm 'contact distance'.

Straightness Index

To calculate branch straightness, the 'actual' lengths of primary, secondary and tertiary axon branches (from the distal tips) were measured between nodes using the freehand line tool in FIJI. These values divided by the direct distances between nodes, measured using the straight-line tool.

Branch Recoil

To calculate branch recoil following ablation, the distance between branch nodes, from the rear-most aspect of the nodes was measured at 5 second intervals using the straight-line tool in FIJI. These values were normalised by division with the original distance between the nodes prior to ablation.

Active zone density

Active zone densities in axon terminals were calculated manually in FIJI using the multi-point tool. Bouton areas were calculated by tracing around boutons using the freehand selection tool.

Bibliography

Ackman, J.B., Burbridge, T.J. & Crair, C.C., 2012. Retinal waves coordinate patterned activity throughout the developing visual system. *Nature*, 490, pp.219–25.

Ahmari, S.E., Buchanan, J. & Smith, S.J., 2000. Assembly of presynaptic active zones from cytoplasmic transport packets. *Nature Neuroscience*, 3, pp.445–51.

Alsina, B., Vu, T. & Cohen-Cory, S., 2001. Visualizing synapse formation in arborizing optic axons *in vivo*: dynamics and modulation by BDNF. *Nature Neuroscience*, 4, pp.1093–101.

Anderson, M.S., Halpern, M.E. & Keshishian, H., 1988. Identification of the neuropeptide transmitter proctolin in *Drosophila* larvae: characterization of muscle fiber-specific neuromuscular endings. *Journal of Neuroscience*, 8(1), pp.242–55.

Andreae, L.C. & Burrone, J., 2015. Spontaneous Neurotransmitter Release Shapes Dendritic Arbors via Long-Range Activation of NMDA Receptors. *Cell Reports*, 10(6), pp.873–82.

Andreae, L.C., Fredj, N. Ben & Burrone, J., 2012. Independent Vesicle Pools Underlie Different Modes of Release during Neuronal Development. *Journal of Neuroscience*, 32(5), pp.1867–74.

Andrews, G.L. et al., 2008. Dscam Guides Embryonic Axons By Netrin-Dependent And Independent Functions. *Development*, 135(23), pp.3839–48.

Arstikaitis, P. *et al.*., 2011. Proteins that promote filopodia stability, but not number, lead to more axonal-dendritic contacts. *PLoS ONE*, 6(3), pp.1–12.

Ashworth, R. & Bolsover, S.R., 2002. Spontaneous activity-independent intracellular calcium signals in the developing spinal cord of the zebrafish embryo. *Developmental Brain Research*, 139, pp.131–7.

Banovic, D. *et al.*., 2010. *Drosophila* neuroligin 1 promotes growth and postsynaptic differentiation at glutamatergic neuromuscular junctions. *Neuron*, 66(5), pp.724–38.

Barrow, S.L. *et al.*., 2009. Neuroligin1: a cell adhesion molecule that recruits PSD-95 and NMDA receptors by distinct mechanisms during synaptogenesis. *Neural development*, 4(1), p.17.

Bate, C.M., 1976a. Embryogenesis of an insect nervous system 1. A map of the thoracic and abdominal neuroblasts in Locusta migratoria. *Jounal of Embryology and Experimental Morphology*, 35(1), pp.107–23.

Bate, C.M., 1976b. Pioneer neurones in an insect embryo. *Nature*, 260, pp.54–56.

Bate, M., Rushton, E. & Currie, D. a, 1991. Cells with persistent twist expression are the embryonic precursors of adult muscles in *Drosophila*. *Development*, 113(1), pp.79–89.

Belote, J.M. & Baker, B.S., 1982. Sex determination in *Drosophila* melanogaster: analysis of transformer-2, a sex-transforming locus. *PNAS*, 79(5), pp.1568–72.

Bemben, M.A. *et al.*., 2014. CaMKII phosphorylation of neuroligin-1 regulates excitatory synapses. *Nature Neuroscience*, 17(1), pp.56–64.

Blankenship, A.G. *et al.*., 2011. The role of neuronal connexins 36 and 45 in shaping spontaneous firing patterns in the developing retina. *Journal of Neuroscience*, 31(27), pp.9998–10008.

Boucard, A.A. *et al.*., 2005. A splice code for trans-synaptic cell adhesion mediated by binding of neuroligin 1 to α- and β-neurexins. *Neuron*, 48(2), pp.229–36.

Bozdagi, O. *et al.*., 2010. Persistence of coordinated long-term potentiation and dendritic spine enlargement at mature hippocampal CA1 synapses requires N-cadherin. *Journal of Neuroscience*, 30(30), pp.9984–9.

Bradley, P. & Berry, M., 1976a. Quantitative effects of climbing fibre deafferentation on the adult Purkinje cell dendritic tree. *Brain Research*, 112(1), pp.133–40.

Bradley, P. & Berry, M., 1976b. The growth of the dendritic trees of Purkinje cells in irradiated agranular cerebellar cortex. *Brain Research*, 35(2), pp.123–43.

Brandon, E.P. *et al.*., 2003. Aberrant patterning of neuromuscular synapses in choline acetyltransferase-deficient mice. *The Journal of neuroscience*, 23(2), pp.539–49.

Bray, D., 1984. Axonal growth in response to experimentally applied mechanical tension. *Developmental Biology*, 102(2), pp.379–89.

Brierley, D.J. *et al.*., 2009. Dendritic targeting in the leg neuropil of *Drosophila*: The role of midline signalling molecules in generating a myotopic map. *PLoS Biology*, 7(9), pp.1–16.

Broadie, K. & Bate, M., 1993. Activity-dependent development of the neuromuscular synapse during *Drosophila* embryogenesis. *Neuron*, 11(4), pp.607–19.

Burrows, M. & Newland, P.L., 1994. Convergence of mechanosensory afferents from different classes of exteroceptors onto spiking local interneurons in the locust. *Journal of Neuroscience*, 14(5 Pt 2), pp.3341–50.

Chagnac-Amitai, Y., Luhmann, H.J. & Prince, D. a, 1990. Burst Generating and Regular Spiking Layer-5 Pyramidal Neurons of Rat Neocortex Have Different Morphological Features. *Journal of Comparative Neurology*, 296, pp.598–613.

Chen, S.X. *et al.*., 2010. Neurexin-neuroligin cell adhesion complexes contribute to synaptotropic dendritogenesis via growth stabilization mechanisms *in vivo*. *Neuron*, 67(6), pp.967–83.

Chen, T.W. *et al.*., 2013. Ultrasensitive fluorescent proteins for imaging neuronal activity. *Nature*, 499, pp.295–300.

Chen, Y.-C. *et al.*., 2012. *Drosophila* neuroligin 2 is required presynaptically and postsynaptically for proper synaptic differentiation and synaptic transmission. *Journal of Neuroscience*, 32(45), pp.16018–30.

Chia, P.H. *et al.*., 2014. Local F-actin network links synapse formation and axon branching. *Cell*, 156, pp.1–6.

Chia, P.H., Patel, M.R. & Shen, K., 2012. NAB-1 instructs synapse assembly by linking adhesion molecules and F-actin to active zone proteins. *Nature Neuroscience*, 15(2), pp.234–42.

Chiba, a *et al.*., 1993. Growth cone choices of *Drosophila* motoneurons in response to muscle fiber mismatch. *Journal of Neuroscience*, 13(2), pp.714–32.

Chih, B. *et al.*., 2004. Disorder-associated mutations lead to functional inactivation of neuroligins. *Human Molecular Genetics*, 13(14), pp.1471–7.

Chih, B., Engelman, H. & Scheiffele, P., 2005. Control of Excitatory and Inhibitory Synapse Formation by Neuroligins. *Science*, 307, pp.1324–8.

Chih, B., Gollan, L. & Scheiffele, P., 2006. Alternative Splicing Controls Selective Trans-Synaptic Interactions of the Neuroligin-Neurexin Complex. *Neuron*, 51(2), pp.171–78.

Choi, B.J. *et al.*., 2014. Miniature Neurotransmission Regulates *Drosophila* Synaptic Structural Maturation. *Neuron*, 82(3), pp.618–34.

Chubykin, A.A. *et al.*., 2007. Activity-Dependent Validation of Excitatory versus Inhibitory Synapses by Neuroligin-1 versus Neuroligin-2. *Neuron*, 54(6), pp.919–31.

Citri, A. & Malenka, R.C., 2008. Synaptic Plasticity : Multiple Forms , Functions , and Mechanisms. *Neuropsychopharmacology Reviews*, 33, pp.18–41.

Coleman, P.D. & Riesen, A.H., 1968. Environmental effects on cortical dendritic fields. *Journal of Anatomy*, 102(3), pp.363–74.

Cook, R. K., Christensen, S. J., Deal, J. A., Coburn, R. A., Deal, M. E., Gresens, J. M., … Cook, K. R. (2012). The generation of chromosomal deletions to provide extensive coverage and subdivision of the Drosophila melanogaster genome. Genome Biology, 13.

Cooper, M.W. & Smith, S.J., 1992. A real-time analysis of growth cone target-cell interactions during the formation of stable contacts between hippocampal-neurons in culture. *Journal Of Neurobiology*, 23, pp.814–28.

Costanzo, E.M., Barry, J. a & Ribchester, R.R., 2000. Competition at silent synapses in reinnervated skeletal muscle. *Nature Neuroscience*, 3(7), pp.694–700.

Craig, A.M. *et al.*., 2006. How to build a central synapse: clues from cell culture. *Trends in Neurosciences*, 29(1), pp.1–23.

Crisp, S. *et al.*., 2008. The development of motor coordination in *Drosophila* embryos. *Development*, 3717, pp.3707–17.

Crompton, D. *et al.*., 1995. Essential and neural transcripts from the *Drosophila* shaking-B locus are differentially expressed in the embryonic mesoderm and pupal nervous system. *Developmental biology*, 170(1), pp.142–58.

Currie, D. a & Bate, M., 1991. The development of adult abdominal muscles in *Drosophila*: myoblasts express twist and are associated with nerves. *Development*, 113(1), pp.91–102.

Dahlhaus, R. *et al.*., 2010. Overexpression of the cell adhesion protein neuroligin-1 induces learning deficits and impairs synaptic plasticity by altering the ratio of excitation to inhibition in the hippocampus. *Hippocampus*, 20(2), pp.305–22.

Dailey, M.E. & Smith, S.J., 1996. The dynamics of dendritic structure in developing hippocampal slices. *Journal of Neuroscience*, 16(9), pp.2983–94.

Dalva, M.B., McClelland, A.C. & Kayser, M.S., 2007. Cell adhesion molecules: signalling functions at the synapse. *Nature reviews. Neuroscience*, 8(3), pp.206–20.

Damke, H. *et al.*., 1994. Induction of mutant dynamin specifically blocks endocytic coated vesicle formation. *Journal of Cell Biology*, 127(4), pp.915–34.

Daniels, R.W. *et al.*., 2006. A single vesicular glutamate transporter is sufficient to fill a synaptic vesicle. *Neuron*, 49(1), pp.11–6.

Daniels, R.W. *et al.*., 2008. Visualizing glutamatergic cell bodies and synapses in *Drosophila* larval and adult CNS. *Journal of Comparative Neurology*, 508(1), pp.131–52.

Dascenco, D. et al., 2015. Slit and Receptor Tyrosine Phosphatase 69D Confer Spatial Specificity to Axon Branching via Dscam1. *Cell*, 162(5), pp.1140–54.

David, J.D., See, W.M. & Higginbotham, C.A., 1981. Fusion of chick embryo skeletal myoblasts: Role of calcium influx preceding membrane union. *Developmental Biology*, 82(2), pp.297–307.

Dean, C. *et al.*., 2003. Neurexin mediates the assembly of presynaptic terminals. *Nature Neuroscience*, 6(7), pp.708–16.

Dégenètais, E. *et al.*., 2002. Electrophysiological properties of pyramidal neurons in the rat prefrontal cortex: an *in vivo* intracellular recording study. *Cerebral cortex*, 12(1), pp.1–16.

Desprat, N. *et al.*., 2008. Tissue Deformation Modulates Twist Expression to Determine Anterior Midgut Differentiation in *Drosophila* Embryos. *Developmental Cell*, 15(3), pp.470–7.

Doherty, K.R. *et al.*., 2005. Normal myoblast fusion requires myoferlin. *Development*, 132(24), pp.5565–75.

Dudanova, I. *et al.*., 2007. Deletion of α-Neurexins Does Not Cause a Major Impairment of Axonal Pathfinding or Synapse Formation. *Journal of Comparative Neurology*, 504(3), pp.287–97.

Durand, C.M. *et al.*., 2012. SHANK3 mutations identified in autism lead to modification of dendritic spine morphology via an actin-dependent mechanism. *Molecular psychiatry*, 17(1), pp.71–84.

Edwards, J.S. & Huntford, R., 1998. Fridtjof Nansen : from the neuron to the North Polar Sea. *Endeavour*, 22(2), pp.76–80.

Ekker, S.C. & Larson, J.D., 2001. Morphant technology in model developmental systems. *Genesis*, 30(3), pp.89–93.

van Elburg, R.A.J. & van Ooyen, A., 2010. Impact of dendritic size and dendritic topology on burst firing in pyramidal cells. *PLoS Computational Biology*, 6(5), pp.1–19.

Feller, M.B. *et al.*., 1996. Requirement for Cholinergic Synaptic Transmission in the Propagation of Spontaneous Retinal Waves. *Science*, 272, pp.1182–7.

Feng, J. *et al.*., 2006. High frequency of neurexin 1β signal peptide structural variants in patients with autism. *Neuroscience Letters*, 409(1), pp.10–3.

Ferreira, T. *et al.*., 2014. Dendrite architecture organized by transcriptional control of the F-actin nucleator Spire. *Development*, 141, pp.650–60.

Fiala, J.C. *et al.*., 1998. Synaptogenesis via dendritic filopodia in developing hippocampal area CA1. *Journal of Neuroscience*, 18(21), pp.8900–11.

Fisher, Y. E., Yang, H. H., Isaacman-Beck, J., Xie, M., Gohl, D. M., & Clandinin, T. R. (2017). FlpStop, a tool for conditional gene control in Drosophila. eLife, 6.

Fouquet, W. *et al.*., 2009. Maturation of active zone assembly by *Drosophila* Bruchpilot. *Journal of Cell Biology*, 186(1), pp.129–45.

Fredj, N.B. *et al.*., 2010. Synaptic activity and activity-dependent competition regulates axon arbor maturation, growth arrest, and territory in the retinotectal projection. *Journal of Neuroscience*, 30(32), pp.10939–51.

Friedman, H.V. *et al.*., 2000. Assembly of new individual excitatory synapses: time course and temporal order of synaptic molecule recruitment. *Neuron*, 27, pp.57–69.

Gonzalez-bellido, P.T. *et al.*., 2010. Overexpressing Temperature-Sensitive Dynamin Decelerates Phototransduction and Bundles Microtubules in *Drosophila* photoreceptors. *Journal of Neuroscience*, 29(45), pp.14199–210.

Graf, E.R. *et al.*., 2004. Neurexins induce differentiation of GABA and glutamate postsynaptic specializations via neuroligins. *Cell*, 119(7), pp.1013–26.

Greiner, B. *et al.*., 2004. Neural organisation in the first optic ganglion of the nocturnal bee Megalopta genalis. *Cell and Tissue Research*, 318(2), pp.429–37.

Grigliatti, T., Hall, L., Rosenbluth, R., Suzuki, D., 1973. Temperature-sensitive mutations in *Drosophila* melanogaster. XIV. A selection of immobile adults. Molecular Genetics and Genomics. 120(2), pp.107-14.

Grueber, W.B. *et al.*., 2003. Dendrites of Distinct Classes of *Drosophila* Sensory Neurons Show Different Capacities for Homotypic Repulsion. *Current Biology*, 13, pp.618–26.

Grueber, W.B., Jan, L.Y. & Jan, Y.N., 2002. Tiling of the *Drosophila* epidermis by multidendritic sensory neurons. *Development*, 129, pp.2867–78.

Grueber, W.B. & Sagasti, A., 2010. Self-avoidance and Tiling : Mechanisms. *Cold Spring Harbor Laboratory Press*, 2, pp.1–16.

Gu, X., Olson, C. & Spitzer, C., 1994. Spontaneous Neuronal Calcium Spikes and Waves during Early Differentiation. *Journal of Neuroscience*, 14(11), pp.6325–35.

Haas, K., Li, J. & Cline, H.T., 2006. AMPA receptors regulate experience-dependent dendritic arbor growth *in vivo*. *PNAS*, 103(32), pp.12127–31.

Haberman, A. *et al*.., 2012. The synaptic vesicle SNARE neuronal synaptobrevin promotes endolysosomal degradation and prevents neurodegeneration. *Journal of Cell Biology*, 196(2), pp.261–76.

Hamada, F.N. et al., 2008. An internal thermal sensor controlling temperature preference in *Drosophila*. *Nature*, 454, pp.217–22.

Harris, K.M., Jensen, F.E. & Tsao, B., 1992. Three-dimensional structure of dendritic spines and synapses in rat hippocampus (CA1) at postnatal day 15 and adult ages: implications for the maturation of synaptic physiology and long-term potentiation. *Journal of Neuroscience*, 12(7), pp.2685–705.

Harrison, R.G., 1904. An experimental study of the relation of the nervous system to the developing muscula- ture in the embryo of the frog. *American Journal of Anatomy*. 3, pp.197-220

Hassan, B.A. & Hiesinger, P.R., 2015. Beyond Molecular Codes: Simple Rules to Wire Complex Brains. *Cell*, 163(2), pp.285–91.

Haverkamp, J., 1986. Anatomical and Physiological Development of the *Xenopus* Embryonic Motor System in the Absence of Neural Activity. *Journal of Neuroscience*, 6(5), pp.1338–48.

Haverkamp, L.J. & Oppenheim, R.W., 1986. Behavioral Development in the Absence of Neural Activity : Effects of Chronic Immobilization on Amphibian Embryos. *Journal of Neuroscience*, 6(5), pp.1332–7.

Hebbar, S. & Fernandes, J.J., 2005. A role for Fas II in the stabilization of motor neuron branches during pruning in *Drosophila*. *Developmental Biology*, 285(1), pp.185–99.

Heiman, M.G. & Shaham, S., 2009. DEX-1 and DYF-7 Establish Sensory Dendrite Length by Anchoring Dendritic Tips during Cell Migration. *Cell*, 137(2), pp.344–55.

Heiman, M.G. & Shaham, S., 2010. Twigs into branches: how a filopodium becomes a dendrite. *Current Opinion in Neurobiology*, 20(1), pp.86–91.

Hitchcock, P.F., 1989. Exclusionary dendritic interactions in the retina of the goldfish. *Development*, 106(3), pp.589–98.

Houenou, L.J. *et al*.., 1987. Neuromuscular Development Following Tetrodotoxin-Induced Inactivity in Mouse Embryos. *Journal of Neurobiology*, 21(8), pp.1249–1261.

Hua, J.Y. *et al*.., 2005. Regulation of axon growth *in vivo* by activity-based competition. *Nature*, 434, pp.1022–26.

Hummel, T. et al., 2003. Axonal Targeting of Olfactory Receptor Neurons in *Drosophila* Is Controlled by Dscam. *Neuron*, 37(37), pp.221–31.

Hutchinson, D. *et al*.., 2008. Differential outgrowth of axons and their branches is regulated by localized calcium transients. *Journal of Neuroscience*, 148(4), pp.825–32.

Ichtchenko, K. *et al.*., 1995. Neuroligin 1: A splice site-specific ligand for β-Neurexins. *Cell*, 81(3), pp.435–43.

Irie, M. *et al.*., 1997. Binding of Neuroligins to PSD-95. *Science*, 277, pp.1511–5.

Jamain, S. *et al.*., 2003. Mutations of the X-linked genes encoding neuroligins NLGN3 and NLGN4 are associated with autism. *Nature Genetics*, 34(1), pp.27–9.

Javaherian, A. & Cline, H.T., 2005. Coordinated motor neuron axon growth and neuromuscular synaptogenesis are promoted by CPG15 *in vivo*. *Neuron*, 45(4), pp.505–12.

Jefferis, G.S. *et al.*., 2001. Target neuron prespecification in the olfactory map of *Drosophila*. *Nature*, 414, pp.204–8.

Jinushi-Nakao, S. *et al.*., 2007. Knot/Collier and Cut Control Different Aspects of Dendrite Cytoskeleton and Synergize to Define Final Arbor Shape. *Neuron*, 56(6), pp.963–78.

Johns, D.C. et al., 1999. Inducible Genetic Suppression of Neuronal Excitability. *The Journal of Neuroscience*, 19(5), pp.1691–7.

Jontes, J.D., Buchanan, J. & Smith, S.J., 2000. Growth cone and dendrite dynamics in zebrafish embryos: early events in synaptogenesis imaged *in vivo*. *Nature Neuroscience*, 3, pp.231–7.

Kaas, J.H., 1997. Topographic Maps Are Fundamental to Sensory Processing. *Brain Research Bullitin*, 44(2), pp.107–12.

Kaethner, R.J. & Stuermer, C.A.O., 1994. Growth behavior of retinotectal axons in live zebrafish embryos under TTX-induced neural impulse blockade. *Journal of Neurobiology*, 25(7), pp.781–96.

Kaethner, R.J. & Stuermer, C. a, 1992. Dynamics of terminal arbor formation and target approach of retinotectal axons in living zebrafish embryos: a time-lapse study of single axons. *Journal of Neuroscience*, 12, pp.3257–71.

Kalil, K. & Dent, E.W., 2014. Branch management: mechanisms of axon branching in the developing vertebrate CNS. *Nature reviews. Neuroscience*, 15(1), pp.7–18.

Kalil, K., Li, L. & Hutchins, B.I., 2011. Signaling Mechanisms in Cortical Axon Growth, Guidance, and Branching. *Frontiers in Neuroanatomy*, 5, pp.1–15.

Kalus, P. *et al.*., 2000. The dendritic architecture of prefrontal pyramidal neurons in schizophrenic patients. *Neuroreport*, 11(16), pp.3621–5.

Kaneko, M. *et al.*., 2000. Disruption of Synaptic Transmission or Clock-Gene Product Oscillations in Circadian Pacemaker Cells of *Drosophila* Cause Abnormal Behavioral Rhythms. *Journal of Neurobiology*, 3(3), pp.207–33.

Karuppudurai, T. *et al.*., 2014. A Hard-Wired Glutamatergic Circuit Pools and Relays UV Signals to Mediate Spectral Preference in *Drosophila*. *Neuron*, 81(3), pp.603–15.

Kater, S.B. & Rehder, V., 1992. Regulation of Neuronal Growth Cone Filopodia by Intracellular Calcium. *Journal of Neuroscience*, 12(8), pp.3175–86.

Kaufmann, N. *et al.*., 2002. *Drosophila* liprin-α and the receptor phosphatase Dlar control synapse morphogenesis. *Neuron*, 34(1), pp.27–38.

Kaufmann, W.E. & Moser, H.W., 2000. Dendritic Anomalies in Disorders Associated with Mental Retardation. *Cerebral Cortex*, 10, pp.981–91.

Kim, H.-G. *et al.*., 2008. Disruption of neurexin 1 associated with autism spectrum disorder. *American Journal of Human Genetics*, 82(January), pp.199–207.

Kim, J. *et al.*., 2008. Neuroligin-1 is required for normal expression of LTP and associative fear memory in the amygdala of adult animals. *PNAS*, 105(26), pp.9087–92.

Kimura, H. *et al.*., 2006. Potential dual molecular interaction of the *Drosophila* 7-pass transmembrane cadherin Flamingo in dendritic morphogenesis. *Journal of Cell Science*, 119(6), pp.1118–29.

Kirkby, L.A. *et al.*., 2013. A role for correlated spontaneous activity in the assembly of neural circuits. *Neuron*, 80(5), pp.1129–44.

Kittel, R.J. *et al.*., 2006. Bruchpilot Promotes Active Zone Assembly, Ca2+ Channel Clustering, and Vesicle Release. *Science*, 312, pp.1051–54.

Ko, J. *et al.*., 2009. LRRTM2 Functions as a Neurexin Ligand in Promoting Excitatory Synapse Formation. *Neuron*, 64(6), pp.791–8.

Ko, J. *et al.*., 2011. Neuroligins/LRRTMs prevent activity- and Ca 2+/calmodulin-dependent synapse elimination in cultured neurons. *Journal of Cell Biology*, 194(2), pp.323–34.

Kohsaka, H. & Nose, A., 2009. Target recognition at the tips of postsynaptic filopodia: accumulation and function of Capricious. *Development*, 136(7), pp.1127–35.

Kohsaka, H., Takasu, E. & Nose, A., 2007. *In vivo* induction of postsynaptic molecular assembly by the cell adhesion molecule Fasciclin2. *Journal of Cell Biology*, 179(6), pp.1289–300.

Komuro, H. & Rakic, P., 1996. Intracellular Ca2+ fluctuations modulate the rate of neuronal migration. *Neuron*, 17(2), pp.275–85.

Kosaka, T. & Ikeda, K., 1983. Reversible blockage of membrane retrieval and endocytosis in the garland cell of the temperature-sensitive mutant of *Drosophila* melanogaster, shibirets1. *Journal of Cell Biology*, 97(2), pp.499–507.

Kwon, H.-B. *et al.*., 2012. Neuroligin-1-dependent competition regulates cortical synaptogenesis and synapse number. *Nature neuroscience*, 15(12), pp.1667–74.

Lamoureux, P. *et al.*., 2002. Mechanical tension can specify axonal fate in hippocampal neurons. *Journal of Cell Biology*, 159(3), pp.499–508.

Landgraf, M. *et al.*., 2003. Embryonic origins of a motor system: Motor dendrites form a myotopic map in *Drosophila*. *PLoS Biology*, 1(2), pp.221–30.

Lee, H., Dean, C. & Isacoff, E., 2010. Alternative Splicing of Neuroligin Regulates the Rate of Presynaptic Differentiation. *Journal of Neuroscience*, 30(34), pp.11435–46.

Lee, T. & Luo, L., 1999. Mosaic Analysis with a Repressible Neurotechnique Cell Marker for Studies of Gene Function in Neuronal Morphogenesis. *Neuron*, 22, pp.451–61.

Leevers, S.J. *et al.*., 1996. The *Drosophila* phosphoinositide 3-kinase Dp110 promotes cell growth. *EMBO journal*, 15(23), pp.6584–94.

Lefebvre, J.L. *et al.*., 2012. Protocadherins mediate dendritic self-avoidance in the mammalian nervous system. *Nature*, 488, pp.517–21.

Li, J. *et al.*., 2007. Crucial Role of *Drosophila* Neurexin in Proper Active Zone Apposition to Postsynaptic Densities, Synaptic Growth, and Synaptic Transmission. *Neuron*, 55(5), pp.741–55.

Li, L. *et al.*., 2014. *Drosophila* Syd-1, Liprin-α, and protein phosphatase 2A B' subunit Wrd function in a linear pathway to prevent ectopic accumulation of synaptic materials in distal axons. *Journal of Neuroscience*, 34(25), pp.8474–87.

Li, W. *et al.*., 2004. BTB/POZ-zinc finger protein abrupt suppresses dendritic branching in a neuronal subtype-specific and dosage-dependent manner. *Neuron*, 43(6), pp.823–34.

Link, E. et al., 1992. Tetanus Toxin Action : Inhibition of Neurotransmitter Release Linked to Synaptobrevin Proteolysis. *BIOCHEMICAL AND BIOPHYSICAL RESEARCH COMMUNICATIONS*, 189(2), pp.1017–23.

Liu, X.F., Tari, P.K. & Haas, K., 2009. PKMζ Restricts Dendritic Arbor Growth by Filopodial and Branch Stabilization within the Intact and Awake Developing Brain. *Journal of Neuroscience*, 29(39), pp.12229–35.

Lohmann, C., Finski, A. & Bonhoeffer, T., 2005. Local calcium transients regulate the spontaneous motility of dendritic filopodia. *Nature neuroscience*, 8(3), pp.305–12.

Lohmann, C., Myhr, K. & Wong, R.O.L., 2002. Transmitter-evoked local calcium release stabilizes developing dendrites. *Nature*, 418, pp.174–77.

Mahr, A. & Aberle, H., 2006. The expression pattern of the *Drosophila* vesicular glutamate transporter: a marker protein for motoneurons and glutamatergic centers in the brain. *Gene Expression Patterns*, 6(3), pp.299-309.

Mainen, Z.F. & Sejnowski, T.J., 1996. Influence of dendritic topology on firing patterns in model neurons. *Neurocomputing*, 382, pp.363–6.

Mason, A. & Larkman, A., 1990. Correlations between morphology and electrophysiology of pyramidal neurons in slices of rat visual cortex. II. Electrophysiology. *Journal of Neuroscience*, 10(5), pp.1415–28.

Matkovic, T. *et al.*., 2013. The bruchpilot cytomatrix determines the size of the readily releasable pool of synaptic vesicles. *Journal of Cell Biology*, 202(4), pp.667–83.

Mattila, P.K. & Lappalainen, P., 2008. Filopodia: molecular architecture and cellular functions. *Nature reviews. Molecular cell biology*, 9(6), pp.446–54.

Mauss, A. *et al.*., 2009. Midline signalling systems direct the formation of a neural map by dendritic targeting in the *Drosophila* motor system. *PLoS Biology*, 7(9), pp.1–18.

Mclaughlin, T. & Leary, D.D.M.O., 2005. Molecular Gradients and Development of Retinotopic Maps. *Annual Reviews of Neuroscience*, 28, pp.327–55.

Meyer, M.P. & Smith, S.J., 2006. Evidence from *in vivo* imaging that synaptogenesis guides the growth and branching of axonal arbors by two distinct mechanisms. *Journal of Neuroscience*, 26(13), pp.3604–14.

Millard, S.S. *et al.*., 2007. DSCAM2 mediates axonal tiling in the visual system. *Nature*, 447, pp.720–24.

Misgeld, T. *et al.*., 2002. Roles of neurotransmitter in synapse formation: development of neuromuscular junctions lacking choline acetyltransferase. *Neuron*, 36(4), pp.635–48.

Missler, M. *et al.*., 2003. Alpha-neurexins couple Ca2+ channels to synaptic vesicle exocytosis. *Nature*, 423, pp.939–48.

Missler, M., Südhof, T.C. & Bierderer, T., 2012. Synaptic Cell Adhesion. *Cold Spring Harbor Laboratory Press*, 970, pp.97–128.

Monastirioti, M. *et al.*., 1995. Octopamine Immunoreactivity in the Fruit Fly *Drosophila* melanogaster. *Journal of Comparative Neurology*, 356(2), pp.37–54.

Mondin, M. *et al.*., 2011. Neurexin-Neuroligin Adhesions Capture Surface-Diffusing AMPA Receptors through PSD-95 Scaffolds. *Journal of Neuroscience*, 31(38), pp.13500–15.

Monier, B. *et al.*., 2010. An actomyosin-based barrier inhibits cell mixing at compartmental boundaries in *Drosophila* embryos. *Nature Cell Biology*, 12(1), pp.60–5.

Montague, P.R. & Friedlander, M.J., 1989. Expression of an intrinsic growth strategy by mammalian retinal neurons. *PNAS*, 86(18), pp.7223–7.

Montague, P.R. & Friedlander, M.J., 1991. Morphogenesis and Territorial Retinal Ganglion Cells Coverage by Isolated Mammalian. *Journal of Neuroscience*, 11(5), pp.1440–57.

Moody, W.J. & Bosma, M.M., 2005. Ion channel development, spontaneous activity, and activity-dependent development in nerve and muscle cells. *Physiological Reviews*, 85, pp.883–941.

Muhammad, K. *et al.*., 2015. Presynaptic spinophilin tunes neurexin signalling to control active zone architecture and function. *Nature Communications*, 6, pp.1–15.

Nadeau, H. *et al.*., 2000. ROMK1 (Kir1.1) causes apoptosis and chronic silencing of hippocampal neurons. *Journal of Neurophysiology*, 84(2), pp.1062–75.

Narahashi, T. et al., 1960. Stabilization and rectification of muscle fiber membrane by tetrodotoxin. *American Journal of Physiology*, 198(5), pp.934–8.

Neale, E.A., Bowers, L.M. & Smith, T.G., 1993. Early dendrite development in spinal cord cell cultures: A quantitative study. *Journal of Neuroscience Research*, 34(1), pp.54–66.

Newland, P.L. & Burrows, M., 1997. Processing of tactile information in neuronal networks controlling leg movements of the locust. *Journal of Insect Physiology*, 43(2), pp.107–23.

Nguyen, T. & Südhof, T.C., 1997. Binding properties of neuroligin 1 and neurexin 1β reveal function as heterophilic cell adhesion molecules. *Journal of Biological Chemistry*, 272(41), pp.26032–26039.

Niell, C.M., 2006. Theoretical analysis of a synaptotropic dendrite growth mechanism. *Journal of Theoretical Biology*, 241(1), pp.39–48.

Niell, C.M., Meyer, M.P. & Smith, S.J., 2004. *In vivo* imaging of synapse formation on a growing dendritic arbor. *Nature Neuroscience*, 7(3), pp.254–60.

Nikolaou, N. & Meyer, M.P., 2015. Lamination Speeds the Functional Development of Visual Circuits. *Neuron*, 88(5), pp.999–1013.

Nitabach, M.N., Blau, J. & Holmes, T.C., 2002. Electrical silencing of *Drosophila* pacemaker neurons stops the free-running circadian clock. *Cell*, 109(4), pp.485–95.

van Ooyen, A. *et al.*., 2002. The effect of dendritic topology on firing patterns in model neurons. *Network: Computation in Neural Systems*, 13(3), pp.311–325.

Owald, D. *et al.*., 2010. A Syd-1 homologue regulates pre- and postsynaptic maturation in *Drosophila*. *Journal of Cell Biology*, 188(4), pp.565–79.

Owald, D. *et al.*., 2012. Cooperation of Syd-1 with Neurexin synchronizes pre- with postsynaptic assembly. *Nature Neuroscience*, 15(9), pp.1219–26.

Pack-Chung, E. *et al.*., 2007. A *Drosophila* kinesin required for synaptic bouton formation and synaptic vesicle transport. *Nature Neuroscience*, 10(8), pp.980–9.

Pakkenberg, B. *et al.*., 2003. Aging and the human neocortex. *Experimental Gerontology*, 38(1–2), pp.95–9.

Palkovits, M., Magyar, P. & Szentágothai, J., 1971. Quantitative histological analysis of the cerebellar cortex in the cat. II. Cell numbers and densities in the granular layer. *Brain Research*, 32(1), pp.15–30.

Panzer, J.A., Song, Y. & Balice-gordon, R.J., 2006. *In vivo* Imaging of Preferential Motor Axon Outgrowth to and Synaptogenesis at Prepatterned Acetylcholine Receptor Clusters in Embryonic Zebrafish Skeletal Muscle. *Journal of Neuroscience*, 26(3), pp.934–47.

Paradis, S. *et al.*., 2001. Homeostatic Control of Presynaptic Release Is Triggered by Postsynaptic Membrane Depolarization. *Neuron*, 30(3), pp.737–49.

Parks, A. L., Cook, K. R., Belvin, M., Dompe, N. a, Fawcett, R., Huppert, K., … Francis-Lang, H. L. (2004). Systematic generation of high-resolution deletion coverage of the Drosophila melanogaster genome. *Nature Genetics*, *36*(3), 288–92.

Peixoto, R.T. *et al.*., 2012. Transsynaptic Signaling by Activity-Dependent Cleavage of Neuroligin-1. *Neuron*, 76(2), pp.396–409.

Penn, A.A. *et al.*., 1998. Competition in Retinogeniculate Patterning Driven by Spontaneous Activity. *Science*, 279, pp.2108–12.

Perry, V.H. & Linden, R., 1982. Evidence for dendritic competition in the developing retina. *Nature*, 297, pp.683–5.

Pfeiffer, B. D., Truman, J. W., & Rubin, G. M. (2012). Using translational enhancers to increase transgene expression in Drosophila. Proceedings of the National Academy of Sciences, 109(17), 6626–31.

Rajan, I. & Cline, H.T., 1998. Glutamate Receptor Activity Is Required for Normal Development of Tectal Cell Dendrites *In vivo*. *Journal of Neuroscience*, 18(19), pp.7836–46.

Rajan, I., Witte, S. & Cline, H.T., 1999. NMDA receptor activity stabilizes presynaptic retinotectal axons and postsynaptic optic tectal cell dendrites *in vivo*. *Journal of Neurobiology*, 38(3), pp.357–68.

Ranganayakulu, G., Schlulz, R., Olsen, E., 1996. Wingless Signaling Inducesnautilus Expression in the Ventral Mesoderm of the *Drosophila* Embryo. *Developmental Biology*. 176(1), pp.143-8.

Ritzenthaler, S. & Chiba, A., 2002. Myopodia (postsynaptic filopodia) participate in synaptic target recognition. *Journal of Neurobiology*, 55(1), pp.31–40.

Rossi, F.M. *et al.*., 2001. Requirement of the nicotinic acetylcholine receptor β2 subunit for the anatomical and functional development of the visual system. *PNAS*, 98(11), pp.6453–8.

Ruthazer, E.S., Li, J. & Cline, H.T., 2006. Stabilization of axon branch dynamics by synaptic maturation. *Journal of Neuroscience*, 26(13), pp.3594–603.

Sabo, S.L., Gomes, R. a & McAllister, a K., 2006. Formation of presynaptic terminals at predefined sites along axons. *Journal of Neuroscience*, 26(42), pp.10813–25.

Sagasti, A. *et al.*., 2005. Repulsive interactions shape the morphologies and functional arrangement of zebrafish peripheral sensory arbors. *Current Biology*, 15(9), pp.804–14.

Sanes, J.R. & Masland, R.H., 2015. The Types of Retinal Ganglion Cells : Current Status and Implications for Neuronal Classification. *Annual Reviews of Neuroscience*, 38, pp.221–48.

Scheiffele, P. *et al.*., 2000. Neuroligin expressed in nonneuronal cells triggers presynaptic development in contacting axons. *Cell*, 101(6), pp.657–69.

Schmidt, J.T. *et al.*., 2000. MK801 increases retinotectal arbor size in developing zebrafish without affecting kinetics of branch elimination and addition. *Journal of Neurobiology*, 42(3), pp.303–314.

Schmidt, J.T., Fleming, M.R. & Leu, B., 2004. Presynaptic Protein Kinase C Controls Maturation and Branch Dynamics of Developing Retinotectal Arbors: Possible Role in Activity-Driven Sharpening. *Journal of Neurobiology*, 58(3), pp.328–40.

Schmucker, D. *et al.*., 2000. *Drosophila* DSCAM Is an Axon Guidance Receptor Exhibiting Extraordinary Molecular Diversity. *Cell*, 101, pp.671–84.

Schnell, E. *et al.*., 2012. Neuroligin-1 Overexpression in Newborn Granule Cells *In vivo*. *PLoS ONE*, 7(10), pp.1–11.

Schwartz, E.L., 1977. Spatial mapping in the primate sensory projection: Analytic structure and relevance to perception. *Biological Cybernetics*, 25(4), pp.181–94.

Shapira, M. *et al.*., 2003. Unitary assembly of presynaptic active zones from Piccolo-Bassoon transport vesicles. *Neuron*, 38(2), pp.237–52.

Shatz, C.J. & Stryker, M.P., 1986. Prenatal Tetrodotoxin Infusion Blocks Segregation of Retinogeniculate Afferents. *Science*, 242, pp.87–9.

Shepherd, D. & Laurent, G., 1992. Embryonic Development of a Population of Spiking Local Interneurones in the Locust. *Journal of Comparative Neurology*, 319, pp.438–53.

Siddiqui, T.J. *et al.*., 2010. LRRTMs and Neuroligins Bind Neurexins with a Differential Code to Cooperate in Glutamate Synapse Development. *Brain Research*, 30(22), pp.7495–506.

Siechen, S. *et al.*., 2009. Mechanical tension contributes to clustering of neurotransmitter vesicles at presynaptic terminals. *PNAS*, 106(31), pp.12611–6.

Siegler, M. V & Burrows, M., 1986. Receptive fields of motor neurons underlying local tactile reflexes in the locust. *Journal of Neuroscience*, 6(February), pp.507–13.

Sin, W.C. *et al.*., 2002. Dendrite growth increased by visual activity requires NMDA receptor and Rho GTPases. *Nature*, 419(6906), pp.475–80.

Sink, H. & Whitington, P.M., 1991. Early ablation of target muscles modulates the arborisation pattern of an identified embryonic *Drosophila* motor axon. *Development*, 113(2), pp.701–7.

Smith, D.H., Wolf, J.A. & Meaney, D.F., 2001. A New Strategy to Produce Sustained Growth of Central Nervous System Axons: Continuous Mechanical Tension. *Tissue Engineering*, 7(2), pp.131–9.

Soba, P. *et al.*., 2007. *Drosophila* Sensory Neurons Require DSCAM for Dendritic Self-Avoidance and Proper Dendritic Field Organization. *Neuron*, 54, pp.403–16.

Soler-Llavina, G.J. *et al.*., 2011. The neurexin ligands, neuroligins and leucine-rich repeat transmembrane proteins, perform convergent and divergent synaptic functions *in vivo*. *PNAS*, 108(40), pp.16502–9.

Song, J.Y. *et al.*., 1999. Neuroligin 1 is a postsynaptic cell-adhesion molecule of excitatory synapses. *PNAS*, 96(3), pp.1100–5.

Spitzer, N.C. *et al.*., 2000. Coding of neuronal differentiation by calcium transients. *BioEssays*, 22(9), pp.811–7.

Stramer, B. *et al.*., 2010. Clasp-mediated microtubule bundling regulates persistent motility and contact repulsion in *Drosophila* macrophages *in vivo*. *Journal of Cell Biology*, 189(4), pp.681–9.

Südhof, T.C., 2013. A molecular machine for neurotransmitter release: synaptotagmin and beyond. *Nature Medicine*, 19(10), pp.1227–31.

Südhof, T.C., 2008. Neuroligins and neurexins link synaptic function to cognitive disease. *Nature*, 455, pp.903–11.

Sugimura, K. *et al.*., 2004. Development of morphological diversity of dendrites in *Drosophila* by the BTB-zinc finger protein abrupt. *Neuron*, 43(6), pp.809–22.

Sugita, S. *et al.*., 2001. A stoichiometric complex of neurexins and dystroglycan in brain. *Journal of Cell Biology*, 154(2), pp.435–445.

Sun, M. *et al.*., 2011. Neuroligin 2 is required for synapse development and function at the *Drosophila* neuromuscular junction. *Journal of Neuroscience*, 31(2), pp.687–99.

Suster, M.L. *et al.*., 2003. Targeted expression of tetanus toxin reveals sets of neurons involved in larval locomotion in *Drosophila*. *Journal of Neurobiology*, 55(2), pp.233–46.

Sweeney, S.T. *et al.*., 1995. Targeted expression of tetanus toxin light chain in *Drosophila* specifically eliminates synaptic transmission and causes behavioral defects. *Neuron*, 14(2), pp.341–51.

Tabuchi, K. *et al.*., 2007. A Neuroligin-3 Mutation Implicated in Autism Increases Inhibitory Synaptic Transmission in Mice. *Science*, 318(5847), pp.71–6.

Talavage, T.M. *et al.*., 2004. Tonotopic organization in human auditory cortex revealed by progressions of frequency sensitivity. *Journal of Neurophysiology*, 91(3), pp.1282–96.

Tang, F., Dent, E.W. & Kalil, K., 2003. Spontaneous calcium transients in developing cortical neurons regulate axon outgrowth. *Journal of Neuroscience*, 23(3), pp.927–36.

Taniguchi, H. *et al.*., 2007. Silencing of neuroligin function by postsynaptic neurexins. *Journal of Neuroscience*, 27(11), pp.2815–24.

Tripodi, M. *et al.*., 2008. Structural homeostasis: Compensatory adjustments of dendritic arbor geometry in response to variations of synaptic input. *PLoS Biology*, 6(10), pp.2172–87.

Tsetsenis, T. et al., 2014. Direct Visualization of Trans -Synaptic Neurexin – Neuroligin Interactions during Synapse Formation. *Journal of Neuroscience*, 34(45), pp.15083–96.

Truman, J.W. & Reiss, S.E., 1976. Dendritic Reorganization of an Identified Motoneuron During Metamorphosis of the Tobacco Hornworm Moth. *Science*, 192, pp.477–9.

Turner, D.A. *et al.*., 1995. Morphometric and electrical properties of reconstructed hippocampal CA3 neurons recorded *in vivo*. *Journal of Comparative Neurology*, 356(4), pp.580–94.

Tyler, W.J., 2012. The mechanobiology of brain function. *Nature reviews. Neuroscience*, 13(12), pp.867–78.

Ushkaryov, Y. a *et al.*., 1992. Neurexins: synaptic cell surface proteins related to the alpha-latrotoxin receptor and laminin. *Science*, 257(5066), pp.50–6.

Usui, T. *et al.*., 1999. Flamingo, a seven-pass transmembrane cadherin, regulates planar cell polarity under the control of Frizzled. *Cell*, 98(5), pp.585–95.

Varoqueaux, F. *et al.*., 2006. Neuroligins Determine Synapse Maturation and Function. *Neuron*, 51(6), pp.741–54.

Varoqueaux, F. *et al.*., 2002. Total arrest of spontaneous and evoked synaptic transmission but normal synaptogenesis in the absence of Munc13-mediated vesicle priming. *PNAS*, 99(13), pp.9037–42.

Vassar, R. *et al.*., 1994. Topographic Organization of Sensory Projection to the Olfactory Bulb. *Cell*, 79, pp.981–91.

Vaughn, J.E., 1989. Fine structure of synaptogenesis in the vertebrate central nervous system. *Synapse*, 3, pp.255–85.

Vaughn, J.E., Barber, R.P. & Sims, T.J., 1988. Dendritic development and preferential growth into synaptogenic fields: a quantitative study of Golgi-impregnated spinal motor neurons. *Synapse*, 2(1), pp.69–78.

Vaughn, J.E., Henrikson, C.K. & Grieshaber, J.A., 1974. A quantitative study of synapses on motor neuron dendritic growth cones in developing mouse spinal cord. *Journal of Cell Biology*, 60(3), pp.664–72.

Verhage, M. *et al.*., 2000. Synaptic assembly of the brain in the absence of neurotransmitter secretion. *Science*, 287, pp.864–9.

Wagh, D.A. *et al.*., 2006. Bruchpilot, a Protein with Homology to ELKS/CAST, Is Required for Structural Integrity and Function of Synaptic Active Zones in *Drosophila*. *Neuron*, 49, pp.833–44.

Walter, J., Henke-fahle, S. & Bonhoeffer, F., 1987. Avoidance of posterior tectal membranes by temporal retinal axons. *Development*, 913, pp.909–13.

Wang, J. *et al.*., 2002. *Drosophila* DSCAM Is Required for Divergent Segregation of Sister Branches and Suppresses Ectopic Bifurcation of Axons. *Neuron*, 33, pp.559–71.

Washbourne, P. *et al.*., 2004. Cycling of NMDA Receptors during Trafficking in Neurons before Synapse Formation. *Journal of Neuroscience*, 24(38), pp.8253–64.

Wässle, H., Boycott, B.B. & Illing, R.B., 1981. Morphology and Mosaic of on- and off-Beta Cells in the Cat Retina and Some Functional Considerations. *Precedings of the Royal Society of London. Series B, Biological Sciences*, 212, pp.177–95.

Wei, C. *et al.*., 2009. Calcium flickers steer cell migration. *Nature*, 457(7231), pp.901–5.

Wiesel, T.N. & Hubel, D.H., 1963. Responses in Striate Deprived of Vision Cortex of One Eye. *Journal of Neurophysiology*, 26, pp.1003–17.

Wojtowicz, W.M. *et al.*., 2004. Alternative Splicing of *Drosophila* DSCAM Generates Axon Guidance Receptors that Exhibit Isoform-Specific Homophilic Binding. *Cell*, 118, pp.619–33.

Wong, R.O.L. & Ghosh, A., 2002. Activity-dependent regulation of dendritic growth and patterning. *Nature reviews. Neuroscience*, 3, pp.803–12.

Wong, W.T. *et al.*., 2000. Rapid dendritic remodeling in the developing retina: dependence on neurotransmission and reciprocal regulation by Rac and Rho. *Journal of Neuroscience*, 20(13), pp.5024–36.

Wu, C.F. & Ganetzky, B., 1980. Genetic alteration of nerve membrane excitability in temperature-sensitive paralytic mutants of *Drosophila* melanogaster. *Nature*, 286(5775), pp.814–16.

Wu, G.Y. *et al.*., 1999. Dendritic dynamics *in vivo* change during neuronal maturation. *Journal of Neuroscience*, 19(11), pp.4472–83.

Wu, G.Y. & Cline, H.T., 1998. Stabilization of dendritic arbor structure *in vivo* by CaMKII. *Science*, 279(5348), pp.222–6.

Xing, G. *et al.*., 2014. *Drosophila* neuroligin3 regulates neuromuscular junction development and synaptic differentiation. *Journal of Biological Chemistry*, 289(46), pp.31867–77.

Xu, J., Xiao, N. & Xia, J., 2010. Thrombospondin 1 accelerates synaptogenesis in hippocampal neurons through neuroligin 1. *Nature Neuroscience*, 13(1), pp.22–24.

Yang, C.R., Seamans, J.K. & Gorelova, N., 1996. Electrophysiological and morphological properties of layers V-VI principal pyramidal cells in rat prefrontal cortex *in vitro*. *Journal of Neuroscience*, 16(5), pp.1904–21.

Yuste, R. & Bonhoeffer, T., 2001. Morphological changes indendritic spines associated with long-term synaptic plasticity. *Annual Reviews of Neuroscience*, 24, pp.1071–89.

Yuste, R., Peinado, A. & Katz, L.C., 1992. Neuronal Domains in Developing Neocortex. *Science*, 257, pp.665–9.

Zhai, R.G. *et al.*., 2001. Assembling the presynaptic active zone: A characterization of an active zone precursor vesicle. *Neuron*, 29(1), pp.131–43.

Zhan, X. *et al.*., 2004. Analysis of DSCAM Diversity in Regulating Axon Guidance in *Drosophila* Mushroom Bodies. *Neuron*, 43, pp.673–86.

Zhu, H. *et al.*., 2006. Dendritic patterning by DSCAM and synaptic partner matching in the *Drosophila* antennal lobe. *Nature Neuroscience*, 9(3), pp.349–55.

Zito, K. *et al.*., 1999. Watching a synapse grow: noninvasive confocal imaging of synaptic growth in *Drosophila*. *Neuron*, 22(4), pp.719–29.

Ziv, N.E. & Smith, S.J., 1996. Evidence for a role of dendritic filopodia in synaptogenesis and spine formation. *Neuron*, 17, pp.91–102.

Zou, D. & Cline, H.T., 1999. Postsynaptic Calcium / Calmodulin-Dependent Protein Kinase II Is Required to Limit Elaboration of Presynaptic and Postsynaptic Neuronal Arbors. *Journal of Neuroscience*, 19(20), pp.8909–18.

Zschätzsch, M. *et al.*., 2014. Regulation of branching dynamics by axon-intrinsic asymmetries in Tyrosine Kinase Receptor signaling. *eLife*, 2014(3), pp.1–24.